UNIVERSITY OF CALIFORNIA, SAN DIEGO

Sustainable Developments in Eliminating Charging and Correlative Multi-modal Imaging techniques for Serial Block-face Scanning Electron Microscopy

A dissertation submitted in partial satisfaction of the requirements for the degree, Doctor of Philosophy

in

Chemistry

by

Donald Dewane Johnson, Jr.

Committee in charge:

Professor Mark H. Ellisman, Chair
Professor Susan S. Taylor, Co-Chair
Professor Adah Almutairi
Professor Judy Kim
Professor Elizabeth Komives

2015

The dissertation of Donald Dewane Johnson, Jr. is approved, and it is acceptable in the quality and form for publication on microfilm and electronically:

_____

_____

_____

_____
Co-Chair

_____
Chair

University of California, San Diego

2015

DEDICATION

I dedicate this dissertation to my wife, Noelle Rebecca Johnson, and our daughter, Elizabeth Elsie Johnson.

In loving memory of my best friend, Brian Hicks, and my grandfather, Chester Thomas.

EPIGRAPH

“I will love you regardless of what you chose to do with your life as long as you strive to be the best at it.” – Chester M. Thomas

TABLE OF CONTENTS

LIST OF ABBREVIATIONS

AgNP	Silver nanoparticle
AlNP	Aluminum nanoparticle
AuNP	Gold Nanoparticle
BSA	Bovine serum albumin
BSE	Backscattered electron
CL	Cathodoluminescence
CLEM	Correlated light and electron microscopy
cTEM	Conventional transmission electron microscopy
Cy5	Cyanine - 5
DHL	Duane-Hunt limit
DCC	Dicyclohexylcarbodiimide
dSTORM	Direct stochastic optical reconstruction microscopy
EDS	Energy Dispersive X-ray Spectroscopy
EFA	Edge function analysis
EGFP	Efficient green flourescent protein
FITC	Flourescein isocyanate
FOV	Field of view
GFP	Green flourescent protein
GG	Gene gun
NC	Negative Control
PALM	Photoactivated localization Microscopy
PC	Positive Control
ROI	Region of Interest
SBEM	Serial block-face Scanning Electron Microscopy
SE	Secondary electron
SEM	Scanning Electron Microscopy
SNR	Signal-to-noise ratio
ssUCP	Solid-state upconverting particles
TCH	Thiocarbohydrazide
TEM	Transmission Electron Microscopy
UCNP	Upconverting Nanoparticle
WT	Wildtype
XRM	X-ray microscopy
XRT	X-ray tomography

LIST OF FIGURES

LIST OF TABLES

LIST OF SUPPLEMENTAL FILES

KDEL_HV_Matrix_Corannulene: Run4_KDEL_HVMatrix_Corannulene (Converted).mov

Matrix_VP_Corannulene: Matrix_run3_corannulene_VP(Converted).mov

ACKNOWLEDGEMENTS

First and foremost, I would like to thank my committee for putting up with me. Judy, Betsy and Susan have always been the most supportive faculty in the Chemistry & Biochemistry Department. Judy was one of the first people in the department to welcome me here, helping me select a proper division for a home. Betsy was my first year advisor and sat on my second year exam committee. If it were not for Betsy, I would not be at this point my education at the University of California, San Diego. Finally, Mark, a man that has put up with my many personal and research related struggles. I know that Mark took a chance in taking me in; nonetheless, Mark took me in as his graduate student when others would rather see me gone. I am grateful for his generosity and willingness to advise me on my projects. In my time, I have found Mark to be a very humble person for his accomplishments as a scientist. He humbled me. It has been an honor to work under him.

Behind every great principal investigator, there is a great lab. I would like to thank Thomas Deerinck, Eric Bushong, Ranjan Ramachandra, Steve Peltier and James Bouwer for advising and assisting me through the tough experiments. I learned a lot from these people through our weekly serial blockface meetings and was able to successfully craft experiments following the weekly feedback from these meetings.

My thin sectioning and microscope training was not possible without people like Andrea Thor and Mason Mackey. Mason has not only been a great friend but a great help in developing the skills necessary to tackle my projects in

lab. Andrea has also been a great help in training me on thin sectioning and other wet lab techniques important to accomplishing my projects. I am in deep debt to these people for their time and dedication.

When I first joined the lab, I was shocked to find people that cared about my success. Whether it was the Nathaniel working with me on using his microtubes to label with my upconverting nanophosphors, or Alex's help in teaching me to use IMOD and other imaging software. Tapi was always helpful in getting advice on experiments and other lab related matters. Tristan not only helps me on the JEOL-JSM5000 SEM upstairs many times but also acted as an extension of that kindness that is prevalent in the Ellisman lab. Junru and Daniela were always open to helping me on the mammalian cell lines. I owe much of my training in this area to them.

To my collaborators, Josh Collins and Jay Siegel, thank you for your passing on material to me. For Josh, it has been great working with you on the upconverting nanophoshors, learning all the different morphologies and compositions that could be made. For Jay, thank you for taking a graduate student's idea for improving conductivity in resin seriously in sending some corrannulene for the initial experiments.

To Eileen M. Spain, Adrian Hightower, and George Patterson, thank you for guiding me to this point in my career. Each one of you set me on a path to the next endeavor with the best intentions at heart. If it were not for the opportunity to work with you, I would not be at this point my training.

If it was not Betsy talking to me about my worst days, and there were many terrible days. If it was not Judy listening to my problems in her office, and there were a few occurrences. My wife, my other spiritual half, my best friend and the only person I can truly trust on this earth has been there for me. She has rushed clothes to the lab when I have spilled a solvent (completely inert) on me. She has taken time off to be there for me when I have taken my major exams. She has stayed up late and even warmed up dinner when I forget to eat. She has been there for our daughter when I have had to work late in the lab. I cannot think of any word, or phrase that can address my gratitude beyond a simple thank you. If this process has done one thing, it has surely proven to me that my wife, Noelle Johnson, is the most brilliant, selfless, kindest, strong-minded person in my life.

Speaking of strong-minded individuals, I would like to thank my daughter, Elizabeth, for bringing me my morning coffee, for being sweet, brilliant, and jovial. If I ever needed a happy pill, that is my little girl. In my darkest times, she reminded me with that I still have something to fight for. All she has to say is, “Daddy!” It was therapy for me to build Lego spaceships with my daughter, race hot wheels and go biking. It was therapy to take her to the San Diego Zoo or Wild Animal Park, or even Legoland in the last year. I thank her for all of those times when she made my day.

I would like to thank my mother-in-law, Jeanne, and my step father-in-law, Charles Van Horn for opening their home to my family and letting me

decompress after a rough week of experiments. They were also instrumental in taking our daughter some weekends, so I could work in the lab.

To my Aunt Essie Abbott, cousins Jim and Eric, thank you for listening to me talk about my projects. You may not have understood me, but you helped me get over the day. To my brother Vincent, thanks for being the biggest, baddest, coolest big brother a “little guy” like me could ever have. You always provide perspective, and I appreciate that.

A “brother” that helped me start my interest in science is my late best friend, Brian Hicks. He was my roommate at St. Mary’s hospital in Rochester, MN. We spent our days cracking open different types of root beer to see which could be notable over the metallic taste in our mouths from the chemotherapy. We eventually settled on Barq’s rootbeer. Our mothers would buy cases after this conclusion for every time we went in for treatment. We would then pretend to feel safe enough to ask about our conditions. It was like taking a crash course in imaging for me as I wondered over the use of Magnetic Resonance Imaging (MRI). Brian cared more about the biology. It was root beer and a show for us. We were told at some point that we only had three more months to live. I was at peace many years ago with this fact. I was obviously sad to not go with him, but I promised myself years later that I would do something that we were not able to do and that was grow our hair out. So, the entire time I have been in this program, I have been silently acknowledging a friend who always made me smile and still makes me smile. Thank you, Brian, for always being there in spirit.

And finally, to the man that only spent five years getting to know me but impacted my life and many others in such a positive way, my grandfather, Chester Thomas. Very brief, my grandfather grew up on a farm in the middle of nowhere Louisiana with an 11th grade education, however, he managed to climb the ranks to become an executive officer for Gulf Oil. During this time, he cut lawns with his mower and taught all his grandsons the importance of gardening. He created one of the first multi-racial vanpools for his company and worked tirelessly to make sure every nephew, daughter and son had all the opportunities in the world to make it. He was the most selfless man I ever knew. I can remember wanting to be the first to finish cutting my segment of the lawn. His response, “A gardener will be a great gardener if they are always improving their technique and questioning their work.” Basically, slow down and pay attention to the details. He died two months after saying that, and I imagine his words today. I know he would first say he expected a little more, but then hug me and say that he is proud to have me as a grandson. I know I stand on his shoulders. For this reason, I dedicate my thesis to the memory of my grandfather.

For Chapter II, Tom was especially helpful in the resin conductivity project. He was instrumental in the development of using matrices as scaffolds for directing metal coordination for enhanced conductivity. Eric assisted in the development of reconstituted iron dextran systems. Ranjan was instrumental in optimizing our analytical efforts. James was also helpful in advising on some of the first quantitative measurements. James was also a major therapist for me, as he understood my situation before coming to the Ellisman lab. For his time

talking to me, I appreciate all the advice he ever gave me about continuing on and I appreciate that. Jay Siegel provided the corannulene compound. Junru was key in genetically labeling cell monolayers. Thank you for collaborating with me on this project.

For Chapter III, Eric was instrumental in the slot grid development and cell labeling protocols. Josh Collins was instrumental in the solid-state synthesis of the yttrium sulfoxide particles. Tom and Christine Kim were key in generating the SBEM data. Thank you for your assistance in this project. Bushong, E.A., Johnson, Jr., D.D., Kim, K.Y., Terada, M., Hatori, M., Peltier, S.T. Panda, S., Merkle, A. and Ellisman, M.H., X-Ray Microscopy as an Approach to Increasing Accuracy and Efficiency of Serial Block-Face Imaging for Correlated Light and Electron Microscopy of Biological Specimens. **2014**, Microscopy and Microanalysis, 21, pp 231-238.

For Chapter IV, Josh was instrumental in the development of the nanophosphor particles. Most of the labeling protocols involved were developed by Junru and Tom. Thank you for your assistance in this project.

VITA

2008	Bachelor of Arts, Occidental College
2008-2010	National Institutes of Health, National Institute for Biomedical Imaging and Bioengineering
2010-2015	Teaching Assistant, Department of Chemistry & Biochemistry, University of California, San Diego
2010-2015	Graduate Student Fellow, Department of Chemistry & Biochemistry, University of California, San Diego
2011-2015	National Institutes of Health Molecular Biophysics Training Grant Fellow
2012	Master of Science, University of California, San Diego
2015	Doctor of Philosophy, University of California, San Diego

PUBLICATIONS

Developments to improve specimen conductivity in epoxy resins for serial block-face scanning electron microscopy, D.D. Johnson, Jr., T.J. Deerinck, E.A. Bushong, J. Bouwer, R. Ramachandra, S. Peltier, A. Thor, J. Siegel and M.H. Ellisman, (Manuscript in Draft)

Targeted approach to imaging membrane proteins using small water-soluble upconverting nanophophors, D.D. Johnson, Jr., T.J. Deerinck, E.A. Bushong, S. Peltier, D. Boassa, J. Collins, and M.H. Ellisman, (Manuscript in Draft)

X-Ray Microscopy as an Approach to Increasing Accuracy and Efficiency of Serial Block-Face Imaging for Correlated Light and Electron Microscopy of Biological Specimens. E.A. Bushong, D.D. Johnson, Jr., K.Y. Kim, M. Terada, M. Hatori, S.T. Peltier, S. Panda, A. Merkle and M.H. Ellisman, **2014**, Microscopy and Microanalysis, 21, pp 231-238.

Marangoni Flow of Ag Nanoparticles from the Fluid-Fluid Interface, D.D. Johnson, Jr., B. Kang, J.L. Vigorita, A. Amram, and E.M. Spain, *J. Phys. Chem. A* (invited), **2008**, 112. 9318.

FIELDS OF STUDY

Major Field: Chemistry & Biochemistry (Materials Chemistry and Imaging Development

ABSTRACT OF THE DISSERTATION

Sustainable Developments in Eliminating Charging and Correlative Multi-modal Imaging techniques for Serial Block-face Scanning Electron Microscopy

by

Donald Dewane Johnson, Jr.

Doctor of Philosophy in Chemistry

University of California, San Diego, 2015

Professor Mark H. Ellisman, Chair
Professor Susan S. Taylor, Co-Chair

Serial block-face scanning electron microscopy (SBEM) promises to revolutionize structural biology and neuroanatomical research by allowing the 3-dimensional reconstruction of relatively large regions of tissue and cell arrays at

near nanometer-scale resolution. This approach employs an automated ultra-microtome fitted into a scanning electron microscope that images the specimen surface, or block-face, following each iterative nanometer thin cut. However, a principal limitation of this approach is the resolution obtainable using backscatter electrons at low accelerating voltages due to the build up of electrostatic charges on the block-face, otherwise known as “charging.” Herein, we present a specimen preparation protocol that implements heavy metal staining, and a series of methods for use of conductive materials, as either a dopant, covalent linker, or metal coordinated matrix (scaffold), in the epoxy resin. These approaches in staining and enhancing resin conductivity lead to substantial improvement in contrast and image resolution for accelerating voltages at, or below, 2.0keV for SBEM. To build connections from the 3-dimensional data sets obtained by SBEM to other imaging modalities for broader context and insight, developments in region of interest (ROI) tracking across light, x-ray and electron microscopy using upconverting nanoparticles, as fiducial markers and labels, have led to advanced efficiency in the correlated microscopy workflow. As a result, a universal fiducial/marker ties together the representing datasets for multi-modal imaging, and adds further context to the specimen’s region of interest.

Chapter I

Methods for multi-modal imaging and characterization of biological specimens

1.1. Introduction

Over the past decade, interest in the ability to view a biological specimen over multiple imaging platforms have exponentially grown with the interest in understanding the underlying chemical and macromolecular interactions that lead to cellular function (Burnett *et al*. 2014, Deernick *et al.* 2010). Indeed, developments in super resolution light microscopy were the steps that reinvigorated interest in defining some perspective in imaging scales (Schroff and Betzig *et al.* 2007). At the same time, improvements to conventional electron microscopes in camera, detectors, and electron beams set up a revolution in the development of alternative techniques. As a result of growth in both realms, there is now feasibility and interest in developing methods and techniques that bridge both realms.

The rest of this chapter will serve as an introduction to the individual instruments, components and techniques of this imaging toolbox, describing the historical timeline of development, applications and associated technological advancements. Specifically, this chapter will focus on strengths and weaknesses of each imaging modality and their functional relationships. Finally, the conclusion of this chapter will address current goals and establish the importance of materials and methods developed in this dissertation.

1.2. Light microscopy

With visible light and an organized arrangement of lenses, light microscopes have been the primary imaging source for viewing into smaller scale

biological environments since Van Leeuwenhoek (1632-1723) popularized the instrument for biologist. While light microscopes were useful for biologist, they did not become useful for chemist until the development of fluorescence microscopy in the mid 20th century. Stains such as 4', 6-diamidino-2-phenylindole (DAPI) and fluorescein isothiocyanate (FITC) were utilized to chemically target small molecules, proteins and other macromolecules in the cell (citation). Genetic targeting of genes became visible by fluorescence microscopy with the use of efficient green fluorescent protein (EGFP). Multi-channel genetic targeting was the following step in the direct evolution methodologies utilized by Tsien *et al*.

A signal was usually detectable by fluorescence microscopy, however, it was not possible to resolve macromolecular level resolution until the advancements made at the turn of the 20th century in light microscopy, with the development of super resolution microscopy (Patterson *et al.* 2010). The ability to see down to the nanoscale, was no small feat, requiring the violation of Abbe's law of limiting resolution (Betzig *et al*. 1996). With the ability to peer into the nanoscale just by the use of visible light, many molecular level studies

The remainder of this section on light microscopy will be broken into areas dedicated to the techniques, their strengths and weaknesses. Not all visible light techniques will be addressed. In particular, each sub-category of this type of microscopy will serve as a background to the developments and future goals addressed the proceeding chapters of this dissertation.

1.2.1. Super resolution microscopy: PALM and dSTORM

The use of visible light has always limited resolution to 70 microns (Betzig *et al.* 1996). This limitation is calculated by using the Abbe law of limiting resolution. To overcome this limitation of visible light, photons from neighboring flourophores must be identified and localized.

By tuning to a stochastically sparse set of flourophores at a specific excitation wavelength, single-fluorophores can then be excited and imaged. As each fluorophore emits its photons, other fluorescent single molecules can also begin to emit photons causing potential accumulation of active fluorophores in the region of interest (ROI). To overcome this issue, photoactivated localization microscopy (PALM) utilizes photobleaching to effectively quench the initially active fluorophore; whereas, direct stochastic optical reconstruction microscopy (dSTORM) reversibly switches off the fluorophore emission.

Once either process begins, it repeats itself until all of the fluorophores are imaged. The timing is based on how fast it takes to generate a high-emissive state and bleach, or generate a non-emissive state. For each cycle, the density of activated fluorophores is kept low to avoid overlapping individual fluorophores. An image is collected for each cycle and stored into an image sequence for image processing.

During the localization process, fluorophores positions from each of image of a sequence are calculated with a precision typically higher than the diffraction limit (1-10nm). A Gaussian function, or two dimensions, is taken to generate

information on the position of the centers of all the localized fluorophores, building up the super-resolution PALM, or dSTORM, final image. The final image is therefore limited by the precision of each fluorophore localization and the number of localization rather than by diffraction (Schroff *et al.* 2008).

As a result of the single point emission cycles and localization parameters, dynamic trafficking of small molecules has been an issue for this modality. Typically, for live cell imaging, slower cellular processes have been imaged as early as 2007 (Hess *et al.* 2007). Both PALM and dSTORM are also limited to x,y plane resolution, making them incapable of three-dimensional whole volume resolution.

1.2.2. Two-photon excitation microscopy

Although fluorescence microscopy, in particular confocal microscopy, is a popular technique for live cell imaging, there are several major deficiencies. High-energy excitation wavelengths for live cell imaging tend to lead to phototoxicity in the cell. Specimens that are subjected to the high-energy excitation source also deal with larger elements of scattering. As a result, there is limited penetration depth for collecting a whole volume data set. To overcome these issues, two-photon excitation microscopes pulse a red shifted laser source. The source is generally an infrared laser. At low-energy excitation wavelengths, phototoxicity and scattering diminish while penetration depth and spatial resolution significantly improve.

Maria Goeppert-Mayer first described the principle photo-physical process, two-photon absorption, in her 1931 doctorial dissertation (Denk and Strickler, 1990). The two-photon absorption process is based on the idea that two low energy photons are absorbed by a fluorophore simultaneously. The resulting absorption will generate enough energy to excite the fluorophore. It was not until 1961, when the two-photon excitation process excited calcium difluoride, doped with europium. In 1990, Winfred Denk pioneered the development of two-photon microscopy (Denk and Svoboda, 1997). A Ti-sapphire laser, used in studies described in this dissertation, has a pulse width of approximately <30 femtoseconds, with a repetition rate of about 80MHz. This allows high photon density and flux required for simultaneous two-photon absorption and is tunable across a wide range of wavelengths.

1.2.3. Continuous wave low energy light microscopy

With the advent of low energy excitable flourophores, such as upconverting nanoparticles and BODIPY dyes, interest in non-pulsed low energy light microscopy has emerged (Johnson and Bushong *et al*. 2014). Using the same Ti-sapphire laser, except not pulsing the laser output, low energy infrared excitation wavelengths are utilized in this light microscopy technique. Most two-photon systems are ideal setups for this technique. Otherwise, an infrared lasing source is directly attached to a confocal system with no modulator.

Continuous wave, or non-pulsed, low energy light microscopy avoids all the auto-fluorescence problems that arise in two-photon imaging. This eliminates potential false signals in tissue and cell monolayers. Also, just like two-photon, continuous wave also avoids all the specimen damage that arises from a high-energy beam.

1.3. Transmission Electron Microscopy

Instead of using visible light to image a sample, transmission electron microscopy (TEM) uses collected electrons that have gone through the sample and not been deflected by the dense organization of atoms in the sample. Why would we consider electrons as a source for visualizing the sub-micrometer world and not ultraviolet (UV) light? An electron's wavelength is significantly smaller than UV and visible light. In fact, if calculated to determine the appropriate resolution constraints by taking the Abbe diffraction limit, $d = \lambda/2n\sin\Theta$. When the wavelength, λ, is low, the diffraction-limited spot is small. Smaller spots correspond to higher resolution limits for the type of imaging technique.

The electron beam is focused by a series of electromagnetic lens organized along the beam path, under ultrahigh vacuum. Each lens provides a tunable current, which allows the user to adjust the electron's applied force as it passes through the lens. Once the electron passes through the sample and onto the phosphorescent screen, the shadowed areas of the sample resolve macromolecular details as high as 1nm depending on the TEM.

The first TEM was built in 1931 by Max Knoll and Ernst Ruska. It was not until 1933 that this group developed the first TEM with a resolution improvement over visible light, and it was not until 1939 that the instrument was made commercially available. Further advancements by Ruska (citation) led to the first TEM with 100kX magnification. As a result, Ruska received the 1986 Nobel Prize in Physics for his work on “the development of the electron microscope and electron microscopy.”

Since the development and improvements to TEM, chemist and biologist have benefited greatly from this technique. In particular, the developments in structural determination of macromolecular structure are driven by this imaging technique. For the remainder of this section, TEM incorporated techniques will be discussed that relate to this dissertation. The advantages and disadvantages of these techniques will be discussed in detail.

1.3.1. Serial Section Electron Microscopy

After embedding a heavy metal stained biological specimen in epoxy resin, 60-80nm thin sections are taken and imaged by a conventional transmission electron microscope (cTEM). Iterative sectioning and imaging of a biological specimen is known as serial section electron microscopy (ssEM). Serial section microscopy had its initial advantages. A 3-dimensional data set of a biological specimen could be processed at nanoscale resolution. Details about

ultrastruture and macromolecular interactions were either validated or described by this technique.

Although this technique popularized serial sectioning for electron microscopy, there were many downsides to utilizing this technique. For one, someone had to learn to section at a nanometer precision and accuracy without any errors. Training for this degree of sectioning takes time and the person may never be great enough to iteratively section 100 slices to get a data set. Also, each slice is going to have compression or distortion as a result of the knife. Another issue is orientation and alignment. Each slice has to have the appropriate orientation and alignment to make sure the ROI is consistent from section to section. This has resulted in customized sample holders, TEM sample chambers and other high throughput methods.

1.3.2. Cryo-electron microscopy

Most TEM staining methods require the use of some heavy metal and solution conditions that would otherwise alter the native state of the biological specimen or macromolecule. In defining a native state, this relates to the perfect preservation of structure and potential function of a biological specimen. For chemist, this is especially important as potential chemical environments can be altered by the change in larger scale physiological changes (Tseng *et al*. 2015; Adrian *et al*. 1984).

Cryo electron microscopy (cryo-EM) is a process by which the biological specimen is frozen to < -180°C in by a timely plunge freezing method and kept at this temperature for imaging purposes. The specimen does not undergo any metal staining or other chemical treatments that would otherwise alter the macromolecular and ultra-structural environment of the specimen. The biological specimen is in its most native state. This is very major point to make as every other technique disregards the native state of the specimen, excluding some *in vivo* confocal probe methods. There is little to no contrast in the resulting micrograph as a result of the lack of metal stains. However, when the sample is tilted iteratively along a single axis, the collection of images combine to apply some perspective to structural details. Following application of the various image processing constraints and approximations, the final 3-dimensional reconstruction is completed.

Many viruses, proteins and other macromolecular structures have been characterized by this method as a result (Parent *et al*. 2014). There has also been a growing interest in developing nanomaterials for cryo-EM. For example, Chien *et al.* use polymer-peptide nanomaterials as scaffolds for delivery of drugs to targets (Randolph and Chien, 2012). These targets are identified by a stimuli-response, such as the upregulation of matrix metalloprotease – 9 (MMP-9) in cancer cells. Work in the development of synthetic virus capsids has been recently characterized cryo-EM. In all, this is a burgeoning field for TEMs, with a growing interest in the structural biology and nanoscience communities.

The largest pitfall of this technique is that we are imaging vitreous ice embedded tissue/cells with a 120 - 300kV electron beam. The generating heat from the electron beam will essentially bore a hole in the field of view (FOV). Techniques have been developed to avoid this issue, however, if not mindful of this, one can damage the ROI during imaging. The other issue with this method is that the resulting raw micrographs generated are noisy and require extensive image processing. There has yet been a way to address this issue, however, interest in developing a conductive vitreous ice block has been considered as a way to reduce noise and enhance contrast.

1.4. Scanning Electron Microscopy

Rather than reading electrons that have gone through a sample, scanning electron microscopy (SEM) utilizes one, two, or multiple combinations of signals emitted from the surface of the biological specimen. The electrons are directed to the surface of the sample by a rastering pattern. When a biological specimen is dosed with electrons from the electron beam source, the surface of the specimen will emit detectable secondary electrons (SE), back-scattered electrons (BSE), characteristic x-rays, and light (cathodoluminescence, or CL). Most SEMs are fitted with a secondary electron detector (SED) and backscatter electron detector (BSED); although some may either have a third attachment for detecting light or x-rays. Manfred von Ardenne built the first SEM in 1937 where

he also studied the various detection modes available to this technique. It was not commercialized until 1965 (Smith *et al*. 1955).

Since the commercialization of this microscope, many materials scientist have used to this technique to study sub-micrometer details. Chemists have utilized the detection of x-rays as a means to understand the elemental composition of a material, whereas; biologist started using SEM once there was a way to make biological materials conductive. The sample, whatever it may be must be conductive in order for the electrons, from the electron beam to dissipate.

When a sample is not conductive, the electrons from the electron beam source have no mean free path to dissipate. As a result, the electrons collect on the surface of the sample effectively deflect the raster beam, or electron beam, as it moves along the surface of the sample. The resulting image is distorted and pixelated with lower resolution and distorted contrast. This phenomenon is known as sample “charging.” As a result, in order for the SEM to work out high-resolution detail in a sample, the sample must be conductive.

There are various ways to make a sample conductive. Sputter coating gold, platinum, or carbon onto a surface is very common. For biological specimens, heavy metal staining methods have yielded interest in developing techniques similar to serial section electron microscopy. Osmium has proven to be the most optimal heavy metal for most methods. This staining method calls for the impregnation and chemical crosslinking of osmium to unsaturated lipids and other unsaturated hydrocarbon features in the tissue/cellular sample. Once this oxidation step is completed, a cross linker is chemically added to the sample,

known as thiocarbohydrazide. This sets up another Osmium stable sight for covalent chemical attachment. Once done, the sample is usually taken through a series of other heavy metal treatment steps, or taken on to sectioning and/or imaging.

Sample preparation may be important to driving improved resolution and contrast; however, the detection of emitted signals from the sample is also a relevant and vital point of development in this imaging technique. Detection of the types of signals yields important and different results. This is due to the physical process by which these electrons are emitted from the surface.

For example, secondary electrons (SE) are emitted from the surface of a sample following an inelastic collision between an electron from the raster beam and an electron within the sample. Most electrons from the surface of a sample are secondary electrons, ejected from the k-shell of the sample as a result of a violent transfer of energy from the raster beam electrons. Secondary electrons are low energy ionized electrons as a result of the energy transfer from the inelastic collision. The prolific abundance of these low energy electrons is what drove the first SEMs to have secondary electron detectors.

It was not until interest in detecting higher energy electrons that originate at the electron beam. Backscatter electrons (BSE) are the result of elastic scattering with the sample electrons. Due to the minimal potential in elastically colliding with an electron (from sample), especially at low raster beam energies, this signal is fairly weak to detect in low atomic number (low - Z) elements, whereas; higher atomic number (high - Z) elements, like heavy metals, favorably

elastically scatter for detection. As a result, heavy metals, like osmium, are ideal chemical labels for this imaging detection mode.

The following subsections will relate to use of these detection modes as specialized techniques for SEM. These techniques are not all the techniques developed as a result of SEM. Each subsection will build context for this dissertation. The context will build the argument for advancements accomplished and addressed in each following chapter by the author and relevant collaborators.

1.4.1. Low Voltage Scanning Electron Microscopy

Approaches to addressing lower landing energies (Accelerating voltages < 5kV) have become an equally important development piece for improving SEMs and the associated techniques. The driving force for selecting lower landing energies has been the development of improved detection sources. Other advancements have addressed the sample stage, working distance constraints and adjustments to the electron beam source (Joy *et al*. 1995). Why is there interest in low voltage SEM, rather than utilizing higher voltages? To address this point, issues in imaging at higher landing energies must be addressed.

At higher landing energies, assuming a conductive sample, the detectable signal produced is a product of not only interactions with the surface, but also interactions at a finite depth below the surface. Monte Carlo simulations model these finite penetration distances. For a conductive sample, there is enhanced

spatial resolution, in BSE mode, and more BSEs for a detector. Nonetheless, higher voltages result in reduced contrast as a result of reaching deeper finite distances in the sample. Higher landing energies reduce image contrast and serve to detect heavy metal environments. This is problematic for biological specimens where osmium staining loses contrast in high voltage imaging cases, whereas, heavy metal sputter coating techniques are not susceptible to loss in contrast under the same conditions. Spatial resolution is not usually the interest of most sample characterizations and advancements in low voltage microscopy have yielded improved 3.0nm resolution for SEMs. As a result, assuming a conductive sample, high voltage imaging reduces contrast in chemically metal stained samples and yields unnecessary improved spatial resolution at the cost of reduced contrast.

At lower energies, improvements in contrast result in reduced heavy metal staining of tissue/cells, addressing a more native state of the biology of the sample. Also relevant, controlled chemical treatment of biological specimens is the ideal approach, especially when addressing macromolecular details and interactions. Since the advent of low voltage scanning electron microscopy (LVSEM), advancements and interdisciplinary developments in chemical and genetic targeting techniques have grown prominent. In particular, the development of mini singlet oxygen generator (miniSOG) protein not only built on correlated light and electron microscopy techniques but also proved to demonstrate routes in targeting heavy metal stains for electron microscopy (Shu *et al.* 2011). Since this development, interest has gained momentum in

distinguishing metal labels by inelastic scattering yield. Known as a two-color electron microscopy (Ramachandra *et al*. 2014), two metals have been chemically associated as a duel labeling approach for electron microscopy using the miniSOG protein. The two metals undergo chemical analysis by electron energy loss spectroscopy transmission electron microscopy (EELS-TEM). Following chemical analysis by EELS, the areas are identified and marked by modeling and other image processing methods. The next steps in this work include exploiting the scattering properties of metals at varied atomic numbers (Z), where scaling the contrast in a BSE derived image versus a SE derived image will yield distinguishable metal probes.

When the sample is not conductive, sample charging is prevalent in high voltage imaging cases. Non-conductive samples are becoming an increasingly large problem for structural biologist. Most biological specimens for electron microscopy are embedded in a non-conductive epoxy based polymer that is chemically initiated by a tertiary amine. The polymer hardens by a curing a method, and is the scaffold for which one can thin section the tissue/cell monolayer for imaging. Since the development of osmium staining protocols, low voltage SEM has been on the rise as a preferred technique amongst structural biologist. Nonetheless, structural biologists are limited to studying densely metal stained biological tissues, such as brain slices. Cell monolayers, kidney tissue, and other vascularized specimens are prone to charging under low voltage imaging conditions, but less than under high voltage conditions. To overcome this issue, low voltage imaging conditions are safe enough to consider varying

the vacuum pressure of the sample chamber. At high atmospheric pressures, charged contaminants within the sample chamber assist in dissipating charge from the sample. So, as a result of reaching lower landing energies, techniques in studying non-conductive samples in variable pressure environments were developed to overcome sample charging.

Although variable pressure has been the answer to imaging non-conductive samples with low voltage SEM, the original benefits of enhanced contrast and superficial resolution are negatively affected. Hence, recent interest has grown in developing conductive resins for the cell monolayers and other resin rich specimens. Specifically, this dissertation will address the routes taken to develop conductive resins for low voltage SEM systems.

1.4.2. Energy Dispersive X-ray Spectroscopy

Primarily used as an analytical technique for elemental analysis, or chemical characterization, energy dispersive x-ray spectroscopy (EDS) measures characteristic x-rays that have been emitted from the specimen surface. These characteristic x-rays result from high-energy shell electrons occupying ground states as a result of the ejection of a ground state electron. Each element on the periodic table will emit x-rays at a specific energy. The number and energy of the x-rays emitted from the specimen are measured by an energy dispersive spectrometer. As a result, one could plot this energy profile and map out elements in a give specimen. For biological specimens, carbon,

oxygen, nitrogen, sulfur are typical signals; nonetheless, for a metal stained biological specimen, the heavy metals are also profiled.

Since charging is a prevalent issue in scanning electron microscopy, it would be naïve to assume that charging does effect the measuring of emitted x-rays. In fact, the emission of high-energy x-rays from a specimen is perturbed by the collection of electrostatic potentials on the surface of the specimen. When the incident beam forces the ejection of a ground state electron, that electron has to go somewhere. When the specimen is conductive, ground state electrons from the specimen including electrons from the incident beam dissipate into the sample stage and other electrical grounding sources. When the specimen is nonconductive, electrons not dissipating from the specimen collect and inhibit the ejection of ground state electrons. As a result, as you reach detection of higher energy x-rays on an EDS, there is a drop off in signal. This drop off in signal is known as the Duane – Hunt limit. This drop off in characteristic x-ray detection will used as an analytical tool for measuring conductivity later on in this dissertation.

1.4.3. Serial Block-face Scanning Electron Microscopy

With the growth of serial section electron microscopy, low voltage SEM and advancements in image processing, it was a matter of time before a ultramicrotome would get placed into an SEM. Serial blockface scanning electron microscopy (SBEM) is an increasingly popular imaging technique

developed by Winfried Denk in 2004 at the Max Planck Institute of Neurobiology. With a ultramicrotome in the specimen chamber, set to slice a block of epoxy embedded tissue/cell monolayer at nanometer accuracy, the ultramicrotome takes iterative slices of the block.

Figure 1.1., Serial Block-face Scanning Electron Microscopy is a destructive process by which nanometer thick slice of a specimen are shaved off the surface at almost perfect precision and accuracy with a diamond knife. Following every fresh cut, a micrograph is taken of the fresh surface. Following a series of cutting and image collection cycles, the images stacked into a three-dimensional data set. All data sets for this study were collected on the MERLIN SBSEM using the backscatter detector (Denk and Hortzmann *et al*., 2004).

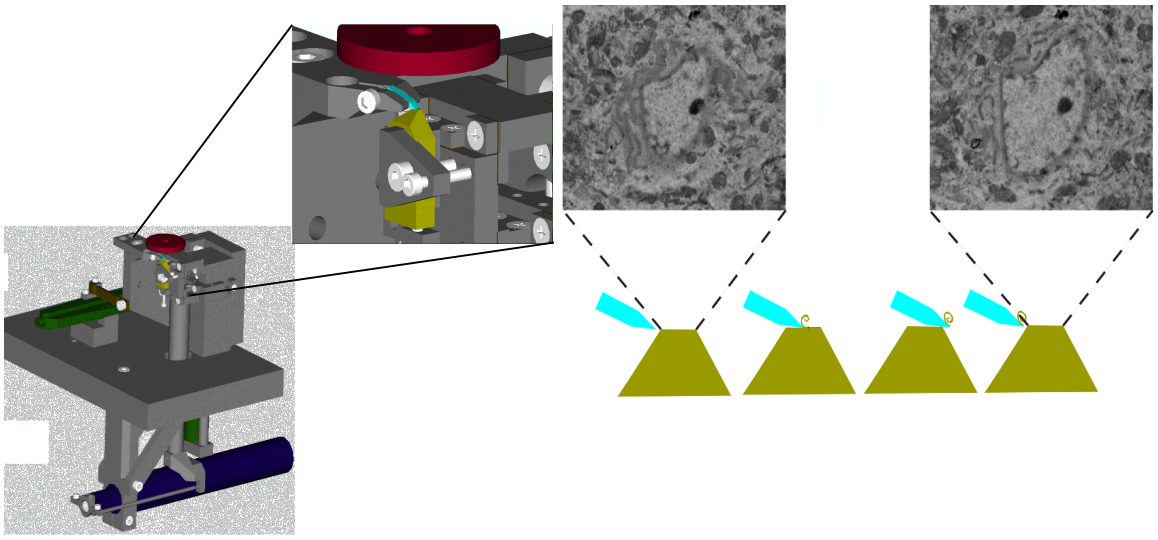

Shown in Figure 1.1., between each slice, there is a raster scan of the surface and resulting in detection by the backscatter electron detector (BSED). These micrographs are collected using low landing energies. The tissue/cell monolayer block is mounted on an aluminum pin and attached by a conductive silver epoxy resin. A diamond plane shaped knife is used to shave away layers of a fixed thickness (50-100 nm) between each collected micrograph. The resulting set of micrographs are collected, aligned and assembled by set thickness into a three-dimensional volume.

Even though a specimen block is grounded by silver epoxy resin and the aluminum pin it sits on is grounded, the specimen block is still prone to charging. Random shifts in the raster beam, which result from electrostatic potentials on the surface of the specimen, are especially not ideal for this collection as shifts in the raster beam correspond to shifts in the micrograph. This also causes defocusing in the image, along with distortions in contrast. Efforts are made during image processing making adjustments in the geometric distortions but there are limits. For example, image alignment constraints may be adjusted to distorted images, however, the specimen was never originally physically shifted along the x,y-axis.

Advancements in variable pressure SEM (VPSEM) at low landing energies have yielded the ability to image cell monolayers and other resin rich specimen environments. Also, improvements to backscatter detectors and the electron beam column have yielded ways to reach lower landing energies.

Hence, there are advancements being made in other areas to limit specimen/resin charging and enhance specimen contrast and resolution. As detector and beam development growth have started to solve charging issues, advancements addressed in this dissertation have been made to improve specimen/resin conductivity.

1.4.4. Cathodoluminescence

Of all the emitted signals from the surface of a sample, visible light is one of the few signals detected. Cathodoluminescence (CL) is a technique that measures emitted photons from the surface of a phosphorescent rich biological rich sample. Optical attachments over the specimen surface, such as the elliptical mirror utilized for this imaging modality, direct the emitting photons to a fiber optic source. From this point, the emitted photons are transferred via the fiber optic wire to a monochromator and separated into component wavelengths for detection by a photomultiplier tube (PMT) (citation). Usually, the electron beam operates at low landing energies, due to the interest in producing more secondary electrons from the specimen surface. Some CL systems come with preselected red, green, blue wavelength filters; however, it is also possible to manually tune the monochromator to the desired wavelengths for detection.

For the longest time, CL has been utilized as a tool for imaging and studying semiconductors, ceramics, and other phosphorescent materials. It was not until recently that cathodoluminescence was used to study biological

specimens. Most of the growth has been as a result of novel flourophores that all emit photons as a result of excitation from the electron beam. In particular, gold nanoparticles, conjugated to secondary antibodies for immunohistochemistry, emit plasmons visible by CL.

Although it is minor, two problems with CL limit the system from growing into a popular approach amongst biochemist. One problem lies in the working distance established between the elliptical mirror and the specimen surface. Distances between the specimen surface and the elliptical mirror must be precise to reach optimal signal detection levels. Also important, this distance must be fairly accurate as signals varying based on distance and can affect the consistency of an experiment. Another problem with CL for biological specimens is that this technique requires a conductive surface, so the specimens are heavy metal stained and grown on conductive coverslips. If not conductive, charging can lead to reduced image contrast and resolution as a result of electrostatic potentials shifting the raster beam. Shifts in the raster beam cause the photons from the specimen to emit at non-ideal angles.

Interest has grown to into incorporating CL into SBEM. The aim is to be able to add a secondary correlation for fiducials identified and mapped in both light and x-ray measurements. A CL image taken while the sample is oriented could be a last step orientation technique before sectioning. Any changes in the mapped area could be instantaneously tracked by this combination.

Immunohistochemical staining techniques could also be coupled to developed to follow two-color phosphorescent staining under SBEM.

1.5. X-ray microscopy

X-rays, unlike visible light, do not reflect or refract easily, and are invisible to the human eye. Hence, the ideal detection approach is the use of charge-coupled device (CCD). Use of soft x-rays as a source for imaging started as early as the late 1940s, and used synchrotron sources at particle accelerator stations at our national laboratories (citation, Kirkpatrick and Baez). Recently, popularity amongst microscopist has grown in generating soft x-rays from laser-produced plasmas. As a result, interest has grown in the redevelopment of x-ray microscopy techniques. Improvements in soft x-ray generation and detection have lead to high resolution (30 nanometer) imaging of biological specimens. This makes the resolution for x-ray microscopy better than using visible light microscopes but close to that of electron microscopy. As a result, x-ray microscopy is an ideal choice for bridging correlations between light and electron microscopy.

A growing interest in understanding three dimensional structure and function of macromolecules in larger context to the ultrastructure has lead to the development of x-ray tomography. Rotating specimen 360 degrees, a short exposure image is taken for every angle. The images are normalized to a series of reference images and applied into a 3D volume of the specimen. As shown in

Figure 1.2., the final raw dataset can be viewed and further filtered for the specified use. From these data sets, scaled connections can be drawn between the ultrastructure and the corresponding macromolecules.

Figure 1.2., Three dimensional reconstruction viewer and image processing software for X-ray microscope. By this method and others such as Amaris and Image J, filters and difference points can be used to map the fiducial markers.

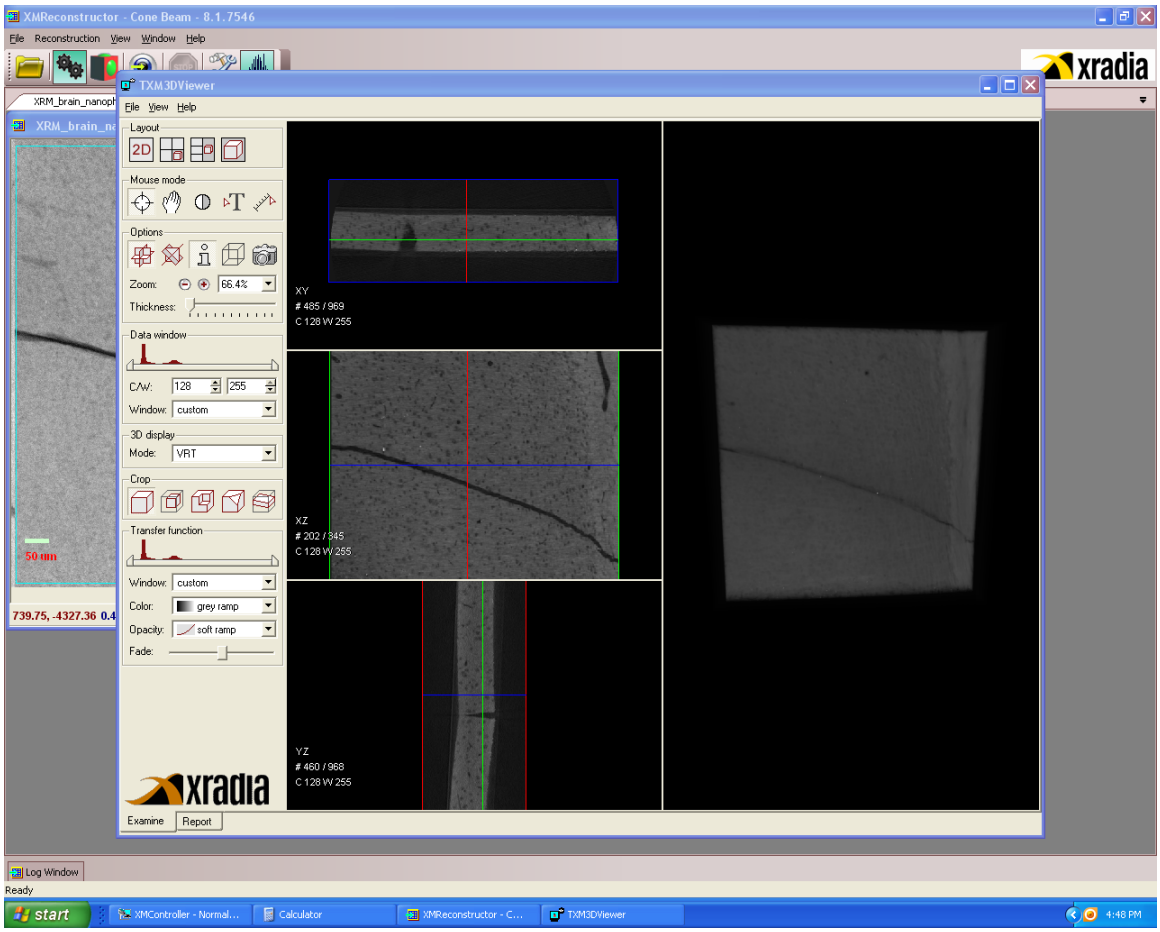
XMReconstructor - Cone Beam - 8.1.7546
File Reconstruction View Window Help
xradia
TXM3DViewer
File View Help
Layout
2D
Mouse mode
Options
Zoom: 66.4%
Thickness:
Data window
C/W: 128 255
Window: custom
3D display
Mode: VRT
Crop
Transfer function
Window: custom
Color: grey ramp
Opacity: soft ramp
Fade:
XY
485 / 969
C 128 W 255
XZ
202 / 845
C 128 W 255
YZ
460 / 968
C 128 W 255
xradia
Examine
Report
50 um
739.75, -4327.36 0.4
Log Window
Ready
start
XMController - Normal...
Calculator
XMReconstructor - C...
TXM3DViewer
4:48 PM

Potential small molecule interactions can be hypothesized for electron microscopy, and/or super-resolution microscopy studies.

For example, a labeled surface protein can be tracked by light and transferred to x-ray microscopy for further study. If a metal is attached or the fluorescent label has a x-ray excitation band, the labeled surface proteins can be confirmed for the position, and the location can be mapped for SBEM. To assist in this endeavor development in the randomized placement of fiducial markers has made this bridging of techniques possible (Bushong and Johnson *et al*. 2014).

Although there have been major advancements in the development of x-ray microscopy, minor issues still plague this imaging modality. For one, the sample has to be position to allow a mean free path for x-rays to reach the detector. For SBEM, the specimen is usually mounted on an aluminum pin. It the sample block is oriented to avoid the pin, the area is still small and hard to image due to the altering geometry and density of the specimen. Efforts in varying the beam energy, based on the angle of tilt, have yielded promising results. Another issue with the current x-ray microscopes is that most of the details between elements are overlooked because it would require multiple soft x-ray sources to generate a multi-channel imaging system. This would be ideal for discrimination of heavy metal stains from labeled targets. Currently, x-ray source filtering and other automated algorithms are the approach for this technique. Another issue with these imaging systems is that there has been little development in designing an x-ray system capable of gaining contrast for non-heavy metal stained

specimens. Essentially, a correlative technique but geared toward cryo-electron microscopy where a frozen slice can be imaged by x-ray and carried over to EM. This would only serve to expand the correlative light, x-ray and electron microscopy efforts made by building on the growing work in cryo-EM.

Chapter II

Developments in improving specimen and resin conductivity for Serial block-face scanning electron microscopy

2.1. Introduction

As discussed in Chapter I: Section 1.4.3., serial block-face scanning microscopy (SBEM) of biological specimens is an all-in-one volume-imaging microscope that is growing in popularity throughout the biological sciences research community. SBEM is a scanning electron microscope with an ultramicrotome built into the specimen stage. Following collection of an image, the ultramicrotome sections a 50-70 nanometer thick slice from the specimen. The newly exposed specimen surface is imaged, and the microtome sections another slice. The process repeats iteratively, and each image is collected. Following the imaging process, the images are cross-correlated, aligned and stitched together to form a volume. These data sets get as large as 1000 slices and a 16k x 16k pixel resolution.

Since the development of this imaging technique, efforts have been made in specimen preparation for improving contrast and resolution of the image (Denk and Hortzmann, 2005). Initially reached as a problem for SBEM, specimens and the embedding resin are prone to the collection of electrons on the surface. These electrons, coming from the incident raster beam, are unable to dissipate because there is no mean free path for the flow of electrons from the surface of the specimen. In environments, where there is little to no specimen and more resin, the collection of electrons is larger. This phenomenon, where electrons collect on the surface of a specimen and generate electrostatic potentials, is known as charging (Joy *et al*. 1995). It is very common problem with non-conductive specimens in scanning electron microscopes.

Although not clear, collection of electrons on the surface of a specimen may generate heat. Over time, localized heating may assist with potential chemical breakdown of the epoxy resin, or even the specimen itself. Degeneration of the resin, as a result of heating, can spur from free radical reactions initiated by the saturation of electrons on the surface. Even in a semi-conductive sample, saturation of electrons/flow of electrons from the incident beam will still generate the necessary heat to initiate any free radical reactions, which could compromise the resin.

The resin in question is a tertiary amine initiated epoxy resin. The resin was never meant, nor synthesized to withstand the direct dose of an electron beam. Thin sections, which were comprised of the specimen and resin, are usually carefully placed onto a silicon wafer for SEM. For TEM, thin sections are carefully placed onto a TEM grid. Since the underlying scaffolds (copper grid or silicon wafer) grounds thin sections, there has not been interest to make the resin conductive until the development of SBEM. The epoxy resin is mixed together from four components. As shown in Figure 2.1., the tertiary amine (component **C**) acts as an initiator in opening the first epoxy ring of either component **A** or **D**. The initiation reaction has been observed to be active at room temperature, however, the most optimal temperature for this reaction is at 65-70°C. Following initiation, the opened epoxy undergoes an addition elimination reaction with the malimide intermediate (component **B**). This reaction is essential to the step-wise covalent patterning of the two epoxy monomer subunits. Also shown in Figure 2.1., the rigidity of the resin is achieved by the simultaneous polymerization with the other

active epoxy groups. The patterning of **AB** or **DB** subunits is random; nonetheless, the content is controllable for every batch reaction.

Figure 2.1., Reaction scheme for one-pot synthesis of epoxy resin polymer. R groups represented are characteristic of the brand of epoxy resin used in our studies. Component C acts as the initiator in this reaction. Epoxy functionality not reacted in this scheme is representative of the potential simultaneous reactivity and further cross-linking at those sites, adding the overall rigidity of the structure.

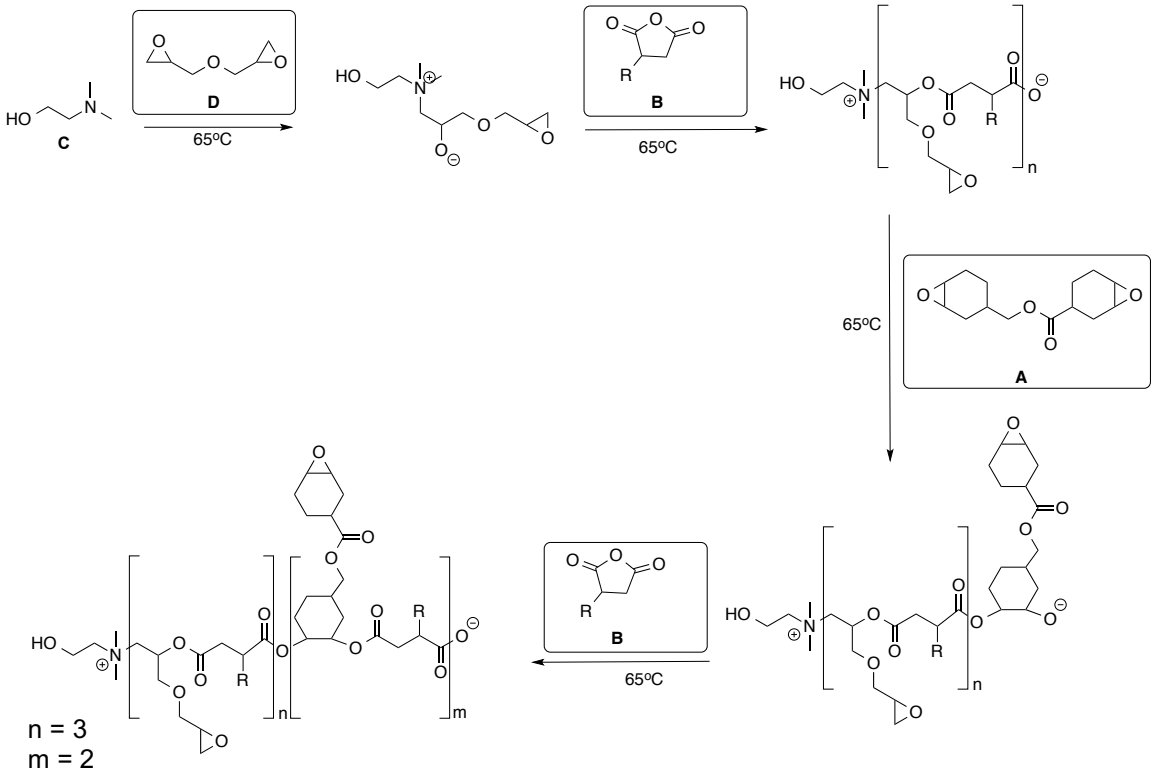
HO
C
D
65ºC
HO
B
65ºC
HO
n
65ºC
A
HO
B
65ºC
HO
n
m
n = 3
m = 2

This chapter will address specimen/resin charging with advancements in specimen and resin preparation. Specifically, all methods relating to the advancements in resin conductivity will be the focus of this chapter. The goals will also highlight the driving biological interest; however, the biological interest will not be the focus of this chapter. Also, the advancements made will highlight issues in the thermal stability of the epoxy resins. In all, this chapter will introduce work on ways to overcome specimen/resin charging and achieve optimal preservation, resolution, and contrast as a result.

2.1.1. Specimen and Resin Charging

With the growth of SBEM, problems with specimen charging have become common. When a specimen is "charging," (as shown in Figure 2.2.) this is usually due to poor grounding of the specimen. Electrons from the incident electron beam are collecting on the surface of the specimen, causing localized electrostatic charges. This leads to beam deflection, which gets perceived as distortions in the resulting micrograph. Since the specimen is getting sectioned (nanometer scale), intuition would dictate that charging should not be a problem since the electrons are collecting near the surface. However, collection time of high-resolution images (16k x 16k) is long, giving the specimen time to collect electrons. Also, electrostatic charges may be deeper than the section thickness, building on the problem. To solve this problem, a heavy metal staining protocol has been developed to provide specimen contrast, resolution and improved conductivity (citations). The heavy metal staining protocol incorporates a combination of transition metals and small

molecules, building on the traditional osmium staining protocols, but also incorporating other metals such as lead and iron.

Most notably, charging of the resin in porous biological specimens and cell monolayers has been a major issue. Introducing and/or chemically modifying the resin will reduce resin charging. This will improve the ability to image porous biological specimens and cell monolayers. Chemical modifications to the resin must be easy to reproduce and be mass producible. Additives to the resin as a dopant tend to have varying meso/micro scale concentrations of the additive. This makes imaging difficult, as some areas may be more conductive than other areas. Nonetheless, chemical modifications can potentially homogenize the resin more than using additives.

Combinations and incorporations of heavy metal staining methods have since taken resin conductivity into consideration. A mechanism that is being considered is the fixing the specimens in iron-conjugated gelatin. In particular, the development of a metal coordinated matrix acts a scaffold for the cell monolayer/tissue before embedding in the resin. Proceeding sections in this chapter will highlight the blending of cell/tissue staining techniques with methods to improve conductivity of the resin.

2.1.2. Resin Thermal Stability and the Electron Beam

As shown in Figure 2.2., a non-conductive sample is prone to charge saturation form the electrons from the incident beam not properly dissipating in time from the surface of the specimen. Whereas, a conductive sample would

equally dissipate as much charge as it receives from the incident beam. So, ideally, a conductive sample would be the best condition for imaging under SBEM. Nonetheless, even in a conductive sample, the passage of electrons would still produce some form of heat that would lead to free radical reactions and degeneration of the resin matrix. The relationship of thermal conductivity to electrical conductivity in a metal is known as the Wiedemann-Franz law (citation). Efforts in addressing thermal conductivity may be less related to the chemical composition of the resin, and more related to the mechanical design of the specimen stage. As a result, this thesis will not address any advancement in this area, as it does not require the development of any chemical characterization/synthetic techniques.

2.2. Methods Development and Results

This section will address methods defined as approaches to improving resin conductivity. Also important, methods in improving specimen conductivity will be addressed this section. There were many approaches taken, so the successful methods will be outlined first and in chronological order. Other approaches will be mentioned to address any questions, but should be considered failures, as the reasons for their failure will be outlined in the Discussion section of this chapter. In total, this section will serve to highlight the step-wise application of developed hypothesis and the results of each route described.

Figure 2.2., Sample “charging” and charge balance, or conductivity. When a sample is unable to dissipate as many electrons as it will receive from the incident electron beam, this is known as “charging.” Negative charging is when the sample is usually visualized at accelerating voltages >1.5keV. Whereas, positive charging is characteristic at accelerating voltages <1.5keV. When a sample is capable of dissipating as many electrons as it receives from the incident electron beam, it is at charge balance. However, in reality, charge dissipation is also a function of beam dose, magnification and scan rate.

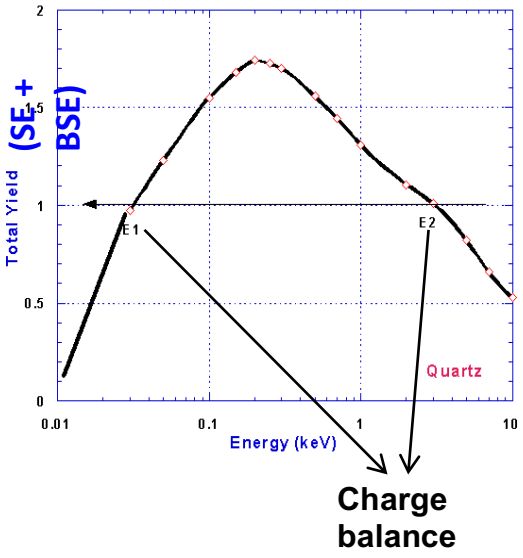

Charge balance

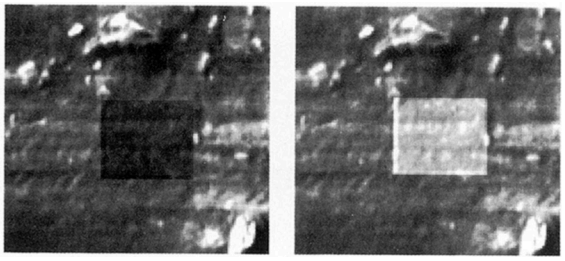

Positive charging (~ < 1.5 KeV)

Negative charging (~ > 1.5 KeV)

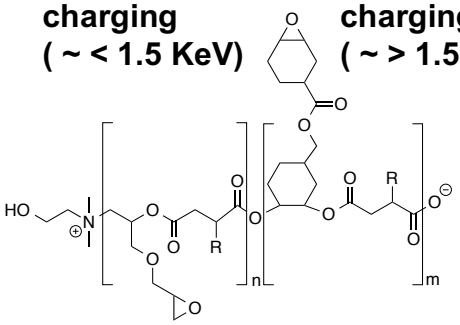

2.2.1. Sample Preparation

All animals were used according to a protocol approved by the Institutional Animal Use and Care Committee at the University of California, San Diego following AAALAC guidelines. Mice were anesthetized with ketamine / xylazine and transcardially perfused with Tyrode's solution followed by 2.5%wt glutaraldehyde / 2%wt formaldehyde in 0.15M cacodylate buffer containing 2mM $CaCl_2$. The brain was removed and postfixed on ice in the same fixative solution for 2 hours and then cut into 100 m thick slices on a vibrating microtome. The slices were post-fixed at 4°C overnight before heavy metal staining protocol as detailed in Section 2.2.2.

2.2.2. Heavy metal staining biological specimens for SBEM

Before solving the resin conductivity problem, development of an ideal heavy metal staining method for serial blockface scanning electron microscopy (SBEM) was necessary. This staining approach incorporates existing heavy metal staining methods, along with additional steps in low content staining and dehydration.

For cell monolayer samples, which are usually grown on poly-d-lysine coated Maktek dishes, the cells are fixed in 2%wt paraformaldehyde, 2mM calcium chloride and 5%wt glutaraldehyde. Cells are washed for 1 hour in 0.30M cacodylate buffer containing 2mM calcium chloride. Afterwards, cells are incubated in a 0.15M cacodylate buffer solution containing 15%wt potassium ferrocyanide, 15%wt calcium chloride and 2%wt osmium tetroxide for 1 hour and

agitated every 10 minutes. This is the first heavy metal staining reaction. Meanwhile, a 10%wt solution of thiocarbohydrazide (TCH) is prepared incubated at 60°C for 1 hour. Once an hour has passed for first the heavy metal staining, cells are washed in double distilled water three times for 15 minutes. Cells are treated in the filtered TCH solution for 20 minutes. Once done, the cells are washed in double distilled water and incubated once more in 2%wt osmium tetroxide for 30 minutes. The cells washed once more in double distilled water and incubated overnight in 1%wt uranyl acetate at 4°C. The following day, cells are washed in double distilled water (ddH_2O) three times for 15 minutes. Meanwhile, an aqueous solution containing 6.6%wt lead nitrate in 0.25M aspartic acid (pH 5.5) is made and incubated for 30 minutes at 60°C. Once done, the lead aspartic acid solution is incubated with the cells at 60°C for 30 minutes. Following this final metal treatment and washing in ddH_2O three times for 15 minutes, the cell monolayer undergoes a series of solvent exchange steps as outlined in the proceeding portion of this section. Solvent exchanges involve going from 100%wt ddH_2O to 100% ethanol. The cover slip, containing the cell monolayer, is separated from the plastic maktek dish. Once separated, the cells are exchanged into 100%wt acetone. Once in 100%wt acetone, a gradient is set up to eventually exchange out all the acetone for 100% epoxy resin. Once fully exchanged, and the cells fully embedded in the epoxy resin, the resin treated at 60°C for 24-72 hours.

For tissue samples, which are usually thin sectioned to 100 micrometer slices by a vibratome, the tissue is fixed in 2%wt paraformaldehyde, 2mM calcium

chloride and 5%wt glutaraldehyde. The tissue is washed for 1 hour in 0.30M cacodylate buffer containing 2mM calcium chloride. Afterwards, the tissue slices are incubated in a 0.15M cacodylate buffer solution containing 15%wt potassium ferrocyanide, 15%wt calcium chloride and 2%wt osmium tetroxide for 1 hour and agitated every 10 minutes. This is the first heavy metal staining reaction. Meanwhile, a 10%wt solution of thiocarbohydrazide (TCH) is prepared incubated at 60°C for 1 hour. Once an hour has passed for first the heavy metal staining, the tissue slices are washed in double distilled water three times for 15 minutes. Tissue slices are treated in the filtered TCH solution for 20 minutes. Once done, the tissue slices are washed in double distilled water and incubated once more in 2%wt osmium tetroxide for 30 minutes. The tissue slices are washed once more in double distilled water and incubated overnight in 1%wt uranyl acetate at 4°C. The following day, tissue slices are washed in double distilled water (ddH_2O) three times for 15 minutes.

Meanwhile, an aqueous solution containing 6.6%wt lead nitrate in 0.25M aspartic acid (pH 5.5) is made and incubated for 30 minutes at 60°C. Once done, the lead aspartic acid solution is incubated with the tissue slices at 60°C for 30 minutes. Following this final metal treatment and washing in ddH_2O three times for 15 minutes, the tissue slices undergo a series of solvent exchange steps as outlined in the proceeding portion of this section. Solvent exchanges involve going from 100%wt ddH_2O to 100%wt ethanol.

Figure 2.3., Heavy metal staining of tissue and cells dissipates charge collection from incident beam. Using the 3View heavy metal staining protocol, tissue and cells are stained with osmium, lead and other heavy metals. However, in areas where there is no tissue or cells (just resin), the area collects large amounts of charge, which can lead to issues in contrast and resolution. Especially the case with SBEM, distortions in the incident raster beam lead to distortions in the image slice, making alignments and three dimensional stacking processes difficult to achieve.

Mouse Kidney - Bowman's Capsule (SBFSEM)

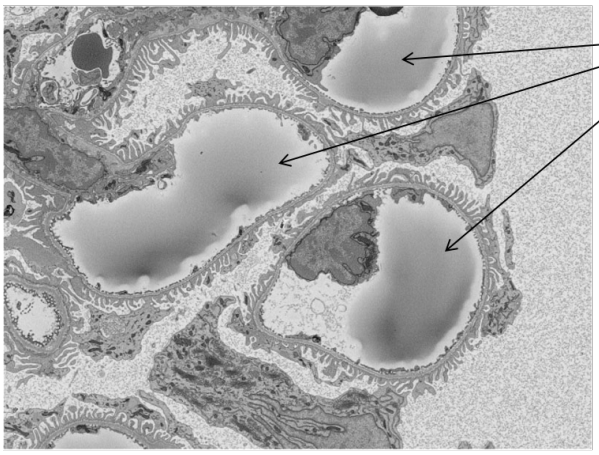

Image courtesy Tom Deerinck

Areas where charge is being collected by the lack of charge dissipation

Mouse Brain – Cortex volume (SBFSEM)

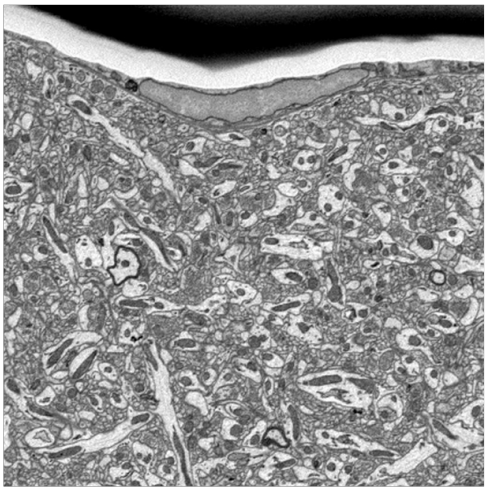

Movie courtesy Eric Bushong

Fixation of cells and tissue, followed by the series of heavy metal staining that is carried out are meant to not only provide contrast and resolution under BSE detection but make the biological specimen conductive, reducing any potential charging effects. As a result, biological specimens like brain slices from *mus musculus* (mouse), where there is a denser area for metal staining, undergoes reduced charging except where are blood vessels and capillaries. As shown above in Figure 2.3., areas where there are no heavy metals are susceptible to charging as these areas are not grounded to the specimen stage. As a result, biological specimens like mouse kidney, or lung, have major issues with charging. Cell monolayers are not even able to be imaged under high vacuum, so variable pressure SBEM is commonly used for these samples. Other metal staining methods incorporate the use of staining a gelatin, or BSA, matrix, which is used to fill the open areas in tissue, or cell monolayer. The implementation and combination of osmium staining with matrix scaffolds will be discussed in detail in proceeding portions of this section.

2.2.3. Multi-walled Carbon Nanotubes as Dopants in the Epoxy resin

Incorporation of an already known conductive material was the first step valuing the promise of this project. Little interest at this point was in seeing the viability of this approach in biological systems. Multi-walled carbon nanotubes (MWCNTs) were immediately identified as conductive dopant materials for improving the resin conductivity.

During the embedding process for cell monolayers, incremental increases in ethanol concentration are completed when reaching a 100%wt concentration in ethanol. Removing the solvents and introducing the new solvent combination in three incremental washes completes each increment. The ethanol is exchanged out four times. A new gradient, using acetone is incorporated starting at 75%wt ethanol/25%wt acetone by an increasing acetone concentration. The acetone will react with the Maktek dish, so we separate the coverslip from the Maktek dish and place in a glass petri dish. Once the acetone reaches 100%wt in concentration, Durcupan resin is introduced at increasing concentration ratios to a decreasing acetone concentration. At 50%wt Durcupan resin, MWCNTs are introduced, at a given concentration. The resulting 100%wt resin, with MWCNTs, is exchanged out four times to remove any acetone. The final embedding step, which is 100%wt Durcupan resin in a given concentration of MWCNTs, is layer on the glass slide. The glass slide is sandwiched by two mold-release coated glass slides. The sandwiched glass slides containing the embedded cell monolayer are placed in the oven at 65-70°C to initiate the polymerization reaction. The resin polymerization takes 24-72 hours to complete.

During the embedding process for tissue, incremental increases in ethanol concentration are completed at a 100%wt concentration of ethanol. The ethanol is exchanged out four times. A new gradient, using acetone is incorporated starting at 75%wt ethanol/25%wt acetone. Make sure that the tissue is not in a container that will react with the acetone. Eventually, the acetone concentration reaches 100%wt after increasing by 25%wt increments. The 100%wt acetone

concentration is exchanged out four times. After this process is completed, a starting concentration of 75%wt acetone/25%wt Durcupan resin is introduced to the tissue slice. At the 50%wt acetone/50%wt Durcupan resin exchange step, the multi-walled carbon nanotubes are pre-blended into the acetone:resin mixture before introducing to the tissue slice. The pre-blending of MWCNTs was achieved by a combination of mechanical stirring and ultrasonication at 10°C to avoid any potential initiation of the resin polymerization. Depending on the concentration, other mixing techniques such as milling were utilized. The preblended concentration of the MWCNTs was maintained during every solvent exchange step until the tissue was embedded in 100%wt Durcupan resin/MWCNTs. The resin/MWCNT mix was exchanged out several times to remove any acetone. The final tissue embedded in 100%wt Durcupan resin, with MWCNTs at a given concentration, was placed sandwiched by two mold release coated glass slides. The glass slides containing the embedded tissue sample was placed in the oven to initiate the polymerization reaction. The resin polymerization takes 24 to 72 hours to complete.

Depending on the concentration of MWCNTs, a low viscosity epoxy resin is incorporated into the embedding ratios to assist in the blending process. At concentrations of MWCNTs exceeding 4%wt, Durcupan concentration is reduced to 50% of whatever the concentration of the low viscosity resin (Spurrs resin). So, at 50%wt acetone, there is a 1:1 ratio Durcupan:Spurrs resin combination to lower the viscosity during blending. The resulting 1:1 concentration of resins is

maintained and even polymerized, as the concentration (>4%wt) of MWCNTs cannot blend into 100%wt Durcupan.

Figure 2.4., Multi-walled carbon nanotubes are reducing charging in epoxy resin, however, are difficult to disperse. Collection of a three dimensional volume using SBEM of *mus musculus* brain tissue is carried out. The sample has been embedded in multi-walled carbon nanotube doped resin at 2.0%wt. A ROI is selected and imaged by detection of both secondary electrons and backscatter electrons. Images are collected at areas above and at the tissue. A volume is collected of the brain tissue.

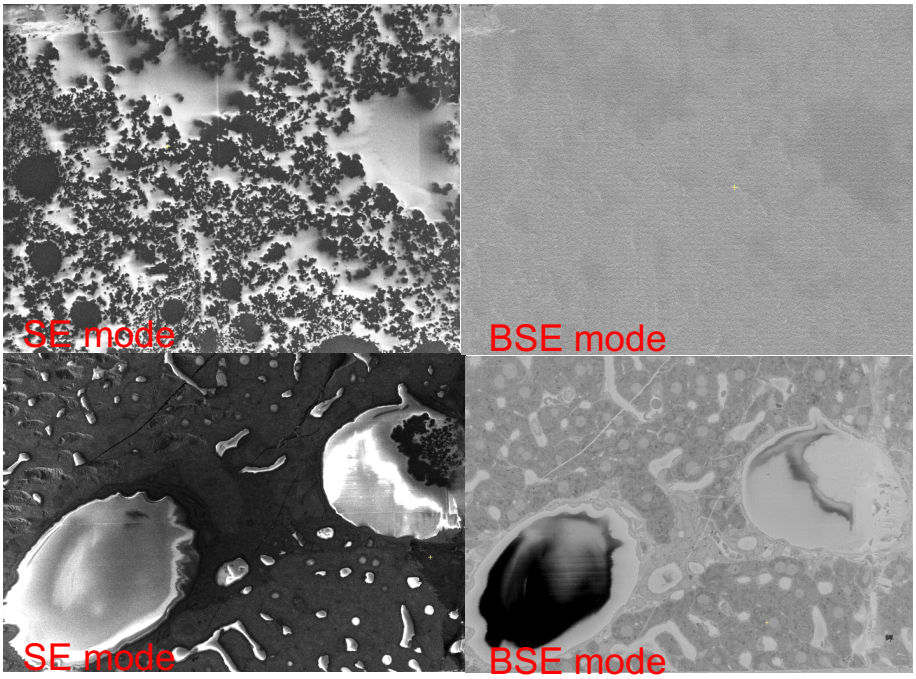

Resin (No Tissue)

Tissue

Even though concentrations as high as 4%wt MWCNTs was tested for charge reduction under SBEM, charge reduction was achievable at 2%wt MWCNTs, as shown in Figure 2.4. In cases where there is free resin, MWCNTs is detectable by secondary electron mode. Islands of knotted black balls are the MWCNTs. Where there is a knotted up ball of MWCNTs, there is no charging detected in by the backscatter electron (BSED). These knotted black balls of MWCNTs become a problem when the block face is sectioned down to the tissue. In tissue, a lack of MWCNTs in the capillary leads to charging. Whereas, knotted black balls of MWCNTs made it into the other capillary and eliminated the charging by grounding the area to the metal specimen stub.

2.2.4. Corannulene as a Dopant in the Epoxy Resin

Knotted black balls of MWCNTs were too large to make into capillaries and vessels. To address the size of MWCNTs while still using large sp^2 hybridized carbon networks, or multi-cyclic aromatic structures, corannulene was proposed as a candidate for replacing the MWCNTs as a conductive dopant for epoxy resins. This section details the incorporation of corannulene into our epoxy resins.

During the embedding process for cell monolayers, incremental increases in ethanol concentration are completed when reaching a 100%wt concentration in ethanol. Removing the solvents and introducing the new solvent combination in three incremental washes completes each increment. The ethanol is exchanged out four times. A new gradient, using acetone is incorporated starting at 75%wt ethanol/25%wt acetone by an increasing acetone concentration. The acetone will

react with the Maktek dish, so we separate the coverslip from the Maktek dish and place in a glass petri dish. Once the acetone reaches 100%wt in concentration, Durcupan resin is introduced at increasing concentration ratios to a decreasing acetone concentration. At 50%wt Durcupan resin, corannulene is introduced, at a given concentration. The resulting 100%wt resin, with corannulene, is exchanged out four times to remove any acetone. The final embedding step, which is 100%wt Durcupan resin in a given concentration of corannulene, is layered on the glass slide. The glass slide is sandwiched by two mold-release coated glass slides. The sandwiched glass slides containing the embedded cell monolayer are placed in the oven at 65-70°C to initiate the polymerization reaction. The resin polymerization takes 24-72 hours to complete.

During the embedding process for tissue, incremental increases in ethanol concentration are completed at a 100%wt concentration of ethanol. The ethanol is exchanged out four times. A new gradient, using acetone is incorporated starting at 75%wt ethanol/25%wt acetone. Make sure that the tissue is not in a container that will react with the acetone. Eventually, the acetone concentration reaches 100%wt after increasing by 25%wt increments. The 100%wt acetone concentration is exchanged out four times. After this process is completed, a starting concentration of 75%wt acetone/25%wt Durcupan resin is introduced to the tissue slice. At the 50%wt acetone/50%wt Durcupan resin exchange step, the multi-walled carbon nanotubes are pre-blended into the acetone:resin mixture before introducing to the tissue slice. The pre-blending of corannulene was achieved by a combination of mechanical stirring and ultrasonication at 10°C to

avoid any potential initiation of the resin polymerization. Depending on the concentration, other mixing techniques such as milling were utilized. The pre-blended concentration of the corannulene was maintained during every solvent exchange step until the tissue was embedded in 100%wt Durcupan resin/corannulene. The resin/corannulene mix was exchanged out four times to remove any acetone. The final tissue embedded in 100%wt Durcupan resin, with corannulene at a given concentration, was placed sandwiched by two mold release coated glass slides. The glass slides containing the embedded tissue sample was placed in the oven to initiate the polymerization reaction. The resin polymerization takes 24-72 hours to complete.

Depending on the concentration of corannulene, a low viscosity epoxy resin is incorporated into the embedding ratios to assist in the blending process. At concentrations of corannulene exceeding 10%wt, Durcupan concentration is reduced to 50% of whatever the concentration of the low viscosity resin (Spurrs resin). So, at 50%wt acetone, there is a 1:1 ratio Durcupan:Spurrs resin combination to lower the viscosity during blending. The resulting 1:1 concentration of resins is maintained and even polymerized, as the concentration (>10%wt) of corannulene cannot blend into 100%wt Durcupan.

At low concentrations (5%wt) of corannulene, pre-blending was achievable with mechanical stirring. Thin sections of resin with corannulene dopant did not have any places of aggregated corannulene at concentrations lower than 10%wt. The aggregation of corannulene was a large factor in not completely understanding its conductive properties. For analytical purposes, corannulene concentration had

to be controlled. To achieve this feat, corannulene would need to be incorporated into the resin structure.

2.2.5. Corannulene modified for covalent incorporation into the epoxy resin

To eliminate aggregation of corannulene and effectively distribute the multi-cyclic aromatic structure throughout the resin, a method for covalent incorporation into the epoxy resin was worked out and executed. Before covalent incorporation into the epoxy polymer is achieved, corannulene needs to be modified with epoxy functionality by synthetic organic techniques. This section will describe the synthesis of a modified corannulene with epoxy functionality.

Before the synthesis of epoxy modified corannulene can begin, 1 mole of 9-hydroxynonanoic acid is treated in 2 moles of ($SOCl_2$) in pyridine. The crude product is exchanged into dichloromethane and purified by flash column chromatography, and the fractions are checked by thin layer chromotagraphy (TLC). To a round bottom flask, 1 mole of aluminum chloride is added to 0.50 moles of 10-chlorononanoyl chloride and 0.50 moles of corannulene and refluxed at 100°C for 1 hour. The crude is filtered and recrystallized into concentrated into 50%wt methanol and 2 molar potassium hydroxide. The resulting product is filtered and solubilized into 80%wt methanol and 2 molar potassium hydroxide with 1 mole of hydrazine at 100°C for 4 hours. The crude is washed with dichloromethane twice, where the product exchanges into the organic layer. Once done, 1 mole of 2-(bromomethyl)oxirane is combined with the two washes of alcohol modified corannulene in dichloromethane. The reaction takes 4 hours to

complete under room temperature. Any excess reactants from the reaction are separated by a flash column (1:10, ethylacetate:dichloromethane), and the fractions are checked by TLC. H^1 Nuclear Magnetic Resonance and electrospray ionization mass spectroscopy (ESI-MS) was utilized to confirm the structure. Once confirmed, dichloromethane was evaporated off, leaving the purified compound.

Following synthesis of corannulene modified linker, now known as component **E**, component **B** is recalculated to one of three mole ratios of component **E**. The entire volume is scaled down by 10 fold to account for the low yielding component **E**. To a single batch, the mole ratio of **A**:**D**:**E** was varied by 3:2:X, where X = 2, 3, and 6.

2.2.6. Protein/Gelatin Matrix as scaffolds for coordinating transition metals

To build on corannulene and introduce higher permitvity for the resins, a gelatin, or protein matrix, is utilized as a scaffold for coordinating transition metals, such as iron (Fe), and more osmium. This section will lay out the method for making these protein/gelatin matrixes as for further enhancing the conductivity of these polymeric resins.

2.2.6.1. BSA as a scaffold for coordinating transition metals

To a 1.5 mL centrifuge tube, aliquot 0.8 mL of 1X phosphate buffer solution (PBS). Carefully place 0.1 g BSA powder on top of the buffer, and spin down the 1.5 mL centrifuge tube for about 5 minutes. BSA should solubilize into the 1X PBS. Do not stir, shake, or vortex the tube. Repeat the adding of BSA three more times

for a total of 0.4 g BSA. You may need to gently stir in any BSA that is left stuck to sides of tube afterwards.

Meanwhile, fix cells with 2.5% glutaraldehyde in 1X PBS for 20 minutes. Rinse cells twice with 1X PBS for 10 minutes. Add 500 uL iron-dextran (Fe(dex)) (100 mg/mL solution from Sigma) to 500 uL BSA solution. Vortex briefly and spin down briefly. Remove the 1X PBS from the cells and wash the cells with ddH_2O three times 15 minutes. Add 70 uL 2.5% glutaraldehyde to the BSA-Fe(dex) solution. Immediately vortex for 1 sec and aliquot thin layer onto cells. Glutaraldehyde should begin crosslinking and hardening the BSA-Fe(dex) matrix. Once hardened, add cold 2.5% glutaraldehyde in 0.3M cacodylate buffer to the cells and allow to sit for at least 30 minutes on ice. Wash the cells briefly in 0.3M cacodylate buffer a few times with buffer. Following this step, process the matrix embedded cell monolayers by the osmium heavy staining protocol described in Section 2.2.2. Following heavy metal staining, the matrix is dehydrated, water to ethanol to acetone, and embedded in the epoxy modified corannulene resin and polymerized for 24-72 hours at 60°C, as described in Section 2.2.2.

2.2.6.2. Gelatin as a scaffold for coordinating transition metals

Hela cells are grown on sterilized Aclar film treated with poly-d-lysine. Cell monlayers are fixed 2%wt glutaraldehyde with 3mM CaCl2 in 100mM sodium cacodylate for 60 minutes. Following this, cell monolayers are rinsed five times for 10 minutes in 100mM cold cacodylate buffer. The cell monolayers are blocked for 5 minutes with 20mM glycine in cold cacodylate buffer. Cells are reacted with

diaminobenzadine (DAB) with 0.03%wt hydrogen peroxide (H_2O_2) for 5 minutes (APEX2-KDEL or H2B). Once done, the cell monolayers are washed six times for 2 minutes in cold cacodylate buffer. Cells are brought to room temperature. A freshly prepared solution of 10%wt gelatin with 0.5%wt tannic acid (LMW EM grade) and 1%wt (10mg/ml) iron dextran (Fe(dex)) in 100mM cacodylate buffer, at 50°C, is added on top of the cells to form a thin layer. The cell monolayers are incubated on ice for 1 minute. A cold primary fixative is added to the thin layer for 20 minutes. The matrix embedded cell monolayers are rinsed six times for 2 minutes in cold cacodylate buffer. Following this step, process the matrix embedded cell monolayers by the osmium heavy staining protocol described in Section 2.2.2. Following heavy metal staining, the matrix is dehydrated, water to ethanol to acetone, and embedded in the epoxy modified corannulene resin and polymerized for 24-72 hours at 60°C, as described in Section 2.2.2.

2.2.7. Serial Block-face Imaging

SBEM data was collected with a 3View unit (Gatan, Inc., Pleasanton, CA, USA) installed on a Merlin field emission SEM (Carl Zeiss Microscopy, Jena, Germany). The retinal volume was collected at 2.0keV accelerating voltage, with a raster size of 19k x 39k and pixel dwell time of 0.5sec. The pixel size was 5.7 nm and section thickness was 70 nm. The astrocyte volume was collected at 2.0 keV, with a raster of 20k x 20k and pixel dwell time of 1.0sec. The pixel size was 4.5nm and section thickness was 90 nm.

2.3. Discussion

Considering the methods and materials provided, this section of this chapter aims to address and discuss the use of the techniques and methods accomplished and their viability for eliminating charging in biological specimens. Also introduced, binary and relative analytical techniques novel in use to the field will also be addressed. From this section, this dissertation aims to lay out specific conclusions and achievements in the area of charge reduction, leading to enhanced contrast and resolution, for serial block-face scanning electron microscopy.

2.3.1. Edge function analysis is a quantitative tool for assessing specimen charging

When measuring the conductivity of the resin under scanning electron microscopy (SEM), one could evaluate charging as a proportional relational measure of conductivity. Resin charging is associated with collection of electrons on the surface of the sample. When the electrons are dissipating from the surface of the sample as fast as they are being collected, the sample is conductive. For epoxy resins, this is a major issue as charge collects on the surface and rarely dissipates. In cases where the epoxy resins are thick (>100 microns) and imaged over long iterative periods of time, this can be an even greater issue as the charge collection may damage the resin and potentially the sample ultrastructure, effecting the sectioning of the material over time. In assessing resin charging, no direct measurement has been developed to relate charging to conductivity quantitatively.

Most measures of charging and conductivity are qualitative, meaning that they are relative to the parameters of the instrument.

In initially addressing specimen conductivity through charging quantitatively, we measure the mean pixel intensity along surface of SEM images collected in Figure 2.5.a. Samples are subjected to a limited and consistent beam dose at 10k times magnification. Following exposure, the magnification is adjusted to 5k times magnification, and an image is collected. When the sample is conductive, as shown in the two left SEM image panels, there is no difference in pixel intensity. When the difference in pixel intensity is graphed for every line crossing perpendicular to the white box, averaged and normalized, the resulting average difference in pixel intensity is a step-function. As a result, when the sample is not conductive, as shown in the two right image panels, there is a significant difference in pixel intensity.

The pixel intensity can vary from line to line along the “box edge” drawn in figure 1a. So, all the pixel intensities are collected along the “box edge” and averaged. The resulting average value is irrelevant just as long as the average is a significant difference from zero average height. Hence, this method yields a binary answer. The data generated via this measuring tool depends on a consistently accurate pressurized environment. The beam current needs to be consistent. The specimen to raster beam working distance needs to be consistent. The brightness and contrast knobs have to be consistent. And, the timing of adjustments in magnification has to be automated. Hence, it is only possible to

infer a yes, or no, answer to understanding sample conductivity through charging via edge function analysis.

Figure 2.5., Calculating the relative difference in mean pixel intensity as a function of specimen charging is a quantitative measure for assessing potential conductive resins. In (a.), pixel intensity is plotted across the edge of a box to provide the step function. The difference in pixel intensity varies along the box; so all lines were sorted and averaged (shown in b.) to plot mean pixel intensity and solve for the average height, H_{av}. While all specimens were exposed to the raster beam, the number of scans and specimen dose was monitored to make sure all measurements were relatable (as shown in c.).

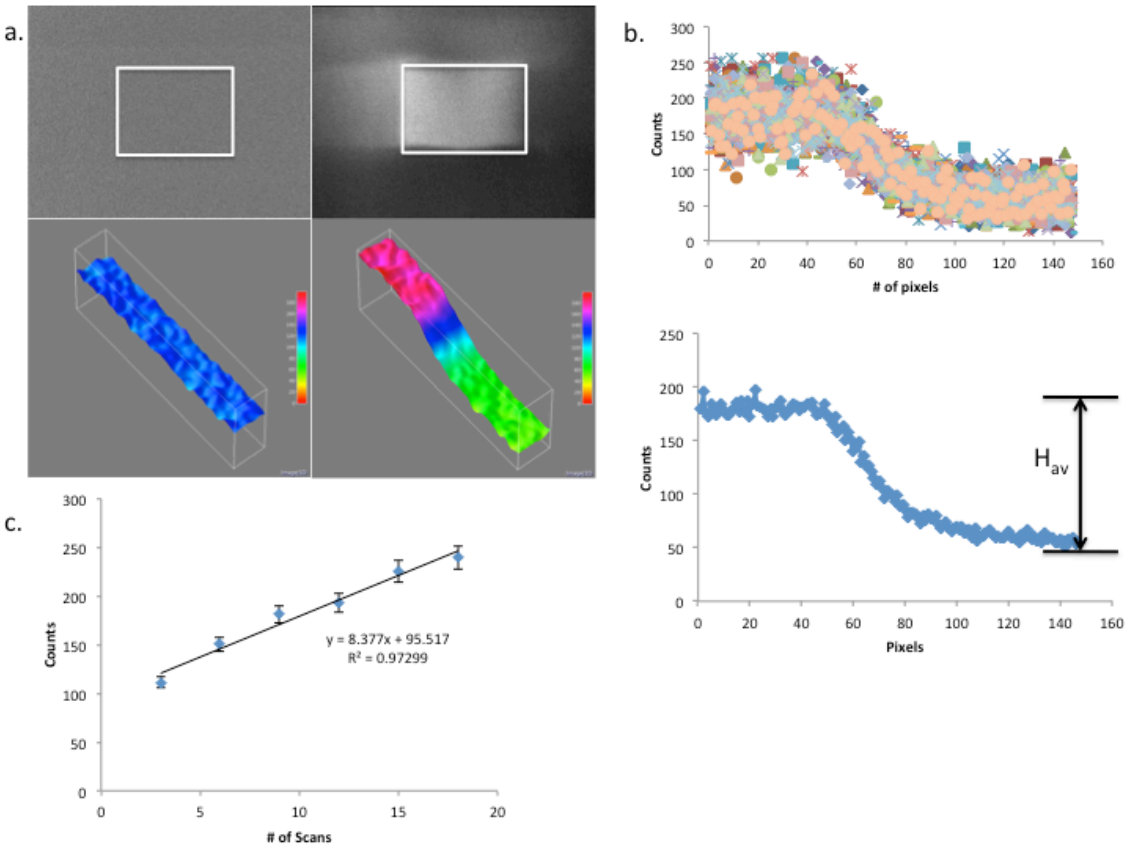
a.
b.
Counts
# of pixels
Pixels
H_{av}
c.
Counts
# of Scans
y = 8.377x + 95.517
R² = 0.97299

All samples are exposed to the same beam dose while not saturating the detector and causing potential false negatives for this technique. This measurement was taken for every sample before beginning the experiment. This measurement also assisted the normalization process when comparing specimens that varied by 0.01 microns in working distance from the raster beam, and/or varied slightly in beam current. The number of scans was then determined by the lowest possible threshold of signal. If a higher number of scans was selected, the threshold would be too high to measure the presence of charging.

The step-function value is valuable in screening all possible candidate materials for improving conductivity of the resin. As shown in Table 1.1., various candidates of materials, known to be conductive or useful in electron transfer, were tested against a positive and negative control. The negative control was epoxy resin, without any conductive dopants. The positive control was epoxy resin, that is doped with MWCNTs, as an ideal conductor for these resins. Knowing not only candidates but conditions for the material are major parameters for measuring and quantifying the charging amongst all the samples. As a result, methods aimed at quantifying degrees of charging are developed and utilized to further assess materials incorporated into the resin.

Table 1.1., Approaches taken to address sample charging and their relative outcomes. Various candidates of dopants and a conjugate were tested by three separate scanning electron microscopes. The data generated using edge function analysis was compared used to assess the best possible conditions for the dopant. EDS-SEM was then used to assess the relative charging between each dopant and/or conjugate. All candidates were confirmed for potential enhancements, or failure, by SBEM.

MATERIAL/ ROUTE	CHARGING THRESHOLD	CONCENTRATIONS TESTED
MWCNTS	2.0keV at 2%wt	0.5,1.0, 1.5, 2.0, 2.5, 3.0, 3.5, 4.0, … 20.0%wt
CORRANULENE	1.3-1.8keV at 10%wt	5, 10, 15, 20%wt
CORRANULENE (EPOXY CONJUGATE)	1.8keV at o = 6	o = 2, 3, 6, 9
PERYLENE DIANHYDRIDE	Failed	10, 20%wt
CORRANULENE (-CF3)	1.3-1.8keV at 10%wt	10%wt
CORRANULENE (-DIESTER)	1.3-1.8keV at 10%wt	10%wt
HEMOGLOBIN	Failed	10, 20%wt
IRON (GELATIN)	1.4keV at 20%wt	10, 20%wt
IRON (BSA)	1.5-1.8keV at 50%wt	10, 20, 50%wt

2.3.2. Energy-Dispersive X-ray Spectroscopy and evaluating the Duane-Hunt limit

As mentioned earlier, edge function analysis only provides a binary assessment for studying sample conductivity through determining whether a material is charging, or not. In order to compare degrees of conductivity while imaging the epoxy resin, there had to be a way to quantify the current in a sample. This measurement could be done via electron beam-induced current. The issue with this assessment is that the epoxy resin had to be of a set volumne and shape for every measurement. Also important, the biological specimen in question has to provide a consistent geometric motif to avoid differences in measure current per area. To overcome these issues, energy-dispersive x-ray spectroscopy scanning

electron microscopy (EDS SEM) was used to get closer at quantitating the permittivity of these samples without having to loose flexibility in the use of biological specimen or dimensions of the epoxy resin block.

Energy dispersive spectroscopy on a scanning electron microscope measures x-rays emitted from a sample. These x-rays are generated by the excitation and emission of k-shell electron on the surface of the sample. So, when 10keV of accelerating voltage is delivered to the sample, it is expected (for a conductive sample) for 10keV of x-ray energy to return back to the EDS detector. When a sample is non-conductive, or semi-conductive, the returning x-ray energy is less. As a result, the spectral readout demonstrates a drop off in x-ray energy.

Mathematically, EDS SEM can be used to address charging by quantifying the drop off in emitting x-ray energy. In order to quantitatively measure degrees of charging, we take the limit of the energy curve as it approaches zero on the y-axis. This is known as the Duane-Hunt limit, in which the drop off in emitted x-ray photons is directly proportional to degrees of charging. From differences in x-ray photon emission drop off, one can relate to charging of sample surfaces, and profile materials at differing conditions for optimization. As a shown in Figure 2.6.b, when the beam energy is set to 20keV, the measured x-ray photon energy should be 20keV, however, the signal (y-axis, x-ray signal) approaches zero as the beam energy approaches 10keV.

If the signal reaches zero before 20keV, the sample is charging. When comparing the negative control (neg) to the two concentrations of MWCNTs in resin, the MWCNT signals are closer to approaching zero at 10keV than the

negative control. The negative control has no conductive material and is just resin. So, just as edge function analysis has shown MWCNTs to eliminate charging, EDS SEM data has shown charge dissipation significantly improved compared to the negative control, as shown in figure 2.6.b. When studying the charging properties visually by SBEM, wherever there were MWCNTs, charging was eliminated. As a result, the positive control has MWCNTs doped at 4%wt. Cell monolayer/tissue studies with MWCNTs, and other conductive additives, have been tested by this technique.

Figure 2.6., Energy-dispersive x-ray spectroscopy scanning electron microscopy (EDS SEM) is a technique useful in measuring relative degrees of charging between samples, as shown in (a.). To confirm results generated from edge function analysis, MWCNTs in epoxy resin were measured by EDS SEM, as plotted in (b.).

a.

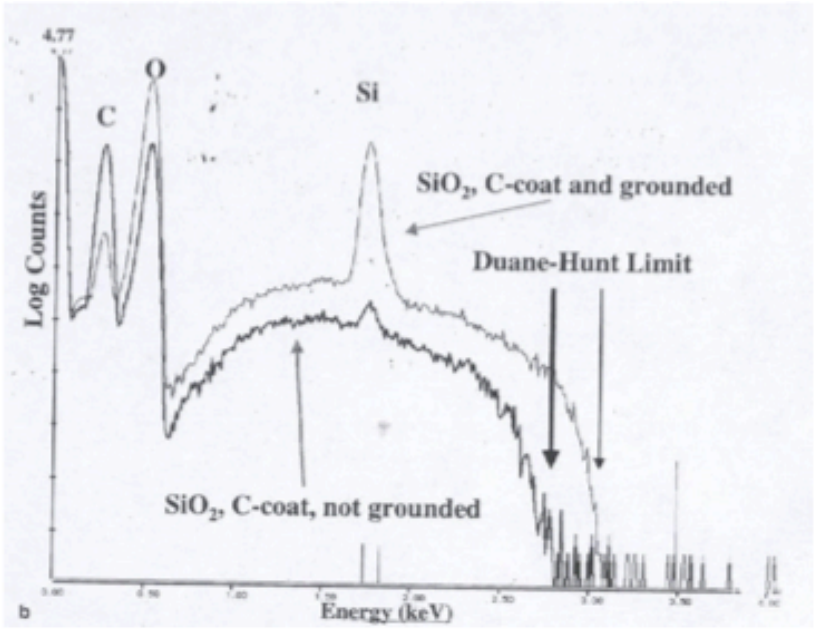
4.77
C
O
Si
SiO_2, C-coat and grounded
Duane-Hunt Limit
Log Counts
SiO_2, C-coat, not grounded
Energy (keV)
b

b.

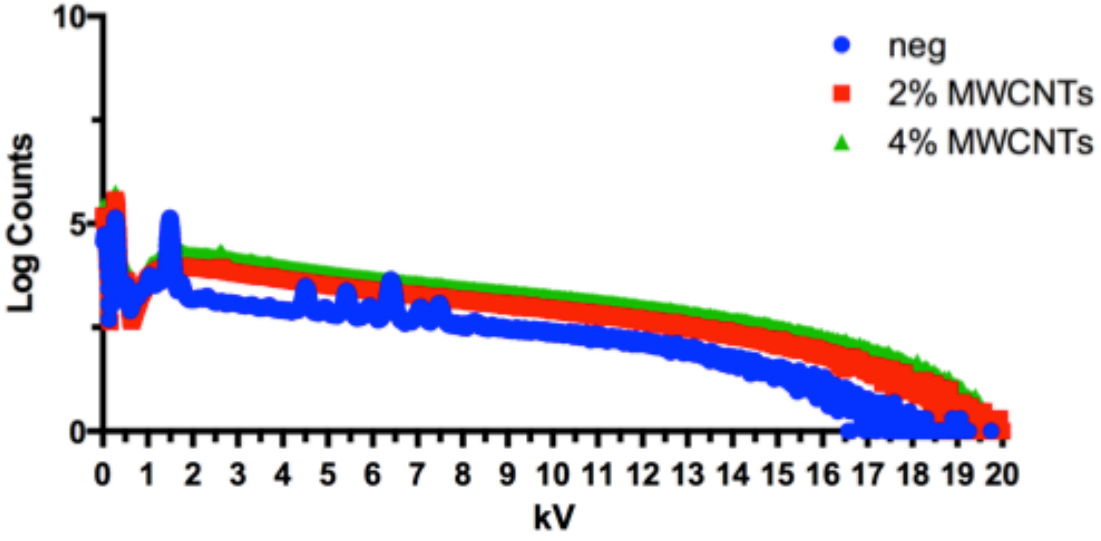
neg
2% MWCNTs
4% MWCNTs
Log Counts
10
5
0
0 1 2 3 4 5 6 7 8 9 10 11 12 13 14 15 16 17 18 19 20
kV

2.3.3. Doping MWCNTs into the epoxy resin

The most robust method in eliminating charging has been using multi-walled carbon nanotubes (MWCNTs). As long as MWCNTs are in the region of interest (ROI), there is no charging in that area. Edge function analysis and EDS SEM experiments utilized MWCNTs as a positive control after extensive experimentation regarding the appropriate parameters for preparing and blending MWCNTs into the resin. From a 2%wt MWCNT concentration in epoxy resin, for both tissue and cells, charge dissipation is immediate up to 1.8keV, as shown in Figure 2.5., by edge function analysis. MWCNTs were postulated as potential charge dissipaters due to their widely known conductive properties (reference). The choice in selecting multi-walled over single-walled nanotubes was mainly due to taking advantage of the highly dense sp^2-hybridized orbital composition, in which unhydridized p_z-orbitals are overlapping one another stabilizing one another by this overlapping nature (reference). Concentrations were prepared as high as 20%wt MWCNTs in the epoxy resins, as described in table 1.1. Mixing was not optimal at any MWCNT concentration in the epoxy resin.

The issue in using carbon nanotubes is that this material poorly disperses in resin. It is especially a problem in porous tissue samples where there is a chance no carbon nanotubes are present in highly vascularized regions, blood vessels and especially in capillaries. Shown in Figure 2.4., brain tissue has been embedded in a 2%wt MWCNT resin and imaged by our serial block scanning electron microscope (SBEM). A thin layer (10 microns) of resin on top of the slice of brain tissue is imaged in both the secondary electron channel and backscatter

electron channel. The secondary electron channel reveals that the presence of MWCNTs, as they are the black knotted balls. MWCNT dispersion has been very consistent, as these nanotubes tend to “knot up” into balls. The sizes of these balls range from 500 nanometers to 5 micrometers. The backscatter electron channel is the standard channel used for the SBEM system. Also, the heavy metal stains used in providing contrast to the specimen can be imaged in this channel. Charging is generally associated with darker regions in these images. In the top right image panel in Figure 2.4., these darkened areas are where there are no MWCNTs, demonstrating that MWCNTs are withdrawing charge from the corresponding resin ROI.

When sectioning down to the brain tissue and imaging in both channels, MWCNTs are present where there is no resin charging. Hence, MWCNTs are ideal materials for dissipating electrons and making the epoxy resins conductive. Studies in cell monolayers yielded similar issues in getting the MWCNTs dispersed in the resin. Another issue with MWCNTs was the ability to see the sample in preparation for SBEM. The doped MWCNTs made the resin black and opaque, unable to see a tissue by another light microscope before cutting and mounting the area. With advances in correlated microscopy and the introduction of x-ray microscopy as novel multimodal imaging platform for biological and chemically driven projects, a sample prepared with doped MWCNTs can be scanned by x-ray tomography and an ROI can be selected before placing the sample into the SBEM. As a result, once ways in dispersing this material can be solved, such as

functionalized epoxy MWCNT derivatives, this would be the most optimal way to making the epoxy resin conductive for SBEM.

2.3.4. Doping corannulene and other polyaromatic derivatives

Since MWCNTs were effective in eliminating charge, but not effective in dispersion, the focus on use of nanomaterials as conductive dopants switched to smaller polyaromatic systems. In particular, the use of corannulene, and other polyaromatic derivatives, as conductive dopants in porous tissue and cell monolayers have problems in dispersing into the epoxy resin. In using EDS SEM (Figure 2.7. a and b), significant charge reduction was noted in certain areas and poor charge dissipation in other areas of a sample doped with corannulene. Upon deeper investigation by taking an 80nm thin section and viewing the same areas by TEM, conducting areas had accumulated agglomerations of corannulene, whereas, non-conducting areas had no accumulated amounts of corannulene. Imaging of these areas by SBEM testing concluded that the EDS SEM data was accurate in assessing the varying degrees of charging. Eventually, the n-value of EDS SEM testing couple with SBEM data started to show large variability in optimized charge dissipation for corannulene. So, a continuation of agglomerations is leading to a continued problem in uniformed conductivity in the epoxy resin material.

Corannulene is a polyaromatic structure with 5-fold rotational symmetry. The structure is chosen as a candidate for improving the conductivity of the epoxy resin due its similarity in being an sp^2 hybridized network of carbons with

unhybridized p_z orbitals for potential overlap with other corannulene structures in the resin, if in close proximity ($1/r^2$). Concentrations of corannulene, above 10%wt, have marginal improvement in conducting, as shown by Figure 2.7. Also important, variations in EDS spectral data collected by area for a given sample improved for epoxy resin samples at, or above, 10%wt concentration in corannulene. From this data, we can infer that we are reaching a saturation limit in doped corannulene.

However, randomization of corannulene at varied concentrations is still a real problem and associated with poor dispersion. Also important, doped corannulene at, or above, 10%wt requires various combinations of mixing and blending (ultrasonciation, mechanical stirring, blending with spurs resin) usually leaving bubbles in the resin, which are hard to remove in later embedding steps. On a molecular level, it would be ideal to control the distances in corannulene interaction. To solve this and the blending issue, corannulene is prepared as a monomer for covalent incorporation into the epoxy polymer structure.

Figure 2.7., Evaluating charging in corannulene doped tissue samples. SBEM of kidney tissue embedded in 10%wt Corannulene (a.). EDS SEM of serial dilutions of corannulene in resin demonstrates a trend charge reduction (b.).

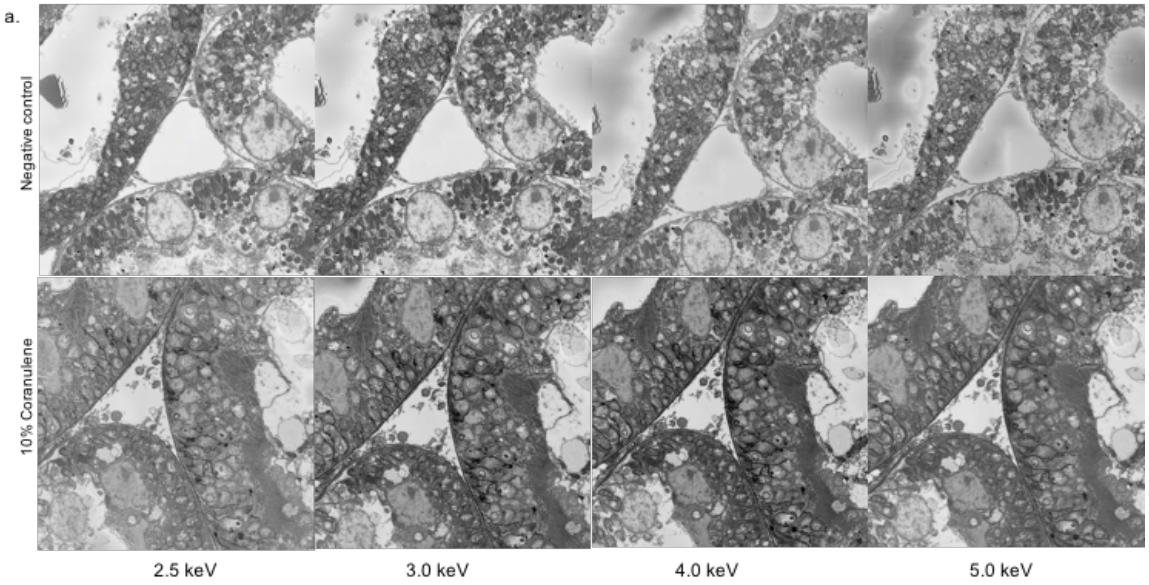
a.
Negative control
10% Coranulene
2.5 keV
3.0 keV
4.0 keV
5.0 keV

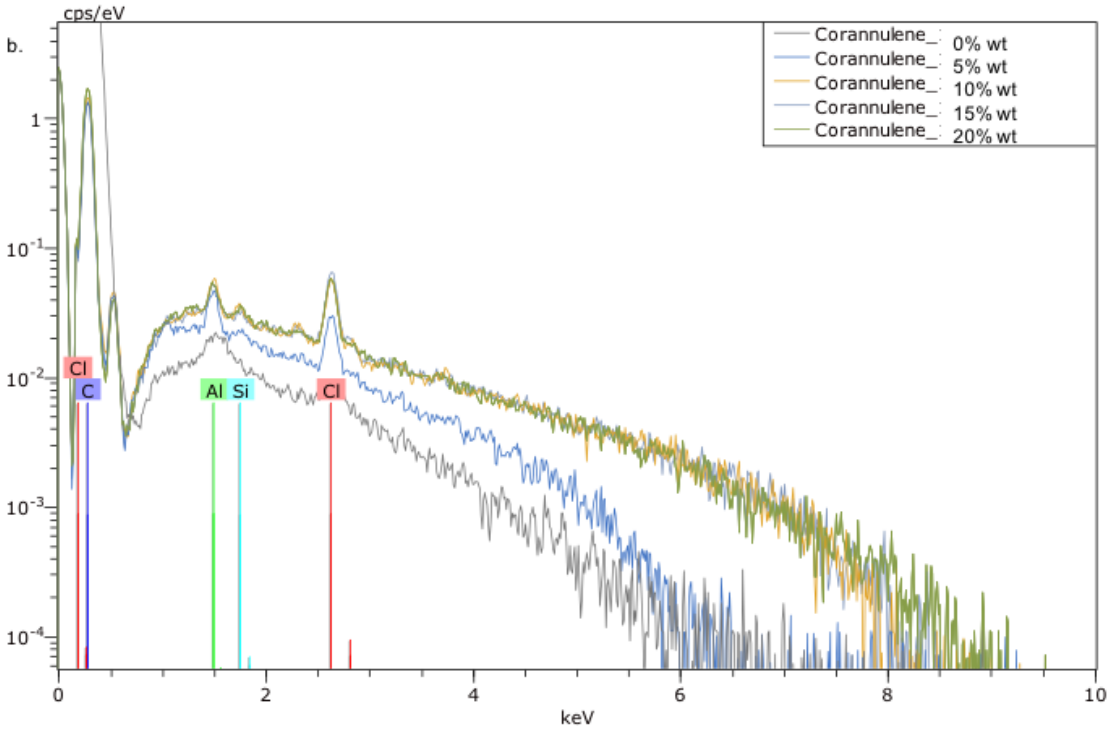
b.
cps/eV
Corannulene_ 0% wt
Corannulene_ 5% wt
Corannulene_ 10% wt
Corannulene_ 15% wt
Corannulene_ 20% wt
Cl
C
Al
Si
Cl
keV

Other polyaromatic derviatives have been investigated by edge function analysis and SBEM as potential improvements to the dispersion and conductivity of the resin. Polyaromatic derivatives such as perylene dianhydride have led to no improvements in charge dissipation. Corannulene $-CF_3$ and diester derivatives have led to no significant improvements in charge dissipation over corannulene. As a result, these approaches were immediately halted, and only considered to further support the successes of other approaches taken.

2.3.5. Conjugating epoxy-corannulene monomer to the resin

Corannulene as a subunit to the polymer structure yielded monodispersed charge dissipation by SBEM and EDS SEM, as shown in Figure 2.8. The corannulene epoxy monomer was characterized by electrospray ionization mass spectroscopy (ESI-MS) for the exact mass (448.24 m/z). The combination of unique hydrogens (H) on the polyaromatic ring, in combination with the sterically hundered hydrogens on the three-membered epoxy ring confirm the structure by H nuclear magnetic resonance spectroscopy. Further characterization by infrared spectroscopy yielded no carbonyl groups, or alcohol groups.

Covalent incorporation of corannulene into the polymer structure is depended on the synthesis of an epoxy corannulene monomer. The epoxy corannulene monomer is blended with the other components to yield a n:m:o molar ratio of 2:3:x, where x = 3 and 6. SBEM volume collection of a HeLa cell monolayer embedded in an o = 3 resin at 2.0keV in high vacuum (Figure 2.8.), yields partially improved charging. The key improvement is that the charging is monodispersed

throughout the resin, rather localized. In comparing to the volume in figure 5b, the degree of charging is greatly diminished.

Figure 2.8., EDS SEM (scatter plot) and SBEM of cell monolayers embedded in corannulene conjugated resin. For corannulene (dopant), two sites varied significantly in concentration, whereas, the conjugate is evenly dispersed throughout the resin. As a result, the corannulene conjugate yields enhanced conductivity for the resin. For the first time, cell monolayers can be imaged by SBEM.

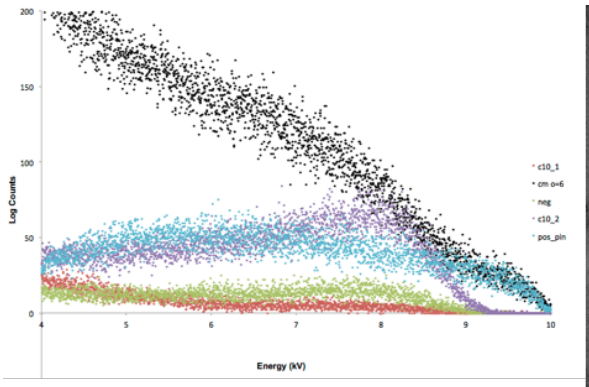
Log Counts
Energy (kV)
c10_1
cm o=6
neg
c10_2
pos_pin

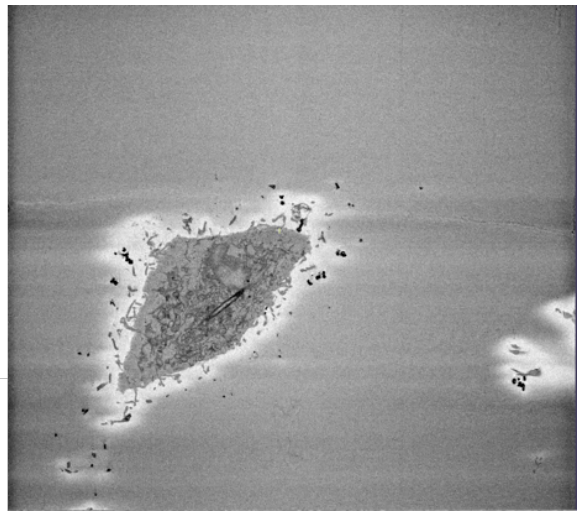

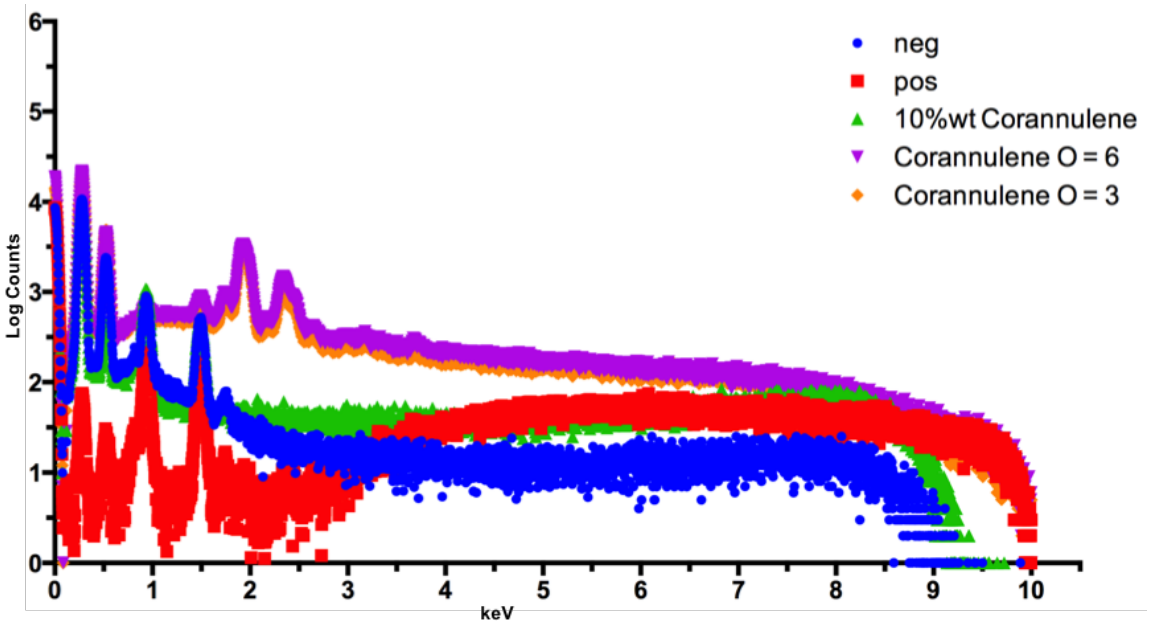
neg
pos
10%wt Corannulene
Corannulene O = 6
Corannulene O = 3
Log Counts
keV

By EDS SEM, higher concentration block polymers have been consistent with improved charge dissipation, as shown in Figure 2.8. The difference in drop off of x-ray photons was not significant between the o = 3 and 6 conjugates. However, the drop off was close to, if not similar to the positive control, which was the aluminum pin. Covalent incorporation of corannulene into the resin structure as a repeating block has yielded improved dispersion. Thin sections have yielded no agglomerations, while EDS SEM and SBEM data have yielded improved charge dissipation. Cell monolayers yielded improvements to charge dissipation, as shown in Figure 2.8. However, when the beam energy is increased to >2.2keV, the highest concentrated corannulene epoxy resin undergoes charging. Once the beam is blanked, meaning it is turned off, then imaged at lower energy (such that there is charge balance), the mean pixel intensity can be measured as a function of time. Pixel intensity, whether it be darker, or lighter, is directly proportional to charging. In following this measured decay in pixel intensity, a measured decay in charging can be calculated. This decay is indicative of an RC circuit decay. Only conductive, or partially conductive, materials undergo an RC decay. As a result, corannulene, as a subunit in the epoxy resin based polymeric structure is assisting in the elimination of charge from the surface of the resin. Nonetheless, there is a limit to this mechanism in handling the charge load.

Studies on the concentration of corannulene as a function of improved charge dissipation by EDS SEM has led to the use of an o = 6 molar ratio corannulene epoxy monomer, as this is the highest concentration achievable without compromising the bulk properties of the resin. Concentrations higher than

o = 6, such as 9, 12, and 15, all yielded poorly hardened resins. This is important to consider as the resin is the principle scaffold in ultra thin sectioning of the biological specimen. A polymerized resin, that has not hardened enough to accept the tensile force of the incident diamond knife will damage the knife. Also relevant, there will be inaccuracies in the section thickness as this is important in image reconstruction. All of the other components were scaled by molar mass appropriately to accommodate the increased concentration of corannulene in the epoxy resin.

2.3.6. Heavy metal stained gelatin matrix for cell monolayers

It was previously noted that when a mouse was not profuse properly, leaving blood in portions of tissue, veins and capillaries, these areas would not collect any charge (as shown in Figure 2.3. in Bowman's Capsule). So, to build on this information, we postulated the use of hemoglobin as this protein carries four iron heme porphyrins that could lend to improving conductivity in the resin. Characterization of cell monolayers with hemoglobin fixed, with paraformaldehyde, into a gelatin matrix was done by edge function analysis, EDS SEM, and SBEM.

Initial experiments by EDS SEM on serial dilutions of red blood cells in cured resin demonstrated some charge dissipation, but not significantly improved at 10keV over corannulene or even MWCNTs. Measurements were taken at multiple points in the resin to check for cellular distribution. As expected, there were no small agglomerations of blood cells, as it was pre-fixed into a gelatin matrix. Charge dissipation was usually consistent with the local cellular concentration.

Hemoglobin was considered as a possible target for our gelatin matrix due to the iron heme complexes. Similar to the red blood cell test, studies using hemoglobin in cured resin demonstrated variability in local concentrations.

To homogenize the distribution of hemoglobin, 15%wt gelatin was blended at 45°C in 0.3M cacodylate buffer with 5%wt bovine serum albumin (BSA). The BSA assists in establishing a charged environment for retaining the hemoglobin in gelatin. Using Klaus HeLa cells, this gelatin matrix was applied and tested by EDS SEM and is currently finishing testing by SBEM. EDS SEM data was inconclusive as there was a marginal improvement, however, there seemed to be improved distribution throughout the sample.

Considering the improvements of using a gelatin matrix and the potential of iron heme as a charge dissipation source, iron (II) dextran is incorporated as a replacement to the hemoglobin. As a small molecule, this simplifies the system for further chemical modifications. EDS SEM data has been collected on cell monolayers embedded with this iron, as shown in Figure 2.9. The data is conclusively demonstrating major improvements in charge dissipation. When comparing to the negative control, the drop off in emitted x-ray energy is much closer the to the energy of the incident raster beam. The calculated drop off was around 9.5keV for the iron doped matrix (gelatin). Iron dextran was rendered ineffective at concentrations below 5mg/mL by edge function analysis, so 5mg/mL is considered initially as the best concentration while not compromising the transparency of the resin. Eventually, SBEM data sets revealed 25mg/mL to be the better concentration for higher energy imaging and high vacuum data

collection. The transparency of the resin has been ruled out by use of the x-ray microscope and other modalities within the correlated microscopy suite.

Figure 2.9., EDS SEM and SBEM of cell monolayer embedded with iron (dextran) BSA matrix (scaffold). In (a.), EDS SEM of iron (dextran) in BSA matrix is compared to corannulene conjugate and found to be just as optimal as the resin conjugate. When imaging the iron (dextran) BSA matrix by SBEM at 1.5keV in high vacuum (b.), there is no charging noted when collecting the 3D volume.

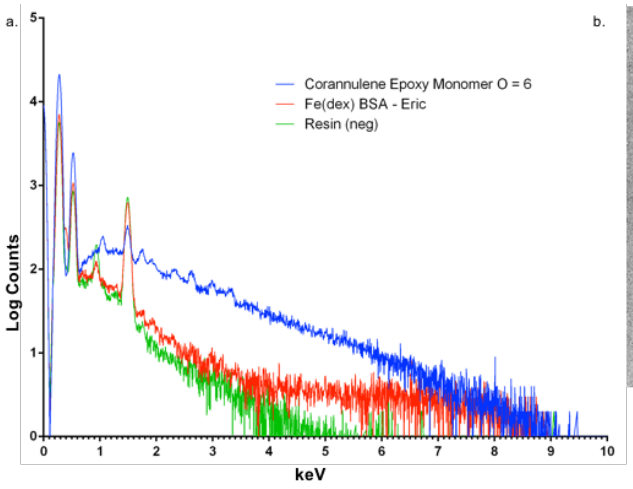
a.
Corannulene Epoxy Monomer O = 6
Fe(dex) BSA - Eric
Resin (neg)
Log Counts
keV
0
1
2
3
4
5
6
7
8
9
10

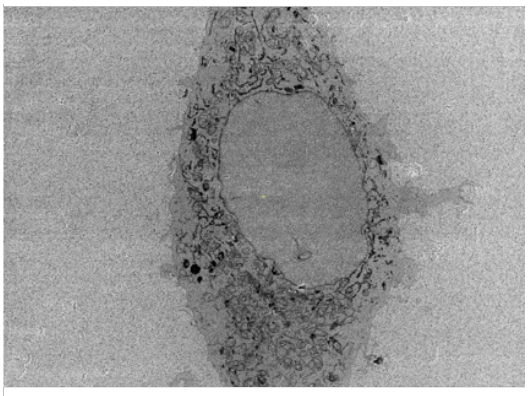
b.

A different route utilizes BSA as the scaffold/matrix for iron dextran instead of gelatin. Because tannic acid is not used in this method, there is no need to use gelatin. Regardless of the matrix, BSA or gelatin, both use 25mg/mL of iron dextran. By EDS SEM, as shown in Figure 2.9., use of BSA does not change the improvement by measuring the Duane-Hunt limit. The only measured difference in matrix is in the protocol, where BSA is not heated and cooled to harden. Iron dextran is active additive in improving conductivity for the specimen. BSA is hardened by crosslinking with paraformaldehyde. As a result, thin sections of BSA/iron matrix yields a more monodispersed network of iron atoms. Whereas, with gelatin, iron is sometimes found clustered in agglomerations of large colloids. SBEM experiments, on both matrices, have shown improved dispersion, with little to no charging at 1.5keV in high vacuum. Even more interesting is the charge decay that takes place when the beam dose is accelerated, then reduced.

Volume collection of epoxy resin and cell monolayers by SBEM yielded little, to no charging at 1.5keV in high vacuum, using both gelatin and BSA. To build on the techniques and tools developed, iron matrix (BSA or gelatin) embedded cell monolayers were polymerized in the newly formed corannulene epoxy resin, where corannulene is a monomeric repeat. We postulated that the conductive epoxy resin is getting assistance in charge transfer from the iron embedded matrix scaffold, further enhancing charge dissipation. As shown in figures 2.8. and 2.9., there is no measured difference in the use of corannulene as a monomeric repeat for this system for the iron/matrix system. When there was a layer of resin, not yet removed and above the iron/matrix, improvements made directly to the resin

improved imaging parameters for finding the ROI. Otherwise, the epoxy resin would charge and make it difficult to set up the run. So, the iron/matrix can eliminate charging at low landing energies without improvements.

In acknowledging contributors to Chapter II, Tom was especially helpful in the resin conductivity project. He was instrumental in the development of using matrices as scaffolds for directing metal coordination for enhanced conductivity. Eric assisted in the development of reconstituted iron dextran systems. Ranjan was instrumental in optimizing our analytical efforts. James was also helpful in advising on some of the first quantitative measurements. James was also a major therapist for me, as he understood my situation before coming to the Ellisman lab. For his time talking to me, I appreciate all the advice he ever gave me about continuing on and I appreciate that. Jay Siegel provided the corannulene compound. Junru was key in genetically labeling cell monolayers. Thank you for collaborating with me on this project.

Chapter III

X-Ray Microscopy as an Approach to Increasing Accuracy and Efficiency of Serial Block-Face Imaging for Correlated Light and Electron Microscopy of Biological Specimens.

3.1. Introduction

Serial block-face scanning electron microscopy (SBEM) of biological specimens is a relatively new volume imaging technique that is rapidly growing in popularity throughout the biological sciences research community. Most notably, this approach is proving of great value for 3D visualization of nervous system ultrastructure, particularly when details of synaptic and other subcellular elements must be located and quantified (Holcomb, et al., 2013; Wilke, et al., 2013), but also where it is important to construct connectomic models of regional brain circuits (Helmstaedter, 2013). In addition, SBEM is increasingly used to perform nanohistology on a wide variety of tissue systems, including systems as diverse as lung (West, et al., 2010), liver (Hatori, et al., 2012), tendons (Pingel, et al., 2014), kidney (Arkill, et al., 2014), and cell cultures (Puhka, et al., 2012). Serial block-face imaging entails the iterative process of imaging a specimen block-face (usually using back-scattered electrons) followed by the removal of a thin layer of epoxy-embedded tissue from the block-face, either using ion abrasion (FIB-SEM) (Heymann, et al., 2009; Knott, et al., 2008) or a diamond knife (Denk & Horstmann, 2004; Leighton, 1981). The current home-made or commercial systems have automated the process so that the SEM operates in SBEM mode, allowing for the collection of much larger EM volumes than could easily be collected using standard serial section TEM, and importantly, avoiding the section compression artifacts associated with serial section TEM. Several reviews have compared volume EM methods, some highlighting the advantages and potential of SBEM (Kleinfeld, et al., 2011; Peddie & Collinson, 2014).

FIB-SEM and diamond knife-based SBEM are both destructive techniques, allowing only a single opportunity to collect images of an object of interest, which is usually buried within the volume of the starting specimen block. Additionally, typical experiments carried out with both techniques can require days or weeks of automated SBEM machine process time. More often in the case of diamond knife-based SBEM, data collection runs can involve months of acquisition time to obtain volumes of the scale and resolution required to contain a suitable portion of a neuronal network with adequate ultrastructural detail to assess connectivity. Consequentially, any methods that can improve the precision and efficiency of SBEM imaging would greatly enhance the power of the technique and the availability of rare imaging resources.

Nevertheless, targeting specific areas or structures for SBEM imaging presents challenges. First, as mentioned above, samples must be intensely stained with heavy metals in order to allow for back-scatter imaging of the tissue and to prevent charging artifacts in the SEM. This staining process generally results in tissue samples that are completely opaque to light, complicating efforts to find and track regions of interest (ROIs) for SBEM imaging. Second, once a sample is placed in the SEM for imaging, only the freshly prepared block-face is visible. This can create uncertainty when deciding where to collect data from the sample surface in order to reach an ROI deep within the sample accurately and efficiently. In practice it is common to collect a larger volume than necessary in order to ensure that the ROI is captured. This practice results in either wasted microscope time and/or a sacrifice in image quality due to lower resolution scans.

X-ray microscopy (XRM) is a tomographic technique that uses x-ray illumination to interrogate the interiors of optically-opaque samples in a non-destructive manner (Stock, 2009). Modern laboratory-based x-ray microscopes (XRM) are capable of producing 3D tomographic reconstructions routinely with sub-micron isotropic resolution. Numerous protocols have been developed for imaging various biological specimens with XRM (Metscher, 2009). One common approach is to stain tissue with osmium tetroxide, a stain that is presently critical for the conductive infiltration of tissue for SBEM imaging. This suggests that XRM may be capable of imaging samples prepared for SBEM. There have been initial efforts to use XRM as an intermediate step in a multiscale, correlated imaging workflow (Burnett, et al., 2014; Sengle, et al., 2013). In this report, we describe our efforts to use XRM as part of an improved SBEM correlative imaging workflow.

3.2. Methods Development and Results

This section will address methods defined as approaches to improving correlation between imaging modalities. Also important, methods in establishing quality controls between tissue staining protocols. There were a number of approaches taken, so the methods will be outlined in chronological order. Other approaches will be mentioned to address any details. In total, this section will serve to highlight the step-wise application of developed hypothesis and the results of each route described.

3.2.1. Sample Preparation

All animals were used according to a protocol approved by the Institutional Animal Use and Care Committee at the University of California, San Diego following AAALAC guidelines. Mice were anesthetized with ketamine / xylazine and transcardially perfused with Tyrode's solution followed by 2.5%wt glutaraldehyde / 2%wt formaldehyde in 0.15M cacodylate buffer containing 2mM $CaCl_2$. The brain was removed and postfixed on ice in the same fixative solution for 2 hours and then cut into 100 m thick slices on a vibrating microtome. The slices were post-fixed at 4°C overnight before further processing. For iontophoretic dye-filling and photooxidation, a mouse was perfused with 4%wt formaldehyde / 0.1%wt glutaraldehyde in 0.1M PBS. The brain was postfixed on ice for 2 hours and then cut into 100 m thick slices. An astrocyte in the hippocampus was filled with 5%wt Lucifer yellow (LY) and then postfixed in 4%wt formaldehyde / 0.1%wt glutaraldehyde for 1 hour. LY fluorescence was imaged and the slice was bathed in 100 mM glycine-PBS buffer to quench excess aldehydes, washed with PBS, and then bathed for 5 minutes in PBS containing 0.15%wt 3,3'-diaminobenzidine tetrahydrochloride (DAB) and 0.1%wt potassium cyanide. The tissue was then illuminated with a LY filter set until LY fluorescence was replaced with light brown precipitate in transmitted light mode. The tissue was washed with PBS and then stained for SBEM imaging, as described below. For MiniSOG photooxidation, a mouse expressing MiniSOG and tdTomato in a subpopulation of retinal ganglion cells (RGCs) was transcardially perfused with 4%wt formaldehyde / 0.1%wt glutaraldehyde in 0.1M PBS. The retina was dissected and post-fixed with 4%wt

formaldehyde in 0.1M PBS on ice for 2 hours and then cut into 100 m thick vertical slices. The tdTomato expressed RGCs were imaged and the retina was fixed with 2.5%wt glutaraldehyde, 2.5mM CaCl2 in 0.15 M cacodylate buffer (CB) pH 7.4, and the tissue was rinsed five times with ice-cold CB, and blocked for 30 minutes with 10mM KCN, 20mM aminotriazole, 50mM glycine, and 0.01%wt hydrogen peroxide in CB. Freshly prepared DAB in CB was added to the retina, and RGCs were illuminated with 450-490 nm light from a xenon lamp for 10-15 minutes until a light brown reaction product was observed in place of the green fluorescence of MiniSOG. The tissue was then processed for SBEM.

3.2.2. SBEM Staining

Tissue was prepared for SBEM as previously described (Deerinck, et al., 2010). Briefly, tissue was washed with buffer and then placed into 2%wt OsO4 / 1.5%wt potassium ferrocyanide in either 0.15M cacodylate buffer containing 2 mM $CaCl_2$ or 0.1M PBS for LY photooxidized specimens. The slices were left for 30 minutes on ice and then 30 minutes a room temperature. After thorough washing in double distilled water, the slices were placed into 0.5%wt thiocarbohydrazide for 30 minutes. The slices were again washed and then stained with 2%wt aq. OsO4 for 30 min. The slices were washed and then placed into 2%wt aq. uranyl acetate overnight at 4°C. The slices were washed with water at room temp and then stained with en bloc lead aspartate for 30 minutes at 60°C. The slices were washed with water and then dehydrated on ice in 70%wt, 90%wt, 100%wt, 100%wt ethanol solutions for 10 minutes at each step. The slices were then washed twice

in dry acetone and then placed into 50:50 Durcupan ACM:acetone overnight. The slices were transferred to 100%wt Durcupan resin overnight in vacuum chamber. The slices were then flat embedded between glass slides coated with mould-release compound and left in oven at 60°C for 48 hours.

3.2.3. XRM Sample Preparation

Generally, small blocks of tissue (maximum dimension < 5mm) were cut from glass slides and then mounted with cyanoacrylate glue to the top of aluminum rods. For some samples, a rhodium-flashed copper finder grid was affixed to one face of the specimen using 5-minute epoxy. Alternatively, one face of the specimen was covered with a small aliquot of poly-L-lysine solution and left for 2-3 minutes. The lysine solution was briefly washed off under a stream of water and then the specimen was allowed to air dry. Tungsten (IV) carbide powder (2 m particles; Sigma-Aldrich Corp., St. Louis, MO, USA) was temporarily suspended in distilled water by vortexing 0.1 g powder in 10 mL water. A small drop was placed on the surface of the sample previously coated with lysine. The sample was allowed to rest for 2 minutes and then wash briefly rinsed several times under a stream of distilled water and allowed to dry.

3.2.4. Biolistic labeling

Nanophosphor particles (NaYSO4: Yb,Er) with a diameter of 1 m were kindly provided by Intelligent Material Solutions, Inc. (San Diego, CA, USA). A 2 mg/mL solution of nanophosphor particles in 95%wt isopropanol/5%wt acetone

was deposited within Tefzel tubing to create bullets for a Helios gene gun (Bio-Rad Laboratories, Hercules, CA, USA), as previously described (O'Brien & Lummis, 2011). The nanophosphor particles were shot into slices of brain tissue at 160 psi with a 2 cm distance between the tip of the gun nozzle and the tissue slice. The slice was then washed briefly in buffer, imaged by light microscopy, and subsequently processed for SBEM staining.

3.2.5. Light Microscopy

Prior to photo-oxidation, LY-filled cells were imaged on a Leica SPEII using a 63X oil objective (NA 1.30). Brain slices containing nanophosphor particles were imaged on a Radiance 2000 microscope (Bio-Rad) equipped with a Ti-sapphire infrared laser (Spectra-Physics, Santa Clara, CA, USA). The slices were initially imaged with a 10X objective (Nikon, NA 0.3) with pulsed-mode illumination (980 nm) and then continuous wave illumination (980 nm), in order to collect nanophosphor and autofluorescence signal, respectively. Sub-regions were then imaged with a 40X objective (Nikon, NA 1.30) using continuous wave illumination at 980 nm, simultaneously collecting fluorescence and transmitted light images.

3.2.6. X-ray Microscopy

Most XRM work was performed on a MicroXCT-200 instrument (Zeiss X-Ray Microscopy, Pleasanton, CA, USA). This architecture combines both geometric (as found in conventional microCT constructs) and optical magnification (lens-coupled post-sample magnification) as well as optimized scintillation

technologies to yield high-contrast sub-micron 3D reconstructions of a sample. XRM tilt series were generally collected at 40 kV and 4W power (100 A current), unless otherwise noted. A Zeiss Xradia 510 Versa was utilized for these studies as well, as indicated in Figure 3.

3.2.7. Serial Block-face Imaging

SBEM data was collected with a 3View unit (Gatan, Inc., Pleasanton, CA, USA) installed on a Merlin field emission SEM (Carl Zeiss Microscopy, Jena, Germany). The retinal volume was collected at 2.0kV accelerating voltage, with a raster size of 19k x 39k and pixel dwell time of 0.5sec. The pixel size was 5.7 nm and section thickness was 70 nm. The astrocyte volume was collected at 2.0 kV, with a raster of 20k x 20k and pixel dwell time of 1.0sec. The pixel size was 4.5nm and section thickness was 90 nm.

3.2.8. Image Analysis

XRM volumes were generated from XRM tilt series using XMReconstructor (Xradia). Scaling, rotation, transformation of images to find best alignment between features of interest was performed in Photoshop (Adobe Systems Inc., San Jose, CA, USA) or Imaris (Bitplane AG, Zurich, Switzerland).

2D affine transformation was performed using SciPy LinearNDInterpolator. In order to estimate the location of a target ROI on the SEM stage coordinates, fiducial markers were chosen near the ROI and their SEM stage coordinates were collected, as well as their coordinates in a previously acquired XRM volume. The

two sets of coordinates were then used to calculate the SEM coordinates for the ROI based on the XRM coordinates of the ROI.

3.3. Discussion

Considering the methods and materials provided, this section of this chapter aims to address and discuss the use of the techniques and methods accomplished and their viability for correlating biological specimens across light, x-ray and electron microscopy. Also introduced, the novelty in region of interest tracking techniques novel in use to the field will also be addressed. From this section, this dissertation aims to lay out specific conclusions and achievements in the area of universal markers and multi-modal imaging for correlative microscopy.

3.3.1. XRM Imaging of SBEM-Stained Tissue

In order to test the applicability of XRM to imaging typical SBEM samples, 100 m thick slices of mouse brain were stained with heavy metals stains for SBEM imaging and embedded in epoxy resin (Figure 3.1. a and b). Following conductive infiltration with heavy metals, the tissue was rendered completely opaque to light. Acquisition of low magnification 2D XRM projection images of the specimens was sufficient to reveal considerable detail, including basic cytoarchitecture, white matter tracts, vasculature, and cracks and other defects within the samples (Figure 3.1.c). The resolution achieved in XRM volumes collected at 20X (optical) magnification was sufficient to allow for the unambiguous identification of individual somata of neurons and other cell types, large dendritic processes, and

occasionally nucleoli within otherwise transparent nuclei (Figure 3.1. d and e). Subtle differences in cytoplasmic staining were even detectable, most likely revealing interneurons typically displaying dark cytoplasm in electron micrographs.

Figure 3.1., X-ray microscopy (XRM) allow for high-resolution imaging of tissue stained for serial block-face scanning electron microscopy (SBEM) (a., b.). While it is possible to easily identify anatomical features within a brain slice using light microscopy, the tissue is completely opaque to light following staining for SBEM. In (c.), a two-dimensional (2D) projection image with the XRM using a 4x objective and 40kV reveals details within the SBEM-stained tissue slice, including cell layers, vasculature, and white matter tracts. As shown in (d.), a virtual 2D slice from a XRM volume allows for the discrimination of individual cells, dendrites, dark neurons, and nucleoli. The volume was collected with a 20x objective using a 180° sample rotation, 0.1° tilt increments, and 15s exposures (~7.5h total). In (e.), a 3D array trace projection image of the same volume. Scale bar: (c.) 500μm, (d.) 50μm, and (e.) 100μm.

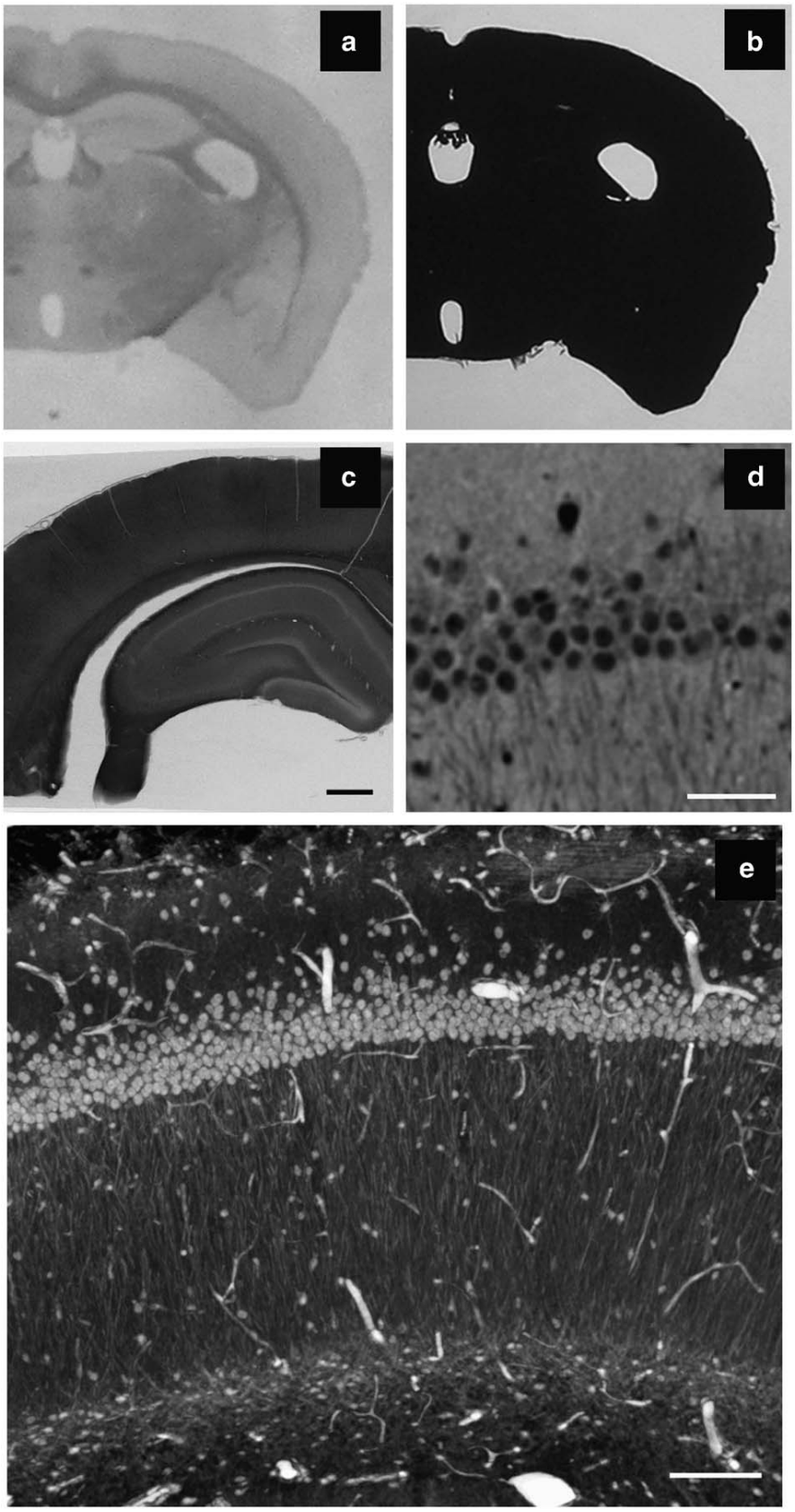
a
b
c
d
e

3.3.2. Finder Grids for Rough Mapping of Specimens

Similar to other efforts to track ROIs within specimens from light to electron microscopy, we experimented with the use of finder grids (Auinger & Small, 2008; McDonald, et al., 2010). Quick-setting epoxy was used to fix a rhodium-plated copper finder grid to the surface of an epoxy-embedded brain slice stained for SBEM. The metal grids did not interfere with the ability to image tissue, even when the tissue was underlying an area of unmeshed metal (Figure 3.2.). Following XRM, specimens were coated with a thin layer of gold-palladium in a sputter coater and the finder grid was carefully removed. The resulting mask image of the finder grid was visible under light microscope and in the SEM. This approach would allow an investigator to target a specific region of the tissue for acquisition of an SBEM volume.

3.3.3. XRM Tracking of Photo-oxidized Specimens

Novel transgenic probes such as MiniSOG and APEX allow for electron-dense labeling of tissue elements in a genetically targeted manner (Martell, et al., 2012; Shu, et al., 2011). To test the use of these probes with XRM imaging, retinas expressing MiniSOG and tdTomato in a subpopulation of RGC were photooxidized in the presence of DAB (Fig3 a,b). Following SBEM staining and resin embedding, XRM imaging of the retina revealed the area of photooxidation with sufficient resolution and sensitivity to detect DAB-labeled RGC dendrites in the inner plexiform layer (IPL). In addition to detecting the DAB labeling, XRM also exposed the presence of blood vessels, tissue cytoarchitecture, and cracks in tissue, which

were all useful landmarks for finding the ROI in the SEM. Based on these landmarks, an SBEM volume was collected in an area shown by XRM to contain DAB-labeled dendrites. When the XRM volume was re-sliced in an oblique orientation to match as closely as possible the cutting plane of the SBEM volume, it was possible to correlate XRM slices very closely with the block-face images collected by SBEM (Fig 3 c, d), confirming that the signals detected by XRM imaging were generated by DAB-labeled dendrites.

Figure 3.2., Finder grids are a simple method for tracking regions of interest between X-ray microscopy (XRM) and serial block-face scanning electron microscopy (SBEM) modalities. In (a.), an electron microscopic finder grid was attached to the surface of a resin-embedded, SBEM-stained slice of brain tissue. The grid landmarks are clearly visible in a computed slice from a XRM volume. In (b.), a second computed slice taken through the tissue shows that tissue structures are visible even in areas laying under areas of solid metal in the finder grid. The volume was collected using a 10Å~ objective, with a 360° sample rotation at 0.2° tilt increments and 8s exposures (~4hrs total). Scale bar is 500 μm.

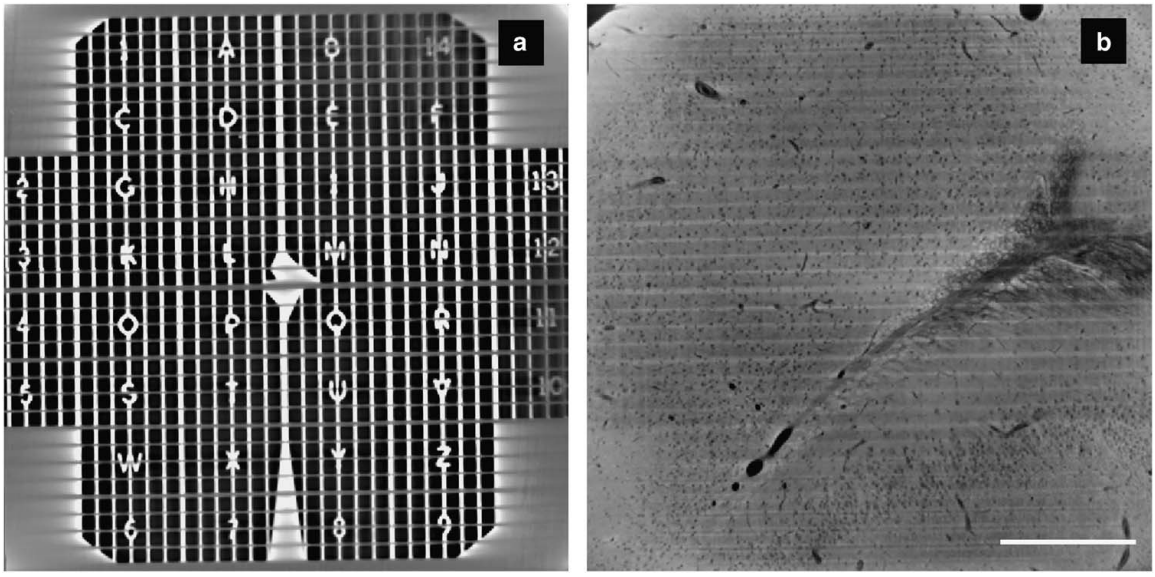
a
b

3.3.4. Tungsten Carbide as a Fiducial Marker

The retina presented a relatively simple specimen, where the search was limited to finding a ROI containing many structures of interest (i.e., RGC dendrites) along a one-dimensional aspect of the specimen (i.e., the vitreal surface of the retinal slice). Many specimens could prove much more challenging in the precision required for ROI tracking. We explored the use of small fiducial markers that would allow us to more accurately target a ROI within an SBEM sample. An astrocyte in a 100 m-thick slice of mouse brain was iontophoretically-filled with LY and subsequently labeled by photooxidation of DAB. The tissue was prepared for SBEM imaging using heavy metal staining and embedded in epoxy resin. Prior to performing XRM on the sample, a layer of 2 m tungsten carbide particles was dispersed on one surface of the specimen. Following XRM reconstruction, the DAB-labeled astrocyte was clearly distinguishable within the tissue slice, as were the tungsten carbide particles at the surface. After the ROI was mounted on an SEM pin, it was possible to identify the tungsten carbide particles by backscatter imaging in the SEM. For several tungsten particles, the SEM stage coordinates and XRM volume coordinates were determined. Using 2D affine transformation, the SEM coordinates of the astrocyte were determined based on the XRM volume coordinates for the cell. Additionally, the XRM data revealed that the astrocyte was located approximately 45 m beneath the surface of the epoxy resin. The SBEM microtome was used to quickly bring the block-face down to a level just above the targeted cell, thus avoiding significant acquisition time for collection of data from an area of little interest. Based on the size of the astrocyte as measured in LM

and XRM volumes, an SBEM volume was collected at the coordinates calculated using the tungsten carbide fiducial markers. The resulting SBEM volume captured the astrocyte perfectly centered within the field of view, while minimizing the raster size and the time spent approaching the cell.

Figure 3.3., Specifically labeled structures for electron microscopy are also visible in X-ray microscopy (XRM) volumes following staining for serial block-face scanning electron microscopy (SBEM). In (a.), tdTomato labeling of retinal ganglion cell co-expressing MiniSOG. In (b.), a light microscopy image of the retina following photooxidation. Small area containing 3,3'-diaminobenzidine tetrahydrochloride (DAB) filled dendrites, corresponding area in (a.) is marked with a dashed box. In (c.) and (d.) bright spots in XRM volume (arrows in left panels) from same area in (a.) and (b.) correspond to DABlabeled dendrites in SBEM images (arrows in center panel, higher magnification in right panels). The XRM volume was collected using a Zeiss Xradia 510 Versa at 40keV and 3W power, 180° sample rotation at 0.1° tilt increments, with 10s exposure time (~6 h total). RGL, retinal ganglion cell layer; IPL, inner plexiform layer; INL, inner nuclear layer; OPL, outer plexiform layer; ONL, outer nuclear layer. Scale bar: (a.) 50μm, (c., d. center panels) 10 μm, and (c., d. right panels) 2.5 μm.

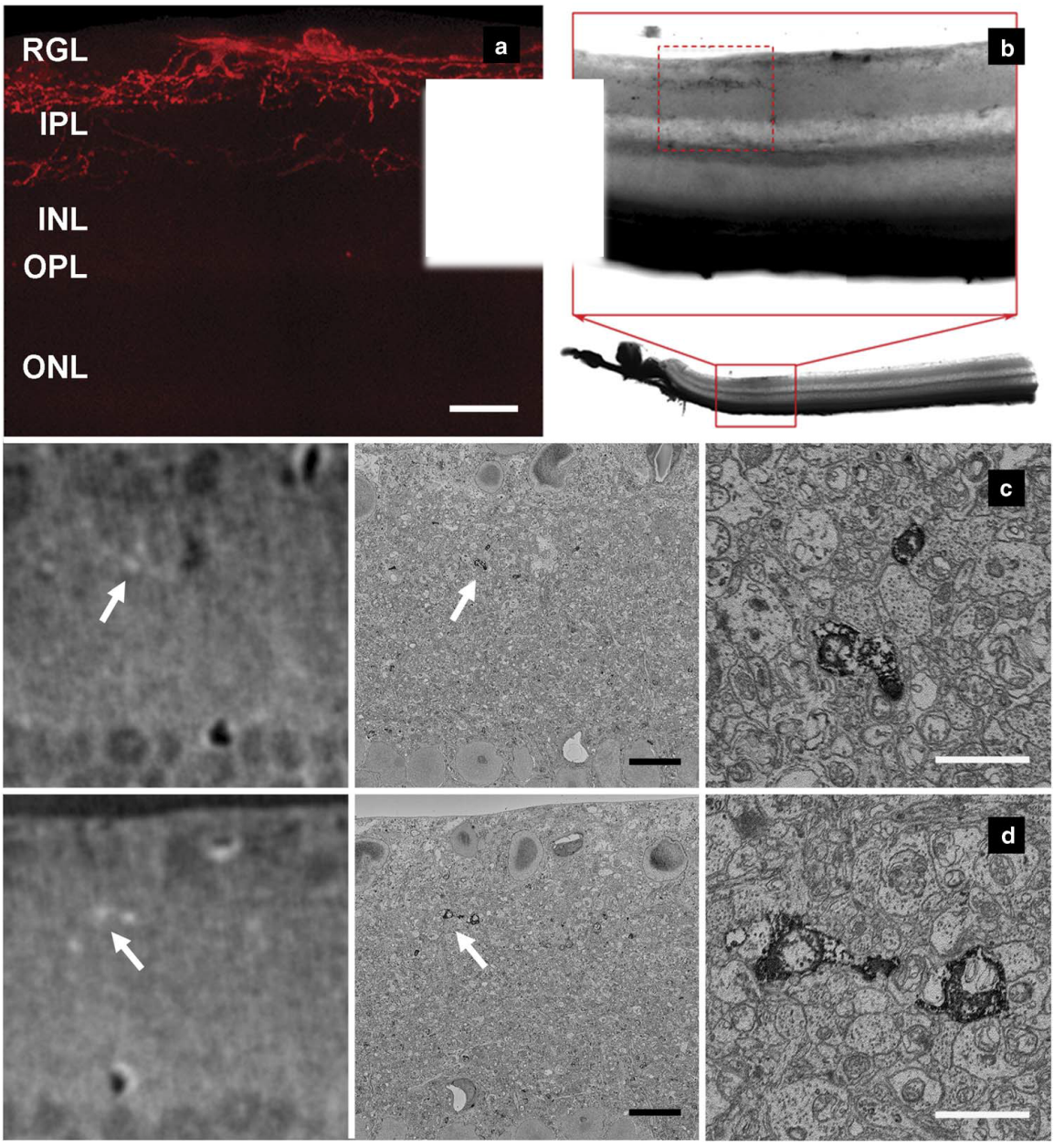
RGL
IPL
INL
OPL
ONL
a
b
c
d

3.3.5. Nanophosphor Particles as Correlated LM-XRM-SBEM Fiducial Markers

We have also explored the use of nanophosphor particles as fiducial markers. Also known as upconverting nanoparticles, nanophosphor particles display phosphorescence emission in response to excitation with infrared wavelength light. They are available in sizes ranging from 70 nm up to 1 m in diameter. In addition, nanophosphor emission is resistant to staining with osmium tetroxide (data not shown).

Figure 3.4., Tungsten carbide particles are effective fiducial markers for precisely tracking regions of interest from X-ray microscopy (XRM) to serial block-face scanning electron microscopy (SBEM). In (a.), a photooxidized astrocyte in tissue stained for SBEM is visible in a computed slice from a XRM. Inset shows a confocal image of the astrocyte before photooxidation. XRM volume was collected at 20keV and 2W power, with a 20Å~ objective using 180° sample rotation with 0.1° tilt increments and 25s exposures (~13hrs total). In (b.) another computed slice from the same volume shows the distribution of tungsten carbide particles on one surface of the sample. Inset shows scanning electron microscopic image of area in white box in (b.), with several tungsten carbide particles visible. In (c.), Computed slice through cross-section of the sample allows for determination of the depth of the astrocyte within the specimen. In (d.), SBEM slice taken from volume collected of the astrocyte, based on the coordinates calculated using tungsten carbide particles. The astrocyte is properly centered in the field of view. Scale bar: (a. inset) 15 μm, (b. inset) 4 μm, (b.) 100 μm, (c.) 50μm, and (d.) 10 μm.

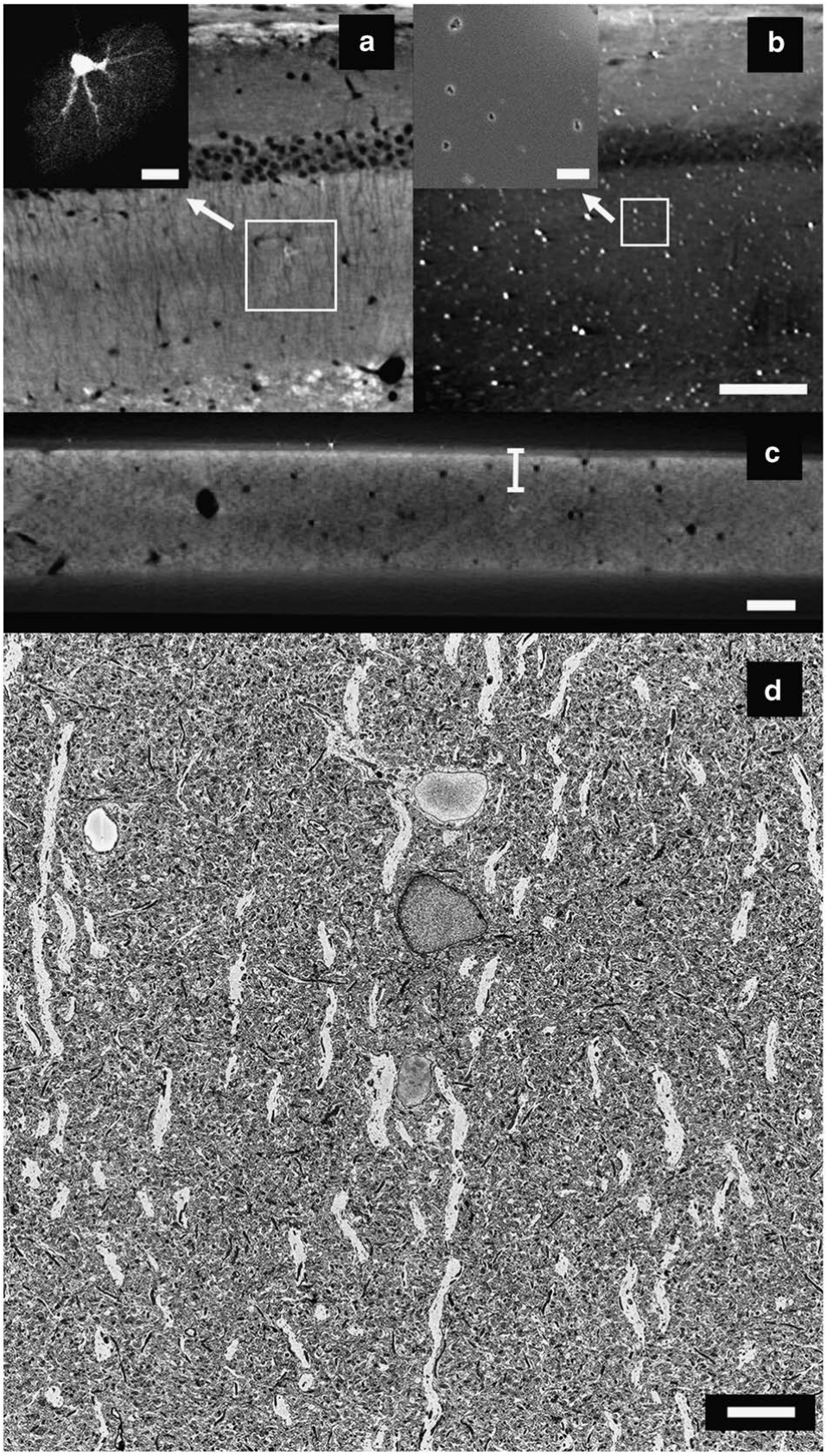
a
b
c
d

Nanophosphor particles (1m diameter) were distributed within brain slices using a helium-powered biolistic device. The brain slices were imaged with 980nm wavelength illumination in continuous wave mode to detect nanophosphor particles and in pulsed mode to image tissue autofluorescence. By combining these images, the distribution of the particles relative to tissue landmarks, such as cell layers, white matter tracts, and vasculature, was determined. The samples were then stained with the SBEM staining protocol and embedded in epoxy resin. The nanophosphor particles were easily detectable at all levels of the tissue slices in XRM volumes of the specimens. With the combination of particles characteristics and biolistic parameters used here, the majority of particles were present within the first few microns of the tissue sample, with a sizable minority having traveled completely through the specimen to the opposite surface. Few nanoparticles were found within the interior of the specimen, with most of these particles found near blood vessels. The distributions of nanophosphor particles within confocal and XRM volumes of an identical FOV were very similar, allowing for the unambiguous identification of an ROI (Figure 3.5.).

Figure 3.5., Nanophosphor particles are useful fiducial particles that can also be used to correlate regions of interest between LM and X-ray microscopy (XRM). In (a.), nanophosphor particles (red) are distributed across a brain slice (green) using a gene gun. In (b.), transmitted light image of nanophosphor particles on one surface of a brain slice. In (c.) computed slice from XRM volume of same field of view as in (b.). Volume was collected with 20Å~ objective using 360° sample rotation with 0.2° tilt increments and 15s exposures (~7.5hrs total). Scale bar: (a.) 200 μm and (b., c.) 50 μm.

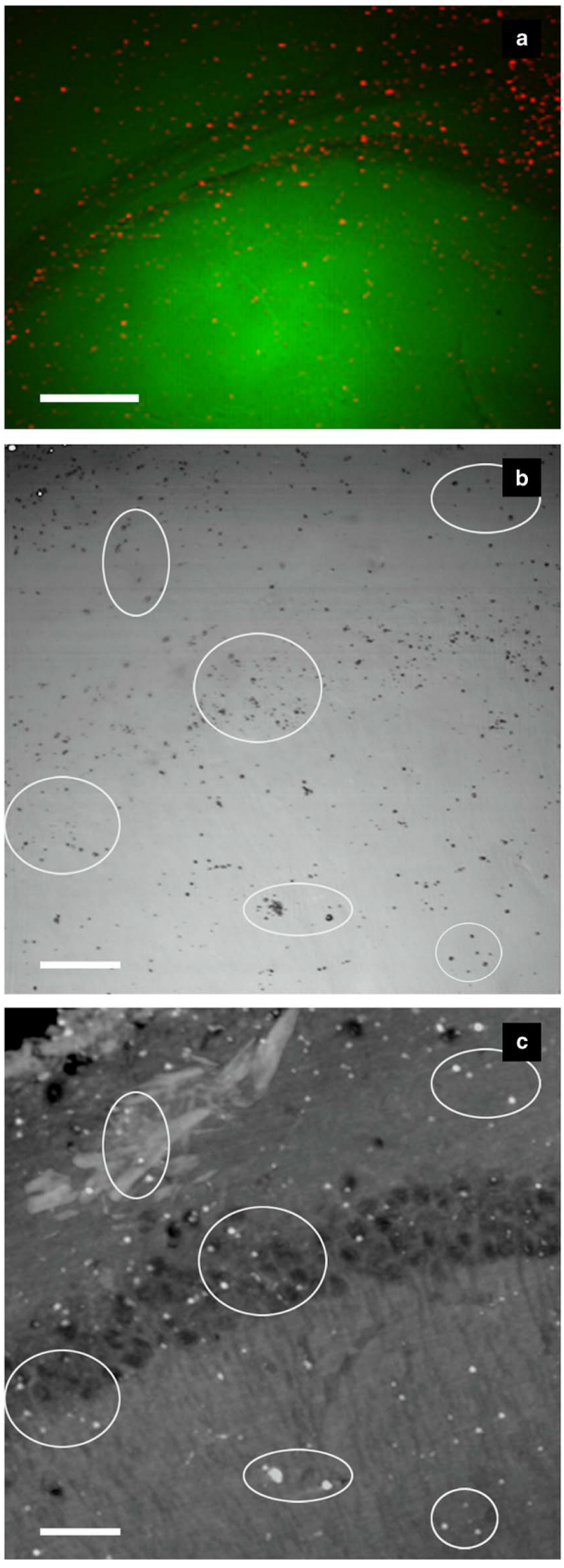
a
b
c

In acknowledging the contributors to Chapter III, Eric was instrumental in the slot grid development and cell labeling protocols. Josh Collins was instrumental in the solid-state synthesis of the yttrium sulfoxide particles. Tom and Christine Kim were key in generating the SBEM data. Thank you for your assistance in this project. Bushong, E.A., Johnson, Jr., D.D., Kim, K.Y., Terada, M., Hatori, M., Peltier, S.T. Panda, S., Merkle, A. and Ellisman, M.H., X-Ray Microscopy as an Approach to Increasing Accuracy and Efficiency of Serial Block-Face Imaging for Correlated Light and Electron Microscopy of Biological Specimens. **2014**, Microscopy and Microanalysis, 21, pp 231-238.

Chapter IV

Targeted approach to imaging membrane proteins and microtubules using small water-soluble upconverting nanophophors

4.1. Introduction

Correlated light, x-ray and electron microscopy are increasingly growing in popularity and use, as an effort is growing in characterizing macromolecular dynamics and the scale of these dynamics. Correlated light, x-ray and electron microscopy addresses three details: generates unique information for each imaging modality, is useful in identifying rare or hard to target structures, and puts all scaled details into context. As a result, correlative microscopy has grown to be an important tool for irreversible imaging parameters (Shu *et al*. 2011).

In particular, serial block face scanning electron microscopy (SBEM) is an imaging technique that is inherently an irreversible imaging process. Also important, the staining used to define image contrast and resolution by SBEM quenches most genetic tag and small molecule fluorescent labels. So, an ROI can be lost from light to electron microscopy. To solve this issue, x-ray microscopy confirms the ROI without destroying the sample (Bushong and Johnson *et al.* 2014). However, the fluorescent label is still quenched, and most likely not resolvable by x-ray microscopy. Hence, a “universal label” that targets the protein, small molecule, or combination and is resolvable by light, x-ray and electron is the next step in the development of correlative microscopy. In particular, this “universal marker” would have to be small, bright, yet provide contrast, and scatter electrons differently from osmium. Quantum dots fit all these criteria, however, they are prone to being quenched by osmium (Han *et al*. 2014). A novel marker, tolerant to osmium but still fulfilling all these criteria, would need to undergo a photophysical mechanism that avoids potential interactions with osmium. Also

important, a universal marker would make a biological specimen capable of being imaged in the reverse order, as long it is not imaged by SBEM.

Low-energy excitation (near-IR wavelengths) of biological specimens is becoming increasingly important to preserving macromolecular and ultra-structural information. Much work on low-energy excitation light microscopy lead to the development of super-resolution light micrscopy methods, such as photoactivated localization micrscopy (PALM) (Betzig 1984). Most fluorescent labels are utilizing higher energy (near ultraviolet) excitation wavelengths, which lead to overheating and tissue damage. Novel strategies involving the use of low energy excitable probes will be useful in preserving ultra-structure. Also important, the use of low energy excitable metal probes will be visible by x-ray and electron microscopy, depending on the properties of the metal probe.

Upconverting nanophosphors, as described in chapter III, are functionalized and utilized as “universal markers” for correlative microscopy. Upconverting nanophosphors (UCPs) are heavy metal crystalline structures doped with heavy metals important in the emission of visible light from the particle. These particles come in various shapes, such as cubes, spheres, diamonds and sheets. Synthesis of these materials yield particle sizes ranging from 10nm to 5μm in diameter. For the scope of this dissertation, we will be discussing the use of ytterbium(Yb)/erbium(Er) and ytterbium(Yb)/Thulium(Tm) doped yttrium host. The cationic species for these synthesis generally vary between barium, lithium and sodium.

The photophysical mechanism, as described by Chatterjee *et al.* and Haase *et al*., involved in fluorescent emission of these nanocrystals is excited by infrared energy at 980nm wavelength. Known as an anti-stokes emission, the mechanism involves upconversion, two-photon excitation and second-harmonic generation. Two metastable excited states are involved, the first serving as an excitation reservoir, and the second as the emitter. These two states are known as the Yb and Er, or Tm respectively. They are situated close to one another and supported by the host metal material. When radiated, both Yb (reservoir) and Er, or Tm, (emitter) ions are excited to a higher energy state. Instead of radiative dissipation of the energy, the Yb (reservoir) ions non-radiatively transmit the excess energy to the Er, or Tm, (emitter) ions, thereby exciting it to a higher energy state (Auzel *et al*. 2004). The Er, or Tm, ions then relax back to the ground state. As a result of the non-radiative transfer of energy to the emitter, the emitted energy is greater than the incident excitation energy.

The upconversion mechanism is very similar to simultaneous two-photon absorption (STPA), which is similar, but requires simultaneous absorption of two low-energy photons to a higher excited state. The simultaneous absorption of two low-energy photons is not occuring with one ion for two-photon upconversion. Instead, the process is shared between the reservoir and the emitter, as described above. When the excited photons return to the ground state, the combined energy of the absorbed photons is released as a single photon of higher energy (Franken *et al*. 1961).

In this chapter, the focus will divert from using upconverting nanophosphors as fiducials for correlative microscopy. The focus will steer towards the use of these upconverting nanophosphors as labels for targeting macromolecular and small molecular structures for correlative microscopy. Synthesis of the particles, characterization of the particles by the various imaging modalities available, coupled with cell labeling experiments will be the focus of this chapter.

4.2. Methods Development and Results

This section will address methods defined as approaches to improving correlation between imaging modalities, with an interest in targeting specific proteins. Also important, methods in establishing quality controls between tissue staining protocols. There were a number of approaches taken, so the methods will be outlined in chronological order. Other approaches will be mentioned to address any details. In total, this section will serve to highlight the step-wise application of developed hypothesis and the results of each route described.

4.2.1. Synthesis of upconverting nanophosphors

4.2.1.1. Lithium yttrium fluoride: ytterbium, erbium

Starting in a round bottom flask with a 1:1 volume of octadecene and oleic acid, all heavy metals are weighed out and added according to their relative molar ratios. For this synthesis, 0.0068 moles of lithium triflouroacetate, 0.00015 moles of erbium triflouroacetate, 0.0058 moles of yttrium triflouroacetate, and 0.0015 moles of ytterbium triflouroacetate added to the octadecene/oleic acid volume.

The round bottom, containing the mixture of solvent and heavy metals, is heated to 140°C, while stirring, under house vacuum for 45 minutes. The reaction mixture will turn a light amber brown during this process. An opaque solution indicates the solution has generated too much oleiate to be successful. The goal of this step is to remove any unwarranted solvents, such as water, ethanol, etc.

Once the reaction mixture has been heated under an induced vacuum to remove unnecessary solvents, the reaction mixture is transferred to a molten salt bath, set to 345°C. Ultrapure nitrogen gas is bubbled through the mixture while the decomposition and final reaction is taking place at 340°C. This reaction is closely monitored for 25 minutes. During the final reaction, hydrogen fluoride (HF) is generated and filtered out of through the bubbling process. Once the reaction has come to completion, an IR laser pen is used to confirm the emission band of the particles. The reaction mixture is removed from the molten salt bath and cooled. The reaction is quenched with 3 mL of octadecene, followed by 10 mL of ethanol and 10-20 mL of hexanes to precipitate out the final product. The particles are iteratively washed 3 times in 1:1, ethanol: hexanes solution. The particles are stored in hexanes once complete with the washes.

4.2.1.2. Lithium yttrium fluoride: ytterbium, thulium

Starting in a round bottom flask with a 1:1 volume of octadecene and oleic acid, all heavy metals are weighed out and added according to their relative molar ratios. For this synthesis, 0.0068 moles of lithium triflouroacetate, 0.000037 moles

of thulium triflouroacetate, 0.0058 moles of yttrium triflouroacetate, and 0.0015 moles of ytterbium triflouroacetate added to the octadecene/oleic acid volume. The round bottom, containing the mixture of solvent and heavy metals, is heated to 140°C, while stirring, under house vacuum for 45 minutes. The reaction mixture will turn a light amber brown during this process. An opaque solution indicates the solution has generated too much oleiate to be successful. The goal of this step is to remove any unwarranted solvents, such as water, ethanol, etc.

Once the reaction mixture has been heated under an induced vacuum to remove unnecessary solvents, the reaction mixture is transferred to a molten salt bath, set to 345°C. Ultrapure nitrogen gas is bubbled through the mixture while the decomposition and final reaction is taking place at 340°C. This reaction is closely monitored for 25 minutes. During the final reaction, hydrogen fluoride (HF) is generated and filtered out of through the bubbling process. Once the reaction has come to completion, an IR laser pen is used to confirm the emission band of the particles. The reaction mixture is removed from the molten salt bath and cooled. The reaction is quenched with 3 mL of octadecene, followed by 10 mL of ethanol and 10-20 mL of hexanes to precipitate out the final product. The particles are iteratively washed 3 times in 1:1, ethanol: hexanes solution. The particles are stored in hexanes once complete with the washes.

4.2.1.3. Lithium yttrium fluoride, ytterbium, holmium

Starting in a round bottom flask with a 1:1 volume of octadecene and oleic acid, all heavy metals are weighed out and added according to their relative molar ratios. For this synthesis, 0.0068 moles of lithium triflouroacetate, 0.000075 moles of holmium triflouroacetate, 0.0058 moles of yttrium triflouroacetate, and 0.0015 moles of ytterbium triflouroacetate added to the octadecene/oleic acid volume. The round bottom, containing the mixture of solvent and heavy metals, is heated to 140°C, while stirring, under house vacuum for 45 minutes. The reaction mixture will turn a light amber brown during this process. An opaque solution indicates the solution has generated too much oleiate to be successful. The goal of this step is to remove any unwarranted solvents, such as water, ethanol, etc.

Once the reaction mixture has been heated under an induced vacuum to remove unnecessary solvents, the reaction mixture is transferred to a molten salt bath, set to 345°C. Ultrapure nitrogen gas is bubbled through the mixture while the decomposition and final reaction is taking place at 340°C. This reaction is closely monitored for 25 minutes. During the final reaction, hydrogen fluoride (HF) is generated and filtered out of through the bubbling process. Once the reaction has come to completion, an IR laser pen is used to confirm the emission band of the particles. The reaction mixture is removed from the molten salt bath and cooled. The reaction is quenched with 3 mL of octadecene, followed by 10 mL of ethanol and 10-20 mL of hexanes to precipitate out the final product. The particles

are iteratively washed 3 times in 1:1, ethanol: hexanes solution. The particles are stored in hexanes once complete with the washes.

4.2.1.4. Sodium yttrium fluoride, ytterbium, erbium

Starting in a round bottom flask with a 1:1 volume of octadecene and oleic acid, all heavy metals are weighed out and added according to their relative molar ratios. For this synthesis, 0.0056 moles of sodium triflouroacetate, 0.00015 moles of erbium triflouroacetate, 0.0029 moles of yttrium triflouroacetate, and 0.00075 moles of ytterbium triflouroacetate added to the octadecene/oleic acid volume. The round bottom, containing the mixture of solvent and heavy metals, is heated to 140°C, while stirring, under house vacuum for 45 minutes. The reaction mixture will turn a light amber brown during this process. An opaque solution indicates the solution has generated too much oleiate to be successful. The goal of this step is to remove any unwarranted solvents, such as water, ethanol, etc.

Once the reaction mixture has been heated under an induced vacuum to remove unnecessary solvents, the reaction mixture is transferred to a molten salt bath, set to 345°C. Ultrapure nitrogen gas is bubbled through the mixture while the decomposition and final reaction is taking place at 340°C. This reaction is closely monitored for 25 minutes. During the final reaction, hydrogen fluoride (HF) is generated and filtered out of through the bubbling process. Once the reaction has come to completion, an IR laser pen is used to confirm the emission band of the particles. The reaction mixture is removed from the molten salt bath and

cooled. The reaction is quenched with 3 mL of octadecene, followed by 10 mL of ethanol and 10-20 mL of hexanes to precipitate out the final product. The particles are iteratively washed 3 times in 1:1, ethanol: hexanes solution. The particles are stored in hexanes once complete with the washes.

4.2.1.5. Sodium yttrium fluoride, ytterbium, thulium

Starting in a round bottom flask with a 1:1 volume of octadecene and oleic acid, all heavy metals are weighed out and added according to their relative molar ratios. For this synthesis, 0.0056 moles of sodium triflouroacetate, 0.000037 moles of thulium triflouroacetate, 0.0029 moles of yttrium triflouroacetate, and 0.00075 moles of ytterbium triflouroacetate added to the octadecene/oleic acid volume. The round bottom, containing the mixture of solvent and heavy metals, is heated to 140°C, while stirring, under house vacuum for 45 minutes. The reaction mixture will turn a light amber brown during this process. An opaque solution indicates the solution has generated too much oleiate to be successful. The goal of this step is to remove any unwarranted solvents, such as water, ethanol, etc.

Once the reaction mixture has been heated under an induced vacuum to remove unnecessary solvents, the reaction mixture is transferred to a molten salt bath, set to 345°C. Ultrapure nitrogen gas is bubbled through the mixture while the decomposition and final reaction is taking place at 340°C. This reaction is closely monitored for 25 minutes. During the final reaction, hydrogen fluoride (HF) is generated and filtered out of through the bubbling process. Once the reaction

has come to completion, an IR laser pen is used to confirm the emission band of the particles. The reaction mixture is removed from the molten salt bath and cooled. The reaction is quenched with 3 mL of octadecene, followed by 10 mL of ethanol and 10-20 mL of hexanes to precipitate out the final product. The particles are iteratively washed 3 times in 1:1, ethanol: hexanes solution. The particles are stored in hexanes once complete with the washes.

4.2.1.6. Sodium yttrium fluoride, ytterbium, holmium

Starting in a round bottom flask with a 1:1 volume of octadecene and oleic acid, all heavy metals are weighed out and added according to their relative molar ratios. For this synthesis, 0.0056 moles of sodium triflouroacetate, 0.000075 moles of thulium triflouroacetate, 0.0029 moles of yttrium triflouroacetate, and 0.00075 moles of ytterbium triflouroacetate added to the octadecene/oleic acid volume. The round bottom, containing the mixture of solvent and heavy metals, is heated to 140°C, while stirring, under house vacuum for 45 minutes. The reaction mixture will turn a light amber brown during this process. An opaque solution indicates the solution has generated too much oleiate to be successful. The goal of this step is to remove any unwarranted solvents, such as water, ethanol, etc.

Once the reaction mixture has been heated under an induced vacuum to remove unnecessary solvents, the reaction mixture is transferred to a molten salt bath, set to 345°C. Ultrapure nitrogen gas is bubbled through the mixture while the decomposition and final reaction is taking place at 340°C. This reaction is

closely monitored for 25 minutes. During the final reaction, hydrogen fluoride (HF) is generated and filtered out of through the bubbling process. Once the reaction has come to completion, an IR laser pen is used to confirm the emission band of the particles. The reaction mixture is removed from the molten salt bath and cooled. The reaction is quenched with 3 mL of octadecene, followed by 10 mL of ethanol and 10-20 mL of hexanes to precipitate out the final product. The particles are iteratively washed 3 times in 1:1, ethanol: hexanes solution. The particles are stored in hexanes once complete with the washes.

4.2.1.7. Barium yttrium fluoride: ytterbium, erbium

Starting in a round bottom flask with a 1:1 volume of octadecene and oleic acid, all heavy metals are weighed out and added according to their relative molar ratios. For this synthesis, 0.0026 moles of barium triflouroacetate, 0.00015 moles of erbium triflouroacetate, 0.0029 moles of yttrium triflouroacetate, and 0.00075 moles of ytterbium triflouroacetate added to the octadecene/oleic acid volume. The round bottom, containing the mixture of solvent and heavy metals, is heated to 140°C, while stirring, under house vacuum for 45 minutes. The reaction mixture will turn a light amber brown during this process. An opaque solution indicates the solution has generated too much oleiate to be successful. The goal of this step is to remove any unwarranted solvents, such as water, ethanol, etc.

Once the reaction mixture has been heated under an induced vacuum to remove unnecessary solvents, the reaction mixture is transferred to a molten salt bath, set to 345°C. Ultrapure nitrogen gas is bubbled through the mixture while

the decomposition and final reaction is taking place at 340°C. This reaction is closely monitored for 25 minutes. During the final reaction, hydrogen fluoride (HF) is generated and filtered out of through the bubbling process. Once the reaction has come to completion, an IR laser pen is used to confirm the emission band of the particles. The reaction mixture is removed from the molten salt bath and cooled. The reaction is quenched with 3 mL of octadecene, followed by 10 mL of ethanol and 10-20 mL of hexanes to precipitate out the final product. The particles are iteratively washed 3 times in 1:1, ethanol: hexanes solution. The particles are stored in hexanes once complete with the washes.

4.2.1.8. Barium yttrium fluoride: ytterbium, thulium

Starting in a round bottom flask with a 1:1 volume of octadecene and oleic acid, all heavy metals are weighed out and added according to their relative molar ratios. For this synthesis, 0.0026 moles of barium triflouroacetate, 0.000037 moles of thulium triflouroacetate, 0.0029 moles of yttrium triflouroacetate, and 0.00075 moles of ytterbium triflouroacetate added to the octadecene/oleic acid volume. The round bottom, containing the mixture of solvent and heavy metals, is heated to 140°C, while stirring, under house vacuum for 45 minutes. The reaction mixture will turn a light amber brown during this process. An opaque solution indicates the solution has generated too much oleiate to be successful. The goal of this step is to remove any unwarranted solvents, such as water, ethanol, etc.

Once the reaction mixture has been heated under an induced vacuum to remove unnecessary solvents, the reaction mixture is transferred to a molten salt

bath, set to 345°C. Ultrapure nitrogen gas is bubbled through the mixture while the decomposition and final reaction is taking place at 340°C. This reaction is closely monitored for 25 minutes. During the final reaction, hydrogen fluoride (HF) is generated and filtered out of through the bubbling process. Once the reaction has come to completion, an IR laser pen is used to confirm the emission band of the particles. The reaction mixture is removed from the molten salt bath and cooled. The reaction is quenched with 3 mL of octadecene, followed by 10 mL of ethanol and 10-20 mL of hexanes to precipitate out the final product. The particles are iteratively washed 3 times in 1:1, ethanol: hexanes solution. The particles are stored in hexanes once complete with the washes.

4.2.2. Surface functionalization of upconverting nanophosphors

Following the synthesis of the various upconverting nanophosphors described in Section 4.2.1. of this dissertation, the surface of these particles are coated with oleic acid. For aqueous solution based experiments, an oily, hydrophobic surface will not work, so we need to exchange out the oleic acid coating for a more water soluble coating. The remainder of this section will describe the procedure for the two coatings used to replace oleic acid. The functionalization will dictate the eventual bio-conjugation of these particles to proteins and antibodies.

4.2.3. Folic acid as a substitute for oleic acid

Surface modification of the upconverting nanophosphors begins with the removal of the passivation ligand. In the cases of the aforementioned synthesis of upconverting nanophosphors, oleic acid is the surface coating. To strip oleic acid coating, the upconverting nanophosphors are washed four times in hexanes to remove any residual ethanol and water. The nanophosphors have been pre-weighed out to 3g, and this weight will be used to determine all other molar quantities. After washing out the particles in hexanes, the particles are left suspended in 10mL of toluene. The final particles should be monodispersed in the solution. To the same vessel, 10mL of dimethylformaldehyde (DMF) is added to the suspended particle solution. There should be two visible liquid phases. A four-fold excess of tetraflouroborate (BF_4^-) is added to vessel. The BF_4^- covers the surface of the particle, removing the oleic acid. The oleic acid is recovered by removing the toluene layer. To ensure all the oleic acid is removed, successive washes toluene with the DMF layer drive any remaining oleic acid from the surface.

Known to be soluble in aqueous environments, folic acid is considered for conjugation to the surface of the upconverting nanophoshor. A 10mL solution of ten-fold excess folic acid is prepared in 20%wt dimethyl sulfoxide (DMSO) and ddH_2O. The solution is added to the DMF layer and washed for 20 minutes on a rocker. Once the wash is complete, the aqueous layer is collected with the folic acid coated particles. Excess BF_4^- and folic acid is removed from the aqueous layer by iterative washes in 200 proof ethanol. After five successive washes in absolute ethanol, the particles are resuspended in 5%wt DMSO in ddH_2O. Any

particles that do not suspend in solution, are collected and weighed to calculate the yield of folic acid coated particles. The particles collected that did not suspend are resuspended in hexanes and undergo the BF_4^- treatment once more. Following the iterative process, all of the folic acid coated particles are suspended in 5%wt DMSO in 0.1M HEPES buffer.

4.2.4. Glutamic acid dendrimers as a substitute for oleic acid

Surface modification of the upconverting nanophosphors begins with the removal of the passivation ligand. In the cases of the aforementioned synthesis of upconverting nanophosphors, oleic acid is the surface coating. To strip oleic acid coating, the upconverting nanophosphors are washed four times in hexanes to remove any residual ethanol and water. The nanophosphors have been pre-weighed out to 3g, and this weight will be used to determine all other molar quantities. After washing out the particles in hexanes, the particles are left suspended in 10mL of hexanes. The final particles should be monodispersed in the solution. To the same vessel, 10mL of dimethylformaldehyde (DMF) is added to the suspended particle solution. There should be two visible liquid phases. A four-fold excess of tetraflouroborate (BF_4^-) is added to vessel. The BF_4^- covers the surface of the particle, removing the oleic acid. The oleic acid is recovered by removing the hexane layer. To ensure all the oleic acid is removed, successive washes hexanes with the DMF layer drive any remaining oleic acid from the surface.

Following surface modification, three prepared glutamic acid dendrimers scaffolds are prepared for replacing BF_4^- on the surface of the particle. A four-fold excess of all three components (ref, glutamic acid paper) is prepared in ddH_2O and reacted with the DMF layer, containing the upconverting nanophosphors. To ensure complete exchange of the glutamic acid dendrimers to the surface of the particle, the organic and aqueous layers are incubated at room temperature on the rocker for 2 hours. Once complete, the DMF layer is removed. Any particles that do not suspend in the aqueous layer are spinned down and removed to check for the reacted product. The suspended particles in the aqueous layer are reacted with dicyclohexylcarbodiimide (DCC), in a 1:1 mole ratio (DCC:Dendrimer), in 5mL of 50%wt DMSO. Since there is no interest in maintaining stereochemistry, N-hydroxybenzotriazole is not a part of this reaction. Following 1 hour of incubation, the particles are precipitated out in hexanes and washed four times to remove any by-products. The particles are resuspended in ddH_2O. Only add 1-5%wt DMSO if there is any issue with agglomerates. The particles that did not suspend in the aqueous solution are treated with BF_4^- and undergo the aforementioned steps to ensure coating of the surface. Following the iterative process, all of the glutamic acid dendrimer coated particles are suspended in 0.1M HEPES buffer.

4.2.5. Functionalizing primary antibody to water soluble particle conjugate

For both glutamic acid and folic acid, exposed amines are reacted with an N-γ-maleimidobutyryl – oxysuccinimide ester (NHS malimide linker) in a pH 9 0.1M HEPES buffer solution. The molar ratio for this reaction is 1:5 coated particle: NHS

malimide linker. This reaction is set up to go for 2 hours at 4°C. Meanwhile, the selected secondary antibody (molar ratio of 1:10 coated particle: primary antibody) is treated with 10nmoles of tris (2-carboxyethyl) phosphine (TCEP) for 2 hours at 4°C. Following the incubation of the two solutions, the TCEP treated antibody solution is added by a 5k molecular weight cut-off spin column to the malimide functionalized particles at pH 7 and incubated at 4°C for 30 minutes. The excess NHS malimide linker is removed by a desalting column before combining with the reducing secondary antibody. An IR laser pen checks the desalting column for any left over particles and checks the eluted solution.

The final crude particle-secondary antibody conjugate is diluted out to 1:100 and aliquoted for long term -80°C storage. An aliquot is left out to test by assaying for the primary antibody/protein target, which is immobilized via poly-d-lysine to a coverslip and imaged by continuous wave low energy fluorescence microscopy.

4.2.6. Immunohistochemical staining of upconverting nanophosphors

Klaus HeLa cells are grown to 70% confluence on sterilzed indium-tin-oxide coverslips. Following this step, the cells are washed 1x HBSS buffer solution, warmed to 37°C, three times. The cells are then fixed in 2%wt paraformaldehyde for 20 minutes. The cells are washed in 0.1M HEPES buffer solution four times to remove any excess paraformaldehyde. The cells were treated with 1x Triton buffer for 30 minutes. The cells were incubated in blocking buffer (2.0%wt BSA, 1.0%wt Goat Serum in 0.1M HEPES buffer solution) for 30 minutes at room temperature.

Meanwhile, a working buffer solution was made from a 100x dilution of the blocking buffer into ddH_2O.

Following blocking the cells, the cells were washed with the working buffer three times for 20 minutes at room temperature. Then the selected primary antibody is incubated with the cells for 48 hours at 4°C. Dilutions of 1:100, 1:500, 1:1000 and 1:5000 are prepared of the primary antibody in the working buffer. A negative control of no primary antibody is set up.

Once the primary antibody has incubated for the 48 hours, the cells are washed once more in working buffer three times for 20 minutes at room temperature. The particle-secondary antibody is prepared in the following dilutions in working buffer: 1:100, 1:500, 1:1000 and 1:5000. These dilutions are incubated on the cells for another 72 hours at 4°C. The negative control is incubated with a 1:100 dilution of the particle-secondary antibody conjugate. While the incubation is taking place, the coverslips are checked to for potential drying of the working solution. More working buffer is applied as the incubation is completing.

Once cells have completed their 72-hour incubation, they are washed three times for 20 minutes at room temperature with working buffer. All dishes of cells are checked by IR pen for any visible emission during the process. A 0.1M HEPES buffer solution is final solution the cells are in before imaging.

4.2.7. Light Microscopy

Klaus HeLa cells containing immunolabel conjugated nanophosphor particles were imaged on a Radiance 2000 microscope (Bio-Rad) equipped with a

Ti-sapphire infrared laser (Spectra-Physics, Santa Clara, CA, USA). The cells were initially imaged with a 10X objective (Nikon, NA 0.3) with pulsed-mode illumination (980 nm) and then continuous wave illumination (980nm), in order to collect nanophosphor and autofluorescence signal, respectively. Sub-regions were then imaged with a 40X objective (Nikon, NA 1.30) using continuous wave illumination at 980nm, simultaneously collecting fluorescence and transmitted light images.

4.2.8. X-ray Microscopy

Most XRM work was performed on a MicroXCT-200 instrument (Zeiss X-Ray Microscopy, Pleasanton, CA, USA). This architecture combines both geometric (as found in conventional microCT constructs) and optical magnification (lens-coupled post-sample magnification) as well as optimized scintillation technologies to yield high-contrast sub-micron 3D reconstructions of a sample. XRM tilt series were generally collected at 40 kV and 4W power (100 A current), unless otherwise noted. A Zeiss Xradia 510 Versa was utilized for these studies as well, as indicated in Figure 3.3.

4.3. Discussion

Considering the methods and materials provided, this section of this chapter aims to address and discuss the use of the techniques and methods accomplished and their viability for correlating biological specimens across light, x-ray and electron microscopy. Also introduced, the novelty in region of interest tracking

techniques novel in use to the field will also be addressed. From this section, this dissertation aims to lay out specific conclusions and achievements in the area of universal markers and multi-modal imaging for correlative microscopy.

4.3.1. Characterization of upconverting nanoparticles

The use of upconverting nanophosphors (UCPs) is becoming a novel tool in multi-scale correlated light, x-ray and electron microscopy. For example, the use of yttrium sulfoxide particles, doped with ytterbium and erbium, as non-specific fiducial markers have led to a novel method in checking for any potential changes in the specimen between heavy metal staining and epoxy resin embedding steps (Bushong and Johnson *et al.* 2014). As shown in figure 1b-d, sizes and shapes are easily made by adjustment of heating times, molar ratios of metal dopants, and cations (lithium, sodium and barium to name a few). Most of the smaller nanoscale particles are made by high temperature (~340-360°C) liquid phase synthetic methods; whereas, the larger micron sized particles are made by higher temperature (~1100-1150°C) solid-state synthetic methods. The host metal, whether it be yttrium, gadolinium, or lanthanum, directs size in conjunction with the molar concentration of ytterbium. However, the major contributor in controlling the size of the particle largely comes from the cation used. For example, barium yttrium fluoride, ytterbium:erbium doped, nanoparticles are usually 4x smaller than lithium yttrium fluoride, ytterbium:erbium doped, nanoparticles.

Figure 4.1., Photo-physics of a upconverting nanoparticle (UCP) as shown in (a.) are primarily driven by a two-photon upconversion process. UCPs come in various sizes and shapes, as shown in (b.), (c.), and (d.).

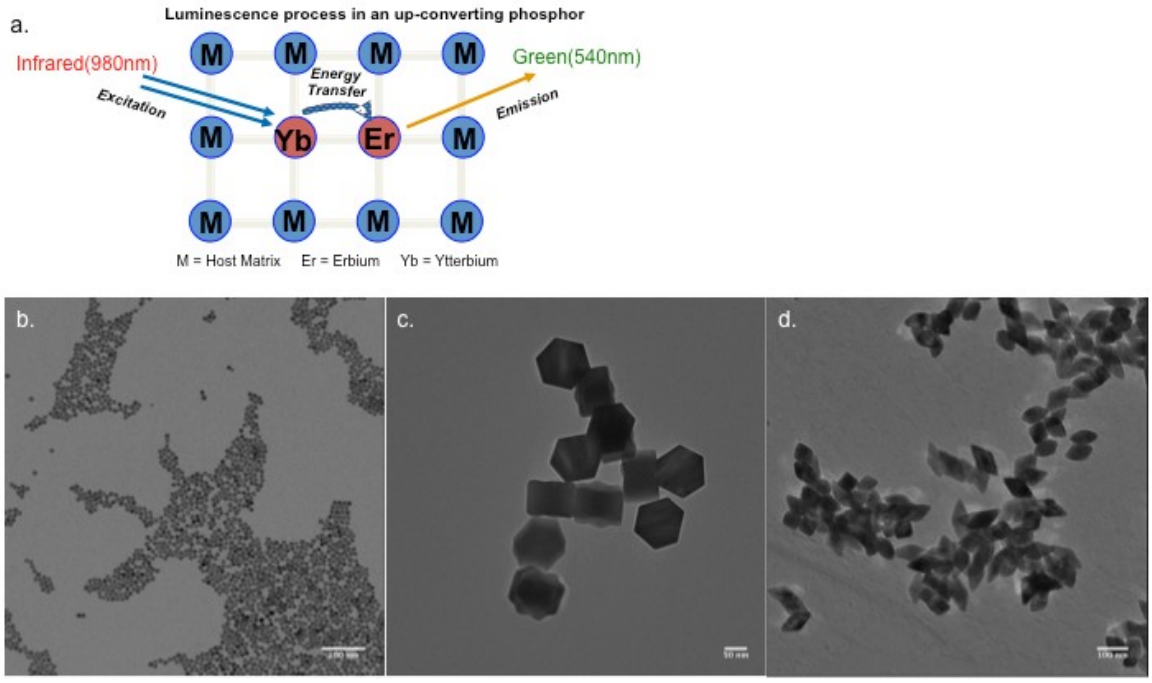
a.
Luminescence process in an up-converting phosphor
Infrared(980nm)
Excitation
Energy Transfer
Green(540nm)
Emission
M
Yb
Er
M = Host Matrix
Er = Erbium
Yb = Ytterbium
b.
c.
d.

The unique photo-physical process of UCPs is mostly based on the two heavy metal dopants. As shown in figure 4.1.a., the ytterbium (Yb) requires two photons of low energy (980nm) to convert to the erbium (Er) and be emitted out at higher energy (540nm). UCP emission undergoes stokes shift when the Er dopant is switched out for thulium (Tm) or holmium (Ho) respectively. Other dopants such as manganese (Mn), neodymium (Nd), europium (Eu) and dysprosium (Dy) are good replacements for Er as the emission source.

Also important to note, upconverting nanoparticles' light emitting properties are inert to osmium staining, thus making them one of the few viable probes for our multi-scale imaging efforts. This is largely due to the difference in the photo-physical mechanism, where two photons are upconverted at one heavy metal to then be emitted as one higher energy photon from another heavy metal. The electronic transitions between metals are buffered by any potential quenching from the osmium tetroxide used to stain the tissue, or cell monolayers.

Herein, I describe the use of UCPs as non-specific fiducial markers for multi-scale correlation across light, x-ray and electron microscopy. So far, work has been accomplished and published on relating fiducials between light and x-ray microscopy. The next step involves mapping the distribution of particles in a biological specimen. From a difference map, potential constrictions and expansions in the specimen can be accounted for while keeping up with the target portion of the volume. Also important, I describe the use of UCPs as a universal probe for multi-scale imaging. So far, immunohistochemistry data is showing some

promise in labeling the particles. Subsequent work will demonstrate the limited but still strategic use of these materials as universal probes.

4.3.2. Developing smaller, water-soluble, brighter particles as probes for multi-scale imaging

The eventual goal has always been to use to smaller, water-soluble, brighter particles as probes for multi-scale imaging. As discussed in the first section, the cation is the major factor in producing a smaller particle, hence, I synthesized barium yttrium fluoride, ytterbium:erbium and ytterbium:thulium doped, nanoparticles. As shown in figure 4.3. a and b, in heating the particles in excess of 370°C for 15 minutes (otherwise known as the decomposition phase of the particle synthesis) after a low-pressure reflux at 140°C for 1 hour, small, spherical nanoparticles are synthesized. These nanoparticles underwent crystalline phase transition during the decomposition phase of the synthesis, from alpha (α) to beta (β) phase transition. The particle distribution is fairly monodispersed at 10 ± 2nm by dynamic light scattering (DLS).

Figure 4.2., Pre and post osmium staining of mouse retina demonstrates limited visibility by most light methods (a.). (b.) is a side by side comparison of a transmission electron micrograph (TEM) and serial blockface scanning electron micrograph (SBEM). (c.) shows the following of phosphors from light to x-ray microscopy (Bushong and Johnson, *et al*. 2014).

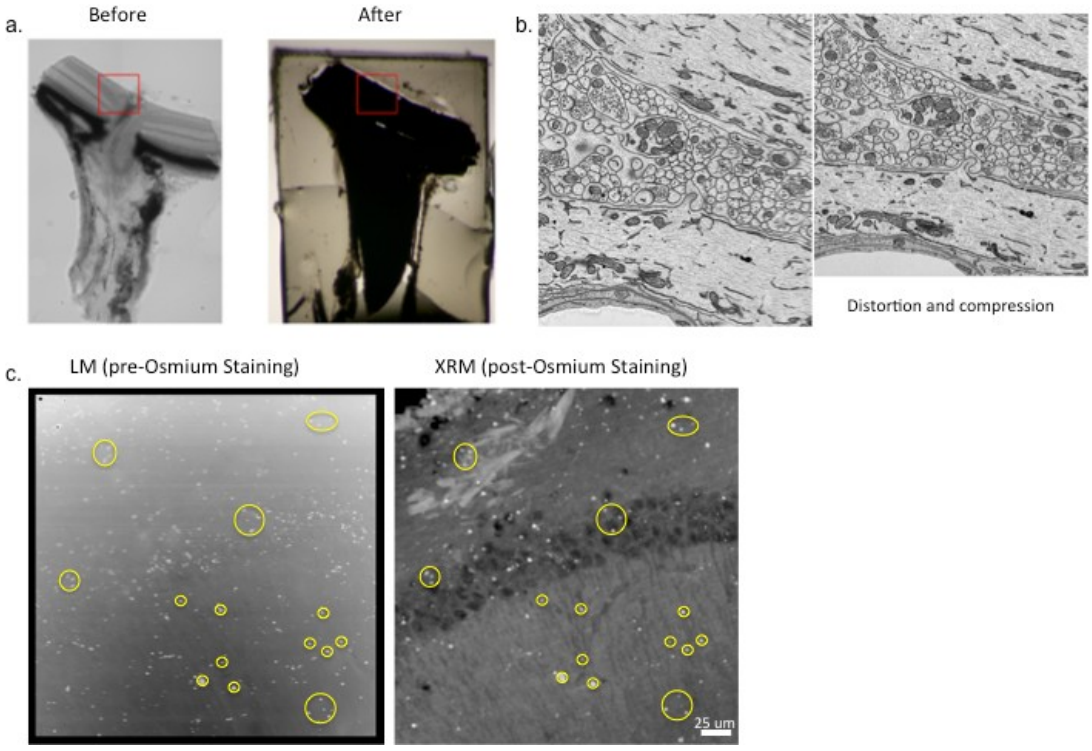
a.
Before
After
b.
Distortion and compression
c.
LM (pre-Osmium Staining)
XRM (post-Osmium Staining)
25 um

Following synthesis of the barium particles, the surface coating post synthesis is oleic acid. A boron fluoride (BF_4^-) treatment is used to remove the oleic acid from the surface of the particle. The BF_4^- coats the surface as a leaving group for whatever ligand of interest is applied. Since we are interested in a water-soluble particle, extensive work has been done to develop water-soluble coatings. One route is the use of glutamic acid dendrimer networks pre-synthesized by solid-phase peptide synthesis. The draw back is that solid-phase peptide synthesis is a tedious process, especially for the combination of desired linkages for the dendrimers to work. As a result, this method is ideal but requires more work than necessary. Another route involves the use of folic acid as a substitute for BF_4^-. Folic acid is not ideal but makes everything easier for the moment.

Following coating of folic acid, the particles undergo a series of washes to remove organics such as dimethylformaldehyde and toluene. Any unreacted folic acid is also removed during these washings. Once the particles are in 10% dimethyl sulfoxide in 0.1M HEPES buffer, the pH is adjusted to 9 and the nanoparticle-folic acid linker are reacted with a NHS maleimide. The excess NHS maleimide is filtered and the particles are brought up in double distilled water and reacted with partially reduced and filtered secondary antibody. Goat anti-rabbit and goat anti-mouse coatings have been made, as shown in Figure 4.3.c.

Figure 4.3., Barium yttrium fluoride, ytterbium:erbium doped, nanoparticles were imaged by TEM [(a.) and (b.)]. These nanoparticles were treated with recoated with folic acid and conjugated to a secondary antibody via a NHS-maleimide (c.).

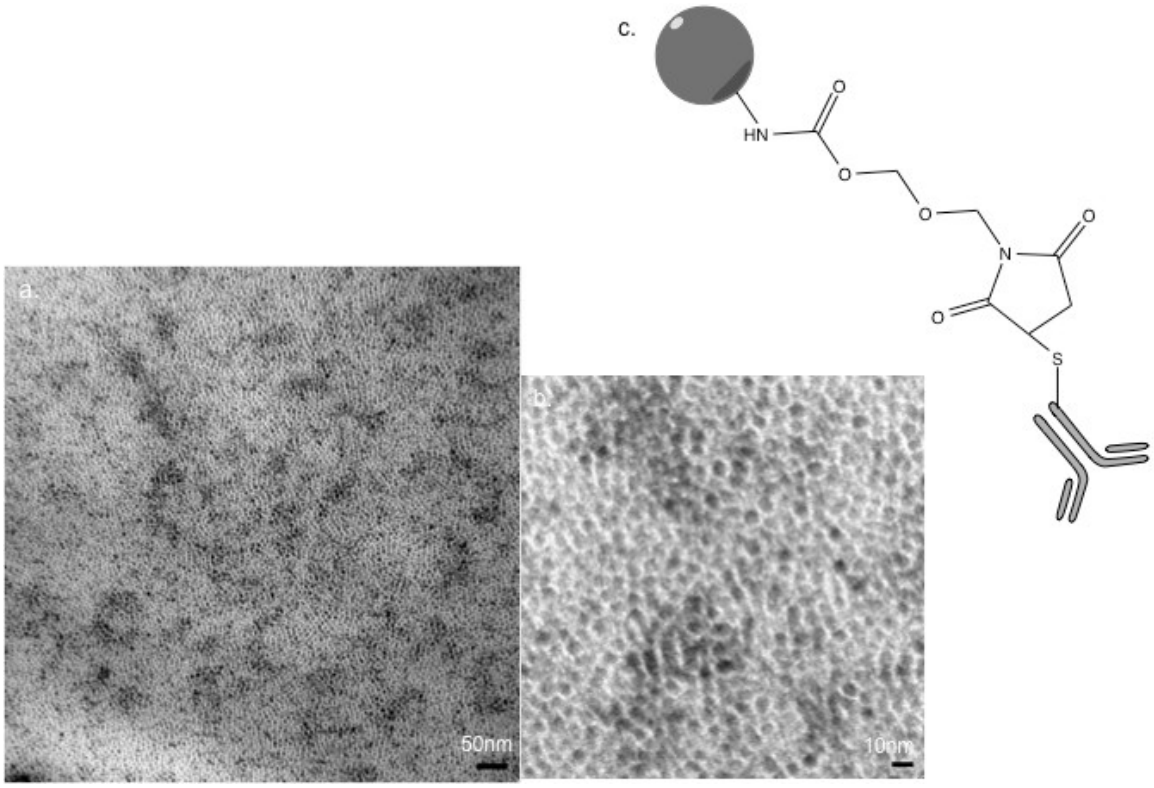
a.
50nm
b.
10nm
c.
HN
O
O
O
O
N
O
O
S

The first target in my studies was synapsin in planaria. Synapsin is ubiquitously expressed in the central nervous system. Using other flourophores, synapsin was fairly easily to label. However, it was difficult to label for the barium anti-rabbit nanoparticles. The planaria membrane was just too hard to remove without effecting the worms ultra-structure of interest. When exposed to harsh treatments for removing the membrane, just to see if we could label the synapsin, the particles barely labeled and provided poor contrast compared to conventional systems.

After plenty of failures with synapsin, cadherin (a membrane protein) ended up being a useful target for the barium anti-rabbit nanoparticles. Cadherin is generally overexpressed in HeLa cells, so I incubated a primary antibody in goat serum for 4 hours, as shown in Figure 4.4.a. Following the washes and incubation of the barium anti-rabbit nanoparticles to cadherin for 18 hours, the cells were washed and imaged by the radiance 2000 in continuous wave (CW) mode. At 20x magnification, there was a clear presence of something fluorescent binding to the cells, as shown in Figure 4.4.b. The issues with this data were not only that it needed to be coupled with controls, but it is also a fairly low-resolution image. The image only piqued the interest of a fairly failure ridden project. So, a series of controls were developed keeping HeLa cells as the cell line of choice. A negative control with no primary antibody was devised to show that the secondary antibodies were not nonspecifically labeling to cells, as shown in Figure 4.5.d. It seems there was no binding of the particle to any biological specimen in this panel. A negative control on the effectiveness of the serum was tested, shown in Figure 4.5.c. Some binding is apparent in this panel, however, there is also random

agglomerations of nanoparticles. This is a promising result for UCP binding but does not answer whether or not the barium anti-rabbit nanoparticles are targeting the cadherin. To test the cadherin primary antibody, we used a Cy5/anti-rabbit conjugate in place of the barium-UCP/anti-rabbit conjugate. The Cy5 emission channel was imaged and yielded binding of the secondary to the cells, as shown in Figure 4.5.b. This not only proves that the primary antibodies are working but also where to look for structure in Figure 4.5.a, where all conditions are consistent with figure 4b except the cells are being imaged at 40x magnification.

Figure 4.5., Four panels demonstrating the binding efficacy of barium anti-rabbit UCPs. Panel (a) is an image following the incubation/wash of the barium anti-rabbit UCPs to the anti-cadherin rabbit primary in goat serum. Panel (b) is an image following the incubation/wash of a Cy5/anti-rabbit conjugate to a anti-cadherin rabbit primary in goat serum. Panel (c) is an image following the incubation/wash of the barium anti-rabbit UCPs to the anti-cadherin rabbit primary in rabbit serum. Panel (d) is an image following the incubation/wash of the barium anti-rabbit UCPs in goat serum.

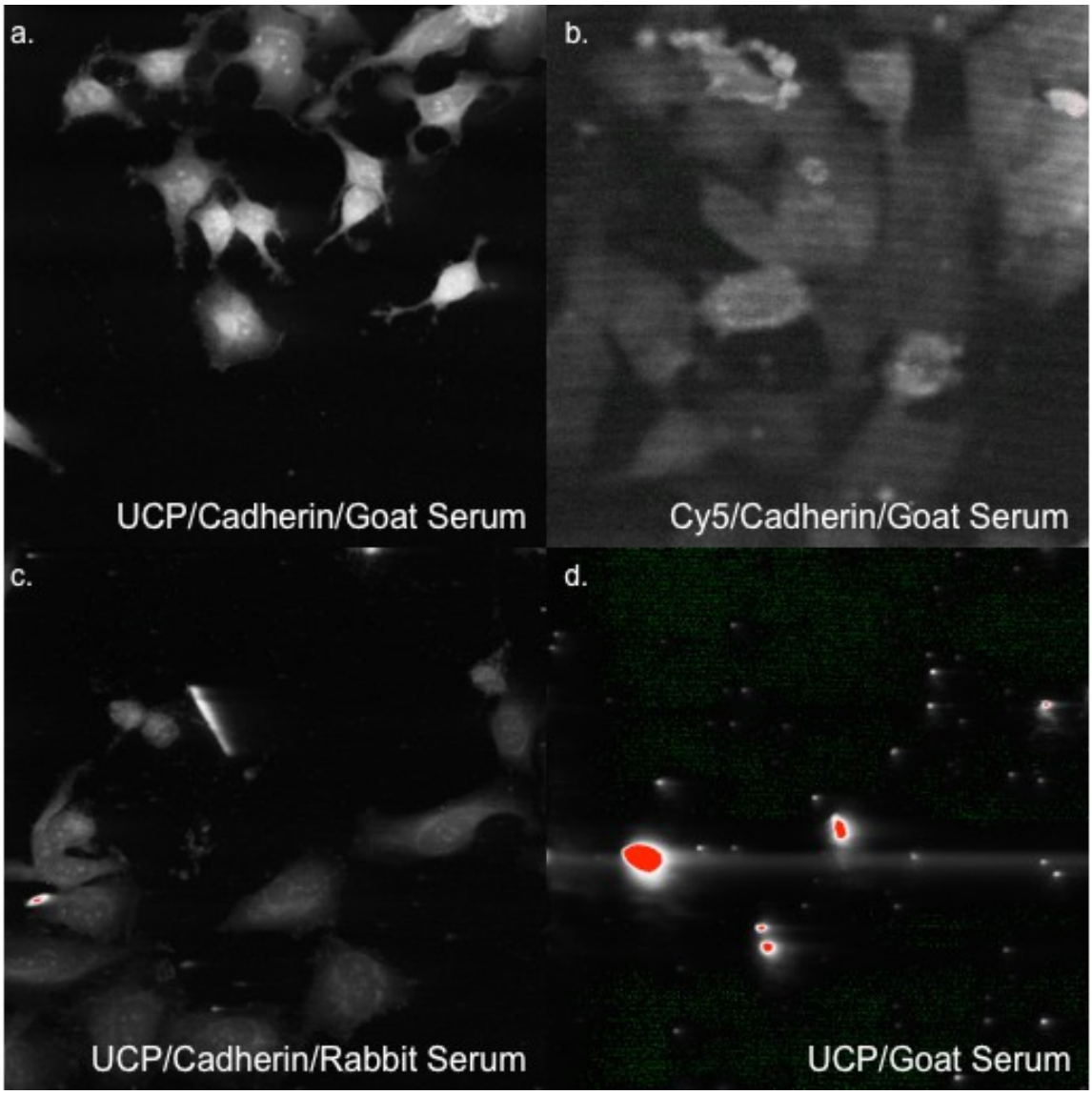
a.
UCP/Cadherin/Goat Serum
b.
Cy5/Cadherin/Goat Serum
c.
UCP/Cadherin/Rabbit Serum
d.
UCP/Goat Serum

Once more, the signal is isolated to the cells pointing to some binding that is specific and not random for the barium anti-rabbit nanoparticle. The down side to this set up of experiments is that we cannot control the expression of cadherin in the cell. To address this issue, we to expressed a new membrane protein target, aquaporin 4 in 293T cells. The aquaporin expression was consistent in the controls with Cy5 labeled cells. An aquaporin 4 knock out (Figure 4.6.) was also consistent with labeling parameters. Coupled with experimental details shown in Figure 4.5., the data demonstrates the potential of using UCP labels as targets for extracellular exposed membrane epitopes under our multi-modal imaging efforts.

Figure 4.6., Transfected 293T cells for overexpression of Aquaporin 4, targeted by $BaYF_4$: Yb, Er (UCP), were compared to the knock down. Cy5 (left) was used as a control against UCP secondary conjugated (right) labels.

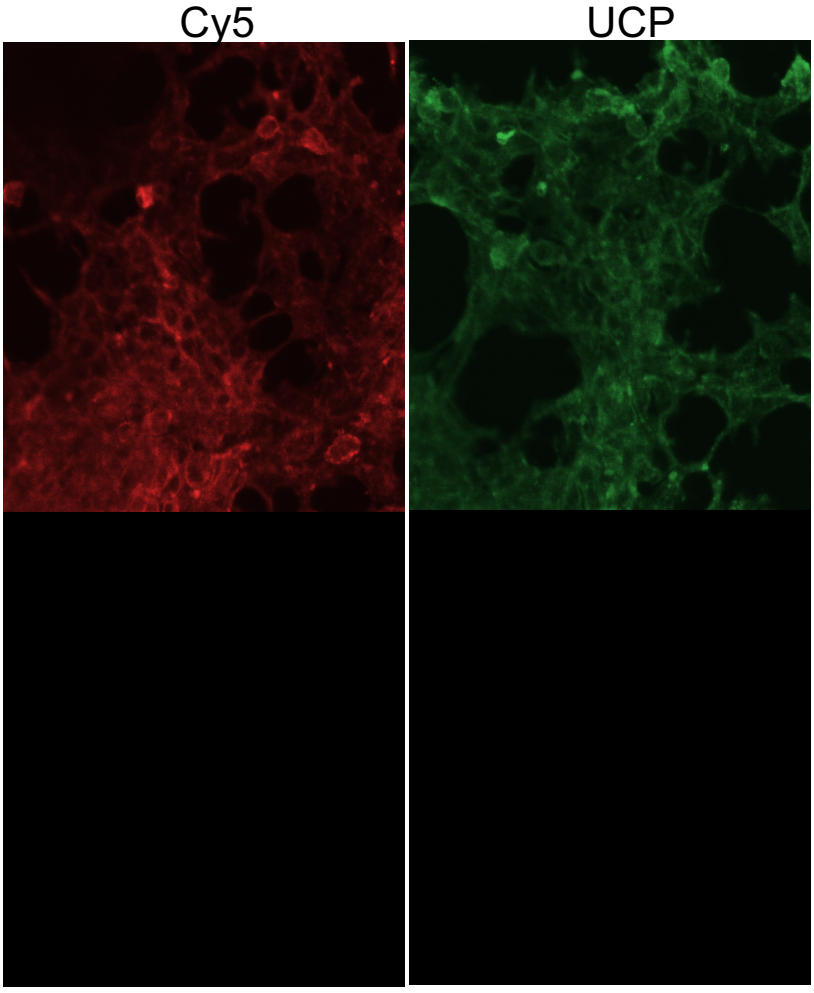

Knock down

In acknowledging the contributors to Chapter IV, Josh was instrumental in the development of the nanophosphor particles. Most of the labeling protocols involved were developed by Junru and Tom. Thank you for your assistance in this project.

Chapter V

Conclusions and Future Perspectives

5.1. Contributions, significance and limitations

Efforts in improving and multi-plexing data upon one another has crossed over into correlative microscopy. In particular, interest in correlating imaging of a biological specimen has left the field open to the need for a universal marker, or probe capable of being identified by multiple modalities. Also important, metal staining protocols has been the major issue for reversibility and imaging under light microscopy. Commonplace fluorescent probes are quenched by osmium tetroxide. Also noteworthy, fluorescent probes, if tolerant to osmium, are lost to the black opacity of the metal stained tissue.

Using upconverting nanoparticles as fiducials aims to revolutionize the way region of interest are tracked across multiple modalities. In having a fiducial that is visible by light, x-ray and electron microscopy, a region of interest can be mapped, scaled and compared under another imaging modality. Software that already exist for mapping ROIs can be designed to be a difference point assessment for evaluating potential compressions or distortions by dehydration and other staining processes.

As labels, UCPs are so far ideal for targeting membrane proteins. As a label, UCPs tag directly to the target and can provide orthogonal information across all modalities. Knock down data for aquaporin 4 clearly demonstrated that we have a tag and a route for tagging the surface of cells. Cadherin data points also clearly demonstrate targeting by UCP immunolabel conjugates.

In drawing connections to the serial block-face scanning electron microscope from the other imaging modalities, UCP development will assist in

quality controlling and following data from other imaging platforms. Workflows for correlated microscopy will be supported by the fiducial marker architecture. Eventually, UCP targeting will be incorporated into correlated light, x-ray and electron microscopy projects driving biological questions.

Efforts in improving contrast and resolution are deeply connected to the continued viability of this instrument. The most important hurdle before this dissertation was overcoming resin charging. This came with improvements to the resin, in terms of assisting charge transfer, via making the resin more conductive. While working out the schematics of the project, efforts were also taken in addressing charging by assembly of a scaffold. A combination of using polyaromatic structures and this matrix will solve the charging issue for SBEM imaging, making this a viable technique at high vacuum. The techniques employed for assessing charging have never been previously considered for SBEM.

5.2. Future Perspectives

Use of the upconverting nanoparticles in crosslinked multi-level liposomes will be the next development for targeting cells and the particular macromolecules. This will become a powerful tool in advancing the x-ray imaging field for identifying lung cancer in patients, as there is no early detection method for lung cancer. This could lead to building multitudes of diagnostics. This could also expand multi-modal correlative microscopy to the medical field.

Use of UCPs as fiducials for quality controlling samples across modalities will be key for staining protocols, which introduce stress to the sample and could

alter the ultra-structure of the biological specimen. Region of interest tracking will be easier with a higher throughput imaging workflow. Details in spacing between individual particles will be key in specifying ROIs for biological specimen. Nanometer level details will be easier to map by this method.

Improvements in contrast and resolution as a result of enhanced conductivity will lead to developments in reduced landing energies for even lower energy SBEM. Details in spatial resolution will become important as this project unfolds. A key contribution is not only the formation of this method for imaging at low energies but the parallel advancement in quantifying permittivity in materials for future projects involving SEM.

Appendix A IMOD Source Code

```
Don-Johnsons-MacBook-Pro:Matrix_10-10-15_VP djohnson$ newstack -bi 2
run3_3VBSED_slice_0*.mrc run3_3VBSED_bin2.st

 RO image file on unit   1 : run3_3VBSED_slice_0000.mrc     Size=     105469 K

 Number of columns, rows, sections .....    9000    6000       1
 Map mode ..............................    1   (16-bit integer)
 Start cols, rows, sects, grid x,y,z ...    0     0     0    9000   6000      1
 Pixel spacing (Angstroms)..............   64.48      64.48      64.48
 Cell angles ...........................   90.000   90.000   90.000
 Fast, medium, slow axes ..............    X    Y    Z
 Origin on x,y,z .......................    0.000       0.000       0.000
 Minimum density .......................  -26010.
 Maximum density .......................  -12060.
 Mean density ..........................  -17027.
 tilt angles (original,current) ........   0.0   0.0   0.0   0.0   0.0   0.0
 Space group,# extra bytes,idtype,lens .        0        0        0        0

     1 Titles :
raw2mrc: Converted to mrc format.                    18-Oct-15  12:56:33


 NEW image file on unit   2 : run3_3VBSED_bin2.st
 section   input min&max       output min&max  &  mean
    0 -23703.00 -13369.25 -23703.00 -13369.25 -17068.54

 RO image file on unit   1 : run3_3VBSED_slice_0001.mrc     Size=     105469 K

 Number of columns, rows, sections .....    9000    6000       1
 Map mode ..............................    1   (16-bit integer)
 Start cols, rows, sects, grid x,y,z ...    0     0     0    9000   6000      1
 Pixel spacing (Angstroms)..............   64.48      64.48      64.48
 Cell angles ...........................   90.000   90.000   90.000
 Fast, medium, slow axes ..............    X    Y    Z
 Origin on x,y,z .......................    0.000       0.000       0.000
 Minimum density .......................  -25566.
 Maximum density .......................  -12374.
 Mean density ..........................  -16824.
 tilt angles (original,current) ........   0.0   0.0   0.0   0.0   0.0   0.0
 Space group,# extra bytes,idtype,lens .        0        0        0        0

     1 Titles :
raw2mrc: Converted to mrc format.                    18-Oct-15  12:56:49
```

```
    1 -23328.25 -13297.25 -23328.25 -13297.25 -16846.05

 RO image file on unit   1 : run3_3VBSED_slice_0002.mrc     Size=     105469 K

 Number of columns, rows, sections .....    9000    6000       1
 Map mode ..............................    1   (16-bit integer)
 Start cols, rows, sects, grid x,y,z ...    0     0     0    9000   6000      1
 Pixel spacing (Angstroms)..............   64.48      64.48      64.48
 Cell angles ...........................   90.000   90.000   90.000
 Fast, medium, slow axes ...............    X    Y    Z
 Origin on x,y,z .......................    0.000       0.000       0.000
 Minimum density .......................  -25489.
 Maximum density .......................  -12127.
 Mean density ..........................  -16661.
 tilt angles (original,current) ........   0.0   0.0   0.0   0.0   0.0   0.0
 Space group,# extra bytes,idtype,lens .        0        0        0        0

    1 Titles :
raw2mrc: Converted to mrc format.                    18-Oct-15  12:57:06

    2 -23630.00 -13370.25 -23630.00 -13370.25 -16658.25

 RO image file on unit   1 : run3_3VBSED_slice_0003.mrc     Size=     105469 K

 Number of columns, rows, sections .....    9000    6000       1
 Map mode ..............................    1   (16-bit integer)
 Start cols, rows, sects, grid x,y,z ...    0     0     0    9000   6000      1
 Pixel spacing (Angstroms)..............   64.48      64.48      64.48
 Cell angles ...........................   90.000   90.000   90.000
 Fast, medium, slow axes ...............    X    Y    Z
 Origin on x,y,z .......................    0.000       0.000       0.000
 Minimum density .......................  -25283.
 Maximum density .......................  -12251.
 Mean density ..........................  -16514.
 tilt angles (original,current) ........   0.0   0.0   0.0   0.0   0.0   0.0
 Space group,# extra bytes,idtype,lens .        0        0        0        0

    1 Titles :
raw2mrc: Converted to mrc format.                    18-Oct-15  12:57:20

    3 -23419.00 -13370.00 -23419.00 -13370.00 -16484.21

 RO image file on unit   1 : run3_3VBSED_slice_0004.mrc     Size=     105469 K
```

```
 Number of columns, rows, sections .....    9000    6000       1
 Map mode ..............................    1   (16-bit integer)
 Start cols, rows, sects, grid x,y,z ...    0     0     0    9000   6000      1
 Pixel spacing (Angstroms)..............   64.48      64.48      64.48
 Cell angles ...........................   90.000   90.000   90.000
 Fast, medium, slow axes ...............    X    Y    Z
 Origin on x,y,z .......................    0.000       0.000       0.000
 Minimum density .......................  -25161.
 Maximum density .......................  -12016.
 Mean density ..........................  -16412.
 tilt angles (original,current) ........   0.0   0.0   0.0   0.0   0.0   0.0
 Space group,# extra bytes,idtype,lens .        0        0        0        0

    1 Titles :
raw2mrc: Converted to mrc format.                    18-Oct-15  12:57:34

    4 -23024.00 -13317.25 -23024.00 -13317.25 -16345.17

 RO image file on unit   1 : run3_3VBSED_slice_0005.mrc     Size=     105469 K

 Number of columns, rows, sections .....    9000    6000       1
 Map mode ..............................    1   (16-bit integer)
 Start cols, rows, sects, grid x,y,z ...    0     0     0    9000   6000      1
 Pixel spacing (Angstroms)..............   64.48      64.48      64.48
 Cell angles ...........................   90.000   90.000   90.000
 Fast, medium, slow axes ...............    X    Y    Z
 Origin on x,y,z .......................    0.000       0.000       0.000
 Minimum density .......................  -24761.
 Maximum density .......................  -12165.
 Mean density ..........................  -16339.
 tilt angles (original,current) ........   0.0   0.0   0.0   0.0   0.0   0.0
 Space group,# extra bytes,idtype,lens .        0        0        0        0

    1 Titles :
raw2mrc: Converted to mrc format.                    18-Oct-15  12:57:52

    5 -23441.50 -12846.50 -23441.50 -12846.50 -16228.54

 RO image file on unit   1 : run3_3VBSED_slice_0006.mrc     Size=     105469 K

 Number of columns, rows, sections .....    9000    6000       1
 Map mode ..............................    1   (16-bit integer)
 Start cols, rows, sects, grid x,y,z ...    0     0     0    9000   6000      1
 Pixel spacing (Angstroms)..............   64.48      64.48      64.48
 Cell angles ...........................   90.000   90.000   90.000
```

```
 Fast, medium, slow axes .....    X    Y    Z
 Origin on x,y,z .....    0.000       0.000       0.000
 Minimum density .....  -24815.
 Maximum density .....  -12137.
 Mean density .....  -16285.
 tilt angles (original,current) .....   0.0   0.0   0.0   0.0   0.0   0.0
 Space group,# extra bytes,idtype,lens .        0        0        0        0

    1 Titles :
raw2mrc: Converted to mrc format.                    18-Oct-15  12:58:04

    6 -23030.50 -13308.00 -23030.50 -13308.00 -16133.99

 RO image file on unit   1 : run3_3VBSED_slice_0007.mrc     Size=     105469 K

 Number of columns, rows, sections .....    9000    6000       1
 Map mode .....    1   (16-bit integer)
 Start cols, rows, sects, grid x,y,z ...    0     0     0    9000   6000      1
 Pixel spacing (Angstroms).....   64.48      64.48      64.48
 Cell angles .....   90.000   90.000   90.000
 Fast, medium, slow axes .....    X    Y    Z
 Origin on x,y,z .....    0.000       0.000       0.000
 Minimum density .....  -24060.
 Maximum density .....  -12152.
 Mean density .....  -16258.
 tilt angles (original,current) .....   0.0   0.0   0.0   0.0   0.0   0.0
 Space group,# extra bytes,idtype,lens .        0        0        0        0

    1 Titles :
raw2mrc: Converted to mrc format.                    18-Oct-15  12:58:16

    7 -22693.00 -13323.50 -22693.00 -13323.50 -16077.33

 RO image file on unit   1 : run3_3VBSED_slice_0008.mrc     Size=     105469 K

 Number of columns, rows, sections .....    9000    6000       1
 Map mode .....    1   (16-bit integer)
 Start cols, rows, sects, grid x,y,z ...    0     0     0    9000   6000      1
 Pixel spacing (Angstroms).....   64.48      64.48      64.48
 Cell angles .....   90.000   90.000   90.000
 Fast, medium, slow axes .....    X    Y    Z
 Origin on x,y,z .....    0.000       0.000       0.000
 Minimum density .....  -22253.
 Maximum density .....  -12026.
 Mean density .....  -16245.
```

```
 tilt angles (original,current) .....   0.0   0.0   0.0   0.0   0.0   0.0
 Space group,# extra bytes,idtype,lens .       0       0       0       0

    1 Titles :
raw2mrc: Converted to mrc format.                  18-Oct-15  12:58:28

    8 -21121.00 -13309.00 -21121.00 -13309.00 -16044.26

 RO image file on unit   1 : run3_3VBSED_slice_0009.mrc     Size=     105469 K

 Number of columns, rows, sections .....    9000    6000       1
 Map mode ..............................    1   (16-bit integer)
 Start cols, rows, sects, grid x,y,z ...    0     0     0    9000   6000      1
 Pixel spacing (Angstroms)..............   64.48      64.48      64.48
 Cell angles ...........................   90.000   90.000   90.000
 Fast, medium, slow axes ...............    X    Y    Z
 Origin on x,y,z .......................    0.000       0.000       0.000
 Minimum density .......................  -22434.
 Maximum density .......................  -12133.
 Mean density ..........................  -16235.
 tilt angles (original,current) .....   0.0   0.0   0.0   0.0   0.0   0.0
 Space group,# extra bytes,idtype,lens .       0       0       0       0

    1 Titles :
raw2mrc: Converted to mrc format.                  18-Oct-15  12:58:42

    9 -20473.50 -13052.25 -20473.50 -13052.25 -16011.07

 RO image file on unit   1 : run3_3VBSED_slice_0010.mrc     Size=     105469 K

 Number of columns, rows, sections .....    9000    6000       1
 Map mode ..............................    1   (16-bit integer)
 Start cols, rows, sects, grid x,y,z ...    0     0     0    9000   6000      1
 Pixel spacing (Angstroms)..............   64.48      64.48      64.48
 Cell angles ...........................   90.000   90.000   90.000
 Fast, medium, slow axes ...............    X    Y    Z
 Origin on x,y,z .......................    0.000       0.000       0.000
 Minimum density .......................  -31402.
 Maximum density .......................  -12106.
 Mean density ..........................  -16225.
 tilt angles (original,current) .....   0.0   0.0   0.0   0.0   0.0   0.0
 Space group,# extra bytes,idtype,lens .       0       0       0       0

    1 Titles :
raw2mrc: Converted to mrc format.                  18-Oct-15  12:58:56
```

```
   10 -23016.50 -13165.25 -23016.50 -13165.25 -15989.90

 RO image file on unit   1 : run3_3VBSED_slice_0011.mrc     Size=     105469 K

 Number of columns, rows, sections .....    9000    6000       1
 Map mode ..............................    1   (16-bit integer)
 Start cols, rows, sects, grid x,y,z ...    0     0     0    9000   6000      1
 Pixel spacing (Angstroms)..............   64.48      64.48      64.48
 Cell angles ...........................   90.000   90.000   90.000
 Fast, medium, slow axes ...............    X    Y    Z
 Origin on x,y,z .......................    0.000       0.000       0.000
 Minimum density .......................  -24107.
 Maximum density .......................  -12068.
 Mean density ..........................  -16218.
 tilt angles (original,current) ........   0.0   0.0   0.0   0.0   0.0   0.0
 Space group,# extra bytes,idtype,lens .        0        0        0        0

     1 Titles :
raw2mrc: Converted to mrc format.                    18-Oct-15  12:59:08

   11 -20692.75 -13112.75 -20692.75 -13112.75 -15966.44

 RO image file on unit   1 : run3_3VBSED_slice_0012.mrc     Size=     105469 K

 Number of columns, rows, sections .....    9000    6000       1
 Map mode ..............................    1   (16-bit integer)
 Start cols, rows, sects, grid x,y,z ...    0     0     0    9000   6000      1
 Pixel spacing (Angstroms)..............   64.48      64.48      64.48
 Cell angles ...........................   90.000   90.000   90.000
 Fast, medium, slow axes ...............    X    Y    Z
 Origin on x,y,z .......................    0.000       0.000       0.000
 Minimum density .......................  -22139.
 Maximum density .......................  -12100.
 Mean density ..........................  -16216.
 tilt angles (original,current) ........   0.0   0.0   0.0   0.0   0.0   0.0
 Space group,# extra bytes,idtype,lens .        0        0        0        0

     1 Titles :
raw2mrc: Converted to mrc format.                    18-Oct-15  12:59:20

   12 -20742.50 -13220.50 -20742.50 -13220.50 -15960.45

 RO image file on unit   1 : run3_3VBSED_slice_0013.mrc     Size=     105469 K
```

```
 Number of columns, rows, sections .....    9000    6000       1
 Map mode ..............................    1   (16-bit integer)
 Start cols, rows, sects, grid x,y,z ...    0     0     0    9000   6000      1
 Pixel spacing (Angstroms)..............   64.48      64.48      64.48
 Cell angles ...........................   90.000   90.000   90.000
 Fast, medium, slow axes ...............    X    Y    Z
 Origin on x,y,z .......................    0.000       0.000       0.000
 Minimum density .......................  -22559.
 Maximum density .......................  -12030.
 Mean density ..........................  -16201.
 tilt angles (original,current) ........   0.0   0.0   0.0   0.0   0.0   0.0
 Space group,# extra bytes,idtype,lens .        0        0        0        0

     1 Titles :
raw2mrc: Converted to mrc format.                    18-Oct-15  12:59:32

    13 -21877.75 -13314.50 -21877.75 -13314.50 -15921.69

 RO image file on unit   1 : run3_3VBSED_slice_0014.mrc     Size=     105469 K

 Number of columns, rows, sections .....    9000    6000       1
 Map mode ..............................    1   (16-bit integer)
 Start cols, rows, sects, grid x,y,z ...    0     0     0    9000   6000      1
 Pixel spacing (Angstroms)..............   64.48      64.48      64.48
 Cell angles ...........................   90.000   90.000   90.000
 Fast, medium, slow axes ...............    X    Y    Z
 Origin on x,y,z .......................    0.000       0.000       0.000
 Minimum density .......................  -22409.
 Maximum density .......................  -11838.
 Mean density ..........................  -16199.
 tilt angles (original,current) ........   0.0   0.0   0.0   0.0   0.0   0.0
 Space group,# extra bytes,idtype,lens .        0        0        0        0

     1 Titles :
raw2mrc: Converted to mrc format.                    18-Oct-15  12:59:44

    14 -20605.50 -13231.75 -20605.50 -13231.75 -15907.61

 RO image file on unit   1 : run3_3VBSED_slice_0015.mrc     Size=     105469 K

 Number of columns, rows, sections .....    9000    6000       1
 Map mode ..............................    1   (16-bit integer)
 Start cols, rows, sects, grid x,y,z ...    0     0     0    9000   6000      1
 Pixel spacing (Angstroms)..............   64.48      64.48      64.48
 Cell angles ...........................   90.000   90.000   90.000
```

```
 Fast, medium, slow axes .....    X    Y    Z
 Origin on x,y,z .....    0.000       0.000       0.000
 Minimum density .....  -31234.
 Maximum density .....  -12187.
 Mean density .....  -16195.
 tilt angles (original,current) .....   0.0   0.0   0.0   0.0   0.0   0.0
 Space group,# extra bytes,idtype,lens .        0        0        0        0

     1 Titles :
raw2mrc: Converted to mrc format.                    18-Oct-15  12:59:56

    15 -23284.00 -13225.50 -23284.00 -13225.50 -15895.62

 RO image file on unit   1 : run3_3VBSED_slice_0016.mrc     Size=     105469 K

 Number of columns, rows, sections .....    9000    6000       1
 Map mode .....    1   (16-bit integer)
 Start cols, rows, sects, grid x,y,z ...    0     0     0    9000   6000      1
 Pixel spacing (Angstroms).....   64.48      64.48      64.48
 Cell angles .....   90.000   90.000   90.000
 Fast, medium, slow axes .....    X    Y    Z
 Origin on x,y,z .....    0.000       0.000       0.000
 Minimum density .....  -21909.
 Maximum density .....  -11941.
 Mean density .....  -16188.
 tilt angles (original,current) .....   0.0   0.0   0.0   0.0   0.0   0.0
 Space group,# extra bytes,idtype,lens .        0        0        0        0

     1 Titles :
raw2mrc: Converted to mrc format.                    18-Oct-15  13:00:12

    16 -20526.25 -13136.00 -20526.25 -13136.00 -15872.44

 RO image file on unit   1 : run3_3VBSED_slice_0017.mrc     Size=     105469 K

 Number of columns, rows, sections .....    9000    6000       1
 Map mode .....    1   (16-bit integer)
 Start cols, rows, sects, grid x,y,z ...    0     0     0    9000   6000      1
 Pixel spacing (Angstroms).....   64.48      64.48      64.48
 Cell angles .....   90.000   90.000   90.000
 Fast, medium, slow axes .....    X    Y    Z
 Origin on x,y,z .....    0.000       0.000       0.000
 Minimum density .....  -22714.
 Maximum density .....  -11617.
 Mean density .....  -16181.
```

```
 tilt angles (original,current) .....   0.0   0.0   0.0   0.0   0.0   0.0
 Space group,# extra bytes,idtype,lens .       0       0       0       0

     1 Titles :
raw2mrc: Converted to mrc format.                  18-Oct-15  13:00:25

    17 -20843.00 -13084.50 -20843.00 -13084.50 -15849.61

 RO image file on unit   1 : run3_3VBSED_slice_0018.mrc     Size=     105469 K

 Number of columns, rows, sections .....    9000    6000       1
 Map mode ..............................    1   (16-bit integer)
 Start cols, rows, sects, grid x,y,z ...    0     0     0    9000   6000      1
 Pixel spacing (Angstroms)..............   64.48      64.48      64.48
 Cell angles ...........................   90.000   90.000   90.000
 Fast, medium, slow axes ...............    X    Y    Z
 Origin on x,y,z .......................    0.000       0.000       0.000
 Minimum density .......................  -22129.
 Maximum density .......................  -11907.
 Mean density ..........................  -16172.
 tilt angles (original,current) .....   0.0   0.0   0.0   0.0   0.0   0.0
 Space group,# extra bytes,idtype,lens .       0       0       0       0

     1 Titles :
raw2mrc: Converted to mrc format.                  18-Oct-15  13:00:40

    18 -20643.25 -13010.50 -20643.25 -13010.50 -15827.93

 RO image file on unit   1 : run3_3VBSED_slice_0019.mrc     Size=     105469 K

 Number of columns, rows, sections .....    9000    6000       1
 Map mode ..............................    1   (16-bit integer)
 Start cols, rows, sects, grid x,y,z ...    0     0     0    9000   6000      1
 Pixel spacing (Angstroms)..............   64.48      64.48      64.48
 Cell angles ...........................   90.000   90.000   90.000
 Fast, medium, slow axes ...............    X    Y    Z
 Origin on x,y,z .......................    0.000       0.000       0.000
 Minimum density .......................  -22043.
 Maximum density .......................  -12001.
 Mean density ..........................  -16172.
 tilt angles (original,current) .....   0.0   0.0   0.0   0.0   0.0   0.0
 Space group,# extra bytes,idtype,lens .       0       0       0       0

     1 Titles :
raw2mrc: Converted to mrc format.                  18-Oct-15  13:00:53
```

```
   19 -20623.25 -13247.50 -20623.25 -13247.50 -15821.99

 RO image file on unit   1 : run3_3VBSED_slice_0020.mrc     Size=     105469 K

 Number of columns, rows, sections .....    9000    6000       1
 Map mode ..............................    1   (16-bit integer)
 Start cols, rows, sects, grid x,y,z ...    0     0     0    9000   6000      1
 Pixel spacing (Angstroms)..............   64.48      64.48      64.48
 Cell angles ...........................   90.000   90.000   90.000
 Fast, medium, slow axes ...............    X    Y    Z
 Origin on x,y,z .......................    0.000       0.000       0.000
 Minimum density .......................  -21695.
 Maximum density .......................  -12038.
 Mean density ..........................  -16165.
 tilt angles (original,current) ........   0.0   0.0   0.0   0.0   0.0   0.0
 Space group,# extra bytes,idtype,lens .        0        0        0        0

     1 Titles :
raw2mrc: Converted to mrc format.                    18-Oct-15  13:01:07

   20 -20935.25 -13139.25 -20935.25 -13139.25 -15803.86

 RO image file on unit   1 : run3_3VBSED_slice_0021.mrc     Size=     105469 K

 Number of columns, rows, sections .....    9000    6000       1
 Map mode ..............................    1   (16-bit integer)
 Start cols, rows, sects, grid x,y,z ...    0     0     0    9000   6000      1
 Pixel spacing (Angstroms)..............   64.48      64.48      64.48
 Cell angles ...........................   90.000   90.000   90.000
 Fast, medium, slow axes ...............    X    Y    Z
 Origin on x,y,z .......................    0.000       0.000       0.000
 Minimum density .......................  -22515.
 Maximum density .......................  -11895.
 Mean density ..........................  -16157.
 tilt angles (original,current) ........   0.0   0.0   0.0   0.0   0.0   0.0
 Space group,# extra bytes,idtype,lens .        0        0        0        0

     1 Titles :
raw2mrc: Converted to mrc format.                    18-Oct-15  13:01:28

   21 -20648.25 -13097.00 -20648.25 -13097.00 -15785.90

 RO image file on unit   1 : run3_3VBSED_slice_0022.mrc     Size=     105469 K
```

```
 Number of columns, rows, sections .....    9000    6000       1
 Map mode ..............................    1   (16-bit integer)
 Start cols, rows, sects, grid x,y,z ...    0     0     0    9000   6000      1
 Pixel spacing (Angstroms)..............   64.48      64.48      64.48
 Cell angles ...........................   90.000   90.000   90.000
 Fast, medium, slow axes ...............    X    Y    Z
 Origin on x,y,z .......................    0.000       0.000       0.000
 Minimum density .......................  -22964.
 Maximum density .......................  -11789.
 Mean density ..........................  -16160.
 tilt angles (original,current) ........   0.0   0.0   0.0   0.0   0.0   0.0
 Space group,# extra bytes,idtype,lens .        0        0        0        0

     1 Titles :
raw2mrc: Converted to mrc format.                    18-Oct-15  13:01:40

   22 -21118.50 -13194.50 -21118.50 -13194.50 -15778.36

 RO image file on unit   1 : run3_3VBSED_slice_0023.mrc     Size=     105469 K

 Number of columns, rows, sections .....    9000    6000       1
 Map mode ..............................    1   (16-bit integer)
 Start cols, rows, sects, grid x,y,z ...    0     0     0    9000   6000      1
 Pixel spacing (Angstroms)..............   64.48      64.48      64.48
 Cell angles ...........................   90.000   90.000   90.000
 Fast, medium, slow axes ...............    X    Y    Z
 Origin on x,y,z .......................    0.000       0.000       0.000
 Minimum density .......................  -26352.
 Maximum density .......................  -11480.
 Mean density ..........................  -16146.
 tilt angles (original,current) ........   0.0   0.0   0.0   0.0   0.0   0.0
 Space group,# extra bytes,idtype,lens .        0        0        0        0

     1 Titles :
raw2mrc: Converted to mrc format.                    18-Oct-15  13:02:11

   23 -21106.25 -13150.75 -21106.25 -13150.75 -15758.13

 RO image file on unit   1 : run3_3VBSED_slice_0024.mrc     Size=     105469 K

 Number of columns, rows, sections .....    9000    6000       1
 Map mode ..............................    1   (16-bit integer)
 Start cols, rows, sects, grid x,y,z ...    0     0     0    9000   6000      1
 Pixel spacing (Angstroms)..............   64.48      64.48      64.48
 Cell angles ...........................   90.000   90.000   90.000
```

```
 Fast, medium, slow axes .....    X    Y    Z
 Origin on x,y,z .....    0.000       0.000       0.000
 Minimum density .....  -27889.
 Maximum density .....  -12025.
 Mean density .....  -16145.
 tilt angles (original,current) .....   0.0   0.0   0.0   0.0   0.0   0.0
 Space group,# extra bytes,idtype,lens .        0        0        0        0

     1 Titles :
raw2mrc: Converted to mrc format.                    18-Oct-15  13:02:23

    24 -21029.25 -13190.00 -21029.25 -13190.00 -15745.79

 RO image file on unit   1 : run3_3VBSED_slice_0025.mrc     Size=     105469 K

 Number of columns, rows, sections .....    9000    6000       1
 Map mode .....    1   (16-bit integer)
 Start cols, rows, sects, grid x,y,z ...    0     0     0    9000   6000      1
 Pixel spacing (Angstroms).....   64.48      64.48      64.48
 Cell angles .....   90.000   90.000   90.000
 Fast, medium, slow axes .....    X    Y    Z
 Origin on x,y,z .....    0.000       0.000       0.000
 Minimum density .....  -22230.
 Maximum density .....  -12050.
 Mean density .....  -16136.
 tilt angles (original,current) .....   0.0   0.0   0.0   0.0   0.0   0.0
 Space group,# extra bytes,idtype,lens .        0        0        0        0

     1 Titles :
raw2mrc: Converted to mrc format.                    18-Oct-15  13:02:35

    25 -20354.00 -13091.25 -20354.00 -13091.25 -15722.15

 RO image file on unit   1 : run3_3VBSED_slice_0026.mrc     Size=     105469 K

 Number of columns, rows, sections .....    9000    6000       1
 Map mode .....    1   (16-bit integer)
 Start cols, rows, sects, grid x,y,z ...    0     0     0    9000   6000      1
 Pixel spacing (Angstroms).....   64.48      64.48      64.48
 Cell angles .....   90.000   90.000   90.000
 Fast, medium, slow axes .....    X    Y    Z
 Origin on x,y,z .....    0.000       0.000       0.000
 Minimum density .....  -22304.
 Maximum density .....  -11883.
 Mean density .....  -16130.
```

```
 tilt angles (original,current) .....   0.0   0.0   0.0   0.0   0.0   0.0
 Space group,# extra bytes,idtype,lens .       0       0       0       0

     1 Titles :
raw2mrc: Converted to mrc format.                  18-Oct-15  13:02:47

   26 -20765.75 -13134.75 -20765.75 -13134.75 -15709.37

 RO image file on unit   1 : run3_3VBSED_slice_0027.mrc     Size=     105469 K

 Number of columns, rows, sections .....    9000    6000       1
 Map mode ..............................    1   (16-bit integer)
 Start cols, rows, sects, grid x,y,z ...    0     0     0    9000   6000      1
 Pixel spacing (Angstroms)..............   64.48      64.48      64.48
 Cell angles ...........................   90.000   90.000   90.000
 Fast, medium, slow axes ..............    X    Y    Z
 Origin on x,y,z .......................    0.000       0.000       0.000
 Minimum density .......................  -30679.
 Maximum density .......................  -11824.
 Mean density ..........................  -16137.
 tilt angles (original,current) .....   0.0   0.0   0.0   0.0   0.0   0.0
 Space group,# extra bytes,idtype,lens .       0       0       0       0

     1 Titles :
raw2mrc: Converted to mrc format.                  18-Oct-15  13:02:59

   27 -22707.00 -13123.75 -22707.00 -13123.75 -15713.08

 RO image file on unit   1 : run3_3VBSED_slice_0028.mrc     Size=     105469 K

 Number of columns, rows, sections .....    9000    6000       1
 Map mode ..............................    1   (16-bit integer)
 Start cols, rows, sects, grid x,y,z ...    0     0     0    9000   6000      1
 Pixel spacing (Angstroms)..............   64.48      64.48      64.48
 Cell angles ...........................   90.000   90.000   90.000
 Fast, medium, slow axes ..............    X    Y    Z
 Origin on x,y,z .......................    0.000       0.000       0.000
 Minimum density .......................  -21838.
 Maximum density .......................  -11797.
 Mean density ..........................  -16126.
 tilt angles (original,current) .....   0.0   0.0   0.0   0.0   0.0   0.0
 Space group,# extra bytes,idtype,lens .       0       0       0       0

     1 Titles :
raw2mrc: Converted to mrc format.                  18-Oct-15  13:03:11
```

```
   28 -20427.75 -12893.50 -20427.75 -12893.50 -15692.41

 RO image file on unit   1 : run3_3VBSED_slice_0029.mrc     Size=     105469 K

 Number of columns, rows, sections .....    9000    6000       1
 Map mode ..............................    1   (16-bit integer)
 Start cols, rows, sects, grid x,y,z ...    0     0     0    9000   6000      1
 Pixel spacing (Angstroms)..............   64.48      64.48      64.48
 Cell angles ...........................   90.000   90.000   90.000
 Fast, medium, slow axes ...............    X    Y    Z
 Origin on x,y,z .......................    0.000       0.000       0.000
 Minimum density .......................  -21773.
 Maximum density .......................  -11969.
 Mean density ..........................  -16123.
 tilt angles (original,current) ........   0.0   0.0   0.0   0.0   0.0   0.0
 Space group,# extra bytes,idtype,lens .        0        0        0        0

     1 Titles :
raw2mrc: Converted to mrc format.                    18-Oct-15  13:03:22

   29 -20338.25 -13044.75 -20338.25 -13044.75 -15677.03

 RO image file on unit   1 : run3_3VBSED_slice_0030.mrc     Size=     105469 K

 Number of columns, rows, sections .....    9000    6000       1
 Map mode ..............................    1   (16-bit integer)
 Start cols, rows, sects, grid x,y,z ...    0     0     0    9000   6000      1
 Pixel spacing (Angstroms)..............   64.48      64.48      64.48
 Cell angles ...........................   90.000   90.000   90.000
 Fast, medium, slow axes ...............    X    Y    Z
 Origin on x,y,z .......................    0.000       0.000       0.000
 Minimum density .......................  -22518.
 Maximum density .......................  -11922.
 Mean density ..........................  -16132.
 tilt angles (original,current) ........   0.0   0.0   0.0   0.0   0.0   0.0
 Space group,# extra bytes,idtype,lens .        0        0        0        0

     1 Titles :
raw2mrc: Converted to mrc format.                    18-Oct-15  13:03:36

   30 -21183.75 -13089.25 -21183.75 -13089.25 -15691.16

 RO image file on unit   1 : run3_3VBSED_slice_0031.mrc     Size=     105469 K
```

```
 Number of columns, rows, sections .....    9000    6000       1
 Map mode ..............................    1   (16-bit integer)
 Start cols, rows, sects, grid x,y,z ...    0     0     0    9000   6000      1
 Pixel spacing (Angstroms)..............   64.48      64.48      64.48
 Cell angles ...........................   90.000   90.000   90.000
 Fast, medium, slow axes ...............    X    Y    Z
 Origin on x,y,z .......................    0.000       0.000       0.000
 Minimum density .......................  -21988.
 Maximum density .......................  -11912.
 Mean density ..........................  -16104.
 tilt angles (original,current) ........   0.0   0.0   0.0   0.0   0.0   0.0
 Space group,# extra bytes,idtype,lens .        0        0        0        0

     1 Titles :
raw2mrc: Converted to mrc format.                    18-Oct-15  13:03:48

   31 -20459.50 -13167.50 -20459.50 -13167.50 -15632.43

 RO image file on unit   1 : run3_3VBSED_slice_0032.mrc     Size=     105469 K

 Number of columns, rows, sections .....    9000    6000       1
 Map mode ..............................    1   (16-bit integer)
 Start cols, rows, sects, grid x,y,z ...    0     0     0    9000   6000      1
 Pixel spacing (Angstroms)..............   64.48      64.48      64.48
 Cell angles ...........................   90.000   90.000   90.000
 Fast, medium, slow axes ...............    X    Y    Z
 Origin on x,y,z .......................    0.000       0.000       0.000
 Minimum density .......................  -21490.
 Maximum density .......................  -11841.
 Mean density ..........................  -16107.
 tilt angles (original,current) ........   0.0   0.0   0.0   0.0   0.0   0.0
 Space group,# extra bytes,idtype,lens .        0        0        0        0

     1 Titles :
raw2mrc: Converted to mrc format.                    18-Oct-15  13:03:59

   32 -20755.25 -13162.50 -20755.25 -13162.50 -15633.93

 RO image file on unit   1 : run3_3VBSED_slice_0033.mrc     Size=     105469 K

 Number of columns, rows, sections .....    9000    6000       1
 Map mode ..............................    1   (16-bit integer)
 Start cols, rows, sects, grid x,y,z ...    0     0     0    9000   6000      1
 Pixel spacing (Angstroms)..............   64.48      64.48      64.48
 Cell angles ...........................   90.000   90.000   90.000
```

```
 Fast, medium, slow axes .....    X    Y    Z
 Origin on x,y,z .....    0.000       0.000       0.000
 Minimum density .....  -22490.
 Maximum density .....  -11840.
 Mean density .....  -16105.
 tilt angles (original,current) .....   0.0   0.0   0.0   0.0   0.0   0.0
 Space group,# extra bytes,idtype,lens .        0        0        0        0

     1 Titles :
raw2mrc: Converted to mrc format.                    18-Oct-15  13:04:12

   33 -20654.00 -13096.75 -20654.00 -13096.75 -15627.76

 RO image file on unit   1 : run3_3VBSED_slice_0034.mrc     Size=     105469 K

 Number of columns, rows, sections .....    9000    6000       1
 Map mode .....    1   (16-bit integer)
 Start cols, rows, sects, grid x,y,z ...    0     0     0    9000   6000      1
 Pixel spacing (Angstroms).....   64.48      64.48      64.48
 Cell angles .....   90.000   90.000   90.000
 Fast, medium, slow axes .....    X    Y    Z
 Origin on x,y,z .....    0.000       0.000       0.000
 Minimum density .....  -21782.
 Maximum density .....  -11746.
 Mean density .....  -16096.
 tilt angles (original,current) .....   0.0   0.0   0.0   0.0   0.0   0.0
 Space group,# extra bytes,idtype,lens .        0        0        0        0

     1 Titles :
raw2mrc: Converted to mrc format.                    18-Oct-15  13:04:25

   34 -20171.50 -13071.25 -20171.50 -13071.25 -15610.45

 RO image file on unit   1 : run3_3VBSED_slice_0035.mrc     Size=     105469 K

 Number of columns, rows, sections .....    9000    6000       1
 Map mode .....    1   (16-bit integer)
 Start cols, rows, sects, grid x,y,z ...    0     0     0    9000   6000      1
 Pixel spacing (Angstroms).....   64.48      64.48      64.48
 Cell angles .....   90.000   90.000   90.000
 Fast, medium, slow axes .....    X    Y    Z
 Origin on x,y,z .....    0.000       0.000       0.000
 Minimum density .....  -21708.
 Maximum density .....  -11815.
 Mean density .....  -16098.
```

```
 tilt angles (original,current) .....   0.0   0.0   0.0   0.0   0.0   0.0
 Space group,# extra bytes,idtype,lens .       0       0       0       0

     1 Titles :
raw2mrc: Converted to mrc format.                  18-Oct-15  13:05:58

   35 -20504.00 -13166.75 -20504.00 -13166.75 -15606.42

 RO image file on unit   1 : run3_3VBSED_slice_0036.mrc     Size=     105469 K

 Number of columns, rows, sections .....    9000    6000       1
 Map mode ..............................    1   (16-bit integer)
 Start cols, rows, sects, grid x,y,z ...    0     0     0    9000   6000      1
 Pixel spacing (Angstroms)..............   64.48      64.48      64.48
 Cell angles ...........................   90.000   90.000   90.000
 Fast, medium, slow axes ..............    X    Y    Z
 Origin on x,y,z .......................    0.000       0.000       0.000
 Minimum density .......................  -21267.
 Maximum density .......................  -11935.
 Mean density ..........................  -16092.
 tilt angles (original,current) .....   0.0   0.0   0.0   0.0   0.0   0.0
 Space group,# extra bytes,idtype,lens .       0       0       0       0

     1 Titles :
raw2mrc: Converted to mrc format.                  18-Oct-15  13:06:11

   36 -20127.75 -13029.50 -20127.75 -13029.50 -15598.02

 RO image file on unit   1 : run3_3VBSED_slice_0037.mrc     Size=     105469 K

 Number of columns, rows, sections .....    9000    6000       1
 Map mode ..............................    1   (16-bit integer)
 Start cols, rows, sects, grid x,y,z ...    0     0     0    9000   6000      1
 Pixel spacing (Angstroms)..............   64.48      64.48      64.48
 Cell angles ...........................   90.000   90.000   90.000
 Fast, medium, slow axes ..............    X    Y    Z
 Origin on x,y,z .......................    0.000       0.000       0.000
 Minimum density .......................  -21536.
 Maximum density .......................  -11949.
 Mean density ..........................  -16090.
 tilt angles (original,current) .....   0.0   0.0   0.0   0.0   0.0   0.0
 Space group,# extra bytes,idtype,lens .       0       0       0       0

     1 Titles :
raw2mrc: Converted to mrc format.                  18-Oct-15  13:06:23
```

```
   37 -20125.75 -13140.00 -20125.75 -13140.00 -15590.76

 RO image file on unit   1 : run3_3VBSED_slice_0038.mrc     Size=     105469 K

 Number of columns, rows, sections .....    9000    6000       1
 Map mode ..............................    1   (16-bit integer)
 Start cols, rows, sects, grid x,y,z ...    0     0     0    9000   6000      1
 Pixel spacing (Angstroms)..............   64.48      64.48      64.48
 Cell angles ...........................   90.000   90.000   90.000
 Fast, medium, slow axes ...............    X    Y    Z
 Origin on x,y,z .......................    0.000       0.000       0.000
 Minimum density .......................  -29847.
 Maximum density .......................  -11937.
 Mean density ..........................  -16116.
 tilt angles (original,current) ........   0.0   0.0   0.0   0.0   0.0   0.0
 Space group,# extra bytes,idtype,lens .        0        0        0        0

     1 Titles :
raw2mrc: Converted to mrc format.                    18-Oct-15  13:06:35

   38 -21975.50 -13084.25 -21975.50 -13084.25 -15642.05

 RO image file on unit   1 : run3_3VBSED_slice_0039.mrc     Size=     105469 K

 Number of columns, rows, sections .....    9000    6000       1
 Map mode ..............................    1   (16-bit integer)
 Start cols, rows, sects, grid x,y,z ...    0     0     0    9000   6000      1
 Pixel spacing (Angstroms)..............   64.48      64.48      64.48
 Cell angles ...........................   90.000   90.000   90.000
 Fast, medium, slow axes ...............    X    Y    Z
 Origin on x,y,z .......................    0.000       0.000       0.000
 Minimum density .......................  -31303.
 Maximum density .......................  -11740.
 Mean density ..........................  -16074.
 tilt angles (original,current) ........   0.0   0.0   0.0   0.0   0.0   0.0
 Space group,# extra bytes,idtype,lens .        0        0        0        0

     1 Titles :
raw2mrc: Converted to mrc format.                    18-Oct-15  13:06:47

   39 -23310.25 -13115.75 -23310.25 -13115.75 -15552.50

 RO image file on unit   1 : run3_3VBSED_slice_0040.mrc     Size=     105469 K
```

```
 Number of columns, rows, sections .....    9000    6000       1
 Map mode ..............................    1   (16-bit integer)
 Start cols, rows, sects, grid x,y,z ...    0     0     0    9000   6000      1
 Pixel spacing (Angstroms)..............   64.48      64.48      64.48
 Cell angles ...........................   90.000   90.000   90.000
 Fast, medium, slow axes ...............    X    Y    Z
 Origin on x,y,z .......................    0.000       0.000       0.000
 Minimum density .......................  -21098.
 Maximum density .......................  -11928.
 Mean density ..........................  -16076.
 tilt angles (original,current) ........   0.0   0.0   0.0   0.0   0.0   0.0
 Space group,# extra bytes,idtype,lens .        0        0        0        0

     1 Titles :
raw2mrc: Converted to mrc format.                    18-Oct-15  13:07:01

   40 -19649.50 -13162.50 -19649.50 -13162.50 -15564.21

 RO image file on unit   1 : run3_3VBSED_slice_0041.mrc     Size=     105469 K

 Number of columns, rows, sections .....    9000    6000       1
 Map mode ..............................    1   (16-bit integer)
 Start cols, rows, sects, grid x,y,z ...    0     0     0    9000   6000      1
 Pixel spacing (Angstroms)..............   64.48      64.48      64.48
 Cell angles ...........................   90.000   90.000   90.000
 Fast, medium, slow axes ...............    X    Y    Z
 Origin on x,y,z .......................    0.000       0.000       0.000
 Minimum density .......................  -31221.
 Maximum density .......................  -11826.
 Mean density ..........................  -16078.
 tilt angles (original,current) ........   0.0   0.0   0.0   0.0   0.0   0.0
 Space group,# extra bytes,idtype,lens .        0        0        0        0

     1 Titles :
raw2mrc: Converted to mrc format.                    18-Oct-15  13:07:12

   41 -22928.50 -13152.50 -22928.50 -13152.50 -15558.58

 RO image file on unit   1 : run3_3VBSED_slice_0042.mrc     Size=     105469 K

 Number of columns, rows, sections .....    9000    6000       1
 Map mode ..............................    1   (16-bit integer)
 Start cols, rows, sects, grid x,y,z ...    0     0     0    9000   6000      1
 Pixel spacing (Angstroms)..............   64.48      64.48      64.48
 Cell angles ...........................   90.000   90.000   90.000
```

```
 Fast, medium, slow axes .....    X    Y    Z
 Origin on x,y,z .....    0.000       0.000       0.000
 Minimum density .....  -21766.
 Maximum density .....  -11804.
 Mean density .....  -16062.
 tilt angles (original,current) .....   0.0   0.0   0.0   0.0   0.0   0.0
 Space group,# extra bytes,idtype,lens .        0        0        0        0

     1 Titles :
raw2mrc: Converted to mrc format.                    18-Oct-15  13:07:22

   42 -20176.75 -13103.00 -20176.75 -13103.00 -15536.08

 RO image file on unit   1 : run3_3VBSED_slice_0043.mrc     Size=     105469 K

 Number of columns, rows, sections .....    9000    6000       1
 Map mode .....    1   (16-bit integer)
 Start cols, rows, sects, grid x,y,z ...    0     0     0    9000   6000      1
 Pixel spacing (Angstroms).....   64.48      64.48      64.48
 Cell angles .....   90.000   90.000   90.000
 Fast, medium, slow axes .....    X    Y    Z
 Origin on x,y,z .....    0.000       0.000       0.000
 Minimum density .....  -21895.
 Maximum density .....  -11774.
 Mean density .....  -16072.
 tilt angles (original,current) .....   0.0   0.0   0.0   0.0   0.0   0.0
 Space group,# extra bytes,idtype,lens .        0        0        0        0

     1 Titles :
raw2mrc: Converted to mrc format.                    18-Oct-15  13:07:31

   43 -20157.25 -13025.75 -20157.25 -13025.75 -15548.53

 RO image file on unit   1 : run3_3VBSED_slice_0044.mrc     Size=     105469 K

 Number of columns, rows, sections .....    9000    6000       1
 Map mode .....    1   (16-bit integer)
 Start cols, rows, sects, grid x,y,z ...    0     0     0    9000   6000      1
 Pixel spacing (Angstroms).....   64.48      64.48      64.48
 Cell angles .....   90.000   90.000   90.000
 Fast, medium, slow axes .....    X    Y    Z
 Origin on x,y,z .....    0.000       0.000       0.000
 Minimum density .....  -21723.
 Maximum density .....  -11570.
 Mean density .....  -16068.
```

```
 tilt angles (original,current) .....   0.0   0.0   0.0   0.0   0.0   0.0
 Space group,# extra bytes,idtype,lens .       0       0       0       0

     1 Titles :
raw2mrc: Converted to mrc format.                  18-Oct-15  13:07:41

   44 -20548.75 -13110.50 -20548.75 -13110.50 -15543.51

 RO image file on unit   1 : run3_3VBSED_slice_0045.mrc     Size=     105469 K

 Number of columns, rows, sections .....    9000    6000       1
 Map mode ..............................    1   (16-bit integer)
 Start cols, rows, sects, grid x,y,z ...    0     0     0    9000   6000      1
 Pixel spacing (Angstroms)..............   64.48      64.48      64.48
 Cell angles ...........................   90.000   90.000   90.000
 Fast, medium, slow axes ..............    X    Y    Z
 Origin on x,y,z .......................    0.000       0.000       0.000
 Minimum density .......................  -22290.
 Maximum density .......................  -11916.
 Mean density ..........................  -16068.
 tilt angles (original,current) .....   0.0   0.0   0.0   0.0   0.0   0.0
 Space group,# extra bytes,idtype,lens .       0       0       0       0

     1 Titles :
raw2mrc: Converted to mrc format.                  18-Oct-15  13:07:57

   45 -20184.50 -12966.75 -20184.50 -12966.75 -15538.39

 RO image file on unit   1 : run3_3VBSED_slice_0046.mrc     Size=     105469 K

 Number of columns, rows, sections .....    9000    6000       1
 Map mode ..............................    1   (16-bit integer)
 Start cols, rows, sects, grid x,y,z ...    0     0     0    9000   6000      1
 Pixel spacing (Angstroms)..............   64.48      64.48      64.48
 Cell angles ...........................   90.000   90.000   90.000
 Fast, medium, slow axes ..............    X    Y    Z
 Origin on x,y,z .......................    0.000       0.000       0.000
 Minimum density .......................  -21902.
 Maximum density .......................  -11740.
 Mean density ..........................  -16065.
 tilt angles (original,current) .....   0.0   0.0   0.0   0.0   0.0   0.0
 Space group,# extra bytes,idtype,lens .       0       0       0       0

     1 Titles :
raw2mrc: Converted to mrc format.                  18-Oct-15  13:12:20
```

46 -20410.25 -13022.50 -20410.25 -13022.50 -15537.26

RO image file on unit 1 : run3_3VBSED_slice_0047.mrc Size= 105469 K

Number of columns, rows, sections 9000 6000 1
Map mode ..... 1 (16-bit integer)
Start cols, rows, sects, grid x,y,z ... 0 0 0 9000 6000 1
Pixel spacing (Angstroms)..... 64.48 64.48 64.48
Cell angles 90.000 90.000 90.000
Fast, medium, slow axes ..... X Y Z
Origin on x,y,z 0.000 0.000 0.000
Minimum density ..... -21651.
Maximum density ..... -11824.
Mean density ..... -16067.
tilt angles (original,current) 0.0 0.0 0.0 0.0 0.0 0.0
Space group,# extra bytes,idtype,lens . 0 0 0 0

1 Titles :
raw2mrc: Converted to mrc format. 18-Oct-15 13:12:30

47 -20512.75 -13137.75 -20512.75 -13137.75 -15538.18

RO image file on unit 1 : run3_3VBSED_slice_0048.mrc Size= 105469 K

Number of columns, rows, sections 9000 6000 1
Map mode ..... 1 (16-bit integer)
Start cols, rows, sects, grid x,y,z ... 0 0 0 9000 6000 1
Pixel spacing (Angstroms)..... 64.48 64.48 64.48
Cell angles 90.000 90.000 90.000
Fast, medium, slow axes ..... X Y Z
Origin on x,y,z 0.000 0.000 0.000
Minimum density ..... -21776.
Maximum density ..... -12031.
Mean density ..... -16056.
tilt angles (original,current) 0.0 0.0 0.0 0.0 0.0 0.0
Space group,# extra bytes,idtype,lens . 0 0 0 0

1 Titles :
raw2mrc: Converted to mrc format. 18-Oct-15 13:12:40

48 -20632.50 -13092.25 -20632.50 -13092.25 -15520.42

RO image file on unit 1 : run3_3VBSED_slice_0049.mrc Size= 105469 K

```
 Number of columns, rows, sections .....    9000    6000       1
 Map mode ..............................    1   (16-bit integer)
 Start cols, rows, sects, grid x,y,z ...    0     0     0    9000   6000      1
 Pixel spacing (Angstroms)..............   64.48      64.48      64.48
 Cell angles ...........................   90.000   90.000   90.000
 Fast, medium, slow axes ...............    X    Y    Z
 Origin on x,y,z .......................    0.000       0.000       0.000
 Minimum density .......................  -21669.
 Maximum density .......................  -11908.
 Mean density ..........................  -16069.
 tilt angles (original,current) ........   0.0   0.0   0.0   0.0   0.0   0.0
 Space group,# extra bytes,idtype,lens .        0        0        0        0

     1 Titles :
raw2mrc: Converted to mrc format.                    18-Oct-15  13:12:50

   49 -20442.50 -13170.25 -20442.50 -13170.25 -15536.11

 RO image file on unit   1 : run3_3VBSED_slice_0050.mrc     Size=     105469 K

 Number of columns, rows, sections .....    9000    6000       1
 Map mode ..............................    1   (16-bit integer)
 Start cols, rows, sects, grid x,y,z ...    0     0     0    9000   6000      1
 Pixel spacing (Angstroms)..............   64.48      64.48      64.48
 Cell angles ...........................   90.000   90.000   90.000
 Fast, medium, slow axes ...............    X    Y    Z
 Origin on x,y,z .......................    0.000       0.000       0.000
 Minimum density .......................  -21959.
 Maximum density .......................  -11787.
 Mean density ..........................  -16065.
 tilt angles (original,current) ........   0.0   0.0   0.0   0.0   0.0   0.0
 Space group,# extra bytes,idtype,lens .        0        0        0        0

     1 Titles :
raw2mrc: Converted to mrc format.                    18-Oct-15  13:13:04

   50 -20690.50 -12981.50 -20690.50 -12981.50 -15534.29

 RO image file on unit   1 : run3_3VBSED_slice_0051.mrc     Size=     105469 K

 Number of columns, rows, sections .....    9000    6000       1
 Map mode ..............................    1   (16-bit integer)
 Start cols, rows, sects, grid x,y,z ...    0     0     0    9000   6000      1
 Pixel spacing (Angstroms)..............   64.48      64.48      64.48
 Cell angles ...........................   90.000   90.000   90.000
```

```
 Fast, medium, slow axes .....    X    Y    Z
 Origin on x,y,z .....    0.000       0.000       0.000
 Minimum density .....  -21516.
 Maximum density .....  -11671.
 Mean density .....  -16061.
 tilt angles (original,current) .....   0.0   0.0   0.0   0.0   0.0   0.0
 Space group,# extra bytes,idtype,lens .        0        0        0        0

     1 Titles :
raw2mrc: Converted to mrc format.                    18-Oct-15  13:13:14

   51 -20453.75 -13153.50 -20453.75 -13153.50 -15518.25

 RO image file on unit   1 : run3_3VBSED_slice_0052.mrc     Size=     105469 K

 Number of columns, rows, sections .....    9000    6000       1
 Map mode .....    1   (16-bit integer)
 Start cols, rows, sects, grid x,y,z ...    0     0     0    9000   6000      1
 Pixel spacing (Angstroms).....   64.48      64.48      64.48
 Cell angles .....   90.000   90.000   90.000
 Fast, medium, slow axes .....    X    Y    Z
 Origin on x,y,z .....    0.000       0.000       0.000
 Minimum density .....  -21355.
 Maximum density .....  -11869.
 Mean density .....  -16056.
 tilt angles (original,current) .....   0.0   0.0   0.0   0.0   0.0   0.0
 Space group,# extra bytes,idtype,lens .        0        0        0        0

     1 Titles :
raw2mrc: Converted to mrc format.                    18-Oct-15  13:13:23

   52 -19876.00 -13069.75 -19876.00 -13069.75 -15519.59

 RO image file on unit   1 : run3_3VBSED_slice_0053.mrc     Size=     105469 K

 Number of columns, rows, sections .....    9000    6000       1
 Map mode .....    1   (16-bit integer)
 Start cols, rows, sects, grid x,y,z ...    0     0     0    9000   6000      1
 Pixel spacing (Angstroms).....   64.48      64.48      64.48
 Cell angles .....   90.000   90.000   90.000
 Fast, medium, slow axes .....    X    Y    Z
 Origin on x,y,z .....    0.000       0.000       0.000
 Minimum density .....  -20888.
 Maximum density .....  -11940.
 Mean density .....  -16060.
```

```
 tilt angles (original,current) .....   0.0   0.0   0.0   0.0   0.0   0.0
 Space group,# extra bytes,idtype,lens .       0       0       0       0

     1 Titles :
raw2mrc: Converted to mrc format.                  18-Oct-15  13:13:33

    53 -19745.25 -13111.25 -19745.25 -13111.25 -15525.71

 RO image file on unit   1 : run3_3VBSED_slice_0054.mrc     Size=     105469 K

 Number of columns, rows, sections .....    9000    6000       1
 Map mode ..............................    1   (16-bit integer)
 Start cols, rows, sects, grid x,y,z ...    0     0     0    9000   6000      1
 Pixel spacing (Angstroms)..............   64.48      64.48      64.48
 Cell angles ...........................   90.000   90.000   90.000
 Fast, medium, slow axes ..............    X    Y    Z
 Origin on x,y,z .......................    0.000       0.000       0.000
 Minimum density .......................  -21504.
 Maximum density .......................  -11646.
 Mean density ..........................  -16056.
 tilt angles (original,current) .....   0.0   0.0   0.0   0.0   0.0   0.0
 Space group,# extra bytes,idtype,lens .       0       0       0       0

     1 Titles :
raw2mrc: Converted to mrc format.                  18-Oct-15  13:13:44

    54 -20178.25 -13127.00 -20178.25 -13127.00 -15514.09

 RO image file on unit   1 : run3_3VBSED_slice_0055.mrc     Size=     105469 K

 Number of columns, rows, sections .....    9000    6000       1
 Map mode ..............................    1   (16-bit integer)
 Start cols, rows, sects, grid x,y,z ...    0     0     0    9000   6000      1
 Pixel spacing (Angstroms)..............   64.48      64.48      64.48
 Cell angles ...........................   90.000   90.000   90.000
 Fast, medium, slow axes ..............    X    Y    Z
 Origin on x,y,z .......................    0.000       0.000       0.000
 Minimum density .......................  -21238.
 Maximum density .......................  -11768.
 Mean density ..........................  -16048.
 tilt angles (original,current) .....   0.0   0.0   0.0   0.0   0.0   0.0
 Space group,# extra bytes,idtype,lens .       0       0       0       0

     1 Titles :
raw2mrc: Converted to mrc format.                  18-Oct-15  13:13:53
```

55 -19841.00 -13114.00 -19841.00 -13114.00 -15502.09

RO image file on unit 1 : run3_3VBSED_slice_0056.mrc Size= 105469 K

Number of columns, rows, sections 9000 6000 1
Map mode ..... 1 (16-bit integer)
Start cols, rows, sects, grid x,y,z ... 0 0 0 9000 6000 1
Pixel spacing (Angstroms)..... 64.48 64.48 64.48
Cell angles 90.000 90.000 90.000
Fast, medium, slow axes ..... X Y Z
Origin on x,y,z 0.000 0.000 0.000
Minimum density ..... -21740.
Maximum density ..... -11891.
Mean density ..... -16050.
tilt angles (original,current) 0.0 0.0 0.0 0.0 0.0 0.0
Space group,# extra bytes,idtype,lens . 0 0 0 0

1 Titles :
raw2mrc: Converted to mrc format. 18-Oct-15 13:14:05

56 -20176.75 -12969.00 -20176.75 -12969.00 -15502.41

RO image file on unit 1 : run3_3VBSED_slice_0057.mrc Size= 105469 K

Number of columns, rows, sections 9000 6000 1
Map mode ..... 1 (16-bit integer)
Start cols, rows, sects, grid x,y,z ... 0 0 0 9000 6000 1
Pixel spacing (Angstroms)..... 64.48 64.48 64.48
Cell angles 90.000 90.000 90.000
Fast, medium, slow axes ..... X Y Z
Origin on x,y,z 0.000 0.000 0.000
Minimum density ..... -21779.
Maximum density ..... -11770.
Mean density ..... -16045.
tilt angles (original,current) 0.0 0.0 0.0 0.0 0.0 0.0
Space group,# extra bytes,idtype,lens . 0 0 0 0

1 Titles :
raw2mrc: Converted to mrc format. 18-Oct-15 13:14:16

57 -20511.75 -12905.75 -20511.75 -12905.75 -15496.87

RO image file on unit 1 : run3_3VBSED_slice_0058.mrc Size= 105469 K

```
 Number of columns, rows, sections .....    9000    6000       1
 Map mode ..............................    1   (16-bit integer)
 Start cols, rows, sects, grid x,y,z ...    0     0     0    9000   6000      1
 Pixel spacing (Angstroms)..............   64.48      64.48      64.48
 Cell angles ...........................   90.000   90.000   90.000
 Fast, medium, slow axes ...............    X    Y    Z
 Origin on x,y,z .......................    0.000       0.000       0.000
 Minimum density .......................  -21864.
 Maximum density .......................  -11725.
 Mean density ..........................  -16055.
 tilt angles (original,current) ........   0.0   0.0   0.0   0.0   0.0   0.0
 Space group,# extra bytes,idtype,lens .        0        0        0        0

     1 Titles :
raw2mrc: Converted to mrc format.                    18-Oct-15  13:14:26

   58 -20161.00 -13128.25 -20161.00 -13128.25 -15508.06

 RO image file on unit   1 : run3_3VBSED_slice_0059.mrc     Size=     105469 K

 Number of columns, rows, sections .....    9000    6000       1
 Map mode ..............................    1   (16-bit integer)
 Start cols, rows, sects, grid x,y,z ...    0     0     0    9000   6000      1
 Pixel spacing (Angstroms)..............   64.48      64.48      64.48
 Cell angles ...........................   90.000   90.000   90.000
 Fast, medium, slow axes ...............    X    Y    Z
 Origin on x,y,z .......................    0.000       0.000       0.000
 Minimum density .......................  -21130.
 Maximum density .......................  -11732.
 Mean density ..........................  -16032.
 tilt angles (original,current) ........   0.0   0.0   0.0   0.0   0.0   0.0
 Space group,# extra bytes,idtype,lens .        0        0        0        0

     1 Titles :
raw2mrc: Converted to mrc format.                    18-Oct-15  13:14:36

   59 -19931.50 -12888.75 -19931.50 -12888.75 -15471.83

 RO image file on unit   1 : run3_3VBSED_slice_0060.mrc     Size=     105469 K

 Number of columns, rows, sections .....    9000    6000       1
 Map mode ..............................    1   (16-bit integer)
 Start cols, rows, sects, grid x,y,z ...    0     0     0    9000   6000      1
 Pixel spacing (Angstroms)..............   64.48      64.48      64.48
 Cell angles ...........................   90.000   90.000   90.000
```

```
 Fast, medium, slow axes .....    X    Y    Z
 Origin on x,y,z .....    0.000       0.000       0.000
 Minimum density .....  -20988.
 Maximum density .....  -12042.
 Mean density .....  -16054.
 tilt angles (original,current) .....   0.0   0.0   0.0   0.0   0.0   0.0
 Space group,# extra bytes,idtype,lens .        0        0        0        0

     1 Titles :
raw2mrc: Converted to mrc format.                    18-Oct-15  13:14:47

   60 -20108.75 -13061.50 -20108.75 -13061.50 -15505.77

 RO image file on unit   1 : run3_3VBSED_slice_0061.mrc     Size=     105469 K

 Number of columns, rows, sections .....    9000    6000       1
 Map mode .....    1   (16-bit integer)
 Start cols, rows, sects, grid x,y,z ...    0     0     0    9000   6000      1
 Pixel spacing (Angstroms).....   64.48      64.48      64.48
 Cell angles .....   90.000   90.000   90.000
 Fast, medium, slow axes .....    X    Y    Z
 Origin on x,y,z .....    0.000       0.000       0.000
 Minimum density .....  -28665.
 Maximum density .....  -11970.
 Mean density .....  -16045.
 tilt angles (original,current) .....   0.0   0.0   0.0   0.0   0.0   0.0
 Space group,# extra bytes,idtype,lens .        0        0        0        0

     1 Titles :
raw2mrc: Converted to mrc format.                    18-Oct-15  13:14:56

   61 -23740.50 -12942.00 -23740.50 -12942.00 -15489.26

 RO image file on unit   1 : run3_3VBSED_slice_0062.mrc     Size=     105469 K

 Number of columns, rows, sections .....    9000    6000       1
 Map mode .....    1   (16-bit integer)
 Start cols, rows, sects, grid x,y,z ...    0     0     0    9000   6000      1
 Pixel spacing (Angstroms).....   64.48      64.48      64.48
 Cell angles .....   90.000   90.000   90.000
 Fast, medium, slow axes .....    X    Y    Z
 Origin on x,y,z .....    0.000       0.000       0.000
 Minimum density .....  -21478.
 Maximum density .....  -11826.
 Mean density .....  -16052.
```

```
 tilt angles (original,current) .....   0.0   0.0   0.0   0.0   0.0   0.0
 Space group,# extra bytes,idtype,lens .       0       0       0       0

     1 Titles :
raw2mrc: Converted to mrc format.                  18-Oct-15  13:15:04

   62 -19702.50 -13052.00 -19702.50 -13052.00 -15502.14

 RO image file on unit   1 : run3_3VBSED_slice_0063.mrc     Size=     105469 K

 Number of columns, rows, sections .....    9000    6000       1
 Map mode ..............................    1   (16-bit integer)
 Start cols, rows, sects, grid x,y,z ...    0     0     0    9000   6000      1
 Pixel spacing (Angstroms)..............   64.48      64.48      64.48
 Cell angles ...........................   90.000   90.000   90.000
 Fast, medium, slow axes ...............    X    Y    Z
 Origin on x,y,z .......................    0.000       0.000       0.000
 Minimum density .......................  -23326.
 Maximum density .......................  -11943.
 Mean density ..........................  -16045.
 tilt angles (original,current) .....   0.0   0.0   0.0   0.0   0.0   0.0
 Space group,# extra bytes,idtype,lens .       0       0       0       0

     1 Titles :
raw2mrc: Converted to mrc format.                  18-Oct-15  13:15:14

   63 -21292.25 -13082.25 -21292.25 -13082.25 -15489.78

 RO image file on unit   1 : run3_3VBSED_slice_0064.mrc     Size=     105469 K

 Number of columns, rows, sections .....    9000    6000       1
 Map mode ..............................    1   (16-bit integer)
 Start cols, rows, sects, grid x,y,z ...    0     0     0    9000   6000      1
 Pixel spacing (Angstroms)..............   64.48      64.48      64.48
 Cell angles ...........................   90.000   90.000   90.000
 Fast, medium, slow axes ...............    X    Y    Z
 Origin on x,y,z .......................    0.000       0.000       0.000
 Minimum density .......................  -22649.
 Maximum density .......................  -12044.
 Mean density ..........................  -16045.
 tilt angles (original,current) .....   0.0   0.0   0.0   0.0   0.0   0.0
 Space group,# extra bytes,idtype,lens .       0       0       0       0

     1 Titles :
raw2mrc: Converted to mrc format.                  18-Oct-15  13:15:23
```

```
   64 -20790.25 -12966.75 -20790.25 -12966.75 -15493.61

 RO image file on unit   1 : run3_3VBSED_slice_0065.mrc     Size=     105469 K

 Number of columns, rows, sections .....    9000    6000       1
 Map mode ..............................    1   (16-bit integer)
 Start cols, rows, sects, grid x,y,z ...    0     0     0    9000   6000      1
 Pixel spacing (Angstroms)..............   64.48      64.48      64.48
 Cell angles ...........................   90.000   90.000   90.000
 Fast, medium, slow axes ...............    X    Y    Z
 Origin on x,y,z .......................    0.000       0.000       0.000
 Minimum density .......................  -25520.
 Maximum density .......................  -11701.
 Mean density ..........................  -16048.
 tilt angles (original,current) ........   0.0   0.0   0.0   0.0   0.0   0.0
 Space group,# extra bytes,idtype,lens .        0        0        0        0

     1 Titles :
raw2mrc: Converted to mrc format.                    18-Oct-15  13:15:32

   65 -20186.50 -13124.00 -20186.50 -13124.00 -15493.82

 RO image file on unit   1 : run3_3VBSED_slice_0066.mrc     Size=     105469 K

 Number of columns, rows, sections .....    9000    6000       1
 Map mode ..............................    1   (16-bit integer)
 Start cols, rows, sects, grid x,y,z ...    0     0     0    9000   6000      1
 Pixel spacing (Angstroms)..............   64.48      64.48      64.48
 Cell angles ...........................   90.000   90.000   90.000
 Fast, medium, slow axes ...............    X    Y    Z
 Origin on x,y,z .......................    0.000       0.000       0.000
 Minimum density .......................  -20829.
 Maximum density .......................  -11798.
 Mean density ..........................  -16045.
 tilt angles (original,current) ........   0.0   0.0   0.0   0.0   0.0   0.0
 Space group,# extra bytes,idtype,lens .        0        0        0        0

     1 Titles :
raw2mrc: Converted to mrc format.                    18-Oct-15  13:15:41

   66 -19883.25 -13034.50 -19883.25 -13034.50 -15491.42

 RO image file on unit   1 : run3_3VBSED_slice_0067.mrc     Size=     105469 K
```

```
 Number of columns, rows, sections .....    9000    6000       1
 Map mode ..............................    1   (16-bit integer)
 Start cols, rows, sects, grid x,y,z ...    0     0     0    9000   6000      1
 Pixel spacing (Angstroms)..............   64.48      64.48      64.48
 Cell angles ...........................   90.000   90.000   90.000
 Fast, medium, slow axes ...............    X    Y    Z
 Origin on x,y,z .......................    0.000       0.000       0.000
 Minimum density .......................  -24519.
 Maximum density .......................  -11839.
 Mean density ..........................  -16049.
 tilt angles (original,current) ........   0.0   0.0   0.0   0.0   0.0   0.0
 Space group,# extra bytes,idtype,lens .        0        0        0        0

     1 Titles :
raw2mrc: Converted to mrc format.                    18-Oct-15  13:15:51

   67 -22459.50 -13091.75 -22459.50 -13091.75 -15495.05

 RO image file on unit   1 : run3_3VBSED_slice_0068.mrc     Size=     105469 K

 Number of columns, rows, sections .....    9000    6000       1
 Map mode ..............................    1   (16-bit integer)
 Start cols, rows, sects, grid x,y,z ...    0     0     0    9000   6000      1
 Pixel spacing (Angstroms)..............   64.48      64.48      64.48
 Cell angles ...........................   90.000   90.000   90.000
 Fast, medium, slow axes ...............    X    Y    Z
 Origin on x,y,z .......................    0.000       0.000       0.000
 Minimum density .......................  -24003.
 Maximum density .......................  -11990.
 Mean density ..........................  -16049.
 tilt angles (original,current) ........   0.0   0.0   0.0   0.0   0.0   0.0
 Space group,# extra bytes,idtype,lens .        0        0        0        0

     1 Titles :
raw2mrc: Converted to mrc format.                    18-Oct-15  13:16:01

   68 -21682.75 -13172.25 -21682.75 -13172.25 -15494.42

 RO image file on unit   1 : run3_3VBSED_slice_0069.mrc     Size=     105469 K

 Number of columns, rows, sections .....    9000    6000       1
 Map mode ..............................    1   (16-bit integer)
 Start cols, rows, sects, grid x,y,z ...    0     0     0    9000   6000      1
 Pixel spacing (Angstroms)..............   64.48      64.48      64.48
 Cell angles ...........................   90.000   90.000   90.000
```

```
 Fast, medium, slow axes .....    X    Y    Z
 Origin on x,y,z .....    0.000       0.000       0.000
 Minimum density .....  -28650.
 Maximum density .....  -11881.
 Mean density .....  -16040.
 tilt angles (original,current) .....   0.0   0.0   0.0   0.0   0.0   0.0
 Space group,# extra bytes,idtype,lens .        0        0        0        0

     1 Titles :
raw2mrc: Converted to mrc format.                    18-Oct-15  13:16:12

   69 -22970.25 -13079.25 -22970.25 -13079.25 -15481.65

 RO image file on unit   1 : run3_3VBSED_slice_0070.mrc     Size=     105469 K

 Number of columns, rows, sections .....    9000    6000       1
 Map mode .....    1   (16-bit integer)
 Start cols, rows, sects, grid x,y,z ...    0     0     0    9000   6000      1
 Pixel spacing (Angstroms).....   64.48      64.48      64.48
 Cell angles .....   90.000   90.000   90.000
 Fast, medium, slow axes .....    X    Y    Z
 Origin on x,y,z .....    0.000       0.000       0.000
 Minimum density .....  -23346.
 Maximum density .....  -11733.
 Mean density .....  -16042.
 tilt angles (original,current) .....   0.0   0.0   0.0   0.0   0.0   0.0
 Space group,# extra bytes,idtype,lens .        0        0        0        0

     1 Titles :
raw2mrc: Converted to mrc format.                    18-Oct-15  13:16:24

   70 -21925.25 -12871.75 -21925.25 -12871.75 -15483.40

 RO image file on unit   1 : run3_3VBSED_slice_0071.mrc     Size=     105469 K

 Number of columns, rows, sections .....    9000    6000       1
 Map mode .....    1   (16-bit integer)
 Start cols, rows, sects, grid x,y,z ...    0     0     0    9000   6000      1
 Pixel spacing (Angstroms).....   64.48      64.48      64.48
 Cell angles .....   90.000   90.000   90.000
 Fast, medium, slow axes .....    X    Y    Z
 Origin on x,y,z .....    0.000       0.000       0.000
 Minimum density .....  -21359.
 Maximum density .....  -12004.
 Mean density .....  -16044.
```

```
 tilt angles (original,current) .....   0.0   0.0   0.0   0.0   0.0   0.0
 Space group,# extra bytes,idtype,lens .       0       0       0       0

     1 Titles :
raw2mrc: Converted to mrc format.                  18-Oct-15  13:16:34

    71 -19667.25 -13070.00 -19667.25 -13070.00 -15485.94

 RO image file on unit   1 : run3_3VBSED_slice_0072.mrc     Size=     105469 K

 Number of columns, rows, sections .....    9000    6000       1
 Map mode ..............................    1   (16-bit integer)
 Start cols, rows, sects, grid x,y,z ...    0     0     0    9000   6000      1
 Pixel spacing (Angstroms)..............   64.48      64.48      64.48
 Cell angles ...........................   90.000   90.000   90.000
 Fast, medium, slow axes ...............    X    Y    Z
 Origin on x,y,z .......................    0.000       0.000       0.000
 Minimum density .......................  -21629.
 Maximum density .......................  -11918.
 Mean density ..........................  -16045.
 tilt angles (original,current) .....   0.0   0.0   0.0   0.0   0.0   0.0
 Space group,# extra bytes,idtype,lens .       0       0       0       0

     1 Titles :
raw2mrc: Converted to mrc format.                  18-Oct-15  13:16:43

    72 -19730.25 -13119.75 -19730.25 -13119.75 -15485.80

 RO image file on unit   1 : run3_3VBSED_slice_0073.mrc     Size=     105469 K

 Number of columns, rows, sections .....    9000    6000       1
 Map mode ..............................    1   (16-bit integer)
 Start cols, rows, sects, grid x,y,z ...    0     0     0    9000   6000      1
 Pixel spacing (Angstroms)..............   64.48      64.48      64.48
 Cell angles ...........................   90.000   90.000   90.000
 Fast, medium, slow axes ...............    X    Y    Z
 Origin on x,y,z .......................    0.000       0.000       0.000
 Minimum density .......................  -21159.
 Maximum density .......................  -11767.
 Mean density ..........................  -16031.
 tilt angles (original,current) .....   0.0   0.0   0.0   0.0   0.0   0.0
 Space group,# extra bytes,idtype,lens .       0       0       0       0

     1 Titles :
raw2mrc: Converted to mrc format.                  18-Oct-15  13:16:52
```

```
   73 -19674.75 -13020.25 -19674.75 -13020.25 -15466.33

 RO image file on unit   1 : run3_3VBSED_slice_0074.mrc     Size=     105469 K

 Number of columns, rows, sections .....    9000    6000       1
 Map mode ..............................    1   (16-bit integer)
 Start cols, rows, sects, grid x,y,z ...    0     0     0    9000   6000      1
 Pixel spacing (Angstroms)..............   64.48      64.48      64.48
 Cell angles ...........................   90.000   90.000   90.000
 Fast, medium, slow axes ...............    X    Y    Z
 Origin on x,y,z .......................    0.000       0.000       0.000
 Minimum density .......................  -21395.
 Maximum density .......................  -11936.
 Mean density ..........................  -16038.
 tilt angles (original,current) ........   0.0   0.0   0.0   0.0   0.0   0.0
 Space group,# extra bytes,idtype,lens .        0        0        0        0

     1 Titles :
raw2mrc: Converted to mrc format.                    18-Oct-15  13:17:01

   74 -19893.25 -13034.75 -19893.25 -13034.75 -15479.30

 RO image file on unit   1 : run3_3VBSED_slice_0075.mrc     Size=     105469 K

 Number of columns, rows, sections .....    9000    6000       1
 Map mode ..............................    1   (16-bit integer)
 Start cols, rows, sects, grid x,y,z ...    0     0     0    9000   6000      1
 Pixel spacing (Angstroms)..............   64.48      64.48      64.48
 Cell angles ...........................   90.000   90.000   90.000
 Fast, medium, slow axes ...............    X    Y    Z
 Origin on x,y,z .......................    0.000       0.000       0.000
 Minimum density .......................  -31396.
 Maximum density .......................  -11681.
 Mean density ..........................  -16042.
 tilt angles (original,current) ........   0.0   0.0   0.0   0.0   0.0   0.0
 Space group,# extra bytes,idtype,lens .        0        0        0        0

     1 Titles :
raw2mrc: Converted to mrc format.                    18-Oct-15  13:17:10

   75 -23681.50 -13047.00 -23681.50 -13047.00 -15481.80

 RO image file on unit   1 : run3_3VBSED_slice_0076.mrc     Size=     105469 K
```

```
 Number of columns, rows, sections .....    9000    6000       1
 Map mode ..............................    1   (16-bit integer)
 Start cols, rows, sects, grid x,y,z ...    0     0     0    9000   6000      1
 Pixel spacing (Angstroms)..............   64.48      64.48      64.48
 Cell angles ...........................   90.000   90.000   90.000
 Fast, medium, slow axes ...............    X    Y    Z
 Origin on x,y,z .......................    0.000       0.000       0.000
 Minimum density .......................  -21048.
 Maximum density .......................  -11876.
 Mean density ..........................  -16039.
 tilt angles (original,current) ........   0.0   0.0   0.0   0.0   0.0   0.0
 Space group,# extra bytes,idtype,lens .        0        0        0        0

     1 Titles :
raw2mrc: Converted to mrc format.                    18-Oct-15  13:17:19

   76 -19450.75 -13052.25 -19450.75 -13052.25 -15481.61

 RO image file on unit   1 : run3_3VBSED_slice_0077.mrc     Size=     105469 K

 Number of columns, rows, sections .....    9000    6000       1
 Map mode ..............................    1   (16-bit integer)
 Start cols, rows, sects, grid x,y,z ...    0     0     0    9000   6000      1
 Pixel spacing (Angstroms)..............   64.48      64.48      64.48
 Cell angles ...........................   90.000   90.000   90.000
 Fast, medium, slow axes ...............    X    Y    Z
 Origin on x,y,z .......................    0.000       0.000       0.000
 Minimum density .......................  -29614.
 Maximum density .......................  -11832.
 Mean density ..........................  -16056.
 tilt angles (original,current) ........   0.0   0.0   0.0   0.0   0.0   0.0
 Space group,# extra bytes,idtype,lens .        0        0        0        0

     1 Titles :
raw2mrc: Converted to mrc format.                    18-Oct-15  13:17:28

   77 -25919.00 -12992.50 -25919.00 -12992.50 -15499.76

 RO image file on unit   1 : run3_3VBSED_slice_0078.mrc     Size=     105469 K

 Number of columns, rows, sections .....    9000    6000       1
 Map mode ..............................    1   (16-bit integer)
 Start cols, rows, sects, grid x,y,z ...    0     0     0    9000   6000      1
 Pixel spacing (Angstroms)..............   64.48      64.48      64.48
 Cell angles ...........................   90.000   90.000   90.000
```

```
 Fast, medium, slow axes .....    X    Y    Z
 Origin on x,y,z .....    0.000       0.000       0.000
 Minimum density .....  -21168.
 Maximum density .....  -11830.
 Mean density .....  -16042.
 tilt angles (original,current) .....   0.0   0.0   0.0   0.0   0.0   0.0
 Space group,# extra bytes,idtype,lens .        0        0        0        0

     1 Titles :
raw2mrc: Converted to mrc format.                    18-Oct-15  13:17:37

   78 -19509.50 -12959.50 -19509.50 -12959.50 -15485.64

 RO image file on unit   1 : run3_3VBSED_slice_0079.mrc     Size=     105469 K

 Number of columns, rows, sections .....    9000    6000       1
 Map mode .....    1   (16-bit integer)
 Start cols, rows, sects, grid x,y,z ...    0     0     0    9000   6000      1
 Pixel spacing (Angstroms).....   64.48      64.48      64.48
 Cell angles .....   90.000   90.000   90.000
 Fast, medium, slow axes .....    X    Y    Z
 Origin on x,y,z .....    0.000       0.000       0.000
 Minimum density .....  -29980.
 Maximum density .....  -11762.
 Mean density .....  -16058.
 tilt angles (original,current) .....   0.0   0.0   0.0   0.0   0.0   0.0
 Space group,# extra bytes,idtype,lens .        0        0        0        0

     1 Titles :
raw2mrc: Converted to mrc format.                    18-Oct-15  13:17:47

   79 -24333.25 -12965.25 -24333.25 -12965.25 -15505.25

 RO image file on unit   1 : run3_3VBSED_slice_0080.mrc     Size=     105469 K

 Number of columns, rows, sections .....    9000    6000       1
 Map mode .....    1   (16-bit integer)
 Start cols, rows, sects, grid x,y,z ...    0     0     0    9000   6000      1
 Pixel spacing (Angstroms).....   64.48      64.48      64.48
 Cell angles .....   90.000   90.000   90.000
 Fast, medium, slow axes .....    X    Y    Z
 Origin on x,y,z .....    0.000       0.000       0.000
 Minimum density .....  -21166.
 Maximum density .....  -11847.
 Mean density .....  -16042.
```

```
 tilt angles (original,current) .....   0.0   0.0   0.0   0.0   0.0   0.0
 Space group,# extra bytes,idtype,lens .       0       0       0       0

     1 Titles :
raw2mrc: Converted to mrc format.                  18-Oct-15  13:17:59

   80 -19854.75 -13112.75 -19854.75 -13112.75 -15479.48

 RO image file on unit   1 : run3_3VBSED_slice_0081.mrc     Size=     105469 K

 Number of columns, rows, sections .....    9000    6000       1
 Map mode ..............................    1   (16-bit integer)
 Start cols, rows, sects, grid x,y,z ...    0     0     0    9000   6000      1
 Pixel spacing (Angstroms)..............   64.48      64.48      64.48
 Cell angles ...........................   90.000   90.000   90.000
 Fast, medium, slow axes ...............    X    Y    Z
 Origin on x,y,z .......................    0.000       0.000       0.000
 Minimum density .......................  -21285.
 Maximum density .......................  -11548.
 Mean density ..........................  -16046.
 tilt angles (original,current) .....   0.0   0.0   0.0   0.0   0.0   0.0
 Space group,# extra bytes,idtype,lens .       0       0       0       0

     1 Titles :
raw2mrc: Converted to mrc format.                  18-Oct-15  13:18:15

   81 -19749.25 -13000.75 -19749.25 -13000.75 -15483.47

 RO image file on unit   1 : run3_3VBSED_slice_0082.mrc     Size=     105469 K

 Number of columns, rows, sections .....    9000    6000       1
 Map mode ..............................    1   (16-bit integer)
 Start cols, rows, sects, grid x,y,z ...    0     0     0    9000   6000      1
 Pixel spacing (Angstroms)..............   64.48      64.48      64.48
 Cell angles ...........................   90.000   90.000   90.000
 Fast, medium, slow axes ...............    X    Y    Z
 Origin on x,y,z .......................    0.000       0.000       0.000
 Minimum density .......................  -23783.
 Maximum density .......................  -11878.
 Mean density ..........................  -16036.
 tilt angles (original,current) .....   0.0   0.0   0.0   0.0   0.0   0.0
 Space group,# extra bytes,idtype,lens .       0       0       0       0

     1 Titles :
raw2mrc: Converted to mrc format.                  18-Oct-15  13:18:27
```

82 -20528.75 -13072.75 -20528.75 -13072.75 -15472.13

RO image file on unit 1 : run3_3VBSED_slice_0083.mrc Size= 105469 K

Number of columns, rows, sections 9000 6000 1
Map mode ..... 1 (16-bit integer)
Start cols, rows, sects, grid x,y,z ... 0 0 0 9000 6000 1
Pixel spacing (Angstroms)..... 64.48 64.48 64.48
Cell angles 90.000 90.000 90.000
Fast, medium, slow axes ..... X Y Z
Origin on x,y,z 0.000 0.000 0.000
Minimum density ..... -29137.
Maximum density ..... -11908.
Mean density ..... -16044.
tilt angles (original,current) 0.0 0.0 0.0 0.0 0.0 0.0
Space group,# extra bytes,idtype,lens . 0 0 0 0

1 Titles :
raw2mrc: Converted to mrc format. 18-Oct-15 13:18:38

83 -21901.00 -12854.50 -21901.00 -12854.50 -15482.24

RO image file on unit 1 : run3_3VBSED_slice_0084.mrc Size= 105469 K

Number of columns, rows, sections 9000 6000 1
Map mode ..... 1 (16-bit integer)
Start cols, rows, sects, grid x,y,z ... 0 0 0 9000 6000 1
Pixel spacing (Angstroms)..... 64.48 64.48 64.48
Cell angles 90.000 90.000 90.000
Fast, medium, slow axes ..... X Y Z
Origin on x,y,z 0.000 0.000 0.000
Minimum density ..... -24106.
Maximum density ..... -11977.
Mean density ..... -16039.
tilt angles (original,current) 0.0 0.0 0.0 0.0 0.0 0.0
Space group,# extra bytes,idtype,lens . 0 0 0 0

1 Titles :
raw2mrc: Converted to mrc format. 18-Oct-15 13:19:39

84 -21924.50 -13061.75 -21924.50 -13061.75 -15472.98

RO image file on unit 1 : run3_3VBSED_slice_0085.mrc Size= 105469 K

```
 Number of columns, rows, sections .....    9000    6000       1
 Map mode ..............................    1   (16-bit integer)
 Start cols, rows, sects, grid x,y,z ...    0     0     0    9000   6000      1
 Pixel spacing (Angstroms)..............   64.48      64.48      64.48
 Cell angles ...........................   90.000   90.000   90.000
 Fast, medium, slow axes ...............    X    Y    Z
 Origin on x,y,z .......................    0.000       0.000       0.000
 Minimum density .......................  -27896.
 Maximum density .......................  -11888.
 Mean density ..........................  -16041.
 tilt angles (original,current) ........   0.0   0.0   0.0   0.0   0.0   0.0
 Space group,# extra bytes,idtype,lens .        0        0        0        0

     1 Titles :
raw2mrc: Converted to mrc format.                    18-Oct-15  13:19:48

   85 -23941.25 -13124.50 -23941.25 -13124.50 -15473.66

 RO image file on unit   1 : run3_3VBSED_slice_0086.mrc     Size=     105469 K

 Number of columns, rows, sections .....    9000    6000       1
 Map mode ..............................    1   (16-bit integer)
 Start cols, rows, sects, grid x,y,z ...    0     0     0    9000   6000      1
 Pixel spacing (Angstroms)..............   64.48      64.48      64.48
 Cell angles ...........................   90.000   90.000   90.000
 Fast, medium, slow axes ...............    X    Y    Z
 Origin on x,y,z .......................    0.000       0.000       0.000
 Minimum density .......................  -23631.
 Maximum density .......................  -11769.
 Mean density ..........................  -16042.
 tilt angles (original,current) ........   0.0   0.0   0.0   0.0   0.0   0.0
 Space group,# extra bytes,idtype,lens .        0        0        0        0

     1 Titles :
raw2mrc: Converted to mrc format.                    18-Oct-15  13:19:59

   86 -21128.75 -13136.75 -21128.75 -13136.75 -15474.92

 RO image file on unit   1 : run3_3VBSED_slice_0087.mrc     Size=     105469 K

 Number of columns, rows, sections .....    9000    6000       1
 Map mode ..............................    1   (16-bit integer)
 Start cols, rows, sects, grid x,y,z ...    0     0     0    9000   6000      1
 Pixel spacing (Angstroms)..............   64.48      64.48      64.48
 Cell angles ...........................   90.000   90.000   90.000
```

```
 Fast, medium, slow axes .....    X    Y    Z
 Origin on x,y,z .....    0.000       0.000       0.000
 Minimum density .....  -23810.
 Maximum density .....  -11921.
 Mean density .....  -16039.
 tilt angles (original,current) .....   0.0   0.0   0.0   0.0   0.0   0.0
 Space group,# extra bytes,idtype,lens .        0        0        0        0

     1 Titles :
raw2mrc: Converted to mrc format.                    18-Oct-15  13:20:08

   87 -21186.75 -13126.00 -21186.75 -13126.00 -15466.66

 RO image file on unit   1 : run3_3VBSED_slice_0088.mrc     Size=     105469 K

 Number of columns, rows, sections .....    9000    6000       1
 Map mode .....    1   (16-bit integer)
 Start cols, rows, sects, grid x,y,z ...    0     0     0    9000   6000      1
 Pixel spacing (Angstroms).....   64.48      64.48      64.48
 Cell angles .....   90.000   90.000   90.000
 Fast, medium, slow axes .....    X    Y    Z
 Origin on x,y,z .....    0.000       0.000       0.000
 Minimum density .....  -21467.
 Maximum density .....  -11804.
 Mean density .....  -16038.
 tilt angles (original,current) .....   0.0   0.0   0.0   0.0   0.0   0.0
 Space group,# extra bytes,idtype,lens .        0        0        0        0

     1 Titles :
raw2mrc: Converted to mrc format.                    18-Oct-15  13:20:18

   88 -20257.75 -12971.25 -20257.75 -12971.25 -15472.30

 RO image file on unit   1 : run3_3VBSED_slice_0089.mrc     Size=     105469 K

 Number of columns, rows, sections .....    9000    6000       1
 Map mode .....    1   (16-bit integer)
 Start cols, rows, sects, grid x,y,z ...    0     0     0    9000   6000      1
 Pixel spacing (Angstroms).....   64.48      64.48      64.48
 Cell angles .....   90.000   90.000   90.000
 Fast, medium, slow axes .....    X    Y    Z
 Origin on x,y,z .....    0.000       0.000       0.000
 Minimum density .....  -20799.
 Maximum density .....  -11704.
 Mean density .....  -16012.
```

```
 tilt angles (original,current) .....   0.0   0.0   0.0   0.0   0.0   0.0
 Space group,# extra bytes,idtype,lens .       0       0       0       0

     1 Titles :
raw2mrc: Converted to mrc format.                  18-Oct-15  13:20:27

   89 -19970.50 -13166.25 -19970.50 -13166.25 -15421.67

 RO image file on unit   1 : run3_3VBSED_slice_0090.mrc     Size=     105469 K

 Number of columns, rows, sections .....    9000    6000       1
 Map mode ..............................    1   (16-bit integer)
 Start cols, rows, sects, grid x,y,z ...    0     0     0    9000   6000      1
 Pixel spacing (Angstroms)..............   64.48      64.48      64.48
 Cell angles ...........................   90.000   90.000   90.000
 Fast, medium, slow axes ..............    X    Y    Z
 Origin on x,y,z .......................    0.000       0.000       0.000
 Minimum density .......................  -22507.
 Maximum density .......................  -11888.
 Mean density ..........................  -16040.
 tilt angles (original,current) .....   0.0   0.0   0.0   0.0   0.0   0.0
 Space group,# extra bytes,idtype,lens .       0       0       0       0

     1 Titles :
raw2mrc: Converted to mrc format.                  18-Oct-15  13:20:38

   90 -19955.25 -13219.75 -19955.25 -13219.75 -15478.45

 RO image file on unit   1 : run3_3VBSED_slice_0091.mrc     Size=     105469 K

 Number of columns, rows, sections .....    9000    6000       1
 Map mode ..............................    1   (16-bit integer)
 Start cols, rows, sects, grid x,y,z ...    0     0     0    9000   6000      1
 Pixel spacing (Angstroms)..............   64.48      64.48      64.48
 Cell angles ...........................   90.000   90.000   90.000
 Fast, medium, slow axes ..............    X    Y    Z
 Origin on x,y,z .......................    0.000       0.000       0.000
 Minimum density .......................  -23411.
 Maximum density .......................  -11882.
 Mean density ..........................  -16023.
 tilt angles (original,current) .....   0.0   0.0   0.0   0.0   0.0   0.0
 Space group,# extra bytes,idtype,lens .       0       0       0       0

     1 Titles :
raw2mrc: Converted to mrc format.                  18-Oct-15  13:20:46
```

91 -22283.75 -13065.00 -22283.75 -13065.00 -15440.76

RO image file on unit 1 : run3_3VBSED_slice_0092.mrc Size= 105469 K

Number of columns, rows, sections 9000 6000 1
Map mode ..... 1 (16-bit integer)
Start cols, rows, sects, grid x,y,z ... 0 0 0 9000 6000 1
Pixel spacing (Angstroms)..... 64.48 64.48 64.48
Cell angles 90.000 90.000 90.000
Fast, medium, slow axes ..... X Y Z
Origin on x,y,z 0.000 0.000 0.000
Minimum density ..... -26166.
Maximum density ..... -11500.
Mean density ..... -16039.
tilt angles (original,current) 0.0 0.0 0.0 0.0 0.0 0.0
Space group,# extra bytes,idtype,lens . 0 0 0 0

1 Titles :
raw2mrc: Converted to mrc format. 18-Oct-15 13:20:55

92 -22154.50 -13050.00 -22154.50 -13050.00 -15469.12

RO image file on unit 1 : run3_3VBSED_slice_0093.mrc Size= 105469 K

Number of columns, rows, sections 9000 6000 1
Map mode ..... 1 (16-bit integer)
Start cols, rows, sects, grid x,y,z ... 0 0 0 9000 6000 1
Pixel spacing (Angstroms)..... 64.48 64.48 64.48
Cell angles 90.000 90.000 90.000
Fast, medium, slow axes ..... X Y Z
Origin on x,y,z 0.000 0.000 0.000
Minimum density ..... -28663.
Maximum density ..... -11893.
Mean density ..... -16068.
tilt angles (original,current) 0.0 0.0 0.0 0.0 0.0 0.0
Space group,# extra bytes,idtype,lens . 0 0 0 0

1 Titles :
raw2mrc: Converted to mrc format. 18-Oct-15 13:21:04

93 -24287.50 -13138.50 -24287.50 -13138.50 -15514.92

RO image file on unit 1 : run3_3VBSED_slice_0094.mrc Size= 105469 K

```
 Number of columns, rows, sections .....    9000    6000       1
 Map mode ..............................    1   (16-bit integer)
 Start cols, rows, sects, grid x,y,z ...    0     0     0    9000   6000      1
 Pixel spacing (Angstroms)..............   64.48      64.48      64.48
 Cell angles ...........................   90.000   90.000   90.000
 Fast, medium, slow axes ...............    X    Y    Z
 Origin on x,y,z .......................    0.000       0.000       0.000
 Minimum density .......................  -20936.
 Maximum density .......................  -11635.
 Mean density ..........................  -16014.
 tilt angles (original,current) ........   0.0   0.0   0.0   0.0   0.0   0.0
 Space group,# extra bytes,idtype,lens .        0        0        0        0

     1 Titles :
raw2mrc: Converted to mrc format.                    18-Oct-15  13:21:13

   94 -19261.50 -12913.50 -19261.50 -12913.50 -15422.86

 RO image file on unit   1 : run3_3VBSED_slice_0095.mrc     Size=     105469 K

 Number of columns, rows, sections .....    9000    6000       1
 Map mode ..............................    1   (16-bit integer)
 Start cols, rows, sects, grid x,y,z ...    0     0     0    9000   6000      1
 Pixel spacing (Angstroms)..............   64.48      64.48      64.48
 Cell angles ...........................   90.000   90.000   90.000
 Fast, medium, slow axes ...............    X    Y    Z
 Origin on x,y,z .......................    0.000       0.000       0.000
 Minimum density .......................  -20622.
 Maximum density .......................  -11795.
 Mean density ..........................  -16055.
 tilt angles (original,current) ........   0.0   0.0   0.0   0.0   0.0   0.0
 Space group,# extra bytes,idtype,lens .        0        0        0        0

     1 Titles :
raw2mrc: Converted to mrc format.                    18-Oct-15  13:21:23

   95 -19389.75 -13133.50 -19389.75 -13133.50 -15496.23

 RO image file on unit   1 : run3_3VBSED_slice_0096.mrc     Size=     105469 K

 Number of columns, rows, sections .....    9000    6000       1
 Map mode ..............................    1   (16-bit integer)
 Start cols, rows, sects, grid x,y,z ...    0     0     0    9000   6000      1
 Pixel spacing (Angstroms)..............   64.48      64.48      64.48
 Cell angles ...........................   90.000   90.000   90.000
```

```
 Fast, medium, slow axes .....    X    Y    Z
 Origin on x,y,z .....    0.000       0.000       0.000
 Minimum density .....  -26480.
 Maximum density .....  -11555.
 Mean density .....  -16026.
 tilt angles (original,current) .....   0.0   0.0   0.0   0.0   0.0   0.0
 Space group,# extra bytes,idtype,lens .        0        0        0        0

     1 Titles :
raw2mrc: Converted to mrc format.                    18-Oct-15  13:21:33

   96 -19791.75 -12973.75 -19791.75 -12973.75 -15445.57

 RO image file on unit   1 : run3_3VBSED_slice_0097.mrc     Size=     105469 K

 Number of columns, rows, sections .....    9000    6000       1
 Map mode .....    1   (16-bit integer)
 Start cols, rows, sects, grid x,y,z ...    0     0     0    9000   6000      1
 Pixel spacing (Angstroms).....   64.48      64.48      64.48
 Cell angles .....   90.000   90.000   90.000
 Fast, medium, slow axes .....    X    Y    Z
 Origin on x,y,z .....    0.000       0.000       0.000
 Minimum density .....  -22381.
 Maximum density .....  -11812.
 Mean density .....  -16006.
 tilt angles (original,current) .....   0.0   0.0   0.0   0.0   0.0   0.0
 Space group,# extra bytes,idtype,lens .        0        0        0        0

     1 Titles :
raw2mrc: Converted to mrc format.                    18-Oct-15  13:21:42

   97 -20501.50 -12964.25 -20501.50 -12964.25 -15413.14

 RO image file on unit   1 : run3_3VBSED_slice_0098.mrc     Size=     105469 K

 Number of columns, rows, sections .....    9000    6000       1
 Map mode .....    1   (16-bit integer)
 Start cols, rows, sects, grid x,y,z ...    0     0     0    9000   6000      1
 Pixel spacing (Angstroms).....   64.48      64.48      64.48
 Cell angles .....   90.000   90.000   90.000
 Fast, medium, slow axes .....    X    Y    Z
 Origin on x,y,z .....    0.000       0.000       0.000
 Minimum density .....  -23494.
 Maximum density .....  -11802.
 Mean density .....  -16044.
```

```
 tilt angles (original,current) .....   0.0   0.0   0.0   0.0   0.0   0.0
 Space group,# extra bytes,idtype,lens .       0       0       0       0

     1 Titles :
raw2mrc: Converted to mrc format.                  18-Oct-15  13:21:51

   98 -21546.00 -13022.50 -21546.00 -13022.50 -15471.96

 RO image file on unit   1 : run3_3VBSED_slice_0099.mrc     Size=     105469 K

 Number of columns, rows, sections .....    9000    6000       1
 Map mode ..............................    1   (16-bit integer)
 Start cols, rows, sects, grid x,y,z ...    0     0     0    9000   6000      1
 Pixel spacing (Angstroms)..............   64.48      64.48      64.48
 Cell angles ...........................   90.000   90.000   90.000
 Fast, medium, slow axes ...............    X    Y    Z
 Origin on x,y,z .......................    0.000       0.000       0.000
 Minimum density .......................  -20039.
 Maximum density .......................  -11690.
 Mean density ..........................  -16011.
 tilt angles (original,current) .....   0.0   0.0   0.0   0.0   0.0   0.0
 Space group,# extra bytes,idtype,lens .       0       0       0       0

     1 Titles :
raw2mrc: Converted to mrc format.                  18-Oct-15  13:22:03

   99 -19181.25 -13030.50 -19181.25 -13030.50 -15421.45

 RO image file on unit   1 : run3_3VBSED_slice_0100.mrc     Size=     105469 K

 Number of columns, rows, sections .....    9000    6000       1
 Map mode ..............................    1   (16-bit integer)
 Start cols, rows, sects, grid x,y,z ...    0     0     0    9000   6000      1
 Pixel spacing (Angstroms)..............   64.48      64.48      64.48
 Cell angles ...........................   90.000   90.000   90.000
 Fast, medium, slow axes ...............    X    Y    Z
 Origin on x,y,z .......................    0.000       0.000       0.000
 Minimum density .......................  -20759.
 Maximum density .......................  -11855.
 Mean density ..........................  -16039.
 tilt angles (original,current) .....   0.0   0.0   0.0   0.0   0.0   0.0
 Space group,# extra bytes,idtype,lens .       0       0       0       0

     1 Titles :
raw2mrc: Converted to mrc format.                  18-Oct-15  13:22:16
```

```
  100 -19219.25 -12965.50 -19219.25 -12965.50 -15468.12

 RO image file on unit   1 : run3_3VBSED_slice_0101.mrc     Size=     105469 K

 Number of columns, rows, sections .....    9000    6000       1
 Map mode ..............................    1   (16-bit integer)
 Start cols, rows, sects, grid x,y,z ...    0     0     0    9000   6000      1
 Pixel spacing (Angstroms)..............   64.48      64.48      64.48
 Cell angles ...........................   90.000   90.000   90.000
 Fast, medium, slow axes ...............    X    Y    Z
 Origin on x,y,z .......................    0.000       0.000       0.000
 Minimum density .......................  -20061.
 Maximum density .......................  -11909.
 Mean density ..........................  -16025.
 tilt angles (original,current) ........   0.0   0.0   0.0   0.0   0.0   0.0
 Space group,# extra bytes,idtype,lens .        0        0        0        0

     1 Titles :
raw2mrc: Converted to mrc format.                    18-Oct-15  13:22:24

  101 -18839.50 -13006.25 -18839.50 -13006.25 -15440.83

 RO image file on unit   1 : run3_3VBSED_slice_0102.mrc     Size=     105469 K

 Number of columns, rows, sections .....    9000    6000       1
 Map mode ..............................    1   (16-bit integer)
 Start cols, rows, sects, grid x,y,z ...    0     0     0    9000   6000      1
 Pixel spacing (Angstroms)..............   64.48      64.48      64.48
 Cell angles ...........................   90.000   90.000   90.000
 Fast, medium, slow axes ...............    X    Y    Z
 Origin on x,y,z .......................    0.000       0.000       0.000
 Minimum density .......................  -20721.
 Maximum density .......................  -11821.
 Mean density ..........................  -16043.
 tilt angles (original,current) ........   0.0   0.0   0.0   0.0   0.0   0.0
 Space group,# extra bytes,idtype,lens .        0        0        0        0

     1 Titles :
raw2mrc: Converted to mrc format.                    18-Oct-15  13:22:33

  102 -18795.00 -13045.75 -18795.00 -13045.75 -15473.33

 RO image file on unit   1 : run3_3VBSED_slice_0103.mrc     Size=     105469 K
```

```
 Number of columns, rows, sections .....    9000    6000       1
 Map mode ..............................    1   (16-bit integer)
 Start cols, rows, sects, grid x,y,z ...    0     0     0    9000   6000      1
 Pixel spacing (Angstroms)..............   64.48      64.48      64.48
 Cell angles ...........................   90.000   90.000   90.000
 Fast, medium, slow axes ...............    X    Y    Z
 Origin on x,y,z .......................    0.000       0.000       0.000
 Minimum density .......................  -20324.
 Maximum density .......................  -11842.
 Mean density ..........................  -16020.
 tilt angles (original,current) ........   0.0   0.0   0.0   0.0   0.0   0.0
 Space group,# extra bytes,idtype,lens .        0        0        0        0

     1 Titles :
raw2mrc: Converted to mrc format.                    18-Oct-15  13:22:42

  103 -18677.75 -12993.00 -18677.75 -12993.00 -15432.66

 RO image file on unit   1 : run3_3VBSED_slice_0104.mrc     Size=     105469 K

 Number of columns, rows, sections .....    9000    6000       1
 Map mode ..............................    1   (16-bit integer)
 Start cols, rows, sects, grid x,y,z ...    0     0     0    9000   6000      1
 Pixel spacing (Angstroms)..............   64.48      64.48      64.48
 Cell angles ...........................   90.000   90.000   90.000
 Fast, medium, slow axes ...............    X    Y    Z
 Origin on x,y,z .......................    0.000       0.000       0.000
 Minimum density .......................  -20200.
 Maximum density .......................  -11730.
 Mean density ..........................  -16037.
 tilt angles (original,current) ........   0.0   0.0   0.0   0.0   0.0   0.0
 Space group,# extra bytes,idtype,lens .        0        0        0        0

     1 Titles :
raw2mrc: Converted to mrc format.                    18-Oct-15  13:22:52

  104 -18818.00 -13108.00 -18818.00 -13108.00 -15462.67

 RO image file on unit   1 : run3_3VBSED_slice_0105.mrc     Size=     105469 K

 Number of columns, rows, sections .....    9000    6000       1
 Map mode ..............................    1   (16-bit integer)
 Start cols, rows, sects, grid x,y,z ...    0     0     0    9000   6000      1
 Pixel spacing (Angstroms)..............   64.48      64.48      64.48
 Cell angles ...........................   90.000   90.000   90.000
```

```
 Fast, medium, slow axes .....    X    Y    Z
 Origin on x,y,z .....    0.000       0.000       0.000
 Minimum density .....  -22399.
 Maximum density .....  -11904.
 Mean density .....  -16020.
 tilt angles (original,current) .....   0.0   0.0   0.0   0.0   0.0   0.0
 Space group,# extra bytes,idtype,lens .        0        0        0        0

     1 Titles :
raw2mrc: Converted to mrc format.                    18-Oct-15  13:23:07

   105 -18530.50 -12861.75 -18530.50 -12861.75 -15430.96

 RO image file on unit   1 : run3_3VBSED_slice_0106.mrc     Size=     105469 K

 Number of columns, rows, sections .....    9000    6000       1
 Map mode .....    1   (16-bit integer)
 Start cols, rows, sects, grid x,y,z ...    0     0     0    9000   6000      1
 Pixel spacing (Angstroms).....   64.48      64.48      64.48
 Cell angles .....   90.000   90.000   90.000
 Fast, medium, slow axes .....    X    Y    Z
 Origin on x,y,z .....    0.000       0.000       0.000
 Minimum density .....  -21870.
 Maximum density .....  -11903.
 Mean density .....  -16042.
 tilt angles (original,current) .....   0.0   0.0   0.0   0.0   0.0   0.0
 Space group,# extra bytes,idtype,lens .        0        0        0        0

     1 Titles :
raw2mrc: Converted to mrc format.                    18-Oct-15  13:24:15

   106 -19857.00 -13063.50 -19857.00 -13063.50 -15471.85

 RO image file on unit   1 : run3_3VBSED_slice_0107.mrc     Size=     105469 K

 Number of columns, rows, sections .....    9000    6000       1
 Map mode .....    1   (16-bit integer)
 Start cols, rows, sects, grid x,y,z ...    0     0     0    9000   6000      1
 Pixel spacing (Angstroms).....   64.48      64.48      64.48
 Cell angles .....   90.000   90.000   90.000
 Fast, medium, slow axes .....    X    Y    Z
 Origin on x,y,z .....    0.000       0.000       0.000
 Minimum density .....  -19857.
 Maximum density .....  -11748.
 Mean density .....  -16019.
```

```
 tilt angles (original,current) .....   0.0   0.0   0.0   0.0   0.0   0.0
 Space group,# extra bytes,idtype,lens .       0       0       0       0

     1 Titles :
raw2mrc: Converted to mrc format.                    18-Oct-15  13:24:27

   107 -18847.25 -13050.00 -18847.25 -13050.00 -15426.91

 RO image file on unit   1 : run3_3VBSED_slice_0108.mrc     Size=     105469 K

 Number of columns, rows, sections .....    9000    6000       1
 Map mode ..............................    1   (16-bit integer)
 Start cols, rows, sects, grid x,y,z ...    0     0     0    9000   6000      1
 Pixel spacing (Angstroms)..............   64.48      64.48      64.48
 Cell angles ...........................   90.000   90.000   90.000
 Fast, medium, slow axes ...............    X    Y    Z
 Origin on x,y,z .......................    0.000       0.000       0.000
 Minimum density .......................  -20246.
 Maximum density .......................  -11863.
 Mean density ..........................  -16042.
 tilt angles (original,current) .....   0.0   0.0   0.0   0.0   0.0   0.0
 Space group,# extra bytes,idtype,lens .       0       0       0       0

     1 Titles :
raw2mrc: Converted to mrc format.                    18-Oct-15  13:24:37

   108 -19524.50 -13039.50 -19524.50 -13039.50 -15464.08

 RO image file on unit   1 : run3_3VBSED_slice_0109.mrc     Size=     105469 K

 Number of columns, rows, sections .....    9000    6000       1
 Map mode ..............................    1   (16-bit integer)
 Start cols, rows, sects, grid x,y,z ...    0     0     0    9000   6000      1
 Pixel spacing (Angstroms)..............   64.48      64.48      64.48
 Cell angles ...........................   90.000   90.000   90.000
 Fast, medium, slow axes ...............    X    Y    Z
 Origin on x,y,z .......................    0.000       0.000       0.000
 Minimum density .......................  -21086.
 Maximum density .......................  -11899.
 Mean density ..........................  -16016.
 tilt angles (original,current) .....   0.0   0.0   0.0   0.0   0.0   0.0
 Space group,# extra bytes,idtype,lens .       0       0       0       0

     1 Titles :
raw2mrc: Converted to mrc format.                    18-Oct-15  13:24:48
```

```
  109 -19373.00 -13086.50 -19373.00 -13086.50 -15421.95

 RO image file on unit   1 : run3_3VBSED_slice_0110.mrc     Size=     105469 K

 Number of columns, rows, sections .....    9000    6000       1
 Map mode ..............................    1   (16-bit integer)
 Start cols, rows, sects, grid x,y,z ...    0     0     0    9000   6000      1
 Pixel spacing (Angstroms)..............   64.48      64.48      64.48
 Cell angles ...........................   90.000   90.000   90.000
 Fast, medium, slow axes ...............    X    Y    Z
 Origin on x,y,z .......................    0.000       0.000       0.000
 Minimum density .......................  -20426.
 Maximum density .......................  -11784.
 Mean density ..........................  -16043.
 tilt angles (original,current) ........   0.0   0.0   0.0   0.0   0.0   0.0
 Space group,# extra bytes,idtype,lens .        0        0        0        0

     1 Titles :
raw2mrc: Converted to mrc format.                    18-Oct-15  13:25:00

  110 -18969.00 -13107.75 -18969.00 -13107.75 -15471.58

 RO image file on unit   1 : run3_3VBSED_slice_0111.mrc     Size=     105469 K

 Number of columns, rows, sections .....    9000    6000       1
 Map mode ..............................    1   (16-bit integer)
 Start cols, rows, sects, grid x,y,z ...    0     0     0    9000   6000      1
 Pixel spacing (Angstroms)..............   64.48      64.48      64.48
 Cell angles ...........................   90.000   90.000   90.000
 Fast, medium, slow axes ...............    X    Y    Z
 Origin on x,y,z .......................    0.000       0.000       0.000
 Minimum density .......................  -21739.
 Maximum density .......................  -11585.
 Mean density ..........................  -16021.
 tilt angles (original,current) ........   0.0   0.0   0.0   0.0   0.0   0.0
 Space group,# extra bytes,idtype,lens .        0        0        0        0

     1 Titles :
raw2mrc: Converted to mrc format.                    18-Oct-15  13:25:09

  111 -19343.50 -13158.00 -19343.50 -13158.00 -15430.74

 RO image file on unit   1 : run3_3VBSED_slice_0112.mrc     Size=     105469 K
```

```
 Number of columns, rows, sections .....    9000    6000       1
 Map mode ..............................    1   (16-bit integer)
 Start cols, rows, sects, grid x,y,z ...    0     0     0    9000   6000      1
 Pixel spacing (Angstroms)..............   64.48      64.48      64.48
 Cell angles ...........................   90.000   90.000   90.000
 Fast, medium, slow axes ...............    X    Y    Z
 Origin on x,y,z .......................    0.000       0.000       0.000
 Minimum density .......................  -21446.
 Maximum density .......................  -11879.
 Mean density ..........................  -16044.
 tilt angles (original,current) ........   0.0   0.0   0.0   0.0   0.0   0.0
 Space group,# extra bytes,idtype,lens .        0        0        0        0

     1 Titles :
raw2mrc: Converted to mrc format.                    18-Oct-15  13:25:19

   112 -18855.25 -13032.50 -18855.25 -13032.50 -15472.68

Don-Johnsons-MacBook-Pro:Hela_APEX_20151013_2A_4cell djohnson$
newstack -bi 2 run4_20151014_1_3ViewBS_slice_0*.mrc
run4_20151014_1_3ViewBS_bin2.st

 RO image file on unit   1 : run4_20151014_1_3ViewBS_slice_0000.mrc     Size=
195313 K

 Number of columns, rows, sections .....   10000   10000       1
 Map mode ..............................    1   (16-bit integer)
 Start cols, rows, sects, grid x,y,z ...    0     0     0   10000  10000      1
 Pixel spacing (Angstroms)..............   28.13      28.13      28.13
 Cell angles ...........................   90.000   90.000   90.000
 Fast, medium, slow axes ...............    X    Y    Z
 Origin on x,y,z .......................    0.000       0.000       0.000
 Minimum density .......................  -21751.
 Maximum density .......................  -1469.0
 Mean density ..........................  -12952.
 tilt angles (original,current) ........   0.0   0.0   0.0   0.0   0.0   0.0
 Space group,# extra bytes,idtype,lens .        0        0        0        0

     1 Titles :
raw2mrc: Converted to mrc format.                    18-Oct-15  11:31:57


 NEW image file on unit   2 : run4_20151014_1_3ViewBS_bin2.st
 section   input min&max       output min&max  &  mean
    0 -20038.25  -7639.75 -20038.25  -7639.75 -12379.92
```

```
 RO image file on unit   1 : run4_20151014_1_3ViewBS_slice_0001.mrc     Size=
195313 K

 Number of columns, rows, sections .....   10000   10000       1
 Map mode ..............................    1   (16-bit integer)
 Start cols, rows, sects, grid x,y,z ...    0     0     0   10000  10000      1
 Pixel spacing (Angstroms)..............   28.13      28.13      28.13
 Cell angles ...........................   90.000   90.000   90.000
 Fast, medium, slow axes ...............    X    Y    Z
 Origin on x,y,z .......................    0.000       0.000       0.000
 Minimum density .......................  -21730.
 Maximum density .......................  -2941.0
 Mean density ..........................  -14336.
 tilt angles (original,current) ........   0.0   0.0   0.0   0.0   0.0   0.0
 Space group,# extra bytes,idtype,lens .        0        0        0        0

     1 Titles :
raw2mrc: Converted to mrc format.                    18-Oct-15  11:33:56

     1 -20118.00  -8343.50 -20118.00  -8343.50 -13270.04

 RO image file on unit   1 : run4_20151014_1_3ViewBS_slice_0002.mrc     Size=
195313 K

 Number of columns, rows, sections .....   10000   10000       1
 Map mode ..............................    1   (16-bit integer)
 Start cols, rows, sects, grid x,y,z ...    0     0     0   10000  10000      1
 Pixel spacing (Angstroms)..............   28.13      28.13      28.13
 Cell angles ...........................   90.000   90.000   90.000
 Fast, medium, slow axes ...............    X    Y    Z
 Origin on x,y,z .......................    0.000       0.000       0.000
 Minimum density .......................  -21598.
 Maximum density .......................  -2680.0
 Mean density ..........................  -14331.
 tilt angles (original,current) ........   0.0   0.0   0.0   0.0   0.0   0.0
 Space group,# extra bytes,idtype,lens .        0        0        0        0

     1 Titles :
raw2mrc: Converted to mrc format.                    18-Oct-15  11:34:27

     2 -19812.00  -8535.00 -19812.00  -8535.00 -13249.60

 RO image file on unit   1 : run4_20151014_1_3ViewBS_slice_0003.mrc     Size=
195313 K
```

```
 Number of columns, rows, sections .....   10000   10000       1
 Map mode ..............................    1   (16-bit integer)
 Start cols, rows, sects, grid x,y,z ...    0     0     0   10000  10000      1
 Pixel spacing (Angstroms)..............   28.13      28.13      28.13
 Cell angles ...........................   90.000   90.000   90.000
 Fast, medium, slow axes ...............    X    Y    Z
 Origin on x,y,z .......................    0.000       0.000       0.000
 Minimum density .......................  -21146.
 Maximum density .......................  -3321.0
 Mean density ..........................  -14365.
 tilt angles (original,current) ........   0.0   0.0   0.0   0.0   0.0   0.0
 Space group,# extra bytes,idtype,lens .        0        0        0        0

    1 Titles :
raw2mrc: Converted to mrc format.                    18-Oct-15  11:34:41

    3 -18612.75  -7883.25 -18612.75  -7883.25 -13275.60

 RO image file on unit   1 : run4_20151014_1_3ViewBS_slice_0004.mrc     Size=
195313 K

 Number of columns, rows, sections .....   10000   10000       1
 Map mode ..............................    1   (16-bit integer)
 Start cols, rows, sects, grid x,y,z ...    0     0     0   10000  10000      1
 Pixel spacing (Angstroms)..............   28.13      28.13      28.13
 Cell angles ...........................   90.000   90.000   90.000
 Fast, medium, slow axes ...............    X    Y    Z
 Origin on x,y,z .......................    0.000       0.000       0.000
 Minimum density .......................  -22258.
 Maximum density .......................  -2502.0
 Mean density ..........................  -14391.
 tilt angles (original,current) ........   0.0   0.0   0.0   0.0   0.0   0.0
 Space group,# extra bytes,idtype,lens .        0        0        0        0

    1 Titles :
raw2mrc: Converted to mrc format.                    18-Oct-15  11:34:55

    4 -20119.50  -8337.50 -20119.50  -8337.50 -13291.42

 RO image file on unit   1 : run4_20151014_1_3ViewBS_slice_0005.mrc     Size=
195313 K

 Number of columns, rows, sections .....   10000   10000       1
 Map mode ..............................    1   (16-bit integer)
```

```
 Start cols, rows, sects, grid x,y,z ...    0     0     0   10000  10000      1
 Pixel spacing (Angstroms).............   28.13      28.13      28.13
 Cell angles ...........................   90.000   90.000   90.000
 Fast, medium, slow axes .............    X    Y    Z
 Origin on x,y,z .....................    0.000       0.000       0.000
 Minimum density .....................  -21810.
 Maximum density .....................  -3552.0
 Mean density ........................  -14444.
 tilt angles (original,current) .....   0.0   0.0   0.0   0.0   0.0   0.0
 Space group,# extra bytes,idtype,lens .        0        0        0        0

     1 Titles :
raw2mrc: Converted to mrc format.                    18-Oct-15  11:35:12

     5 -19974.00  -8125.50 -19974.00  -8125.50 -13333.21

 RO image file on unit   1 : run4_20151014_1_3ViewBS_slice_0006.mrc     Size=
195313 K

 Number of columns, rows, sections .....   10000   10000       1
 Map mode ..............................    1   (16-bit integer)
 Start cols, rows, sects, grid x,y,z ...    0     0     0   10000  10000      1
 Pixel spacing (Angstroms).............   28.13      28.13      28.13
 Cell angles ...........................   90.000   90.000   90.000
 Fast, medium, slow axes .............    X    Y    Z
 Origin on x,y,z .....................    0.000       0.000       0.000
 Minimum density .....................  -22217.
 Maximum density .....................  -3052.0
 Mean density ........................  -14426.
 tilt angles (original,current) .....   0.0   0.0   0.0   0.0   0.0   0.0
 Space group,# extra bytes,idtype,lens .        0        0        0        0

     1 Titles :
raw2mrc: Converted to mrc format.                    18-Oct-15  11:35:33

     6 -20221.00  -8131.00 -20221.00  -8131.00 -13314.79

 RO image file on unit   1 : run4_20151014_1_3ViewBS_slice_0007.mrc     Size=
195313 K

 Number of columns, rows, sections .....   10000   10000       1
 Map mode ..............................    1   (16-bit integer)
 Start cols, rows, sects, grid x,y,z ...    0     0     0   10000  10000      1
 Pixel spacing (Angstroms).............   28.13      28.13      28.13
 Cell angles ...........................   90.000   90.000   90.000
```

```
 Fast, medium, slow axes .....    X    Y    Z
 Origin on x,y,z .....    0.000       0.000       0.000
 Minimum density .....  -21012.
 Maximum density .....  -3182.0
 Mean density .....  -14451.
 tilt angles (original,current) .....   0.0   0.0   0.0   0.0   0.0   0.0
 Space group,# extra bytes,idtype,lens .        0        0        0        0

    1 Titles :
raw2mrc: Converted to mrc format.                    18-Oct-15  11:36:27

    7 -20303.75  -8428.00 -20303.75  -8428.00 -13342.12

 RO image file on unit   1 : run4_20151014_1_3ViewBS_slice_0008.mrc     Size=
195313 K

 Number of columns, rows, sections .....   10000   10000       1
 Map mode .....    1   (16-bit integer)
 Start cols, rows, sects, grid x,y,z ...    0     0     0   10000  10000      1
 Pixel spacing (Angstroms).....   28.13      28.13      28.13
 Cell angles .....   90.000   90.000   90.000
 Fast, medium, slow axes .....    X    Y    Z
 Origin on x,y,z .....    0.000       0.000       0.000
 Minimum density .....  -20625.
 Maximum density .....  -3464.0
 Mean density .....  -14518.
 tilt angles (original,current) .....   0.0   0.0   0.0   0.0   0.0   0.0
 Space group,# extra bytes,idtype,lens .        0        0        0        0

    1 Titles :
raw2mrc: Converted to mrc format.                    18-Oct-15  11:36:41

    8 -19029.25  -8424.50 -19029.25  -8424.50 -13392.30

 RO image file on unit   1 : run4_20151014_1_3ViewBS_slice_0009.mrc     Size=
195313 K

 Number of columns, rows, sections .....   10000   10000       1
 Map mode .....    1   (16-bit integer)
 Start cols, rows, sects, grid x,y,z ...    0     0     0   10000  10000      1
 Pixel spacing (Angstroms).....   28.13      28.13      28.13
 Cell angles .....   90.000   90.000   90.000
 Fast, medium, slow axes .....    X    Y    Z
 Origin on x,y,z .....    0.000       0.000       0.000
 Minimum density .....  -23705.
```

```
 Maximum density .....  -3462.0
 Mean density .....  -14502.
 tilt angles (original,current) .....   0.0   0.0   0.0   0.0   0.0   0.0
 Space group,# extra bytes,idtype,lens .        0        0        0        0

     1 Titles :
raw2mrc: Converted to mrc format.                    18-Oct-15  11:37:00

     9 -18277.25  -8655.75 -18277.25  -8655.75 -13380.41

 RO image file on unit   1 : run4_20151014_1_3ViewBS_slice_0010.mrc     Size=
195313 K

 Number of columns, rows, sections .....   10000   10000       1
 Map mode .....    1   (16-bit integer)
 Start cols, rows, sects, grid x,y,z ...    0     0     0   10000  10000      1
 Pixel spacing (Angstroms).....   28.13      28.13      28.13
 Cell angles .....   90.000   90.000   90.000
 Fast, medium, slow axes .....    X    Y    Z
 Origin on x,y,z .....    0.000       0.000       0.000
 Minimum density .....  -32758.
 Maximum density .....   6740.0
 Mean density .....  -14388.
 tilt angles (original,current) .....   0.0   0.0   0.0   0.0   0.0   0.0
 Space group,# extra bytes,idtype,lens .        0        0        0        0

     1 Titles :
raw2mrc: Converted to mrc format.                    18-Oct-15  11:37:19

    10 -21323.50  -4170.00 -21323.50  -4170.00 -13298.26

 RO image file on unit   1 : run4_20151014_1_3ViewBS_slice_0011.mrc     Size=
195313 K

 Number of columns, rows, sections .....   10000   10000       1
 Map mode .....    1   (16-bit integer)
 Start cols, rows, sects, grid x,y,z ...    0     0     0   10000  10000      1
 Pixel spacing (Angstroms).....   28.13      28.13      28.13
 Cell angles .....   90.000   90.000   90.000
 Fast, medium, slow axes .....    X    Y    Z
 Origin on x,y,z .....    0.000       0.000       0.000
 Minimum density .....  -32758.
 Maximum density .....   6486.0
 Mean density .....  -14443.
 tilt angles (original,current) .....   0.0   0.0   0.0   0.0   0.0   0.0
```

Space group,# extra bytes,idtype,lens . 0 0 0 0

1 Titles :
raw2mrc: Converted to mrc format. 18-Oct-15 11:37:34

11 -21238.50 -3248.25 -21238.50 -3248.25 -13342.36

RO image file on unit 1 : run4_20151014_1_3ViewBS_slice_0012.mrc Size= 195313 K

Number of columns, rows, sections 10000 10000 1
Map mode ..... 1 (16-bit integer)
Start cols, rows, sects, grid x,y,z ... 0 0 0 10000 10000 1
Pixel spacing (Angstroms)..... 28.13 28.13 28.13
Cell angles 90.000 90.000 90.000
Fast, medium, slow axes ..... X Y Z
Origin on x,y,z 0.000 0.000 0.000
Minimum density ..... -21837.
Maximum density ..... -3206.0
Mean density ..... -14497.
tilt angles (original,current) 0.0 0.0 0.0 0.0 0.0 0.0
Space group,# extra bytes,idtype,lens . 0 0 0 0

1 Titles :
raw2mrc: Converted to mrc format. 18-Oct-15 11:37:49

12 -20931.75 -8873.75 -20931.75 -8873.75 -13382.81

RO image file on unit 1 : run4_20151014_1_3ViewBS_slice_0013.mrc Size= 195313 K

Number of columns, rows, sections 10000 10000 1
Map mode ..... 1 (16-bit integer)
Start cols, rows, sects, grid x,y,z ... 0 0 0 10000 10000 1
Pixel spacing (Angstroms)..... 28.13 28.13 28.13
Cell angles 90.000 90.000 90.000
Fast, medium, slow axes ..... X Y Z
Origin on x,y,z 0.000 0.000 0.000
Minimum density ..... -26733.
Maximum density ..... -3755.0
Mean density ..... -14496.
tilt angles (original,current) 0.0 0.0 0.0 0.0 0.0 0.0
Space group,# extra bytes,idtype,lens . 0 0 0 0

1 Titles :

raw2mrc: Converted to mrc format. 18-Oct-15 11:38:05

13 -19276.50 -8011.50 -19276.50 -8011.50 -13383.07

RO image file on unit 1 : run4_20151014_1_3ViewBS_slice_0014.mrc Size= 195313 K

Number of columns, rows, sections 10000 10000 1
Map mode ..... 1 (16-bit integer)
Start cols, rows, sects, grid x,y,z ... 0 0 0 10000 10000 1
Pixel spacing (Angstroms)..... 28.13 28.13 28.13
Cell angles 90.000 90.000 90.000
Fast, medium, slow axes ..... X Y Z
Origin on x,y,z 0.000 0.000 0.000
Minimum density ..... -20521.
Maximum density ..... -2724.0
Mean density ..... -14509.
tilt angles (original,current) 0.0 0.0 0.0 0.0 0.0 0.0
Space group,# extra bytes,idtype,lens . 0 0 0 0

1 Titles :
raw2mrc: Converted to mrc format. 18-Oct-15 11:38:24

14 -18282.75 -8365.25 -18282.75 -8365.25 -13395.65

RO image file on unit 1 : run4_20151014_1_3ViewBS_slice_0015.mrc Size= 195313 K

Number of columns, rows, sections 10000 10000 1
Map mode ..... 1 (16-bit integer)
Start cols, rows, sects, grid x,y,z ... 0 0 0 10000 10000 1
Pixel spacing (Angstroms)..... 28.13 28.13 28.13
Cell angles 90.000 90.000 90.000
Fast, medium, slow axes ..... X Y Z
Origin on x,y,z 0.000 0.000 0.000
Minimum density ..... -32758.
Maximum density ..... -3214.0
Mean density ..... -14302.
tilt angles (original,current) 0.0 0.0 0.0 0.0 0.0 0.0
Space group,# extra bytes,idtype,lens . 0 0 0 0

1 Titles :
raw2mrc: Converted to mrc format. 18-Oct-15 11:38:41

15 -21043.50 -8181.75 -21043.50 -8181.75 -13239.24

```
 RO image file on unit   1 : run4_20151014_1_3ViewBS_slice_0016.mrc     Size=
195313 K

 Number of columns, rows, sections .....   10000   10000       1
 Map mode ..............................    1   (16-bit integer)
 Start cols, rows, sects, grid x,y,z ...    0     0     0   10000  10000      1
 Pixel spacing (Angstroms)..............   28.13      28.13      28.13
 Cell angles ...........................   90.000   90.000   90.000
 Fast, medium, slow axes ..............    X    Y    Z
 Origin on x,y,z .......................    0.000       0.000       0.000
 Minimum density .......................  -21874.
 Maximum density .......................  -3084.0
 Mean density ..........................  -14483.
 tilt angles (original,current) ........   0.0   0.0   0.0   0.0   0.0   0.0
 Space group,# extra bytes,idtype,lens .        0        0        0        0

     1 Titles :
raw2mrc: Converted to mrc format.                    18-Oct-15  11:39:14

    16 -20411.75  -8670.25 -20411.75  -8670.25 -13382.50

 RO image file on unit   1 : run4_20151014_1_3ViewBS_slice_0017.mrc     Size=
195313 K

 Number of columns, rows, sections .....   10000   10000       1
 Map mode ..............................    1   (16-bit integer)
 Start cols, rows, sects, grid x,y,z ...    0     0     0   10000  10000      1
 Pixel spacing (Angstroms)..............   28.13      28.13      28.13
 Cell angles ...........................   90.000   90.000   90.000
 Fast, medium, slow axes ..............    X    Y    Z
 Origin on x,y,z .......................    0.000       0.000       0.000
 Minimum density .......................  -21619.
 Maximum density .......................  -3244.0
 Mean density ..........................  -14548.
 tilt angles (original,current) ........   0.0   0.0   0.0   0.0   0.0   0.0
 Space group,# extra bytes,idtype,lens .        0        0        0        0

     1 Titles :
raw2mrc: Converted to mrc format.                    18-Oct-15  11:39:28

    17 -20161.00  -8801.50 -20161.00  -8801.50 -13427.94

 RO image file on unit   1 : run4_20151014_1_3ViewBS_slice_0018.mrc     Size=
195313 K
```

```
 Number of columns, rows, sections .....   10000   10000       1
 Map mode ..............................    1   (16-bit integer)
 Start cols, rows, sects, grid x,y,z ...    0     0     0   10000  10000      1
 Pixel spacing (Angstroms)..............   28.13      28.13      28.13
 Cell angles ...........................   90.000   90.000   90.000
 Fast, medium, slow axes ..............    X    Y    Z
 Origin on x,y,z .......................    0.000       0.000       0.000
 Minimum density .......................  -32758.
 Maximum density .......................   6505.0
 Mean density ..........................  -14551.
 tilt angles (original,current) ........   0.0   0.0   0.0   0.0   0.0   0.0
 Space group,# extra bytes,idtype,lens .        0        0        0        0

     1 Titles :
raw2mrc: Converted to mrc format.                    18-Oct-15  11:39:49

   18 -22322.25  -4713.50 -22322.25  -4713.50 -13438.68

 RO image file on unit   1 : run4_20151014_1_3ViewBS_slice_0019.mrc     Size=
195313 K

 Number of columns, rows, sections .....   10000   10000       1
 Map mode ..............................    1   (16-bit integer)
 Start cols, rows, sects, grid x,y,z ...    0     0     0   10000  10000      1
 Pixel spacing (Angstroms)..............   28.13      28.13      28.13
 Cell angles ...........................   90.000   90.000   90.000
 Fast, medium, slow axes ..............    X    Y    Z
 Origin on x,y,z .......................    0.000       0.000       0.000
 Minimum density .......................  -25788.
 Maximum density .......................  -1687.0
 Mean density ..........................  -12790.
 tilt angles (original,current) ........   0.0   0.0   0.0   0.0   0.0   0.0
 Space group,# extra bytes,idtype,lens .        0        0        0        0

     1 Titles :
raw2mrc: Converted to mrc format.                    18-Oct-15  11:40:08

   19 -16712.50  -7326.50 -16712.50  -7326.50 -12325.80

 RO image file on unit   1 : run4_20151014_1_3ViewBS_slice_0020.mrc     Size=
195313 K

 Number of columns, rows, sections .....   10000   10000       1
 Map mode ..............................    1   (16-bit integer)
```

```
 Start cols, rows, sects, grid x,y,z ...    0     0     0   10000  10000      1
 Pixel spacing (Angstroms).............   28.13      28.13      28.13
 Cell angles ...........................   90.000   90.000   90.000
 Fast, medium, slow axes .............    X    Y    Z
 Origin on x,y,z .....................    0.000       0.000       0.000
 Minimum density .....................  -32758.
 Maximum density .....................  -1835.0
 Mean density ........................  -14521.
 tilt angles (original,current) .....   0.0   0.0   0.0   0.0   0.0   0.0
 Space group,# extra bytes,idtype,lens .        0        0        0        0

     1 Titles :
raw2mrc: Converted to mrc format.                    18-Oct-15  11:44:05

   20 -21106.50  -8219.75 -21106.50  -8219.75 -13437.29

 RO image file on unit   1 : run4_20151014_1_3ViewBS_slice_0021.mrc     Size=
195313 K

 Number of columns, rows, sections .....   10000   10000       1
 Map mode ..............................    1   (16-bit integer)
 Start cols, rows, sects, grid x,y,z ...    0     0     0   10000  10000      1
 Pixel spacing (Angstroms).............   28.13      28.13      28.13
 Cell angles ...........................   90.000   90.000   90.000
 Fast, medium, slow axes .............    X    Y    Z
 Origin on x,y,z .....................    0.000       0.000       0.000
 Minimum density .....................  -31738.
 Maximum density .....................  -3245.0
 Mean density ........................  -14432.
 tilt angles (original,current) .....   0.0   0.0   0.0   0.0   0.0   0.0
 Space group,# extra bytes,idtype,lens .        0        0        0        0

     1 Titles :
raw2mrc: Converted to mrc format.                    18-Oct-15  11:45:06

   21 -20858.50  -8179.00 -20858.50  -8179.00 -13348.52

 RO image file on unit   1 : run4_20151014_1_3ViewBS_slice_0022.mrc     Size=
195313 K

 Number of columns, rows, sections .....   10000   10000       1
 Map mode ..............................    1   (16-bit integer)
 Start cols, rows, sects, grid x,y,z ...    0     0     0   10000  10000      1
 Pixel spacing (Angstroms).............   28.13      28.13      28.13
 Cell angles ...........................   90.000   90.000   90.000
```

```
 Fast, medium, slow axes .....    X    Y    Z
 Origin on x,y,z .....    0.000       0.000       0.000
 Minimum density .....  -21388.
 Maximum density .....  -3096.0
 Mean density .....  -14343.
 tilt angles (original,current) .....   0.0   0.0   0.0   0.0   0.0   0.0
 Space group,# extra bytes,idtype,lens .        0        0        0        0

     1 Titles :
raw2mrc: Converted to mrc format.                    18-Oct-15  11:46:18

   22 -18196.75  -8758.50 -18196.75  -8758.50 -13282.71

 RO image file on unit   1 : run4_20151014_1_3ViewBS_slice_0023.mrc     Size=
195313 K

 Number of columns, rows, sections .....   10000   10000       1
 Map mode .....    1   (16-bit integer)
 Start cols, rows, sects, grid x,y,z ...    0     0     0   10000  10000      1
 Pixel spacing (Angstroms).....   28.13      28.13      28.13
 Cell angles .....   90.000   90.000   90.000
 Fast, medium, slow axes .....    X    Y    Z
 Origin on x,y,z .....    0.000       0.000       0.000
 Minimum density .....  -22315.
 Maximum density .....  -3716.0
 Mean density .....  -14371.
 tilt angles (original,current) .....   0.0   0.0   0.0   0.0   0.0   0.0
 Space group,# extra bytes,idtype,lens .        0        0        0        0

     1 Titles :
raw2mrc: Converted to mrc format.                    18-Oct-15  11:46:36

   23 -20481.00  -8123.50 -20481.00  -8123.50 -13308.12

 RO image file on unit   1 : run4_20151014_1_3ViewBS_slice_0024.mrc     Size=
195313 K

 Number of columns, rows, sections .....   10000   10000       1
 Map mode .....    1   (16-bit integer)
 Start cols, rows, sects, grid x,y,z ...    0     0     0   10000  10000      1
 Pixel spacing (Angstroms).....   28.13      28.13      28.13
 Cell angles .....   90.000   90.000   90.000
 Fast, medium, slow axes .....    X    Y    Z
 Origin on x,y,z .....    0.000       0.000       0.000
 Minimum density .....  -32767.
```

```
 Maximum density .....  -2843.0
 Mean density .....  -14345.
 tilt angles (original,current) .....   0.0   0.0   0.0   0.0   0.0   0.0
 Space group,# extra bytes,idtype,lens .        0        0        0        0

     1 Titles :
raw2mrc: Converted to mrc format.                    18-Oct-15  11:50:48

   24 -24220.75  -8441.50 -24220.75  -8441.50 -13283.45

 RO image file on unit   1 : run4_20151014_1_3ViewBS_slice_0025.mrc     Size=
195313 K

 Number of columns, rows, sections .....   10000   10000       1
 Map mode .....    1   (16-bit integer)
 Start cols, rows, sects, grid x,y,z ...    0     0     0   10000  10000      1
 Pixel spacing (Angstroms).....   28.13      28.13      28.13
 Cell angles .....   90.000   90.000   90.000
 Fast, medium, slow axes .....    X    Y    Z
 Origin on x,y,z .....    0.000       0.000       0.000
 Minimum density .....  -32758.
 Maximum density .....   6640.0
 Mean density .....  -14330.
 tilt angles (original,current) .....   0.0   0.0   0.0   0.0   0.0   0.0
 Space group,# extra bytes,idtype,lens .        0        0        0        0

     1 Titles :
raw2mrc: Converted to mrc format.                    18-Oct-15  11:52:38

   25 -22529.50  -3723.00 -22529.50  -3723.00 -13275.81

 RO image file on unit   1 : run4_20151014_1_3ViewBS_slice_0026.mrc     Size=
195313 K

 Number of columns, rows, sections .....   10000   10000       1
 Map mode .....    1   (16-bit integer)
 Start cols, rows, sects, grid x,y,z ...    0     0     0   10000  10000      1
 Pixel spacing (Angstroms).....   28.13      28.13      28.13
 Cell angles .....   90.000   90.000   90.000
 Fast, medium, slow axes .....    X    Y    Z
 Origin on x,y,z .....    0.000       0.000       0.000
 Minimum density .....  -21903.
 Maximum density .....  -3153.0
 Mean density .....  -14348.
 tilt angles (original,current) .....   0.0   0.0   0.0   0.0   0.0   0.0
```

Space group,# extra bytes,idtype,lens . 0 0 0 0

1 Titles :
raw2mrc: Converted to mrc format. 18-Oct-15 11:52:52

26 -18164.00 -7908.75 -18164.00 -7908.75 -13289.78

RO image file on unit 1 : run4_20151014_1_3ViewBS_slice_0027.mrc Size= 195313 K

Number of columns, rows, sections 10000 10000 1
Map mode ..... 1 (16-bit integer)
Start cols, rows, sects, grid x,y,z ... 0 0 0 10000 10000 1
Pixel spacing (Angstroms)..... 28.13 28.13 28.13
Cell angles 90.000 90.000 90.000
Fast, medium, slow axes ..... X Y Z
Origin on x,y,z 0.000 0.000 0.000
Minimum density ..... -21081.
Maximum density ..... -3006.0
Mean density ..... -14340.
tilt angles (original,current) 0.0 0.0 0.0 0.0 0.0 0.0
Space group,# extra bytes,idtype,lens . 0 0 0 0

1 Titles :
raw2mrc: Converted to mrc format. 18-Oct-15 11:53:08

27 -19266.50 -8295.50 -19266.50 -8295.50 -13280.50

RO image file on unit 1 : run4_20151014_1_3ViewBS_slice_0028.mrc Size= 195313 K

Number of columns, rows, sections 10000 10000 1
Map mode ..... 1 (16-bit integer)
Start cols, rows, sects, grid x,y,z ... 0 0 0 10000 10000 1
Pixel spacing (Angstroms)..... 28.13 28.13 28.13
Cell angles 90.000 90.000 90.000
Fast, medium, slow axes ..... X Y Z
Origin on x,y,z 0.000 0.000 0.000
Minimum density ..... -20308.
Maximum density ..... -3027.0
Mean density ..... -14357.
tilt angles (original,current) 0.0 0.0 0.0 0.0 0.0 0.0
Space group,# extra bytes,idtype,lens . 0 0 0 0

1 Titles :

raw2mrc: Converted to mrc format. 18-Oct-15 11:53:27

28 -18107.25 -7690.00 -18107.25 -7690.00 -13292.38

RO image file on unit 1 : run4_20151014_1_3ViewBS_slice_0029.mrc Size= 195313 K

Number of columns, rows, sections 10000 10000 1
Map mode ..... 1 (16-bit integer)
Start cols, rows, sects, grid x,y,z ... 0 0 0 10000 10000 1
Pixel spacing (Angstroms)..... 28.13 28.13 28.13
Cell angles 90.000 90.000 90.000
Fast, medium, slow axes ..... X Y Z
Origin on x,y,z 0.000 0.000 0.000
Minimum density ..... -32758.
Maximum density 2774.0
Mean density ..... -14381.
tilt angles (original,current) 0.0 0.0 0.0 0.0 0.0 0.0
Space group,# extra bytes,idtype,lens . 0 0 0 0

1 Titles :
raw2mrc: Converted to mrc format. 18-Oct-15 11:53:46

29 -23032.00 -7682.00 -23032.00 -7682.00 -13312.75

RO image file on unit 1 : run4_20151014_1_3ViewBS_slice_0030.mrc Size= 195313 K

Number of columns, rows, sections 10000 10000 1
Map mode ..... 1 (16-bit integer)
Start cols, rows, sects, grid x,y,z ... 0 0 0 10000 10000 1
Pixel spacing (Angstroms)..... 28.13 28.13 28.13
Cell angles 90.000 90.000 90.000
Fast, medium, slow axes ..... X Y Z
Origin on x,y,z 0.000 0.000 0.000
Minimum density ..... -21435.
Maximum density ..... -3815.0
Mean density ..... -14404.
tilt angles (original,current) 0.0 0.0 0.0 0.0 0.0 0.0
Space group,# extra bytes,idtype,lens . 0 0 0 0

1 Titles :
raw2mrc: Converted to mrc format. 18-Oct-15 11:54:07

30 -19600.75 -8426.00 -19600.75 -8426.00 -13332.36

```
 RO image file on unit   1 : run4_20151014_1_3ViewBS_slice_0031.mrc     Size=
195313 K

 Number of columns, rows, sections .....   10000   10000       1
 Map mode ..............................    1   (16-bit integer)
 Start cols, rows, sects, grid x,y,z ...    0     0     0   10000  10000      1
 Pixel spacing (Angstroms)..............   28.13      28.13      28.13
 Cell angles ...........................   90.000   90.000   90.000
 Fast, medium, slow axes ...............    X    Y    Z
 Origin on x,y,z .......................    0.000       0.000       0.000
 Minimum density .......................  -20744.
 Maximum density .......................  -2836.0
 Mean density ..........................  -14398.
 tilt angles (original,current) ........   0.0   0.0   0.0   0.0   0.0   0.0
 Space group,# extra bytes,idtype,lens .        0        0        0        0

     1 Titles :
raw2mrc: Converted to mrc format.                    18-Oct-15  11:54:23

   31 -18565.00  -8193.75 -18565.00  -8193.75 -13330.66

 RO image file on unit   1 : run4_20151014_1_3ViewBS_slice_0032.mrc     Size=
195313 K

 Number of columns, rows, sections .....   10000   10000       1
 Map mode ..............................    1   (16-bit integer)
 Start cols, rows, sects, grid x,y,z ...    0     0     0   10000  10000      1
 Pixel spacing (Angstroms)..............   28.13      28.13      28.13
 Cell angles ...........................   90.000   90.000   90.000
 Fast, medium, slow axes ...............    X    Y    Z
 Origin on x,y,z .......................    0.000       0.000       0.000
 Minimum density .......................  -32758.
 Maximum density .......................   3451.0
 Mean density ..........................  -14337.
 tilt angles (original,current) ........   0.0   0.0   0.0   0.0   0.0   0.0
 Space group,# extra bytes,idtype,lens .        0        0        0        0

     1 Titles :
raw2mrc: Converted to mrc format.                    18-Oct-15  11:54:40

   32 -22567.50  -6411.25 -22567.50  -6411.25 -13277.68

 RO image file on unit   1 : run4_20151014_1_3ViewBS_slice_0033.mrc     Size=
195313 K
```

Number of columns, rows, sections 10000 10000 1
Map mode ..... 1 (16-bit integer)
Start cols, rows, sects, grid x,y,z ... 0 0 0 10000 10000 1
Pixel spacing (Angstroms)..... 28.13 28.13 28.13
Cell angles 90.000 90.000 90.000
Fast, medium, slow axes ..... X Y Z
Origin on x,y,z 0.000 0.000 0.000
Minimum density ..... -21251.
Maximum density ..... -2988.0
Mean density ..... -14356.
tilt angles (original,current) 0.0 0.0 0.0 0.0 0.0 0.0
Space group,# extra bytes,idtype,lens . 0 0 0 0

1 Titles :
raw2mrc: Converted to mrc format. 18-Oct-15 11:54:57

33 -19211.75 -8684.50 -19211.75 -8684.50 -13293.83

RO image file on unit 1 : run4_20151014_1_3ViewBS_slice_0034.mrc Size= 195313 K

Number of columns, rows, sections 10000 10000 1
Map mode ..... 1 (16-bit integer)
Start cols, rows, sects, grid x,y,z ... 0 0 0 10000 10000 1
Pixel spacing (Angstroms)..... 28.13 28.13 28.13
Cell angles 90.000 90.000 90.000
Fast, medium, slow axes ..... X Y Z
Origin on x,y,z 0.000 0.000 0.000
Minimum density ..... -24231.
Maximum density ..... -3103.0
Mean density ..... -14382.
tilt angles (original,current) 0.0 0.0 0.0 0.0 0.0 0.0
Space group,# extra bytes,idtype,lens . 0 0 0 0

1 Titles :
raw2mrc: Converted to mrc format. 18-Oct-15 11:55:10

34 -19500.75 -8349.50 -19500.75 -8349.50 -13319.58

RO image file on unit 1 : run4_20151014_1_3ViewBS_slice_0035.mrc Size= 195313 K

Number of columns, rows, sections 10000 10000 1
Map mode ..... 1 (16-bit integer)

```
 Start cols, rows, sects, grid x,y,z ...    0     0     0   10000  10000      1
 Pixel spacing (Angstroms).............   28.13      28.13      28.13
 Cell angles ...........................   90.000   90.000   90.000
 Fast, medium, slow axes .............    X    Y    Z
 Origin on x,y,z .....................    0.000       0.000       0.000
 Minimum density .....................  -25069.
 Maximum density .....................  -3299.0
 Mean density ........................  -14357.
 tilt angles (original,current) .....   0.0   0.0   0.0   0.0   0.0   0.0
 Space group,# extra bytes,idtype,lens .        0        0        0        0

     1 Titles :
raw2mrc: Converted to mrc format.                    18-Oct-15  11:55:24

   35 -17886.50  -8016.25 -17886.50  -8016.25 -13293.81

 RO image file on unit   1 : run4_20151014_1_3ViewBS_slice_0036.mrc     Size=
195313 K

 Number of columns, rows, sections .....   10000   10000       1
 Map mode ..............................    1   (16-bit integer)
 Start cols, rows, sects, grid x,y,z ...    0     0     0   10000  10000      1
 Pixel spacing (Angstroms).............   28.13      28.13      28.13
 Cell angles ...........................   90.000   90.000   90.000
 Fast, medium, slow axes .............    X    Y    Z
 Origin on x,y,z .....................    0.000       0.000       0.000
 Minimum density .....................  -21893.
 Maximum density .....................  -3205.0
 Mean density ........................  -14392.
 tilt angles (original,current) .....   0.0   0.0   0.0   0.0   0.0   0.0
 Space group,# extra bytes,idtype,lens .        0        0        0        0

     1 Titles :
raw2mrc: Converted to mrc format.                    18-Oct-15  11:55:37

   36 -19916.50  -8685.25 -19916.50  -8685.25 -13327.38

 RO image file on unit   1 : run4_20151014_1_3ViewBS_slice_0037.mrc     Size=
195313 K

 Number of columns, rows, sections .....   10000   10000       1
 Map mode ..............................    1   (16-bit integer)
 Start cols, rows, sects, grid x,y,z ...    0     0     0   10000  10000      1
 Pixel spacing (Angstroms).............   28.13      28.13      28.13
 Cell angles ...........................   90.000   90.000   90.000
```

```
 Fast, medium, slow axes .....    X    Y    Z
 Origin on x,y,z .....    0.000       0.000       0.000
 Minimum density .....  -32758.
 Maximum density .....   6637.0
 Mean density .....  -14396.
 tilt angles (original,current) .....   0.0   0.0   0.0   0.0   0.0   0.0
 Space group,# extra bytes,idtype,lens .        0        0        0        0

     1 Titles :
raw2mrc: Converted to mrc format.                    18-Oct-15  11:55:51

   37 -21858.50  -4718.25 -21858.50  -4718.25 -13332.61

 RO image file on unit   1 : run4_20151014_1_3ViewBS_slice_0038.mrc     Size=
195313 K

 Number of columns, rows, sections .....   10000   10000       1
 Map mode .....    1   (16-bit integer)
 Start cols, rows, sects, grid x,y,z ...    0     0     0   10000  10000      1
 Pixel spacing (Angstroms).....   28.13      28.13      28.13
 Cell angles .....   90.000   90.000   90.000
 Fast, medium, slow axes .....    X    Y    Z
 Origin on x,y,z .....    0.000       0.000       0.000
 Minimum density .....  -23788.
 Maximum density .....  -3040.0
 Mean density .....  -14393.
 tilt angles (original,current) .....   0.0   0.0   0.0   0.0   0.0   0.0
 Space group,# extra bytes,idtype,lens .        0        0        0        0

     1 Titles :
raw2mrc: Converted to mrc format.                    18-Oct-15  11:56:04

   38 -19465.25  -8568.25 -19465.25  -8568.25 -13325.56

 RO image file on unit   1 : run4_20151014_1_3ViewBS_slice_0039.mrc     Size=
195313 K

 Number of columns, rows, sections .....   10000   10000       1
 Map mode .....    1   (16-bit integer)
 Start cols, rows, sects, grid x,y,z ...    0     0     0   10000  10000      1
 Pixel spacing (Angstroms).....   28.13      28.13      28.13
 Cell angles .....   90.000   90.000   90.000
 Fast, medium, slow axes .....    X    Y    Z
 Origin on x,y,z .....    0.000       0.000       0.000
 Minimum density .....  -24995.
```

```
 Maximum density .....  -3543.0
 Mean density .....  -14433.
 tilt angles (original,current) .....   0.0   0.0   0.0   0.0   0.0   0.0
 Space group,# extra bytes,idtype,lens .        0        0        0        0

     1 Titles :
raw2mrc: Converted to mrc format.                    18-Oct-15  11:56:18

   39 -19091.00  -7845.00 -19091.00  -7845.00 -13360.54

 RO image file on unit   1 : run4_20151014_1_3ViewBS_slice_0040.mrc     Size=
195313 K

 Number of columns, rows, sections .....   10000   10000       1
 Map mode .....    1   (16-bit integer)
 Start cols, rows, sects, grid x,y,z ...    0     0     0   10000  10000      1
 Pixel spacing (Angstroms).....   28.13      28.13      28.13
 Cell angles .....   90.000   90.000   90.000
 Fast, medium, slow axes .....    X    Y    Z
 Origin on x,y,z .....    0.000       0.000       0.000
 Minimum density .....  -21808.
 Maximum density .....  -3621.0
 Mean density .....  -14446.
 tilt angles (original,current) .....   0.0   0.0   0.0   0.0   0.0   0.0
 Space group,# extra bytes,idtype,lens .        0        0        0        0

     1 Titles :
raw2mrc: Converted to mrc format.                    18-Oct-15  11:56:34

   40 -19844.50  -8630.75 -19844.50  -8630.75 -13364.27

 RO image file on unit   1 : run4_20151014_1_3ViewBS_slice_0041.mrc     Size=
195313 K

 Number of columns, rows, sections .....   10000   10000       1
 Map mode .....    1   (16-bit integer)
 Start cols, rows, sects, grid x,y,z ...    0     0     0   10000  10000      1
 Pixel spacing (Angstroms).....   28.13      28.13      28.13
 Cell angles .....   90.000   90.000   90.000
 Fast, medium, slow axes .....    X    Y    Z
 Origin on x,y,z .....    0.000       0.000       0.000
 Minimum density .....  -32758.
 Maximum density .....  -2982.0
 Mean density .....  -13861.
 tilt angles (original,current) .....   0.0   0.0   0.0   0.0   0.0   0.0
```

Space group,# extra bytes,idtype,lens . 0 0 0 0

1 Titles :
raw2mrc: Converted to mrc format. 18-Oct-15 12:05:07

41 -22657.50 -7389.50 -22657.50 -7389.50 -12945.31

RO image file on unit 1 : run4_20151014_1_3ViewBS_slice_0042.mrc Size= 195313 K

Number of columns, rows, sections 10000 10000 1
Map mode ..... 1 (16-bit integer)
Start cols, rows, sects, grid x,y,z ... 0 0 0 10000 10000 1
Pixel spacing (Angstroms)..... 28.13 28.13 28.13
Cell angles 90.000 90.000 90.000
Fast, medium, slow axes ..... X Y Z
Origin on x,y,z 0.000 0.000 0.000
Minimum density ..... -22127.
Maximum density ..... -2851.0
Mean density ..... -14505.
tilt angles (original,current) 0.0 0.0 0.0 0.0 0.0 0.0
Space group,# extra bytes,idtype,lens . 0 0 0 0

1 Titles :
raw2mrc: Converted to mrc format. 18-Oct-15 12:05:22

42 -20151.75 -8025.25 -20151.75 -8025.25 -13416.87

RO image file on unit 1 : run4_20151014_1_3ViewBS_slice_0043.mrc Size= 195313 K

Number of columns, rows, sections 10000 10000 1
Map mode ..... 1 (16-bit integer)
Start cols, rows, sects, grid x,y,z ... 0 0 0 10000 10000 1
Pixel spacing (Angstroms)..... 28.13 28.13 28.13
Cell angles 90.000 90.000 90.000
Fast, medium, slow axes ..... X Y Z
Origin on x,y,z 0.000 0.000 0.000
Minimum density ..... -20942.
Maximum density ..... -3415.0
Mean density ..... -14502.
tilt angles (original,current) 0.0 0.0 0.0 0.0 0.0 0.0
Space group,# extra bytes,idtype,lens . 0 0 0 0

1 Titles :

raw2mrc: Converted to mrc format. 18-Oct-15 12:05:35

43 -18254.75 -8273.50 -18254.75 -8273.50 -13420.57

RO image file on unit 1 : run4_20151014_1_3ViewBS_slice_0044.mrc Size= 195313 K

Number of columns, rows, sections 10000 10000 1
Map mode ..... 1 (16-bit integer)
Start cols, rows, sects, grid x,y,z ... 0 0 0 10000 10000 1
Pixel spacing (Angstroms)..... 28.13 28.13 28.13
Cell angles 90.000 90.000 90.000
Fast, medium, slow axes ..... X Y Z
Origin on x,y,z 0.000 0.000 0.000
Minimum density ..... -24347.
Maximum density ..... -2884.0
Mean density ..... -14250.
tilt angles (original,current) 0.0 0.0 0.0 0.0 0.0 0.0
Space group,# extra bytes,idtype,lens . 0 0 0 0

1 Titles :
raw2mrc: Converted to mrc format. 18-Oct-15 12:05:56

44 -20460.75 -8256.25 -20460.75 -8256.25 -13206.14

RO image file on unit 1 : run4_20151014_1_3ViewBS_slice_0045.mrc Size= 195313 K

Number of columns, rows, sections 10000 10000 1
Map mode ..... 1 (16-bit integer)
Start cols, rows, sects, grid x,y,z ... 0 0 0 10000 10000 1
Pixel spacing (Angstroms)..... 28.13 28.13 28.13
Cell angles 90.000 90.000 90.000
Fast, medium, slow axes ..... X Y Z
Origin on x,y,z 0.000 0.000 0.000
Minimum density ..... -20555.
Maximum density ..... -2390.0
Mean density ..... -13539.
tilt angles (original,current) 0.0 0.0 0.0 0.0 0.0 0.0
Space group,# extra bytes,idtype,lens . 0 0 0 0

1 Titles :
raw2mrc: Converted to mrc format. 18-Oct-15 12:06:17

45 -18662.00 -8043.50 -18662.00 -8043.50 -12755.65

```
 RO image file on unit   1 : run4_20151014_1_3ViewBS_slice_0046.mrc     Size=
195313 K

 Number of columns, rows, sections .....   10000   10000       1
 Map mode ..............................    1   (16-bit integer)
 Start cols, rows, sects, grid x,y,z ...    0     0     0   10000  10000      1
 Pixel spacing (Angstroms)..............   28.13      28.13      28.13
 Cell angles ...........................   90.000   90.000   90.000
 Fast, medium, slow axes ..............    X    Y    Z
 Origin on x,y,z .......................    0.000       0.000       0.000
 Minimum density .......................  -25973.
 Maximum density .......................  -3044.0
 Mean density ..........................  -14381.
 tilt angles (original,current) ........   0.0   0.0   0.0   0.0   0.0   0.0
 Space group,# extra bytes,idtype,lens .        0        0        0        0

     1 Titles :
raw2mrc: Converted to mrc format.                    18-Oct-15  12:06:33

   46 -18677.50  -8024.00 -18677.50  -8024.00 -13327.20

 RO image file on unit   1 : run4_20151014_1_3ViewBS_slice_0047.mrc     Size=
195313 K

 Number of columns, rows, sections .....   10000   10000       1
 Map mode ..............................    1   (16-bit integer)
 Start cols, rows, sects, grid x,y,z ...    0     0     0   10000  10000      1
 Pixel spacing (Angstroms)..............   28.13      28.13      28.13
 Cell angles ...........................   90.000   90.000   90.000
 Fast, medium, slow axes ..............    X    Y    Z
 Origin on x,y,z .......................    0.000       0.000       0.000
 Minimum density .......................  -32758.
 Maximum density .......................  -2099.0
 Mean density ..........................  -13416.
 tilt angles (original,current) ........   0.0   0.0   0.0   0.0   0.0   0.0
 Space group,# extra bytes,idtype,lens .        0        0        0        0

     1 Titles :
raw2mrc: Converted to mrc format.                    18-Oct-15  12:06:47

   47 -22068.50  -7641.75 -22068.50  -7641.75 -12643.10

 RO image file on unit   1 : run4_20151014_1_3ViewBS_slice_0048.mrc     Size=
195313 K
```

```
 Number of columns, rows, sections .....   10000   10000       1
 Map mode ..............................    1   (16-bit integer)
 Start cols, rows, sects, grid x,y,z ...    0     0     0   10000  10000      1
 Pixel spacing (Angstroms)..............   28.13      28.13      28.13
 Cell angles ...........................   90.000   90.000   90.000
 Fast, medium, slow axes ..............    X    Y    Z
 Origin on x,y,z .......................    0.000       0.000       0.000
 Minimum density .......................  -22238.
 Maximum density .......................  -2600.0
 Mean density ..........................  -13918.
 tilt angles (original,current) ........   0.0   0.0   0.0   0.0   0.0   0.0
 Space group,# extra bytes,idtype,lens .        0        0        0        0

     1 Titles :
raw2mrc: Converted to mrc format.                    18-Oct-15  12:07:07

   48 -20641.00  -8280.25 -20641.00  -8280.25 -12960.95

 RO image file on unit   1 : run4_20151014_1_3ViewBS_slice_0049.mrc     Size=
195313 K

 Number of columns, rows, sections .....   10000   10000       1
 Map mode ..............................    1   (16-bit integer)
 Start cols, rows, sects, grid x,y,z ...    0     0     0   10000  10000      1
 Pixel spacing (Angstroms)..............   28.13      28.13      28.13
 Cell angles ...........................   90.000   90.000   90.000
 Fast, medium, slow axes ..............    X    Y    Z
 Origin on x,y,z .......................    0.000       0.000       0.000
 Minimum density .......................  -21051.
 Maximum density .......................  -2814.0
 Mean density ..........................  -14459.
 tilt angles (original,current) ........   0.0   0.0   0.0   0.0   0.0   0.0
 Space group,# extra bytes,idtype,lens .        0        0        0        0

     1 Titles :
raw2mrc: Converted to mrc format.                    18-Oct-15  12:07:21

   49 -19334.00  -8696.50 -19334.00  -8696.50 -13371.88

 RO image file on unit   1 : run4_20151014_1_3ViewBS_slice_0050.mrc     Size=
195313 K

 Number of columns, rows, sections .....   10000   10000       1
 Map mode ..............................    1   (16-bit integer)
```

```
 Start cols, rows, sects, grid x,y,z ...    0     0     0   10000  10000      1
 Pixel spacing (Angstroms).............   28.13      28.13      28.13
 Cell angles ...........................   90.000   90.000   90.000
 Fast, medium, slow axes .............    X    Y    Z
 Origin on x,y,z .....................    0.000       0.000       0.000
 Minimum density .....................  -21981.
 Maximum density .....................  -2655.0
 Mean density ........................  -13737.
 tilt angles (original,current) .....   0.0   0.0   0.0   0.0   0.0   0.0
 Space group,# extra bytes,idtype,lens .        0        0        0        0

     1 Titles :
raw2mrc: Converted to mrc format.                    18-Oct-15  12:07:45

   50 -19616.25  -8011.25 -19616.25  -8011.25 -12861.60

 RO image file on unit   1 : run4_20151014_1_3ViewBS_slice_0051.mrc     Size=
195313 K

 Number of columns, rows, sections .....   10000   10000       1
 Map mode ..............................    1   (16-bit integer)
 Start cols, rows, sects, grid x,y,z ...    0     0     0   10000  10000      1
 Pixel spacing (Angstroms).............   28.13      28.13      28.13
 Cell angles ...........................   90.000   90.000   90.000
 Fast, medium, slow axes .............    X    Y    Z
 Origin on x,y,z .....................    0.000       0.000       0.000
 Minimum density .....................  -32429.
 Maximum density .....................  -3385.0
 Mean density ........................  -14506.
 tilt angles (original,current) .....   0.0   0.0   0.0   0.0   0.0   0.0
 Space group,# extra bytes,idtype,lens .        0        0        0        0

     1 Titles :
raw2mrc: Converted to mrc format.                    18-Oct-15  12:07:58

   51 -20292.00  -8611.50 -20292.00  -8611.50 -13418.24

 RO image file on unit   1 : run4_20151014_1_3ViewBS_slice_0052.mrc     Size=
195313 K

 Number of columns, rows, sections .....   10000   10000       1
 Map mode ..............................    1   (16-bit integer)
 Start cols, rows, sects, grid x,y,z ...    0     0     0   10000  10000      1
 Pixel spacing (Angstroms).............   28.13      28.13      28.13
 Cell angles ...........................   90.000   90.000   90.000
```

```
 Fast, medium, slow axes .....    X    Y    Z
 Origin on x,y,z .....    0.000       0.000       0.000
 Minimum density .....  -22610.
 Maximum density .....  -3529.0
 Mean density .....  -14487.
 tilt angles (original,current) .....   0.0   0.0   0.0   0.0   0.0   0.0
 Space group,# extra bytes,idtype,lens .        0        0        0        0

     1 Titles :
raw2mrc: Converted to mrc format.                    18-Oct-15  12:08:11

   52 -20773.50  -8813.00 -20773.50  -8813.00 -13395.75

 RO image file on unit   1 : run4_20151014_1_3ViewBS_slice_0053.mrc     Size=
195313 K

 Number of columns, rows, sections .....   10000   10000       1
 Map mode .....    1   (16-bit integer)
 Start cols, rows, sects, grid x,y,z ...    0     0     0   10000  10000      1
 Pixel spacing (Angstroms).....   28.13      28.13      28.13
 Cell angles .....   90.000   90.000   90.000
 Fast, medium, slow axes .....    X    Y    Z
 Origin on x,y,z .....    0.000       0.000       0.000
 Minimum density .....  -21085.
 Maximum density .....  -1991.0
 Mean density .....  -14461.
 tilt angles (original,current) .....   0.0   0.0   0.0   0.0   0.0   0.0
 Space group,# extra bytes,idtype,lens .        0        0        0        0

     1 Titles :
raw2mrc: Converted to mrc format.                    18-Oct-15  12:08:25

   53 -19227.25  -8920.00 -19227.25  -8920.00 -13386.35

 RO image file on unit   1 : run4_20151014_1_3ViewBS_slice_0054.mrc     Size=
195313 K

 Number of columns, rows, sections .....   10000   10000       1
 Map mode .....    1   (16-bit integer)
 Start cols, rows, sects, grid x,y,z ...    0     0     0   10000  10000      1
 Pixel spacing (Angstroms).....   28.13      28.13      28.13
 Cell angles .....   90.000   90.000   90.000
 Fast, medium, slow axes .....    X    Y    Z
 Origin on x,y,z .....    0.000       0.000       0.000
 Minimum density .....  -20710.
```

```
 Maximum density .....  -3570.0
 Mean density .....  -14496.
 tilt angles (original,current) .....   0.0   0.0   0.0   0.0   0.0   0.0
 Space group,# extra bytes,idtype,lens .        0        0        0        0

     1 Titles :
raw2mrc: Converted to mrc format.                    18-Oct-15  12:08:39

   54 -18914.50  -8733.25 -18914.50  -8733.25 -13413.38

 RO image file on unit   1 : run4_20151014_1_3ViewBS_slice_0055.mrc     Size=
195313 K

 Number of columns, rows, sections .....   10000   10000       1
 Map mode .....    1   (16-bit integer)
 Start cols, rows, sects, grid x,y,z ...    0     0     0   10000  10000      1
 Pixel spacing (Angstroms).....   28.13      28.13      28.13
 Cell angles .....   90.000   90.000   90.000
 Fast, medium, slow axes .....    X    Y    Z
 Origin on x,y,z .....    0.000       0.000       0.000
 Minimum density .....  -24849.
 Maximum density .....  -3438.0
 Mean density .....  -14488.
 tilt angles (original,current) .....   0.0   0.0   0.0   0.0   0.0   0.0
 Space group,# extra bytes,idtype,lens .        0        0        0        0

     1 Titles :
raw2mrc: Converted to mrc format.                    18-Oct-15  12:08:54

   55 -19817.25  -8701.00 -19817.25  -8701.00 -13410.19

 RO image file on unit   1 : run4_20151014_1_3ViewBS_slice_0056.mrc     Size=
195313 K

 Number of columns, rows, sections .....   10000   10000       1
 Map mode .....    1   (16-bit integer)
 Start cols, rows, sects, grid x,y,z ...    0     0     0   10000  10000      1
 Pixel spacing (Angstroms).....   28.13      28.13      28.13
 Cell angles .....   90.000   90.000   90.000
 Fast, medium, slow axes .....    X    Y    Z
 Origin on x,y,z .....    0.000       0.000       0.000
 Minimum density .....  -21129.
 Maximum density .....  -3574.0
 Mean density .....  -14486.
 tilt angles (original,current) .....   0.0   0.0   0.0   0.0   0.0   0.0
```

Space group,# extra bytes,idtype,lens . 0 0 0 0

1 Titles :
raw2mrc: Converted to mrc format. 18-Oct-15 12:09:12

56 -20500.00 -8837.50 -20500.00 -8837.50 -13402.94

RO image file on unit 1 : run4_20151014_1_3ViewBS_slice_0057.mrc Size= 195313 K

Number of columns, rows, sections 10000 10000 1
Map mode ..... 1 (16-bit integer)
Start cols, rows, sects, grid x,y,z ... 0 0 0 10000 10000 1
Pixel spacing (Angstroms)..... 28.13 28.13 28.13
Cell angles 90.000 90.000 90.000
Fast, medium, slow axes ..... X Y Z
Origin on x,y,z 0.000 0.000 0.000
Minimum density ..... -32767.
Maximum density ..... -3062.0
Mean density ..... -14488.
tilt angles (original,current) 0.0 0.0 0.0 0.0 0.0 0.0
Space group,# extra bytes,idtype,lens . 0 0 0 0

1 Titles :
raw2mrc: Converted to mrc format. 18-Oct-15 12:09:38

57 -24060.25 -8494.25 -24060.25 -8494.25 -13407.42

RO image file on unit 1 : run4_20151014_1_3ViewBS_slice_0058.mrc Size= 195313 K

Number of columns, rows, sections 10000 10000 1
Map mode ..... 1 (16-bit integer)
Start cols, rows, sects, grid x,y,z ... 0 0 0 10000 10000 1
Pixel spacing (Angstroms)..... 28.13 28.13 28.13
Cell angles 90.000 90.000 90.000
Fast, medium, slow axes ..... X Y Z
Origin on x,y,z 0.000 0.000 0.000
Minimum density ..... -20963.
Maximum density ..... -3535.0
Mean density ..... -14493.
tilt angles (original,current) 0.0 0.0 0.0 0.0 0.0 0.0
Space group,# extra bytes,idtype,lens . 0 0 0 0

1 Titles :

raw2mrc: Converted to mrc format. 18-Oct-15 12:09:55

58 -18953.75 -8797.75 -18953.75 -8797.75 -13406.20

RO image file on unit 1 : run4_20151014_1_3ViewBS_slice_0059.mrc Size= 195313 K

Number of columns, rows, sections 10000 10000 1
Map mode ..... 1 (16-bit integer)
Start cols, rows, sects, grid x,y,z ... 0 0 0 10000 10000 1
Pixel spacing (Angstroms)..... 28.13 28.13 28.13
Cell angles 90.000 90.000 90.000
Fast, medium, slow axes ..... X Y Z
Origin on x,y,z 0.000 0.000 0.000
Minimum density ..... -28626.
Maximum density ..... -3935.0
Mean density ..... -14502.
tilt angles (original,current) 0.0 0.0 0.0 0.0 0.0 0.0
Space group,# extra bytes,idtype,lens . 0 0 0 0

1 Titles :
raw2mrc: Converted to mrc format. 18-Oct-15 12:10:10

59 -18600.00 -8533.50 -18600.00 -8533.50 -13409.42

RO image file on unit 1 : run4_20151014_1_3ViewBS_slice_0060.mrc Size= 195313 K

Number of columns, rows, sections 10000 10000 1
Map mode ..... 1 (16-bit integer)
Start cols, rows, sects, grid x,y,z ... 0 0 0 10000 10000 1
Pixel spacing (Angstroms)..... 28.13 28.13 28.13
Cell angles 90.000 90.000 90.000
Fast, medium, slow axes ..... X Y Z
Origin on x,y,z 0.000 0.000 0.000
Minimum density ..... -32631.
Maximum density ..... -3370.0
Mean density ..... -14552.
tilt angles (original,current) 0.0 0.0 0.0 0.0 0.0 0.0
Space group,# extra bytes,idtype,lens . 0 0 0 0

1 Titles :
raw2mrc: Converted to mrc format. 18-Oct-15 12:10:28

60 -20531.50 -8403.75 -20531.50 -8403.75 -13452.80

```
 RO image file on unit   1 : run4_20151014_1_3ViewBS_slice_0061.mrc     Size=
195313 K

 Number of columns, rows, sections .....   10000   10000       1
 Map mode ..............................    1   (16-bit integer)
 Start cols, rows, sects, grid x,y,z ...    0     0     0   10000  10000      1
 Pixel spacing (Angstroms)..............   28.13      28.13      28.13
 Cell angles ...........................   90.000   90.000   90.000
 Fast, medium, slow axes ..............    X    Y    Z
 Origin on x,y,z .......................    0.000       0.000       0.000
 Minimum density .......................  -26612.
 Maximum density .......................  -3090.0
 Mean density ..........................  -14210.
 tilt angles (original,current) ........   0.0   0.0   0.0   0.0   0.0   0.0
 Space group,# extra bytes,idtype,lens .        0        0        0        0

     1 Titles :
raw2mrc: Converted to mrc format.                    18-Oct-15  12:10:42

   61 -19755.75  -8209.75 -19755.75  -8209.75 -13179.44

 RO image file on unit   1 : run4_20151014_1_3ViewBS_slice_0062.mrc     Size=
195313 K

 Number of columns, rows, sections .....   10000   10000       1
 Map mode ..............................    1   (16-bit integer)
 Start cols, rows, sects, grid x,y,z ...    0     0     0   10000  10000      1
 Pixel spacing (Angstroms)..............   28.13      28.13      28.13
 Cell angles ...........................   90.000   90.000   90.000
 Fast, medium, slow axes ..............    X    Y    Z
 Origin on x,y,z .......................    0.000       0.000       0.000
 Minimum density .......................  -32741.
 Maximum density .......................  -3128.0
 Mean density ..........................  -14579.
 tilt angles (original,current) ........   0.0   0.0   0.0   0.0   0.0   0.0
 Space group,# extra bytes,idtype,lens .        0        0        0        0

     1 Titles :
raw2mrc: Converted to mrc format.                    18-Oct-15  12:10:54

   62 -20172.75  -8863.75 -20172.75  -8863.75 -13462.49

 RO image file on unit   1 : run4_20151014_1_3ViewBS_slice_0063.mrc     Size=
195313 K
```

```
 Number of columns, rows, sections .....   10000   10000       1
 Map mode ..............................    1   (16-bit integer)
 Start cols, rows, sects, grid x,y,z ...    0     0     0   10000  10000      1
 Pixel spacing (Angstroms)..............   28.13      28.13      28.13
 Cell angles ...........................   90.000   90.000   90.000
 Fast, medium, slow axes ..............    X    Y    Z
 Origin on x,y,z .......................    0.000       0.000       0.000
 Minimum density .......................  -21001.
 Maximum density .......................  -3854.0
 Mean density ..........................  -14586.
 tilt angles (original,current) ........   0.0   0.0   0.0   0.0   0.0   0.0
 Space group,# extra bytes,idtype,lens .        0        0        0        0

     1 Titles :
raw2mrc: Converted to mrc format.                    18-Oct-15  12:11:23

   63 -19327.75  -8603.50 -19327.75  -8603.50 -13470.73

 RO image file on unit   1 : run4_20151014_1_3ViewBS_slice_0064.mrc     Size=
195313 K

 Number of columns, rows, sections .....   10000   10000       1
 Map mode ..............................    1   (16-bit integer)
 Start cols, rows, sects, grid x,y,z ...    0     0     0   10000  10000      1
 Pixel spacing (Angstroms)..............   28.13      28.13      28.13
 Cell angles ...........................   90.000   90.000   90.000
 Fast, medium, slow axes ..............    X    Y    Z
 Origin on x,y,z .......................    0.000       0.000       0.000
 Minimum density .......................  -22016.
 Maximum density .......................  -3430.0
 Mean density ..........................  -14545.
 tilt angles (original,current) ........   0.0   0.0   0.0   0.0   0.0   0.0
 Space group,# extra bytes,idtype,lens .        0        0        0        0

     1 Titles :
raw2mrc: Converted to mrc format.                    18-Oct-15  12:11:36

   64 -19955.25  -8806.75 -19955.25  -8806.75 -13441.06

 RO image file on unit   1 : run4_20151014_1_3ViewBS_slice_0065.mrc     Size=
195313 K

 Number of columns, rows, sections .....   10000   10000       1
 Map mode ..............................    1   (16-bit integer)
```

```
 Start cols, rows, sects, grid x,y,z ...    0     0     0   10000  10000      1
 Pixel spacing (Angstroms)..............   28.13      28.13      28.13
 Cell angles ............................   90.000   90.000   90.000
 Fast, medium, slow axes .............    X    Y    Z
 Origin on x,y,z .......................    0.000       0.000       0.000
 Minimum density ........................  -28984.
 Maximum density ........................  -3146.0
 Mean density ...........................  -14013.
 tilt angles (original,current) .........   0.0   0.0   0.0   0.0   0.0   0.0
 Space group,# extra bytes,idtype,lens .        0        0        0        0

     1 Titles :
raw2mrc: Converted to mrc format.                    18-Oct-15  12:11:51

   65 -21442.75  -8145.00 -21442.75  -8145.00 -13056.26

 RO image file on unit   1 : run4_20151014_1_3ViewBS_slice_0066.mrc     Size=
195313 K

 Number of columns, rows, sections .....   10000   10000       1
 Map mode ...............................    1   (16-bit integer)
 Start cols, rows, sects, grid x,y,z ...    0     0     0   10000  10000      1
 Pixel spacing (Angstroms)..............   28.13      28.13      28.13
 Cell angles ............................   90.000   90.000   90.000
 Fast, medium, slow axes .............    X    Y    Z
 Origin on x,y,z .......................    0.000       0.000       0.000
 Minimum density ........................  -20616.
 Maximum density ........................  -2944.0
 Mean density ...........................  -14513.
 tilt angles (original,current) .........   0.0   0.0   0.0   0.0   0.0   0.0
 Space group,# extra bytes,idtype,lens .        0        0        0        0

     1 Titles :
raw2mrc: Converted to mrc format.                    18-Oct-15  12:12:28

   66 -18289.75  -8585.50 -18289.75  -8585.50 -13435.30

 RO image file on unit   1 : run4_20151014_1_3ViewBS_slice_0067.mrc     Size=
195313 K

 Number of columns, rows, sections .....   10000   10000       1
 Map mode ...............................    1   (16-bit integer)
 Start cols, rows, sects, grid x,y,z ...    0     0     0   10000  10000      1
 Pixel spacing (Angstroms)..............   28.13      28.13      28.13
 Cell angles ............................   90.000   90.000   90.000
```

```
 Fast, medium, slow axes .....    X    Y    Z
 Origin on x,y,z .....    0.000       0.000       0.000
 Minimum density .....  -21099.
 Maximum density .....  -2927.0
 Mean density .....  -13699.
 tilt angles (original,current) .....   0.0   0.0   0.0   0.0   0.0   0.0
 Space group,# extra bytes,idtype,lens .        0        0        0        0

     1 Titles :
raw2mrc: Converted to mrc format.                    18-Oct-15  12:14:42

   67 -20030.75  -8011.75 -20030.75  -8011.75 -12837.19

 RO image file on unit   1 : run4_20151014_1_3ViewBS_slice_0068.mrc     Size=
195313 K

 Number of columns, rows, sections .....   10000   10000       1
 Map mode .....    1   (16-bit integer)
 Start cols, rows, sects, grid x,y,z ...    0     0     0   10000  10000      1
 Pixel spacing (Angstroms).....   28.13      28.13      28.13
 Cell angles .....   90.000   90.000   90.000
 Fast, medium, slow axes .....    X    Y    Z
 Origin on x,y,z .....    0.000       0.000       0.000
 Minimum density .....  -32767.
 Maximum density .....  -3187.0
 Mean density .....  -14618.
 tilt angles (original,current) .....   0.0   0.0   0.0   0.0   0.0   0.0
 Space group,# extra bytes,idtype,lens .        0        0        0        0

     1 Titles :
raw2mrc: Converted to mrc format.                    18-Oct-15  12:15:14

   68 -24201.50  -8818.75 -24201.50  -8818.75 -13476.90

 RO image file on unit   1 : run4_20151014_1_3ViewBS_slice_0069.mrc     Size=
195313 K

 Number of columns, rows, sections .....   10000   10000       1
 Map mode .....    1   (16-bit integer)
 Start cols, rows, sects, grid x,y,z ...    0     0     0   10000  10000      1
 Pixel spacing (Angstroms).....   28.13      28.13      28.13
 Cell angles .....   90.000   90.000   90.000
 Fast, medium, slow axes .....    X    Y    Z
 Origin on x,y,z .....    0.000       0.000       0.000
 Minimum density .....  -32752.
```

```
 Maximum density .....   1831.0
 Mean density .....  -14606.
 tilt angles (original,current) .....   0.0   0.0   0.0   0.0   0.0   0.0
 Space group,# extra bytes,idtype,lens .        0        0        0        0

     1 Titles :
raw2mrc: Converted to mrc format.                    18-Oct-15  12:15:59

   69 -22504.00  -7041.00 -22504.00  -7041.00 -13493.90

 RO image file on unit   1 : run4_20151014_1_3ViewBS_slice_0070.mrc     Size=
195313 K

 Number of columns, rows, sections .....   10000   10000       1
 Map mode .....    1   (16-bit integer)
 Start cols, rows, sects, grid x,y,z ...    0     0     0   10000  10000      1
 Pixel spacing (Angstroms).....   28.13      28.13      28.13
 Cell angles .....   90.000   90.000   90.000
 Fast, medium, slow axes .....    X    Y    Z
 Origin on x,y,z .....    0.000       0.000       0.000
 Minimum density .....  -22785.
 Maximum density .....  -3029.0
 Mean density .....  -14550.
 tilt angles (original,current) .....   0.0   0.0   0.0   0.0   0.0   0.0
 Space group,# extra bytes,idtype,lens .        0        0        0        0

     1 Titles :
raw2mrc: Converted to mrc format.                    18-Oct-15  12:16:39

   70 -20702.25  -8734.00 -20702.25  -8734.00 -13459.59

 RO image file on unit   1 : run4_20151014_1_3ViewBS_slice_0071.mrc     Size=
195313 K

 Number of columns, rows, sections .....   10000   10000       1
 Map mode .....    1   (16-bit integer)
 Start cols, rows, sects, grid x,y,z ...    0     0     0   10000  10000      1
 Pixel spacing (Angstroms).....   28.13      28.13      28.13
 Cell angles .....   90.000   90.000   90.000
 Fast, medium, slow axes .....    X    Y    Z
 Origin on x,y,z .....    0.000       0.000       0.000
 Minimum density .....  -20898.
 Maximum density .....  -2699.0
 Mean density .....  -14605.
 tilt angles (original,current) .....   0.0   0.0   0.0   0.0   0.0   0.0
```

Space group,# extra bytes,idtype,lens . 0 0 0 0

1 Titles :
raw2mrc: Converted to mrc format. 18-Oct-15 12:17:10

71 -19475.50 -8795.00 -19475.50 -8795.00 -13497.82

RO image file on unit 1 : run4_20151014_1_3ViewBS_slice_0072.mrc Size= 195313 K

Number of columns, rows, sections 10000 10000 1
Map mode ..... 1 (16-bit integer)
Start cols, rows, sects, grid x,y,z ... 0 0 0 10000 10000 1
Pixel spacing (Angstroms)..... 28.13 28.13 28.13
Cell angles 90.000 90.000 90.000
Fast, medium, slow axes ..... X Y Z
Origin on x,y,z 0.000 0.000 0.000
Minimum density ..... -32511.
Maximum density ..... -3921.0
Mean density ..... -14577.
tilt angles (original,current) 0.0 0.0 0.0 0.0 0.0 0.0
Space group,# extra bytes,idtype,lens . 0 0 0 0

1 Titles :
raw2mrc: Converted to mrc format. 18-Oct-15 12:17:26

72 -20920.50 -8744.25 -20920.50 -8744.25 -13480.74

RO image file on unit 1 : run4_20151014_1_3ViewBS_slice_0073.mrc Size= 195313 K

Number of columns, rows, sections 10000 10000 1
Map mode ..... 1 (16-bit integer)
Start cols, rows, sects, grid x,y,z ... 0 0 0 10000 10000 1
Pixel spacing (Angstroms)..... 28.13 28.13 28.13
Cell angles 90.000 90.000 90.000
Fast, medium, slow axes ..... X Y Z
Origin on x,y,z 0.000 0.000 0.000
Minimum density ..... -21626.
Maximum density ..... -2844.0
Mean density ..... -14565.
tilt angles (original,current) 0.0 0.0 0.0 0.0 0.0 0.0
Space group,# extra bytes,idtype,lens . 0 0 0 0

1 Titles :

raw2mrc: Converted to mrc format. 18-Oct-15 12:17:39

73 -19837.00 -8796.50 -19837.00 -8796.50 -13462.58

RO image file on unit 1 : run4_20151014_1_3ViewBS_slice_0074.mrc Size= 195313 K

Number of columns, rows, sections 10000 10000 1
Map mode ..... 1 (16-bit integer)
Start cols, rows, sects, grid x,y,z ... 0 0 0 10000 10000 1
Pixel spacing (Angstroms)..... 28.13 28.13 28.13
Cell angles 90.000 90.000 90.000
Fast, medium, slow axes ..... X Y Z
Origin on x,y,z 0.000 0.000 0.000
Minimum density ..... -32758.
Maximum density 2472.0
Mean density ..... -14578.
tilt angles (original,current) 0.0 0.0 0.0 0.0 0.0 0.0
Space group,# extra bytes,idtype,lens . 0 0 0 0

1 Titles :
raw2mrc: Converted to mrc format. 18-Oct-15 12:17:52

74 -21670.50 -6055.25 -21670.50 -6055.25 -13465.43

RO image file on unit 1 : run4_20151014_1_3ViewBS_slice_0075.mrc Size= 195313 K

Number of columns, rows, sections 10000 10000 1
Map mode ..... 1 (16-bit integer)
Start cols, rows, sects, grid x,y,z ... 0 0 0 10000 10000 1
Pixel spacing (Angstroms)..... 28.13 28.13 28.13
Cell angles 90.000 90.000 90.000
Fast, medium, slow axes ..... X Y Z
Origin on x,y,z 0.000 0.000 0.000
Minimum density ..... -32758.
Maximum density ..... -2657.0
Mean density ..... -14436.
tilt angles (original,current) 0.0 0.0 0.0 0.0 0.0 0.0
Space group,# extra bytes,idtype,lens . 0 0 0 0

1 Titles :
raw2mrc: Converted to mrc format. 18-Oct-15 12:18:08

75 -21377.25 -7967.00 -21377.25 -7967.00 -13384.63

```
 RO image file on unit   1 : run4_20151014_1_3ViewBS_slice_0076.mrc     Size=
195313 K

 Number of columns, rows, sections .....   10000   10000       1
 Map mode ..............................    1   (16-bit integer)
 Start cols, rows, sects, grid x,y,z ...    0     0     0   10000  10000      1
 Pixel spacing (Angstroms)..............   28.13      28.13      28.13
 Cell angles ...........................   90.000   90.000   90.000
 Fast, medium, slow axes ...............    X    Y    Z
 Origin on x,y,z .......................    0.000       0.000       0.000
 Minimum density .......................  -23043.
 Maximum density .......................  -2837.0
 Mean density ..........................  -14314.
 tilt angles (original,current) ........   0.0   0.0   0.0   0.0   0.0   0.0
 Space group,# extra bytes,idtype,lens .        0        0        0        0

     1 Titles :
raw2mrc: Converted to mrc format.                    18-Oct-15  12:18:20

   76 -20703.75  -8233.00 -20703.75  -8233.00 -13262.59

 RO image file on unit   1 : run4_20151014_1_3ViewBS_slice_0077.mrc     Size=
195313 K

 Number of columns, rows, sections .....   10000   10000       1
 Map mode ..............................    1   (16-bit integer)
 Start cols, rows, sects, grid x,y,z ...    0     0     0   10000  10000      1
 Pixel spacing (Angstroms)..............   28.13      28.13      28.13
 Cell angles ...........................   90.000   90.000   90.000
 Fast, medium, slow axes ...............    X    Y    Z
 Origin on x,y,z .......................    0.000       0.000       0.000
 Minimum density .......................  -21089.
 Maximum density .......................  -3973.0
 Mean density ..........................  -14584.
 tilt angles (original,current) ........   0.0   0.0   0.0   0.0   0.0   0.0
 Space group,# extra bytes,idtype,lens .        0        0        0        0

     1 Titles :
raw2mrc: Converted to mrc format.                    18-Oct-15  12:18:34

   77 -18608.25  -8945.50 -18608.25  -8945.50 -13477.85

 RO image file on unit   1 : run4_20151014_1_3ViewBS_slice_0078.mrc     Size=
195313 K
```

```
 Number of columns, rows, sections .....   10000   10000       1
 Map mode ..............................    1   (16-bit integer)
 Start cols, rows, sects, grid x,y,z ...    0     0     0   10000  10000      1
 Pixel spacing (Angstroms)..............   28.13      28.13      28.13
 Cell angles ...........................   90.000   90.000   90.000
 Fast, medium, slow axes ..............    X    Y    Z
 Origin on x,y,z .......................    0.000       0.000       0.000
 Minimum density .......................  -32758.
 Maximum density .......................   80.000
 Mean density ..........................  -14599.
 tilt angles (original,current) ........   0.0   0.0   0.0   0.0   0.0   0.0
 Space group,# extra bytes,idtype,lens .        0        0        0        0

     1 Titles :
raw2mrc: Converted to mrc format.                    18-Oct-15  12:18:47

   78 -23528.25  -7634.50 -23528.25  -7634.50 -13490.04

 RO image file on unit   1 : run4_20151014_1_3ViewBS_slice_0079.mrc     Size=
195313 K

 Number of columns, rows, sections .....   10000   10000       1
 Map mode ..............................    1   (16-bit integer)
 Start cols, rows, sects, grid x,y,z ...    0     0     0   10000  10000      1
 Pixel spacing (Angstroms)..............   28.13      28.13      28.13
 Cell angles ...........................   90.000   90.000   90.000
 Fast, medium, slow axes ..............    X    Y    Z
 Origin on x,y,z .......................    0.000       0.000       0.000
 Minimum density .......................  -32767.
 Maximum density .......................  -2875.0
 Mean density ..........................  -14180.
 tilt angles (original,current) ........   0.0   0.0   0.0   0.0   0.0   0.0
 Space group,# extra bytes,idtype,lens .        0        0        0        0

     1 Titles :
raw2mrc: Converted to mrc format.                    18-Oct-15  12:19:00

   79 -24072.50  -7945.25 -24072.50  -7945.25 -13143.58

 RO image file on unit   1 : run4_20151014_1_3ViewBS_slice_0080.mrc     Size=
195313 K

 Number of columns, rows, sections .....   10000   10000       1
 Map mode ..............................    1   (16-bit integer)
```

```
 Start cols, rows, sects, grid x,y,z ...    0     0     0   10000  10000      1
 Pixel spacing (Angstroms).............   28.13      28.13      28.13
 Cell angles ...........................   90.000   90.000   90.000
 Fast, medium, slow axes .............    X    Y    Z
 Origin on x,y,z .....................    0.000       0.000       0.000
 Minimum density .....................  -32758.
 Maximum density .....................  -3939.0
 Mean density ........................  -14665.
 tilt angles (original,current) .....   0.0   0.0   0.0   0.0   0.0   0.0
 Space group,# extra bytes,idtype,lens .        0        0        0        0

     1 Titles :
raw2mrc: Converted to mrc format.                    18-Oct-15  12:19:15

   80 -21374.75  -8810.50 -21374.75  -8810.50 -13561.34

 RO image file on unit   1 : run4_20151014_1_3ViewBS_slice_0081.mrc     Size=
195313 K

 Number of columns, rows, sections .....   10000   10000       1
 Map mode ..............................    1   (16-bit integer)
 Start cols, rows, sects, grid x,y,z ...    0     0     0   10000  10000      1
 Pixel spacing (Angstroms).............   28.13      28.13      28.13
 Cell angles ...........................   90.000   90.000   90.000
 Fast, medium, slow axes .............    X    Y    Z
 Origin on x,y,z .....................    0.000       0.000       0.000
 Minimum density .....................  -21365.
 Maximum density .....................  -2958.0
 Mean density ........................  -13534.
 tilt angles (original,current) .....   0.0   0.0   0.0   0.0   0.0   0.0
 Space group,# extra bytes,idtype,lens .        0        0        0        0

     1 Titles :
raw2mrc: Converted to mrc format.                    18-Oct-15  12:19:27

   81 -18789.25  -7777.75 -18789.25  -7777.75 -12738.92

 RO image file on unit   1 : run4_20151014_1_3ViewBS_slice_0082.mrc     Size=
195313 K

 Number of columns, rows, sections .....   10000   10000       1
 Map mode ..............................    1   (16-bit integer)
 Start cols, rows, sects, grid x,y,z ...    0     0     0   10000  10000      1
 Pixel spacing (Angstroms).............   28.13      28.13      28.13
 Cell angles ...........................   90.000   90.000   90.000
```

```
 Fast, medium, slow axes .....    X    Y    Z
 Origin on x,y,z .....    0.000       0.000       0.000
 Minimum density .....  -27458.
 Maximum density .....  -3738.0
 Mean density .....  -14780.
 tilt angles (original,current) .....   0.0   0.0   0.0   0.0   0.0   0.0
 Space group,# extra bytes,idtype,lens .        0        0        0        0

     1 Titles :
raw2mrc: Converted to mrc format.                    18-Oct-15  12:19:41

   82 -20135.75  -9019.00 -20135.75  -9019.00 -13622.05

 RO image file on unit   1 : run4_20151014_1_3ViewBS_slice_0083.mrc     Size=
195313 K

 Number of columns, rows, sections .....   10000   10000       1
 Map mode .....    1   (16-bit integer)
 Start cols, rows, sects, grid x,y,z ...    0     0     0   10000  10000      1
 Pixel spacing (Angstroms).....   28.13      28.13      28.13
 Cell angles .....   90.000   90.000   90.000
 Fast, medium, slow axes .....    X    Y    Z
 Origin on x,y,z .....    0.000       0.000       0.000
 Minimum density .....  -21789.
 Maximum density .....  -2086.0
 Mean density .....  -14765.
 tilt angles (original,current) .....   0.0   0.0   0.0   0.0   0.0   0.0
 Space group,# extra bytes,idtype,lens .        0        0        0        0

     1 Titles :
raw2mrc: Converted to mrc format.                    18-Oct-15  12:19:55

   83 -20033.50  -8783.25 -20033.50  -8783.25 -13619.58

 RO image file on unit   1 : run4_20151014_1_3ViewBS_slice_0084.mrc     Size=
195313 K

 Number of columns, rows, sections .....   10000   10000       1
 Map mode .....    1   (16-bit integer)
 Start cols, rows, sects, grid x,y,z ...    0     0     0   10000  10000      1
 Pixel spacing (Angstroms).....   28.13      28.13      28.13
 Cell angles .....   90.000   90.000   90.000
 Fast, medium, slow axes .....    X    Y    Z
 Origin on x,y,z .....    0.000       0.000       0.000
 Minimum density .....  -22259.
```

```
 Maximum density .....  -2996.0
 Mean density .....  -14026.
 tilt angles (original,current) .....   0.0   0.0   0.0   0.0   0.0   0.0
 Space group,# extra bytes,idtype,lens .        0        0        0        0

     1 Titles :
raw2mrc: Converted to mrc format.                    18-Oct-15  12:20:08

   84 -20026.50  -7592.00 -20026.50  -7592.00 -13066.34

 RO image file on unit   1 : run4_20151014_1_3ViewBS_slice_0085.mrc     Size=
195313 K

 Number of columns, rows, sections .....   10000   10000       1
 Map mode .....    1   (16-bit integer)
 Start cols, rows, sects, grid x,y,z ...    0     0     0   10000  10000      1
 Pixel spacing (Angstroms).....   28.13      28.13      28.13
 Cell angles .....   90.000   90.000   90.000
 Fast, medium, slow axes .....    X    Y    Z
 Origin on x,y,z .....    0.000       0.000       0.000
 Minimum density .....  -21122.
 Maximum density .....  -3635.0
 Mean density .....  -14683.
 tilt angles (original,current) .....   0.0   0.0   0.0   0.0   0.0   0.0
 Space group,# extra bytes,idtype,lens .        0        0        0        0

     1 Titles :
raw2mrc: Converted to mrc format.                    18-Oct-15  12:20:20

   85 -19432.50  -8868.75 -19432.50  -8868.75 -13567.12

 RO image file on unit   1 : run4_20151014_1_3ViewBS_slice_0086.mrc     Size=
195313 K

 Number of columns, rows, sections .....   10000   10000       1
 Map mode .....    1   (16-bit integer)
 Start cols, rows, sects, grid x,y,z ...    0     0     0   10000  10000      1
 Pixel spacing (Angstroms).....   28.13      28.13      28.13
 Cell angles .....   90.000   90.000   90.000
 Fast, medium, slow axes .....    X    Y    Z
 Origin on x,y,z .....    0.000       0.000       0.000
 Minimum density .....  -32767.
 Maximum density .....  -3118.0
 Mean density .....  -14691.
 tilt angles (original,current) .....   0.0   0.0   0.0   0.0   0.0   0.0
```

Space group,# extra bytes,idtype,lens . 0 0 0 0

1 Titles :
raw2mrc: Converted to mrc format. 18-Oct-15 12:20:42

86 -24364.00 -8941.50 -24364.00 -8941.50 -13572.49

RO image file on unit 1 : run4_20151014_1_3ViewBS_slice_0087.mrc Size= 195313 K

Number of columns, rows, sections 10000 10000 1
Map mode ..... 1 (16-bit integer)
Start cols, rows, sects, grid x,y,z ... 0 0 0 10000 10000 1
Pixel spacing (Angstroms)..... 28.13 28.13 28.13
Cell angles 90.000 90.000 90.000
Fast, medium, slow axes ..... X Y Z
Origin on x,y,z 0.000 0.000 0.000
Minimum density ..... -22339.
Maximum density ..... -3168.0
Mean density ..... -14511.
tilt angles (original,current) 0.0 0.0 0.0 0.0 0.0 0.0
Space group,# extra bytes,idtype,lens . 0 0 0 0

1 Titles :
raw2mrc: Converted to mrc format. 18-Oct-15 12:20:57

87 -20577.25 -8690.50 -20577.25 -8690.50 -13414.59

RO image file on unit 1 : run4_20151014_1_3ViewBS_slice_0088.mrc Size= 195313 K

Number of columns, rows, sections 10000 10000 1
Map mode ..... 1 (16-bit integer)
Start cols, rows, sects, grid x,y,z ... 0 0 0 10000 10000 1
Pixel spacing (Angstroms)..... 28.13 28.13 28.13
Cell angles 90.000 90.000 90.000
Fast, medium, slow axes ..... X Y Z
Origin on x,y,z 0.000 0.000 0.000
Minimum density ..... -23293.
Maximum density ..... -3392.0
Mean density ..... -14658.
tilt angles (original,current) 0.0 0.0 0.0 0.0 0.0 0.0
Space group,# extra bytes,idtype,lens . 0 0 0 0

1 Titles :

raw2mrc: Converted to mrc format. 18-Oct-15 12:21:21

88 -20050.25 -9001.00 -20050.25 -9001.00 -13539.82

RO image file on unit 1 : run4_20151014_1_3ViewBS_slice_0089.mrc Size= 195313 K

Number of columns, rows, sections 10000 10000 1
Map mode ..... 1 (16-bit integer)
Start cols, rows, sects, grid x,y,z ... 0 0 0 10000 10000 1
Pixel spacing (Angstroms)..... 28.13 28.13 28.13
Cell angles 90.000 90.000 90.000
Fast, medium, slow axes ..... X Y Z
Origin on x,y,z 0.000 0.000 0.000
Minimum density ..... -31235.
Maximum density ..... -4170.0
Mean density ..... -14663.
tilt angles (original,current) 0.0 0.0 0.0 0.0 0.0 0.0
Space group,# extra bytes,idtype,lens . 0 0 0 0

1 Titles :
raw2mrc: Converted to mrc format. 18-Oct-15 12:21:33

89 -20984.00 -8879.00 -20984.00 -8879.00 -13544.75

RO image file on unit 1 : run4_20151014_1_3ViewBS_slice_0090.mrc Size= 195313 K

Number of columns, rows, sections 10000 10000 1
Map mode ..... 1 (16-bit integer)
Start cols, rows, sects, grid x,y,z ... 0 0 0 10000 10000 1
Pixel spacing (Angstroms)..... 28.13 28.13 28.13
Cell angles 90.000 90.000 90.000
Fast, medium, slow axes ..... X Y Z
Origin on x,y,z 0.000 0.000 0.000
Minimum density ..... -22416.
Maximum density ..... -3883.0
Mean density ..... -14683.
tilt angles (original,current) 0.0 0.0 0.0 0.0 0.0 0.0
Space group,# extra bytes,idtype,lens . 0 0 0 0

1 Titles :
raw2mrc: Converted to mrc format. 18-Oct-15 12:21:49

90 -19568.75 -8878.50 -19568.75 -8878.50 -13553.57

```
 RO image file on unit   1 : run4_20151014_1_3ViewBS_slice_0091.mrc     Size=
195313 K

 Number of columns, rows, sections .....   10000   10000       1
 Map mode ..............................    1   (16-bit integer)
 Start cols, rows, sects, grid x,y,z ...    0     0     0   10000  10000      1
 Pixel spacing (Angstroms)..............   28.13      28.13      28.13
 Cell angles ...........................   90.000   90.000   90.000
 Fast, medium, slow axes ..............    X    Y    Z
 Origin on x,y,z .......................    0.000       0.000       0.000
 Minimum density .......................  -27259.
 Maximum density .......................  -3695.0
 Mean density ..........................  -14679.
 tilt angles (original,current) ........   0.0   0.0   0.0   0.0   0.0   0.0
 Space group,# extra bytes,idtype,lens .        0        0        0        0

     1 Titles :
raw2mrc: Converted to mrc format.                    18-Oct-15  12:22:07

   91 -20101.00  -9125.50 -20101.00  -9125.50 -13552.81

 RO image file on unit   1 : run4_20151014_1_3ViewBS_slice_0092.mrc     Size=
195313 K

 Number of columns, rows, sections .....   10000   10000       1
 Map mode ..............................    1   (16-bit integer)
 Start cols, rows, sects, grid x,y,z ...    0     0     0   10000  10000      1
 Pixel spacing (Angstroms)..............   28.13      28.13      28.13
 Cell angles ...........................   90.000   90.000   90.000
 Fast, medium, slow axes ..............    X    Y    Z
 Origin on x,y,z .......................    0.000       0.000       0.000
 Minimum density .......................  -22319.
 Maximum density .......................  -4091.0
 Mean density ..........................  -14676.
 tilt angles (original,current) ........   0.0   0.0   0.0   0.0   0.0   0.0
 Space group,# extra bytes,idtype,lens .        0        0        0        0

     1 Titles :
raw2mrc: Converted to mrc format.                    18-Oct-15  12:22:25

   92 -19524.50  -8721.25 -19524.50  -8721.25 -13551.75

 RO image file on unit   1 : run4_20151014_1_3ViewBS_slice_0093.mrc     Size=
195313 K
```

```
 Number of columns, rows, sections .....   10000   10000       1
 Map mode ..............................    1   (16-bit integer)
 Start cols, rows, sects, grid x,y,z ...    0     0     0   10000  10000      1
 Pixel spacing (Angstroms)..............   28.13      28.13      28.13
 Cell angles ...........................   90.000   90.000   90.000
 Fast, medium, slow axes ..............    X    Y    Z
 Origin on x,y,z .......................    0.000       0.000       0.000
 Minimum density .......................  -20755.
 Maximum density .......................  -3506.0
 Mean density ..........................  -14688.
 tilt angles (original,current) ........   0.0   0.0   0.0   0.0   0.0   0.0
 Space group,# extra bytes,idtype,lens .        0        0        0        0

     1 Titles :
raw2mrc: Converted to mrc format.                    18-Oct-15  12:22:40

   93 -19515.50  -9069.50 -19515.50  -9069.50 -13560.51

 RO image file on unit   1 : run4_20151014_1_3ViewBS_slice_0094.mrc     Size=
195313 K

 Number of columns, rows, sections .....   10000   10000       1
 Map mode ..............................    1   (16-bit integer)
 Start cols, rows, sects, grid x,y,z ...    0     0     0   10000  10000      1
 Pixel spacing (Angstroms)..............   28.13      28.13      28.13
 Cell angles ...........................   90.000   90.000   90.000
 Fast, medium, slow axes ..............    X    Y    Z
 Origin on x,y,z .......................    0.000       0.000       0.000
 Minimum density .......................  -27234.
 Maximum density .......................  -3341.0
 Mean density ..........................  -14693.
 tilt angles (original,current) ........   0.0   0.0   0.0   0.0   0.0   0.0
 Space group,# extra bytes,idtype,lens .        0        0        0        0

     1 Titles :
raw2mrc: Converted to mrc format.                    18-Oct-15  12:23:00

   94 -20486.50  -8405.25 -20486.50  -8405.25 -13563.86

 RO image file on unit   1 : run4_20151014_1_3ViewBS_slice_0095.mrc     Size=
195313 K

 Number of columns, rows, sections .....   10000   10000       1
 Map mode ..............................    1   (16-bit integer)
```

```
 Start cols, rows, sects, grid x,y,z ...    0     0     0   10000  10000      1
 Pixel spacing (Angstroms)..............   28.13      28.13      28.13
 Cell angles ............................   90.000   90.000   90.000
 Fast, medium, slow axes .............    X    Y    Z
 Origin on x,y,z .......................    0.000       0.000       0.000
 Minimum density ........................  -32758.
 Maximum density ........................   6244.0
 Mean density ...........................  -14695.
 tilt angles (original,current) .........   0.0   0.0   0.0   0.0   0.0   0.0
 Space group,# extra bytes,idtype,lens .        0        0        0        0

     1 Titles :
raw2mrc: Converted to mrc format.                    18-Oct-15  12:23:18

   95 -23319.50  -5238.75 -23319.50  -5238.75 -13579.18

 RO image file on unit   1 : run4_20151014_1_3ViewBS_slice_0096.mrc     Size=
195313 K

 Number of columns, rows, sections .....   10000   10000       1
 Map mode ...............................    1   (16-bit integer)
 Start cols, rows, sects, grid x,y,z ...    0     0     0   10000  10000      1
 Pixel spacing (Angstroms)..............   28.13      28.13      28.13
 Cell angles ............................   90.000   90.000   90.000
 Fast, medium, slow axes .............    X    Y    Z
 Origin on x,y,z .......................    0.000       0.000       0.000
 Minimum density ........................  -24097.
 Maximum density ........................  -4008.0
 Mean density ...........................  -14726.
 tilt angles (original,current) .........   0.0   0.0   0.0   0.0   0.0   0.0
 Space group,# extra bytes,idtype,lens .        0        0        0        0

     1 Titles :
raw2mrc: Converted to mrc format.                    18-Oct-15  12:23:31

   96 -19599.50  -8736.00 -19599.50  -8736.00 -13600.03

 RO image file on unit   1 : run4_20151014_1_3ViewBS_slice_0097.mrc     Size=
195313 K

 Number of columns, rows, sections .....   10000   10000       1
 Map mode ...............................    1   (16-bit integer)
 Start cols, rows, sects, grid x,y,z ...    0     0     0   10000  10000      1
 Pixel spacing (Angstroms)..............   28.13      28.13      28.13
 Cell angles ............................   90.000   90.000   90.000
```

Fast, medium, slow axes ..... X Y Z
Origin on x,y,z 0.000 0.000 0.000
Minimum density ..... -21360.
Maximum density ..... -3573.0
Mean density ..... -14729.
tilt angles (original,current) 0.0 0.0 0.0 0.0 0.0 0.0
Space group,# extra bytes,idtype,lens . 0 0 0 0

1 Titles :
raw2mrc: Converted to mrc format. 18-Oct-15 12:24:51

97 -19333.00 -9198.00 -19333.00 -9198.00 -13597.29

RO image file on unit 1 : run4_20151014_1_3ViewBS_slice_0098.mrc Size= 195313 K

Number of columns, rows, sections 10000 10000 1
Map mode ..... 1 (16-bit integer)
Start cols, rows, sects, grid x,y,z ... 0 0 0 10000 10000 1
Pixel spacing (Angstroms)..... 28.13 28.13 28.13
Cell angles 90.000 90.000 90.000
Fast, medium, slow axes ..... X Y Z
Origin on x,y,z 0.000 0.000 0.000
Minimum density ..... -32758.
Maximum density ..... -599.00
Mean density ..... -14718.
tilt angles (original,current) 0.0 0.0 0.0 0.0 0.0 0.0
Space group,# extra bytes,idtype,lens . 0 0 0 0

1 Titles :
raw2mrc: Converted to mrc format. 18-Oct-15 12:25:37

98 -21397.25 -8686.75 -21397.25 -8686.75 -13593.42

RO image file on unit 1 : run4_20151014_1_3ViewBS_slice_0099.mrc Size= 195313 K

Number of columns, rows, sections 10000 10000 1
Map mode ..... 1 (16-bit integer)
Start cols, rows, sects, grid x,y,z ... 0 0 0 10000 10000 1
Pixel spacing (Angstroms)..... 28.13 28.13 28.13
Cell angles 90.000 90.000 90.000
Fast, medium, slow axes ..... X Y Z
Origin on x,y,z 0.000 0.000 0.000
Minimum density ..... -22815.

```
 Maximum density .....  -4166.0
 Mean density .....  -14792.
 tilt angles (original,current) .....   0.0   0.0   0.0   0.0   0.0   0.0
 Space group,# extra bytes,idtype,lens .        0        0        0        0

     1 Titles :
raw2mrc: Converted to mrc format.                    18-Oct-15  12:26:58

   99 -20360.50  -8973.25 -20360.50  -8973.25 -13651.23

 RO image file on unit   1 : run4_20151014_1_3ViewBS_slice_0100.mrc     Size=
195313 K

 Number of columns, rows, sections .....   10000   10000       1
 Map mode .....    1   (16-bit integer)
 Start cols, rows, sects, grid x,y,z ...    0     0     0   10000  10000      1
 Pixel spacing (Angstroms).....   28.13      28.13      28.13
 Cell angles .....   90.000   90.000   90.000
 Fast, medium, slow axes .....    X    Y    Z
 Origin on x,y,z .....    0.000       0.000       0.000
 Minimum density .....  -21940.
 Maximum density .....  -3963.0
 Mean density .....  -14774.
 tilt angles (original,current) .....   0.0   0.0   0.0   0.0   0.0   0.0
 Space group,# extra bytes,idtype,lens .        0        0        0        0

     1 Titles :
raw2mrc: Converted to mrc format.                    18-Oct-15  12:27:15

  100 -20323.50  -8593.25 -20323.50  -8593.25 -13632.26

 RO image file on unit   1 : run4_20151014_1_3ViewBS_slice_0101.mrc     Size=
195313 K

 Number of columns, rows, sections .....   10000   10000       1
 Map mode .....    1   (16-bit integer)
 Start cols, rows, sects, grid x,y,z ...    0     0     0   10000  10000      1
 Pixel spacing (Angstroms).....   28.13      28.13      28.13
 Cell angles .....   90.000   90.000   90.000
 Fast, medium, slow axes .....    X    Y    Z
 Origin on x,y,z .....    0.000       0.000       0.000
 Minimum density .....  -23278.
 Maximum density .....  -3352.0
 Mean density .....  -14488.
 tilt angles (original,current) .....   0.0   0.0   0.0   0.0   0.0   0.0
```

Space group,# extra bytes,idtype,lens . 0 0 0 0

1 Titles :
raw2mrc: Converted to mrc format. 18-Oct-15 12:27:29

101 -20626.00 -8518.75 -20626.00 -8518.75 -13398.99

RO image file on unit 1 : run4_20151014_1_3ViewBS_slice_0102.mrc Size= 195313 K

Number of columns, rows, sections 10000 10000 1
Map mode ..... 1 (16-bit integer)
Start cols, rows, sects, grid x,y,z ... 0 0 0 10000 10000 1
Pixel spacing (Angstroms)..... 28.13 28.13 28.13
Cell angles 90.000 90.000 90.000
Fast, medium, slow axes ..... X Y Z
Origin on x,y,z 0.000 0.000 0.000
Minimum density ..... -27216.
Maximum density ..... -3600.0
Mean density ..... -14779.
tilt angles (original,current) 0.0 0.0 0.0 0.0 0.0 0.0
Space group,# extra bytes,idtype,lens . 0 0 0 0

1 Titles :
raw2mrc: Converted to mrc format. 18-Oct-15 12:27:42

102 -19910.75 -9060.50 -19910.75 -9060.50 -13637.50

RO image file on unit 1 : run4_20151014_1_3ViewBS_slice_0103.mrc Size= 195313 K

Number of columns, rows, sections 10000 10000 1
Map mode ..... 1 (16-bit integer)
Start cols, rows, sects, grid x,y,z ... 0 0 0 10000 10000 1
Pixel spacing (Angstroms)..... 28.13 28.13 28.13
Cell angles 90.000 90.000 90.000
Fast, medium, slow axes ..... X Y Z
Origin on x,y,z 0.000 0.000 0.000
Minimum density ..... -30264.
Maximum density ..... -3624.0
Mean density ..... -14703.
tilt angles (original,current) 0.0 0.0 0.0 0.0 0.0 0.0
Space group,# extra bytes,idtype,lens . 0 0 0 0

1 Titles :

raw2mrc: Converted to mrc format. 18-Oct-15 12:28:07

103 -21323.25 -8714.00 -21323.25 -8714.00 -13581.61

RO image file on unit 1 : run4_20151014_1_3ViewBS_slice_0104.mrc Size= 195313 K

Number of columns, rows, sections 10000 10000 1
Map mode ..... 1 (16-bit integer)
Start cols, rows, sects, grid x,y,z ... 0 0 0 10000 10000 1
Pixel spacing (Angstroms)..... 28.13 28.13 28.13
Cell angles 90.000 90.000 90.000
Fast, medium, slow axes ..... X Y Z
Origin on x,y,z 0.000 0.000 0.000
Minimum density ..... -21582.
Maximum density ..... 32513.
Mean density ..... -14687.
tilt angles (original,current) 0.0 0.0 0.0 0.0 0.0 0.0
Space group,# extra bytes,idtype,lens . 0 0 0 0

1 Titles :
raw2mrc: Converted to mrc format. 18-Oct-15 12:28:21

104 -20095.75 -3119.00 -20095.75 -3119.00 -13567.45

RO image file on unit 1 : run4_20151014_1_3ViewBS_slice_0105.mrc Size= 195313 K

Number of columns, rows, sections 10000 10000 1
Map mode ..... 1 (16-bit integer)
Start cols, rows, sects, grid x,y,z ... 0 0 0 10000 10000 1
Pixel spacing (Angstroms)..... 28.13 28.13 28.13
Cell angles 90.000 90.000 90.000
Fast, medium, slow axes ..... X Y Z
Origin on x,y,z 0.000 0.000 0.000
Minimum density ..... -21683.
Maximum density ..... -4115.0
Mean density ..... -14720.
tilt angles (original,current) 0.0 0.0 0.0 0.0 0.0 0.0
Space group,# extra bytes,idtype,lens . 0 0 0 0

1 Titles :
raw2mrc: Converted to mrc format. 18-Oct-15 12:28:35

105 -19743.50 -8718.00 -19743.50 -8718.00 -13600.49

```
 RO image file on unit   1 : run4_20151014_1_3ViewBS_slice_0106.mrc     Size=
195313 K

 Number of columns, rows, sections .....   10000   10000       1
 Map mode ..............................    1   (16-bit integer)
 Start cols, rows, sects, grid x,y,z ...    0     0     0   10000  10000      1
 Pixel spacing (Angstroms)..............   28.13      28.13      28.13
 Cell angles ...........................   90.000   90.000   90.000
 Fast, medium, slow axes ..............    X    Y    Z
 Origin on x,y,z .......................    0.000       0.000       0.000
 Minimum density .......................  -21819.
 Maximum density .......................  -4273.0
 Mean density ..........................  -14725.
 tilt angles (original,current) ........   0.0   0.0   0.0   0.0   0.0   0.0
 Space group,# extra bytes,idtype,lens .        0        0        0        0

     1 Titles :
raw2mrc: Converted to mrc format.                    18-Oct-15  12:28:49

   106 -19884.25  -9110.25 -19884.25  -9110.25 -13607.88

 RO image file on unit   1 : run4_20151014_1_3ViewBS_slice_0107.mrc     Size=
195313 K

 Number of columns, rows, sections .....   10000   10000       1
 Map mode ..............................    1   (16-bit integer)
 Start cols, rows, sects, grid x,y,z ...    0     0     0   10000  10000      1
 Pixel spacing (Angstroms)..............   28.13      28.13      28.13
 Cell angles ...........................   90.000   90.000   90.000
 Fast, medium, slow axes ..............    X    Y    Z
 Origin on x,y,z .......................    0.000       0.000       0.000
 Minimum density .......................  -29295.
 Maximum density .......................  -3605.0
 Mean density ..........................  -14696.
 tilt angles (original,current) ........   0.0   0.0   0.0   0.0   0.0   0.0
 Space group,# extra bytes,idtype,lens .        0        0        0        0

     1 Titles :
raw2mrc: Converted to mrc format.                    18-Oct-15  12:29:01

   107 -20995.00  -8575.50 -20995.00  -8575.50 -13574.87

 RO image file on unit   1 : run4_20151014_1_3ViewBS_slice_0108.mrc     Size=
195313 K
```

```
 Number of columns, rows, sections .....   10000   10000       1
 Map mode ..............................    1   (16-bit integer)
 Start cols, rows, sects, grid x,y,z ...    0     0     0   10000  10000      1
 Pixel spacing (Angstroms)..............   28.13      28.13      28.13
 Cell angles ...........................   90.000   90.000   90.000
 Fast, medium, slow axes ..............    X    Y    Z
 Origin on x,y,z .......................    0.000       0.000       0.000
 Minimum density .......................  -20966.
 Maximum density .......................  -3860.0
 Mean density ..........................  -14737.
 tilt angles (original,current) ........   0.0   0.0   0.0   0.0   0.0   0.0
 Space group,# extra bytes,idtype,lens .        0        0        0        0

     1 Titles :
raw2mrc: Converted to mrc format.                    18-Oct-15  12:29:17

   108 -18533.50  -9012.50 -18533.50  -9012.50 -13615.60

 RO image file on unit   1 : run4_20151014_1_3ViewBS_slice_0109.mrc     Size=
195313 K

 Number of columns, rows, sections .....   10000   10000       1
 Map mode ..............................    1   (16-bit integer)
 Start cols, rows, sects, grid x,y,z ...    0     0     0   10000  10000      1
 Pixel spacing (Angstroms)..............   28.13      28.13      28.13
 Cell angles ...........................   90.000   90.000   90.000
 Fast, medium, slow axes ..............    X    Y    Z
 Origin on x,y,z .......................    0.000       0.000       0.000
 Minimum density .......................  -23328.
 Maximum density .......................  -3747.0
 Mean density ..........................  -14721.
 tilt angles (original,current) ........   0.0   0.0   0.0   0.0   0.0   0.0
 Space group,# extra bytes,idtype,lens .        0        0        0        0

     1 Titles :
raw2mrc: Converted to mrc format.                    18-Oct-15  12:29:31

   109 -21292.25  -8475.00 -21292.25  -8475.00 -13592.98

 RO image file on unit   1 : run4_20151014_1_3ViewBS_slice_0110.mrc     Size=
195313 K

 Number of columns, rows, sections .....   10000   10000       1
 Map mode ..............................    1   (16-bit integer)
```

```
 Start cols, rows, sects, grid x,y,z ...    0     0     0   10000  10000      1
 Pixel spacing (Angstroms).............   28.13      28.13      28.13
 Cell angles ...........................   90.000   90.000   90.000
 Fast, medium, slow axes .............    X    Y    Z
 Origin on x,y,z .....................    0.000       0.000       0.000
 Minimum density .....................  -24612.
 Maximum density .....................  -3982.0
 Mean density ........................  -14657.
 tilt angles (original,current) .....   0.0   0.0   0.0   0.0   0.0   0.0
 Space group,# extra bytes,idtype,lens .        0        0        0        0

     1 Titles :
raw2mrc: Converted to mrc format.                    18-Oct-15  12:29:53

  110 -21316.50  -8509.50 -21316.50  -8509.50 -13548.98

 RO image file on unit   1 : run4_20151014_1_3ViewBS_slice_0111.mrc     Size=
195313 K

 Number of columns, rows, sections .....   10000   10000       1
 Map mode ..............................    1   (16-bit integer)
 Start cols, rows, sects, grid x,y,z ...    0     0     0   10000  10000      1
 Pixel spacing (Angstroms).............   28.13      28.13      28.13
 Cell angles ...........................   90.000   90.000   90.000
 Fast, medium, slow axes .............    X    Y    Z
 Origin on x,y,z .....................    0.000       0.000       0.000
 Minimum density .....................  -23617.
 Maximum density .....................  -3784.0
 Mean density ........................  -14667.
 tilt angles (original,current) .....   0.0   0.0   0.0   0.0   0.0   0.0
 Space group,# extra bytes,idtype,lens .        0        0        0        0

     1 Titles :
raw2mrc: Converted to mrc format.                    18-Oct-15  12:30:08

  111 -20861.75  -8642.00 -20861.75  -8642.00 -13544.73

 RO image file on unit   1 : run4_20151014_1_3ViewBS_slice_0112.mrc     Size=
195313 K

 Number of columns, rows, sections .....   10000   10000       1
 Map mode ..............................    1   (16-bit integer)
 Start cols, rows, sects, grid x,y,z ...    0     0     0   10000  10000      1
 Pixel spacing (Angstroms).............   28.13      28.13      28.13
 Cell angles ...........................   90.000   90.000   90.000
```

```
 Fast, medium, slow axes .....    X    Y    Z
 Origin on x,y,z .....    0.000       0.000       0.000
 Minimum density .....  -23198.
 Maximum density .....  -3727.0
 Mean density .....  -14683.
 tilt angles (original,current) .....   0.0   0.0   0.0   0.0   0.0   0.0
 Space group,# extra bytes,idtype,lens .        0        0        0        0

     1 Titles :
raw2mrc: Converted to mrc format.                    18-Oct-15  12:30:29

   112 -20742.00  -9130.00 -20742.00  -9130.00 -13567.51

 RO image file on unit   1 : run4_20151014_1_3ViewBS_slice_0113.mrc     Size=
195313 K

 Number of columns, rows, sections .....   10000   10000       1
 Map mode .....    1   (16-bit integer)
 Start cols, rows, sects, grid x,y,z ...    0     0     0   10000  10000      1
 Pixel spacing (Angstroms).....   28.13      28.13      28.13
 Cell angles .....   90.000   90.000   90.000
 Fast, medium, slow axes .....    X    Y    Z
 Origin on x,y,z .....    0.000       0.000       0.000
 Minimum density .....  -21858.
 Maximum density .....  -3597.0
 Mean density .....  -14737.
 tilt angles (original,current) .....   0.0   0.0   0.0   0.0   0.0   0.0
 Space group,# extra bytes,idtype,lens .        0        0        0        0

     1 Titles :
raw2mrc: Converted to mrc format.                    18-Oct-15  12:31:12

   113 -20583.50  -9041.00 -20583.50  -9041.00 -13602.70

 RO image file on unit   1 : run4_20151014_1_3ViewBS_slice_0114.mrc     Size=
195313 K

 Number of columns, rows, sections .....   10000   10000       1
 Map mode .....    1   (16-bit integer)
 Start cols, rows, sects, grid x,y,z ...    0     0     0   10000  10000      1
 Pixel spacing (Angstroms).....   28.13      28.13      28.13
 Cell angles .....   90.000   90.000   90.000
 Fast, medium, slow axes .....    X    Y    Z
 Origin on x,y,z .....    0.000       0.000       0.000
 Minimum density .....  -24070.
```

Maximum density ..... -4136.0
Mean density ..... -14795.
tilt angles (original,current) 0.0 0.0 0.0 0.0 0.0 0.0
Space group,# extra bytes,idtype,lens . 0 0 0 0

1 Titles :
raw2mrc: Converted to mrc format. 18-Oct-15 12:31:25

114 -18847.00 -9077.00 -18847.00 -9077.00 -13646.48

RO image file on unit 1 : run4_20151014_1_3ViewBS_slice_0115.mrc Size= 195313 K

Number of columns, rows, sections 10000 10000 1
Map mode ..... 1 (16-bit integer)
Start cols, rows, sects, grid x,y,z ... 0 0 0 10000 10000 1
Pixel spacing (Angstroms)..... 28.13 28.13 28.13
Cell angles 90.000 90.000 90.000
Fast, medium, slow axes ..... X Y Z
Origin on x,y,z 0.000 0.000 0.000
Minimum density ..... -20943.
Maximum density ..... -3231.0
Mean density ..... -14161.
tilt angles (original,current) 0.0 0.0 0.0 0.0 0.0 0.0
Space group,# extra bytes,idtype,lens . 0 0 0 0

1 Titles :
raw2mrc: Converted to mrc format. 18-Oct-15 12:31:43

115 -19293.75 -8241.75 -19293.75 -8241.75 -13141.92

RO image file on unit 1 : run4_20151014_1_3ViewBS_slice_0116.mrc Size= 195313 K

Number of columns, rows, sections 10000 10000 1
Map mode ..... 1 (16-bit integer)
Start cols, rows, sects, grid x,y,z ... 0 0 0 10000 10000 1
Pixel spacing (Angstroms)..... 28.13 28.13 28.13
Cell angles 90.000 90.000 90.000
Fast, medium, slow axes ..... X Y Z
Origin on x,y,z 0.000 0.000 0.000
Minimum density ..... -32758.
Maximum density 6768.0
Mean density ..... -14778.
tilt angles (original,current) 0.0 0.0 0.0 0.0 0.0 0.0

Space group,# extra bytes,idtype,lens . 0 0 0 0

1 Titles :
raw2mrc: Converted to mrc format. 18-Oct-15 12:32:37

116 -22805.25 -5325.75 -22805.25 -5325.75 -13654.56

RO image file on unit 1 : run4_20151014_1_3ViewBS_slice_0117.mrc Size= 195313 K

Number of columns, rows, sections 10000 10000 1
Map mode ..... 1 (16-bit integer)
Start cols, rows, sects, grid x,y,z ... 0 0 0 10000 10000 1
Pixel spacing (Angstroms)..... 28.13 28.13 28.13
Cell angles 90.000 90.000 90.000
Fast, medium, slow axes ..... X Y Z
Origin on x,y,z 0.000 0.000 0.000
Minimum density ..... -24583.
Maximum density ..... -3734.0
Mean density ..... -14792.
tilt angles (original,current) 0.0 0.0 0.0 0.0 0.0 0.0
Space group,# extra bytes,idtype,lens . 0 0 0 0

1 Titles :
raw2mrc: Converted to mrc format. 18-Oct-15 12:32:54

117 -19788.00 -9125.50 -19788.00 -9125.50 -13660.88

RO image file on unit 1 : run4_20151014_1_3ViewBS_slice_0118.mrc Size= 195313 K

Number of columns, rows, sections 10000 10000 1
Map mode ..... 1 (16-bit integer)
Start cols, rows, sects, grid x,y,z ... 0 0 0 10000 10000 1
Pixel spacing (Angstroms)..... 28.13 28.13 28.13
Cell angles 90.000 90.000 90.000
Fast, medium, slow axes ..... X Y Z
Origin on x,y,z 0.000 0.000 0.000
Minimum density ..... -21878.
Maximum density ..... -4182.0
Mean density ..... -14791.
tilt angles (original,current) 0.0 0.0 0.0 0.0 0.0 0.0
Space group,# extra bytes,idtype,lens . 0 0 0 0

1 Titles :

raw2mrc: Converted to mrc format. 18-Oct-15 12:33:29

118 -20289.00 -9125.50 -20289.00 -9125.50 -13654.25

RO image file on unit 1 : run4_20151014_1_3ViewBS_slice_0119.mrc Size= 195313 K

Number of columns, rows, sections 10000 10000 1
Map mode ..... 1 (16-bit integer)
Start cols, rows, sects, grid x,y,z ... 0 0 0 10000 10000 1
Pixel spacing (Angstroms)..... 28.13 28.13 28.13
Cell angles 90.000 90.000 90.000
Fast, medium, slow axes ..... X Y Z
Origin on x,y,z 0.000 0.000 0.000
Minimum density ..... -32758.
Maximum density 6719.0
Mean density ..... -14751.
tilt angles (original,current) 0.0 0.0 0.0 0.0 0.0 0.0
Space group,# extra bytes,idtype,lens . 0 0 0 0

1 Titles :
raw2mrc: Converted to mrc format. 18-Oct-15 12:33:46

119 -21008.00 -4228.25 -21008.00 -4228.25 -13616.14

RO image file on unit 1 : run4_20151014_1_3ViewBS_slice_0120.mrc Size= 195313 K

Number of columns, rows, sections 10000 10000 1
Map mode ..... 1 (16-bit integer)
Start cols, rows, sects, grid x,y,z ... 0 0 0 10000 10000 1
Pixel spacing (Angstroms)..... 28.13 28.13 28.13
Cell angles 90.000 90.000 90.000
Fast, medium, slow axes ..... X Y Z
Origin on x,y,z 0.000 0.000 0.000
Minimum density ..... -32758.
Maximum density 6711.0
Mean density ..... -14793.
tilt angles (original,current) 0.0 0.0 0.0 0.0 0.0 0.0
Space group,# extra bytes,idtype,lens . 0 0 0 0

1 Titles :
raw2mrc: Converted to mrc format. 18-Oct-15 12:34:01

120 -20341.75 -4207.00 -20341.75 -4207.00 -13657.56

```
 RO image file on unit   1 : run4_20151014_1_3ViewBS_slice_0121.mrc     Size=
195313 K

 Number of columns, rows, sections .....   10000   10000       1
 Map mode ..............................    1   (16-bit integer)
 Start cols, rows, sects, grid x,y,z ...    0     0     0   10000  10000      1
 Pixel spacing (Angstroms)..............   28.13      28.13      28.13
 Cell angles ...........................   90.000   90.000   90.000
 Fast, medium, slow axes ..............    X    Y    Z
 Origin on x,y,z .......................    0.000       0.000       0.000
 Minimum density .......................  -32758.
 Maximum density .......................  -88.000
 Mean density ..........................  -14787.
 tilt angles (original,current) ........   0.0   0.0   0.0   0.0   0.0   0.0
 Space group,# extra bytes,idtype,lens .        0        0        0        0

     1 Titles :
raw2mrc: Converted to mrc format.                    18-Oct-15  12:34:14

   121 -22799.25  -8664.25 -22799.25  -8664.25 -13649.07

 RO image file on unit   1 : run4_20151014_1_3ViewBS_slice_0122.mrc     Size=
195313 K

 Number of columns, rows, sections .....   10000   10000       1
 Map mode ..............................    1   (16-bit integer)
 Start cols, rows, sects, grid x,y,z ...    0     0     0   10000  10000      1
 Pixel spacing (Angstroms)..............   28.13      28.13      28.13
 Cell angles ...........................   90.000   90.000   90.000
 Fast, medium, slow axes ..............    X    Y    Z
 Origin on x,y,z .......................    0.000       0.000       0.000
 Minimum density .......................  -21907.
 Maximum density .......................  -3853.0
 Mean density ..........................  -14775.
 tilt angles (original,current) ........   0.0   0.0   0.0   0.0   0.0   0.0
 Space group,# extra bytes,idtype,lens .        0        0        0        0

     1 Titles :
raw2mrc: Converted to mrc format.                    18-Oct-15  12:34:53

   122 -20105.50  -8367.25 -20105.50  -8367.25 -13640.14

 RO image file on unit   1 : run4_20151014_1_3ViewBS_slice_0123.mrc     Size=
195313 K
```

```
 Number of columns, rows, sections .....   10000   10000       1
 Map mode ..............................    1   (16-bit integer)
 Start cols, rows, sects, grid x,y,z ...    0     0     0   10000  10000      1
 Pixel spacing (Angstroms)..............   28.13      28.13      28.13
 Cell angles ...........................   90.000   90.000   90.000
 Fast, medium, slow axes ..............    X    Y    Z
 Origin on x,y,z .......................    0.000       0.000       0.000
 Minimum density .......................  -21042.
 Maximum density .......................  -3636.0
 Mean density ..........................  -14811.
 tilt angles (original,current) ........   0.0   0.0   0.0   0.0   0.0   0.0
 Space group,# extra bytes,idtype,lens .        0        0        0        0

     1 Titles :
raw2mrc: Converted to mrc format.                    18-Oct-15  12:36:16

   123 -19468.25  -8994.75 -19468.25  -8994.75 -13673.19

 RO image file on unit   1 : run4_20151014_1_3ViewBS_slice_0124.mrc     Size=
195313 K

 Number of columns, rows, sections .....   10000   10000       1
 Map mode ..............................    1   (16-bit integer)
 Start cols, rows, sects, grid x,y,z ...    0     0     0   10000  10000      1
 Pixel spacing (Angstroms)..............   28.13      28.13      28.13
 Cell angles ...........................   90.000   90.000   90.000
 Fast, medium, slow axes ..............    X    Y    Z
 Origin on x,y,z .......................    0.000       0.000       0.000
 Minimum density .......................  -20990.
 Maximum density .......................  -3725.0
 Mean density ..........................  -14820.
 tilt angles (original,current) ........   0.0   0.0   0.0   0.0   0.0   0.0
 Space group,# extra bytes,idtype,lens .        0        0        0        0

     1 Titles :
raw2mrc: Converted to mrc format.                    18-Oct-15  12:36:34

   124 -18789.50  -9400.00 -18789.50  -9400.00 -13684.84

 RO image file on unit   1 : run4_20151014_1_3ViewBS_slice_0125.mrc     Size=
195313 K

 Number of columns, rows, sections .....   10000   10000       1
 Map mode ..............................    1   (16-bit integer)
```

```
 Start cols, rows, sects, grid x,y,z ...    0     0     0   10000  10000      1
 Pixel spacing (Angstroms).............   28.13      28.13      28.13
 Cell angles ...........................   90.000   90.000   90.000
 Fast, medium, slow axes .............    X    Y    Z
 Origin on x,y,z .....................    0.000       0.000       0.000
 Minimum density .....................  -26289.
 Maximum density .....................  -4291.0
 Mean density ........................  -14808.
 tilt angles (original,current) .....   0.0   0.0   0.0   0.0   0.0   0.0
 Space group,# extra bytes,idtype,lens .        0        0        0        0

     1 Titles :
raw2mrc: Converted to mrc format.                    18-Oct-15  12:37:13

   125 -19886.75  -9035.75 -19886.75  -9035.75 -13680.40

 RO image file on unit   1 : run4_20151014_1_3ViewBS_slice_0126.mrc     Size=
195313 K

 Number of columns, rows, sections .....   10000   10000       1
 Map mode ..............................    1   (16-bit integer)
 Start cols, rows, sects, grid x,y,z ...    0     0     0   10000  10000      1
 Pixel spacing (Angstroms).............   28.13      28.13      28.13
 Cell angles ...........................   90.000   90.000   90.000
 Fast, medium, slow axes .............    X    Y    Z
 Origin on x,y,z .....................    0.000       0.000       0.000
 Minimum density .....................  -21600.
 Maximum density .....................  -4338.0
 Mean density ........................  -14813.
 tilt angles (original,current) .....   0.0   0.0   0.0   0.0   0.0   0.0
 Space group,# extra bytes,idtype,lens .        0        0        0        0

     1 Titles :
raw2mrc: Converted to mrc format.                    18-Oct-15  12:37:35

   126 -19918.50  -9240.75 -19918.50  -9240.75 -13680.64

 RO image file on unit   1 : run4_20151014_1_3ViewBS_slice_0127.mrc     Size=
195313 K

 Number of columns, rows, sections .....   10000   10000       1
 Map mode ..............................    1   (16-bit integer)
 Start cols, rows, sects, grid x,y,z ...    0     0     0   10000  10000      1
 Pixel spacing (Angstroms).............   28.13      28.13      28.13
 Cell angles ...........................   90.000   90.000   90.000
```

```
 Fast, medium, slow axes .....    X    Y    Z
 Origin on x,y,z .....    0.000       0.000       0.000
 Minimum density .....  -21684.
 Maximum density .....  -3677.0
 Mean density .....  -14801.
 tilt angles (original,current) .....   0.0   0.0   0.0   0.0   0.0   0.0
 Space group,# extra bytes,idtype,lens .        0        0        0        0

     1 Titles :
raw2mrc: Converted to mrc format.                    18-Oct-15  12:38:30

   127 -20233.75  -9113.50 -20233.75  -9113.50 -13674.81

 RO image file on unit   1 : run4_20151014_1_3ViewBS_slice_0128.mrc     Size=
195313 K

 Number of columns, rows, sections .....   10000   10000       1
 Map mode .....    1   (16-bit integer)
 Start cols, rows, sects, grid x,y,z ...    0     0     0   10000  10000      1
 Pixel spacing (Angstroms).....   28.13      28.13      28.13
 Cell angles .....   90.000   90.000   90.000
 Fast, medium, slow axes .....    X    Y    Z
 Origin on x,y,z .....    0.000       0.000       0.000
 Minimum density .....  -32758.
 Maximum density .....   6713.0
 Mean density .....  -14801.
 tilt angles (original,current) .....   0.0   0.0   0.0   0.0   0.0   0.0
 Space group,# extra bytes,idtype,lens .        0        0        0        0

     1 Titles :
raw2mrc: Converted to mrc format.                    18-Oct-15  12:38:43

   128 -22482.75  -4366.50 -22482.75  -4366.50 -13674.12

 RO image file on unit   1 : run4_20151014_1_3ViewBS_slice_0129.mrc     Size=
195313 K

 Number of columns, rows, sections .....   10000   10000       1
 Map mode .....    1   (16-bit integer)
 Start cols, rows, sects, grid x,y,z ...    0     0     0   10000  10000      1
 Pixel spacing (Angstroms).....   28.13      28.13      28.13
 Cell angles .....   90.000   90.000   90.000
 Fast, medium, slow axes .....    X    Y    Z
 Origin on x,y,z .....    0.000       0.000       0.000
 Minimum density .....  -22414.
```

```
 Maximum density .....  -4144.0
 Mean density .....  -14825.
 tilt angles (original,current) .....   0.0   0.0   0.0   0.0   0.0   0.0
 Space group,# extra bytes,idtype,lens .        0        0        0        0

     1 Titles :
raw2mrc: Converted to mrc format.                    18-Oct-15  12:39:41

   129 -20297.00  -8556.50 -20297.00  -8556.50 -13694.98

 RO image file on unit   1 : run4_20151014_1_3ViewBS_slice_0130.mrc     Size=
195313 K

 Number of columns, rows, sections .....   10000   10000       1
 Map mode .....    1   (16-bit integer)
 Start cols, rows, sects, grid x,y,z ...    0     0     0   10000  10000      1
 Pixel spacing (Angstroms).....   28.13      28.13      28.13
 Cell angles .....   90.000   90.000   90.000
 Fast, medium, slow axes .....    X    Y    Z
 Origin on x,y,z .....    0.000       0.000       0.000
 Minimum density .....  -21037.
 Maximum density .....  -4078.0
 Mean density .....  -14846.
 tilt angles (original,current) .....   0.0   0.0   0.0   0.0   0.0   0.0
 Space group,# extra bytes,idtype,lens .        0        0        0        0

     1 Titles :
raw2mrc: Converted to mrc format.                    18-Oct-15  12:40:33

   130 -19320.00  -9495.75 -19320.00  -9495.75 -13716.72

 RO image file on unit   1 : run4_20151014_1_3ViewBS_slice_0131.mrc     Size=
195313 K

 Number of columns, rows, sections .....   10000   10000       1
 Map mode .....    1   (16-bit integer)
 Start cols, rows, sects, grid x,y,z ...    0     0     0   10000  10000      1
 Pixel spacing (Angstroms).....   28.13      28.13      28.13
 Cell angles .....   90.000   90.000   90.000
 Fast, medium, slow axes .....    X    Y    Z
 Origin on x,y,z .....    0.000       0.000       0.000
 Minimum density .....  -32758.
 Maximum density .....  -1630.0
 Mean density .....  -14940.
 tilt angles (original,current) .....   0.0   0.0   0.0   0.0   0.0   0.0
```

Space group,# extra bytes,idtype,lens . 0 0 0 0

1 Titles :
raw2mrc: Converted to mrc format. 18-Oct-15 12:41:50

131 -21724.25 -8441.50 -21724.25 -8441.50 -13799.61

RO image file on unit 1 : run4_20151014_1_3ViewBS_slice_0132.mrc Size= 195313 K

Number of columns, rows, sections 10000 10000 1
Map mode ..... 1 (16-bit integer)
Start cols, rows, sects, grid x,y,z ... 0 0 0 10000 10000 1
Pixel spacing (Angstroms)..... 28.13 28.13 28.13
Cell angles 90.000 90.000 90.000
Fast, medium, slow axes ..... X Y Z
Origin on x,y,z 0.000 0.000 0.000
Minimum density ..... -21306.
Maximum density ..... -4167.0
Mean density ..... -14863.
tilt angles (original,current) 0.0 0.0 0.0 0.0 0.0 0.0
Space group,# extra bytes,idtype,lens . 0 0 0 0

1 Titles :
raw2mrc: Converted to mrc format. 18-Oct-15 12:42:03

132 -19058.50 -8721.25 -19058.50 -8721.25 -13739.77

RO image file on unit 1 : run4_20151014_1_3ViewBS_slice_0133.mrc Size= 195313 K

Number of columns, rows, sections 10000 10000 1
Map mode ..... 1 (16-bit integer)
Start cols, rows, sects, grid x,y,z ... 0 0 0 10000 10000 1
Pixel spacing (Angstroms)..... 28.13 28.13 28.13
Cell angles 90.000 90.000 90.000
Fast, medium, slow axes ..... X Y Z
Origin on x,y,z 0.000 0.000 0.000
Minimum density ..... -32658.
Maximum density ..... -3997.0
Mean density ..... -14750.
tilt angles (original,current) 0.0 0.0 0.0 0.0 0.0 0.0
Space group,# extra bytes,idtype,lens . 0 0 0 0

1 Titles :

raw2mrc: Converted to mrc format. 18-Oct-15 12:42:16

133 -21667.25 -8822.00 -21667.25 -8822.00 -13654.59

RO image file on unit 1 : run4_20151014_1_3ViewBS_slice_0134.mrc Size= 195313 K

Number of columns, rows, sections 10000 10000 1
Map mode ..... 1 (16-bit integer)
Start cols, rows, sects, grid x,y,z ... 0 0 0 10000 10000 1
Pixel spacing (Angstroms)..... 28.13 28.13 28.13
Cell angles 90.000 90.000 90.000
Fast, medium, slow axes ..... X Y Z
Origin on x,y,z 0.000 0.000 0.000
Minimum density ..... -26661.
Maximum density ..... -3497.0
Mean density ..... -14918.
tilt angles (original,current) 0.0 0.0 0.0 0.0 0.0 0.0
Space group,# extra bytes,idtype,lens . 0 0 0 0

1 Titles :
raw2mrc: Converted to mrc format. 18-Oct-15 12:42:29

134 -18383.00 -9489.50 -18383.00 -9489.50 -13800.98

RO image file on unit 1 : run4_20151014_1_3ViewBS_slice_0135.mrc Size= 195313 K

Number of columns, rows, sections 10000 10000 1
Map mode ..... 1 (16-bit integer)
Start cols, rows, sects, grid x,y,z ... 0 0 0 10000 10000 1
Pixel spacing (Angstroms)..... 28.13 28.13 28.13
Cell angles 90.000 90.000 90.000
Fast, medium, slow axes ..... X Y Z
Origin on x,y,z 0.000 0.000 0.000
Minimum density ..... -29366.
Maximum density ..... -4092.0
Mean density ..... -14924.
tilt angles (original,current) 0.0 0.0 0.0 0.0 0.0 0.0
Space group,# extra bytes,idtype,lens . 0 0 0 0

1 Titles :
raw2mrc: Converted to mrc format. 18-Oct-15 12:42:40

135 -18588.25 -9546.25 -18588.25 -9546.25 -13792.87

RO image file on unit 1 : run4_20151014_1_3ViewBS_slice_0136.mrc Size= 195313 K

Number of columns, rows, sections 10000 10000 1
Map mode ..... 1 (16-bit integer)
Start cols, rows, sects, grid x,y,z ... 0 0 0 10000 10000 1
Pixel spacing (Angstroms)..... 28.13 28.13 28.13
Cell angles 90.000 90.000 90.000
Fast, medium, slow axes ..... X Y Z
Origin on x,y,z 0.000 0.000 0.000
Minimum density ..... -23781.
Maximum density ..... -3414.0
Mean density ..... -14651.
tilt angles (original,current) 0.0 0.0 0.0 0.0 0.0 0.0
Space group,# extra bytes,idtype,lens . 0 0 0 0

1 Titles :
raw2mrc: Converted to mrc format. 18-Oct-15 12:42:52

136 -20475.00 -8379.50 -20475.00 -8379.50 -13515.79

RO image file on unit 1 : run4_20151014_1_3ViewBS_slice_0137.mrc Size= 195313 K

Number of columns, rows, sections 10000 10000 1
Map mode ..... 1 (16-bit integer)
Start cols, rows, sects, grid x,y,z ... 0 0 0 10000 10000 1
Pixel spacing (Angstroms)..... 28.13 28.13 28.13
Cell angles 90.000 90.000 90.000
Fast, medium, slow axes ..... X Y Z
Origin on x,y,z 0.000 0.000 0.000
Minimum density ..... -22271.
Maximum density ..... -3793.0
Mean density ..... -14900.
tilt angles (original,current) 0.0 0.0 0.0 0.0 0.0 0.0
Space group,# extra bytes,idtype,lens . 0 0 0 0

1 Titles :
raw2mrc: Converted to mrc format. 18-Oct-15 12:44:06

137 -19378.50 -9170.75 -19378.50 -9170.75 -13809.91

RO image file on unit 1 : run4_20151014_1_3ViewBS_slice_0138.mrc Size= 195313 K

```
 Number of columns, rows, sections .....   10000   10000       1
 Map mode ..............................    1   (16-bit integer)
 Start cols, rows, sects, grid x,y,z ...    0     0     0   10000  10000      1
 Pixel spacing (Angstroms)..............   28.13      28.13      28.13
 Cell angles ...........................   90.000   90.000   90.000
 Fast, medium, slow axes ...............    X    Y    Z
 Origin on x,y,z .......................    0.000       0.000       0.000
 Minimum density .......................  -22353.
 Maximum density .......................  -4093.0
 Mean density ..........................  -14904.
 tilt angles (original,current) ........   0.0   0.0   0.0   0.0   0.0   0.0
 Space group,# extra bytes,idtype,lens .        0        0        0        0

     1 Titles :
raw2mrc: Converted to mrc format.                    18-Oct-15  12:44:20

   138 -19835.75  -9489.00 -19835.75  -9489.00 -13805.37

 RO image file on unit   1 : run4_20151014_1_3ViewBS_slice_0139.mrc     Size=
195313 K

 Number of columns, rows, sections .....   10000   10000       1
 Map mode ..............................    1   (16-bit integer)
 Start cols, rows, sects, grid x,y,z ...    0     0     0   10000  10000      1
 Pixel spacing (Angstroms)..............   28.13      28.13      28.13
 Cell angles ...........................   90.000   90.000   90.000
 Fast, medium, slow axes ...............    X    Y    Z
 Origin on x,y,z .......................    0.000       0.000       0.000
 Minimum density .......................  -21760.
 Maximum density .......................  -3996.0
 Mean density ..........................  -14887.
 tilt angles (original,current) ........   0.0   0.0   0.0   0.0   0.0   0.0
 Space group,# extra bytes,idtype,lens .        0        0        0        0

     1 Titles :
raw2mrc: Converted to mrc format.                    18-Oct-15  12:44:41

   139 -20034.75  -8574.25 -20034.75  -8574.25 -13784.69

 RO image file on unit   1 : run4_20151014_1_3ViewBS_slice_0140.mrc     Size=
195313 K

 Number of columns, rows, sections .....   10000   10000       1
 Map mode ..............................    1   (16-bit integer)
```

```
 Start cols, rows, sects, grid x,y,z ...    0     0     0   10000  10000      1
 Pixel spacing (Angstroms).............   28.13      28.13      28.13
 Cell angles ...........................   90.000   90.000   90.000
 Fast, medium, slow axes .............    X    Y    Z
 Origin on x,y,z .....................    0.000       0.000       0.000
 Minimum density .....................  -22934.
 Maximum density .....................  -2916.0
 Mean density ........................  -14272.
 tilt angles (original,current) .....   0.0   0.0   0.0   0.0   0.0   0.0
 Space group,# extra bytes,idtype,lens .        0        0        0        0

     1 Titles :
raw2mrc: Converted to mrc format.                    18-Oct-15  12:45:42

   140 -20308.25  -8408.25 -20308.25  -8408.25 -13249.90

 RO image file on unit   1 : run4_20151014_1_3ViewBS_slice_0141.mrc     Size=
195313 K

 Number of columns, rows, sections .....   10000   10000       1
 Map mode ..............................    1   (16-bit integer)
 Start cols, rows, sects, grid x,y,z ...    0     0     0   10000  10000      1
 Pixel spacing (Angstroms).............   28.13      28.13      28.13
 Cell angles ...........................   90.000   90.000   90.000
 Fast, medium, slow axes .............    X    Y    Z
 Origin on x,y,z .....................    0.000       0.000       0.000
 Minimum density .....................  -22888.
 Maximum density .....................  -3601.0
 Mean density ........................  -14995.
 tilt angles (original,current) .....   0.0   0.0   0.0   0.0   0.0   0.0
 Space group,# extra bytes,idtype,lens .        0        0        0        0

     1 Titles :
raw2mrc: Converted to mrc format.                    18-Oct-15  12:46:01

   141 -20821.25  -9091.50 -20821.25  -9091.50 -13875.98

 RO image file on unit   1 : run4_20151014_1_3ViewBS_slice_0142.mrc     Size=
195313 K

 Number of columns, rows, sections .....   10000   10000       1
 Map mode ..............................    1   (16-bit integer)
 Start cols, rows, sects, grid x,y,z ...    0     0     0   10000  10000      1
 Pixel spacing (Angstroms).............   28.13      28.13      28.13
 Cell angles ...........................   90.000   90.000   90.000
```

Fast, medium, slow axes ..... X Y Z
Origin on x,y,z 0.000 0.000 0.000
Minimum density ..... -23062.
Maximum density ..... -4066.0
Mean density ..... -14868.
tilt angles (original,current) 0.0 0.0 0.0 0.0 0.0 0.0
Space group,# extra bytes,idtype,lens . 0 0 0 0

1 Titles :
raw2mrc: Converted to mrc format. 18-Oct-15 12:46:15

142 -20750.25 -8743.75 -20750.25 -8743.75 -13771.24

RO image file on unit 1 : run4_20151014_1_3ViewBS_slice_0143.mrc Size= 195313 K

Number of columns, rows, sections 10000 10000 1
Map mode ..... 1 (16-bit integer)
Start cols, rows, sects, grid x,y,z ... 0 0 0 10000 10000 1
Pixel spacing (Angstroms)..... 28.13 28.13 28.13
Cell angles 90.000 90.000 90.000
Fast, medium, slow axes ..... X Y Z
Origin on x,y,z 0.000 0.000 0.000
Minimum density ..... -32767.
Maximum density ..... -3721.0
Mean density ..... -14923.
tilt angles (original,current) 0.0 0.0 0.0 0.0 0.0 0.0
Space group,# extra bytes,idtype,lens . 0 0 0 0

1 Titles :
raw2mrc: Converted to mrc format. 18-Oct-15 12:46:31

143 -24682.00 -8730.00 -24682.00 -8730.00 -13804.49

References

Adrian, M., Dubochet, J., Lepault, J., McDowall, A.W. Cryo-electron microscopy of viruses. *Nature* (1984). **308** (5954): 32-36. Bibcode:1984Natur.308...32A.doi:10.1038/308032a0. PMID 6322001.

Arkill, K.P., Qvortrup, K., Starborg, T., Mantell, J.M., Knupp, C., Michel, C.C., Harper, S.J., Salmon, A.H., Squire, J.M., Bates, D.O. & Neal, C.R. Resolution of the three dimensional structure of components of the glomerular filtration barrier. BMC Nephrol (2014). 15(1), article no. 24.

Auinger, S. & Small, J.V. Correlated light and electron microscopy of the cytoskeleton. Methods Cell Biol (2008). 88, 257–272.

Betzig, E. Proposed Method for molecular optical imaging. *Optics Letters* (1995). **20** (3): 237–239. Bibcode:1995OptL...20..237B. doi:10.1364/OL.20.000237.

Burnett, T.L., Mcdonald, S.A., Gholinia, A., Geurts, R., Janus, M., Slater, T., Haigh, S.J., Ornek, C., Almuaili, F., Engelberg, D.L., Thompson, G.E. & Withers, P.J. Correlative tomography. Sci Rep (2014). 4, article no. 4711.

Bushong, E.A., Johnson, Jr., D.D., Kim, K.Y., Terada, M., Hatori, M., Peltier, S.T. Panda, S., Merkle, A. and Ellisman, M.H., X-Ray Microscopy as an Approach to Increasing Accuracy and Efficiency of Serial Block-Face Imaging for Correlated Light and Electron Microscopy of Biological Specimens. **2014**, Microscopy and Microanalysis, 21, pp 231-238.

Chatterjee, D.K., Yong, Z. Upconverting nanoparticles as nanostructures for photodynamic therapy in cancer cells. (2012). 1(3). 73-82.

Deerinck, T., Bushong, E., Lev-Ram, V., Shu, X., Tsien, R. & Ellisman, M. Enhancing serial block-face scanning electron microscopy to enable high resolution 3-D nanohistology of cells and tissues. Microsc Microanal (2010). 16(Suppl 2), 1138–1139.

Denk, W. & Horstmann, H. Serial block-face scanning electron microscopy to reconstruct three-dimensional tissue nanostructure. PLoS Biol (2004). 2(11), e329.

Denk, W., Strickler, J., Webb, W. Two-photon laser scanning fluorescence microscopy. Science (1990). **248** (4951): 73-6. Bibcode:1990Sci...248...73D.doi:10.1126/science.2321027. PMID 2321027.

Denk, W., Svoboda, K. Photon upmanship: why multiphoton imaging is more than a gimmick. *Neuron* (1997). **18** (3): 351–7. doi:10.1016/S0896-6273(00)81237-4.PMID 9115730.

Hatori, M.,Vollmers, C.,Zarrinpar, A.,Ditacchio, L.,Bushong, E.A., Gill, S., Leblanc, M., Chaix, A., Joens, M., Fitzpatrick, J.A., Ellisman, M.H. & Panda, S. Time-restricted feeding without reducing caloric intake prevents metabolic diseases in mice fed a high-fat diet. Cell Metab (2012). 15(6), 848–860.

Helmstaedter, M. Cellular-resolution connectomics: Challenges of dense neural circuit reconstruction. Nat Methods (2013). 10(6), 501–507.

Heymann, J.A., Shi, D., Kim, S., Bliss, D., Milne, J.L. & Subramaniam, S. 3D imaging of mammalian cells with ion-abrasion scanning electron microscopy. J Struct Biol (2009). 166(1), 1–7.

Holcomb, P.S., Hoffpauir, B.K., Hoyson, M.C., Jackson, D.R., Deerinck, T.J., Marrs, G.S., Dehoff, M.,Wu, J., Ellisman, M.H. & Spirou, G.A. Synaptic inputs compete during rapid formation of the calyx of Held: A new model system for neural development. J Neurosci (2013). 33(32), 12954–12969.

Kleinfeld, D., Bharioke, A., Blinder, P., Bock, D.D., Briggman, K.L., Chklovskii, D.B., Denk, W., Helmstaedter, M., Kaufhold, J.P., Lee, W.C., Meyer, H.S., Micheva, K.D., Oberlaender, M., Prohaska, S., Reid, R.C., Smith, S.J., Takemura, S., Tsai, P.S. & Sakmann, B. Large-scale automated histology in the pursuit of connectomes. J Neurosci (2011). 31(45), 16125–16138.

Knott, G., Marchman, H.,Wall, D. & Lich, B. Serial section scanning electron microscopy of adult brain tissue using focused ion beam milling. J Neurosci (2008). 28(12), 2959–2964.

Leighton, S.B. SEM images of block faces, cut by a miniature microtome within the SEM—a technical note. Scan Electron Microsc (1981). Pt 2, 73–76.

Martell, J.D., Deerinck, T.J., Sancak, Y., Poulos, T.L., Mootha, V.K., Sosinsky, G.E., Ellisman, M.H. & Ting, A.Y. Engineered ascorbate peroxidase as a genetically encoded reporter for electron microscopy. Nat Biotechnol (2012). 30(11), 1143–1148.

Mcdonald, K., Schwarz, H., Muller-Reichert, T., Webb, R., Buser, C. & Morphew, M. “Tips and tricks” for high-pressure freezing of model systems. Methods Cell Biol (2010). 96, 671–693.

Metscher, B.D. MicroCTfor comparativemorphology: Simple staining methods allow high-contrast 3D imaging of diverse non-mineralized animal tissues. BMC

Physiol (2009). 9, article no. 11.

O'brien, J.A. & Lummis, S.C. Nano-biolistics: A method of biolistic transfection of cells and tissues using a gene gun with novel nanometer-sized projectiles. BMC Biotechnol (2011). 11, article no. 66.

Subach, F.V., Patterson, G.H., Renz, M., Lippincott-Schwartz, J., Verkhusha, V.V. Bright monomeric photoactivatable red fluorescent protein for two-color super-resolution sptPALM of live cells. J Am Chem Soc. 2010 May 12.

Parent, K. N., M. L. Erb, G. Cardone, K. Nguyen, E. B. Gilcrease, N. B. Porcek, J. Pogliano, T. S. Baker, and S. R. Casjens OmpA and OmpC are critical host factors for bacteriophage Sf6 entry in Shigella. *Mol. Microbiol.* (2014). 92:47-60.

Peachey, L.D. Thin sections. I. A study of section thickness and physical distortion produced during microtomy. J Biophys Biochem Cytol (1958). 4(3), 233–242.

Peddie, C.J. & Collinson, L.M. Exploring the third dimension: Volume electron microscopy comes of age. Micron (2014). 61C, 9–19.

Pingel, J., Lu, Y., Starborg, T., Fredberg, U., Langberg, H., Nedergaard, A., Weis, M., Eyre, D., Kjaer, M. & Kadler, K.E. 3-D ultrastructure and collagen composition of healthy and overloaded human tendon: Evidence of tenocyte and matrix buckling. J Anat (2014). 224(5), 548–555.

Puhka, M., Joensuu, M., Vihinen, H., Belevich, I. & Jokitalo, E. Progressive sheet-to-tubule transformation is a general mechanism for endoplasmic reticulum partitioning in dividing mammalian cells. Mol Biol Cell (2012). 23(13), 2424–2432.

Randolph, L.M., Chien, M.P., Gianneschi, N.C. Biological stimuli and biomolecules in the assembly and manipulation of nanoscale polymeric particles. (2012). Chem. Sci. 5(3). 1363-1380

Rodriguez, E.A., Ngo, J.T., Palida, S.T., Adams, S.R., Mackey, M.R., Ramachandra, R., Ellisman, M.H. and Tsien, R.Y. (2015). New Molecular Tools for Light and Electron Microscopy. Microscopy and Microanalysis, 21 (Suppl. 3), pp 1-2. doi:10.1017/S143192761500080X.

Shafer, H., Haase, M. Upconverting Nanoparticles (2011). Angew. Chem. Int. Ed. 50, 5808-5829

Sengle, G., Tufa, S.F., Sakai, L.Y., Zulliger, M.A. & Keene, D.R. A correlative method for imaging identical regions of samples by micro-CT, light microscopy, and electron microscopy: Imaging adipose tissue in a model system.

J Histochem Cytochem (2013). 61(4), 263–271.

Shu, X., Lev-Ram, V., Deerinck, T.J., Qi, Y., Ramko, E.B., Davidson, M.W., Jin, Y., Ellisman, M.H. & Tsien, R.Y. A genetically encoded tag for correlated light and electron microscopy of intact cells, tissues, and organisms. PLoS Biol (2011). 9(4), e1001041.

Smith KCA, Oatley, CW (1955). "The scanning electron microscope and its fields of application". *British Journal of Applied Physics* **6** (11): 391–399.Bibcode:1955BJAP....6..391S. doi:10.1088/0508-3443/6/11/304.

Stock, S.R. Microcomputed Tomography: Methodology and Applications. (2009). Boca Raton, FL: CRC Press.

Shroff, H., Galbraith, C.G., Galbraith, J.A., Betzig, E. Live-cell photoactivated localization microscopy of nanoscale adhesion dynamics Nature Methods (2007). 5(5). 417-423.

Tseng, Y. S., B. L. Gurda, P. Chipman, R. McKenna, S. Afione, J. A. Chiorini, N. Muzyczka, N. H. Olson, T. S. Baker, J. Leinschmidt, and M. Agbandje-McKenna (2015) Adeno-Associated Virus serotype 1 (AAV1)- and AAV5-antibody complex structures reveal evolutionary commonalities in parvovirus antigenic reactivity. *J. Virol.* **89:1794-807**.

West, J.B., Fu, Z., Deerinck, T.J., Mackey, M.R., Obayashi, J.T. & Ellisman, M.H. Structure-function studies of blood and air capillaries in chicken lung using 3D electron microscopy. Respir Physiol Neurobiol (2010). 170(2), 202–209.

Wilke, S.A., Antonios, J.K., Bushong, E.A., Badkoobehi, A., Malek, E., Hwang, M., Terada, M., Ellisman, M.H. & Ghosh, A. Deconstructing complexity: Serial block-face electron microscopic analysis of the hippocampal mossy fiber synapse. J Neurosci (2013). 33(2), 507–522.